Universidad Pública de Navarra
Nafarroako Unibertsitate Publikoa

Tesis Doctoral

MEDICAGO TRUNCATULA RESPONSE TO WATER-DEFICIT STRESS

– whole-plant perspectives -

Memoria presentada por **Verónica Castañeda Presa** para optar al grado de Doctora con Mención de "Doctora Internacional"

Pamplona, abril 2021.

https://doi.org/10.48035/Tesis/2454/41129

Universidad Pública de Navarra
Nafarroako Unibertsitate Publikoa

This work was funded by the Spanish Ministry of Economy and Competitiveness (AGL 2011-23738) and the Public University of Navarra/Caja Navarra Foundation (7442-1941/2016).

Verónica Castañeda has been holder of a phD fellowship from the Basque Country Government (BFI-2012-97) and she has received a mobility grant from the Public University of Navarra as well as from the University of Hamburg (13/10/2014 and 20/05/2014, respectively).

A mi madre ♥

ACKNOWLEDGEMENTS

Vaya, parecía que este momento no iba a llegar nunca, pero ¡POR FÍN ESTÁ AQUÍ! Ha sido un camino duro pero que me ha aportado mucho y quiero agradecer a todos los que me habéis ayudado a caminarlo.

En primer lugar: Esther. No sabría cómo empezar a agradecerte todo tu esfuerzo, interés y, sobre todo, paciencia. Gracias por estar siempre dispuesta a ayudarme y a tus muy trabajadas revisiones, por tu buen humor, tu generosidad y comprensión, ha sido un placer conocerte. ¡No habría imaginado una mejor directora!

También quiero agradecer, y mucho, a Gustavo...como siempre, ¡otra tesis que no habría sido lo mismo sin tu ayuda y consejos! Gracias por tu disponibilidad, tu sonrisa mañanera y por tener el capilar siempre listo. A Berta, no sólo me has ayudado mucho con el dichoso SPSS, sino que siempre me has escuchado, el departamento es mucho mejor con personas como tú y te deseo lo mejor!

A mis compañeros de departamento y labo, de alegrías, penas y falta de reactivos Andrés, Carla, Olaya, Iván... A Maribel: gracias preciosa por escucharme y por toda tu ayuda! Gracias por las comidas vegetarianas en buena compañía y por tu honestidad ¡espero que sigamos compartiendo muchos momentos y que te vaya todo tan bien como te mereces! Janix, aunque ya no estás por aquí sé que cotillearás mi tesis para ayudarte a dormir así que que sepas que te agradezco de todo corazón toda tu ayuda y alegría. Has sido un apoyo fundamental para mí y me alegro de llevarme una tan buena amiga. Gracias Libe por tus ideas y sugerencias, ¡ese coco tuyo está desaprovechado! Gracias a los integrantes del departamento, todos tenéis un papel en todas las tesis y trabajos que presentamos: Ana, Morán, Esti, Iker, César, Mercedes, Pedro...gracias por vuestra ayuda!.

Marloncio, ¡¿cómo me voy a olvidar de ti?! Gracias por todo el tiempo que pasamos juntos, aprendí mucho de ti y cada día me sorprendían más tus ganas de aprender y todo tu potencial. Seguro que te irá genial, un besazo enorme y aquí tienes una amiga para lo que necesites! Gracias también a Saray, disfruté mucho con tu TFG y conociéndote, gracias por contagiarme tu amor por la ciencia y tu entusiasmo! A Paola, que no estuviste todo lo que me hubiera gustado, pero aun así me lo pasé genial contigo, gracias por esos momentos y por tu alegría.

I want to thank you Stefanie for greeting me with so much kindness, your help and for everything I have learnt with you. Next time you are in Pamplona with your husband I am inviting you to a

meal by the Arga (I know, not the same). Thank you too, root provider for the roots and the laughs, and thank you Luis for the *negros mañaneros*, your dark humor, your weird music blasting in the lab and for making my stay so much nicer and friendly ☺. Thank you, Colin for welcoming me so kindly into your lab. I am very grateful for your warmth and help the six weeks I spent in London. Thank you, Rosa and Ángel for your time and help as well. Tack Åke, du är inte längre här, men jag kommer alltid att vara tacksam för dig för att trott på mig och för att lära mig så mycket. Inte bara vetenskapen förlorade en stor man med dig. <3. Thank you Samuel and Ele, for making my stay in Stockholm much more than what it was, I am grateful to still have you as friends in my life and just wish the very best to both of you.

Gracias Txus por ser mi mentor. Gracias a ti puedo estar escribiendo esto, y siempre te estaré agradecida por tu ayuda, por relegarme experimentos apenas a regañadientes, contagiarme tus ganas de hacer bien las cosas y por todo tu apoyo todo este tiempo. Gracias por supuesto a vosotros, Félix y Alicia, por acogerme en vuestro laboratorio y confiar en mí, por vuestra cercanía y honestidad, por vuestra inspiración y entusiasmo. Gracias por contar conmigo y por todo lo que me habéis ayudado a crecer.

Davicín, gracias por compartir tus penas y aventuras conmigo, hemos andado mucho juntos y tu apoyo y ejemplo han sido muy importantes para mí. Gracias por ser un amigo de verdad. Espero que sigamos compartiendo muchos vientos pantaneros por mucho tiempo! Gracias también a mis compañeros de nutrición, kite y violín por ayudarme a crecer y a disfrutar de la vida como debe ser! Jessi, gracias por tu amistad y apoyo, has tenido mucho más que ver en esto de lo que te imaginas. A mis tonticas, no os imagináis lo mucho que significa vuestra amistad para mí y que siempre estéis ahí, vuestra alegría y comprensión, sois las mejores <3. A Ainhoa, Alicia, Ana, Edurne, Mariola, Miren, Paula y Rosario, no meras compañeras de trabajo sino amigas. Gracias por escucharme, hacerme reír y por vuestra amistad. Os quiero mucho. Y a Alfredo, por ayudarme a conciliar cuando he necesitado y por los caducados. Gracias también Lucas por la portada (me encanta!) y por mucho más.

Gracias a mi familia madrileña, que, aunque parezca que lejos estáis más cerca de lo que creéis. A mi abuela, que, aunque ya no estás con nosotros siempre te tengo presente. Gracias por tu cariño y alegría, los siento cada día. A mi tía, por tu cariño y dejarme rebañar el cuenco de los pasteles ☺. A mi tío, gracias por ser un ejemplo que seguir de esfuerzo (y cabezonería :D), gracias por tu apoyo todo este tiempo y por tu preocupación. A mi cuñadín y hermanito, gracias por tu apoyo, por todos los momentos de desconexión y por transmitir tanta paz entre la tempestad. Gracias también por poner de tu parte en darme tres sobris perfectos. Gracias Arán por heredar

de tu tía su amor por las plantas (te paso el testigo) y por hacernos la vida más alegre desde que tú estás, y a Dune e Izei por ampliar mi corazoncito a doble.

A mi hermanita, por tu humor sarcástico que siempre me saca una sonrisa, tu preocupación y por apoyarme en todos los momentos duros que he tenido a pesar de la distancia y la falta de tiempo. No hay una hermana mejor. A mis padres...bueno, qué decir, no sería nada sin vosotros ni sin vuestro apoyo. Gracias por escucharme y ayudarme, siempre al pie del cañón. Gracias por comprenderme y hacer todo lo imposible por mi felicidad, y por ser un ejemplo de lo que quiero llegar ser. Os quiero muchísimo a todos.

A mi Kiwi, por tu felicidad permanente, por ser una bolita preciosa que quita el estrés y todas las tristezas, qué haría sin ti y tu aliento. Te quiero mi chiquitina.

A ti, cariño. Gracias por convertir mi paso fugaz por Pamplona en la mejor decisión de mi vida. Gracias por escucharme y apoyarme siempre, por ayudarme a levantar y a aprender de lo bueno y lo malo. Gracias por tus tablas dinámicas y por hacerme más feliz que nunca. Me queda mucho por recorrer, pero sé que esos días que me fallen las fuerzas estarás ahí para dármelas. Te quiero, ahora y siempre. Gracias.

Todas las experiencias que he pasado estos años, buenas y malas, me han enseñado mucho y me han hecho crecer como persona, así que a todos los que han tomado parte en unas u otras: gracias.

ABBREVIATIONS

ABA	Abscisic acid
AAT	Aspartate aminotransferase
acid/AlkINV	Acid/Alkaline invertase
AGPase	ADP-glucose pyrophosphorylase
AlaAT	Alanine aminotransferase
ANOVA	Analysis of variance
AlternatP	Alternative pathway
ASC	Reduced ascorbate
BCAA	Branched-chain amino acids
C	Control
CE	Capillary electrophoresis
CytocP	Cytochrome pathway
DHA	Dehydroascorbate
DTT	1,4-dithiothreitol
DW	Dry weight
EDTA	Ethylenediaminetetraacetic acid
ETC	Electron transport chain
FBPase	Fructose-1,6-bisphosphatase
FC	Fold change
FibR	Fibrous root
FW	Fresh weight
GABA	Gamma-aminobutyric acid
GAPDH	Glyceraldehyde-3-phosphate dehydrogenase
GDH	Glutamate dehydrogenase
GOGAT	Glutamine oxoglutarate aminotransferase/glutamate synthase
G3P	Glycerol-3-phosphate
G6PDH	Glucose-6-phosphate dehydrogenase
GPDH	Glycerol-3-phosphate dehydrogenase
g_s	Stomatal conductance
GS	Glutamine synthase
GSH	Reduced glutathione
GSSG	Oxidized glutathione
hGSH	Reduced homoglutathione

hGSSG	Oxidized homoglutathione
HK	Hexokinase
IDH	Isocitrate dehydrogenase
INV	Invertase
α-KG	α-Ketoglutarate
α-KGDH	α-Ketoglutarate dehydrogenase
MD	Moderate water deficit
MDH	Malate dehydrogenase
ME	Malic enzyme
No-W	No watering
OAT	Ornithine aminotransferase
OPP	Oxidative pentose phosphate
PCA	Principal component analysis
P5C	Δ^1-1-pyrroline-5-carboxylate
P5CS	Δ^1-1-pyrroline-5-carboxylate synthase
PDC	Pyruvate decarboxylase
PEG	Polyethylene glycol
PK	Pyruvate kinase
PMSF	Phenylmethylsulfonyl fluoride
PPFD	Photosynthetic photon flux density
PVPP	Polyvinylpolypyrrolidone
ProDH	Proline dehydrogenase
ROS	Reactive oxygen species
residualR	Residual respiration
RT	Room temperature
SD	Severe water deficit
SE	Sieve element; Standard error
SuSy	Sucrose synthase
tapR	Taproot
TCA	Trichloroacetic acid; Tricarboxylic acid
totalR	Total respiration
UGPase	UDP-glucose pyrophosphorylase
WC	Water content
Ψ_{leaf}	Leaf water potential

RESUMEN

Medicago truncatula es una planta forrajera anual con gran interés agronómico y científico, siendo de hecho empleada como planta modelo en el estudio de la biología de las leguminosas. Teniendo en cuenta el contexto actual del cambio climático, es de vital importancia mantener o aumentar el rendimiento de los cultivos para así poder responder a los requerimientos derivados del constante aumento de la población mundial. Para ello, es imprescindible entender las respuestas adaptativas de las plantas al estrés hídrico, siendo muy útil el empleo de esta planta modelo para su estudio. En este trabajo hemos estudiado el comportamiento de varios órganos vegetales con especial énfasis en el sistema radical, permitiéndonos un conocimiento más integrado de los mecanismos de respuesta al estrés hídrico a nivel de planta entera.

El sistema radical de *M. truncatula* fue estudiado en el **Capítulo 1**, en el cual hicimos una distinción entre la raíz primaria, más gruesa, y las raíces laterales o "raíz fibrosa", mucho más finas. Se estudió entonces el comportamiento de ambos tipos de raíz en condiciones control, remarcando la gran diferencia metabólica entre ambas, teniendo la raíz primaria un papel más activo que como mero almacén de reservas. Además, se observó una mayor resiliencia de la raíz primaria al estrés hídrico, pudiendo tener la modulación de la degradación de la sacarosa y del metabolismo de la prolina un papel esencial en la adaptación del sistema radical al estrés hídrico.

En el **Capítulo 2** hemos abordado diversos tipos de estrés hídrico, empleando para ello condiciones iso-osmóticas de salinidad (NaCl y KCl), falta de riego y un agente osmótico (PEG-6000). Esta comparativa nos permite identificar las semejanzas y diferencias en los mecanismos de respuesta a cada estrés a nivel de planta entera. Por un lado, los resultados obtenidos nos llevaron a descartar el uso de PEG como un compuesto apto para semejar condiciones de sequía, mientras que la exposición de *M. truncatula* a NaCl y KCl provocó respuestas similares, con un ligero mayor efecto negativo en el metabolismo por parte de este último. Al comparar la respuesta a la falta de riego se observó un mayor énfasis en la protección del sistema radical, mientras que la exposición a NaCl conllevó una mayor respuesta a nivel de parte aérea. El estudio del floema nos permitió una mejor comprensión de las respuestas sistémicas de la planta a los diversos tipos de estrés hídrico.

En resumen, este estudio proporciona un mayor conocimiento de la respuesta de *M. truncatula* a condiciones de estrés hídrico a nivel de planta entera y desde un punto de vista bioquímico, metabólico y fisiológico.

ABSTRACT

Medicago truncatula is a forage legume with agricultural but also scientifical interest, being used as a model plant for the study of legumes' biology. Within a climate change context, it is of great importance to maintain/increase plant yield in stressful growth conditions to meet the requirements of the increasing world population. In order to achieve this, it is mandatory to further understand the adaptive response of plants to water-deficit stress, for which the use of this model plant results of great utility. In the present study, the simultaneous study of various plant organs with particular focus on the root system allows us a more integrative understanding of water-deficit response mechanisms from a whole-plant perspective.

The root tissue was studied in **Chapter 1**, distinguishing between the thick taproot and the much thinner fibrous root. The different behaviour of both root types under well-watered as well as under water-deficit conditions was studied from a physiological and metabolic perspective. This study highlighted the active role of the taproot rather than being considered a mere nutrient storage organ. The taproot showed a more resilient nature towards water-deficit stress than the fibrous root, while sucrose cleavage modulation, together with proline metabolism suggested a crucial role of these pathways in the root adaptation to water-deficit stress.

In **Chapter 2** we aimed to address different water-deficit conditions that can affect plant water status, using iso-osmotical conditions of salinity (NaCl and KCl), lack of irrigation and an osmoticum (PEG). This approach allows us to identify the similarities and differences in the mechanisms involved in the response to each stress at the whole-plant level. While PEG was dismissed as a reliable drought-stress mimicker, NaCl and KCl led to similar responses, with a slightly higher negative effect of KCl on plant metabolism. On the other hand, an emphasis on the shoot and root protection was observed for NaCl and no-irrigation stress, respectively. The study of the phloem sap allowed us to better understand the responses to the different water-deficit conditions at a whole-plant level.

In summary, this study provides further insight into the response at the whole-plant level of *M. truncatula* to water-deficit conditions from a biochemical, metabolic and physiological point of view.

TABLE OF CONTENTS

› GENERAL INTRODUCTION

A. LEGUMES – *MEDICAGO TRUNCATULA* AS A MODEL PLANT

Legumes are plants belonging to the *Fabaceae* family (or *Leguminosae*) and, with around 20,000 species, they are the third largest family of higher plants and include many crops of agronomic importance (Gepts *et al.*, 2005). Their economic value does not only derive from being the main source of vegetable protein in human and livestock diets (Tharanathan and Mahadevamma, 2003), but also from their key role in soil organic fertility and N-economy due to their ability to create symbiotic interactions with N-fixing bacteria (Stagnari *et al.*, 2017). According to the edible part and/or its use we can find grain legumes such as pea (*Pisum sativum*), soybean (*Glycine max*), lentil (*Lens culinaris*) and faba bean (*Vicia faba*) in which their unripe pods and/or their seed are consumed mostly by humans, and forage legumes such as alfalfa (*Medicago sativa*) and white clover (*Trifolium repens*), which are usually grazed by livestock or harvested as silage.

Medicago truncatula (barrel medic) is an annual forage legume native to the Mediterranean basin that is well adapted to semi-arid conditions (Lesins and Lesins, 1979). In the 1990's it was chosen as a model species for the study of legume biology due to its small (≈550 Mb for cv. Jemalong A17) diploid (2 × 8 chromosomes) genome, prolific seed production, short life cycle and its ability to self-fertilize (Young *et al.*, 2005). In addition, it is also able to create symbiotic interactions with the model microsymbiont *Sinorhizobium meliloti,* which is one of the best characterized *Rhizobium* species (Galibert *et al.*, 2001). Another key advantage of the use of *M. truncatula* cv. Jemalong is its regenerability, a quite rare characteristic amongst the annual legumes (Barker *et al.*, 1990). *M. truncatula* belongs to the *Trifoliae* tribe and is a close relative of alfalfa and clover. However, while it shares some characteristics with *Lotus japonicus*, another model legume plant, they are phylogenetically different and exhibit nodules of different characteristics. The phylogenetic distance of *Lotus japonicus* to economically important crops is critical in the choice of *M. truncatula* as model legume by many researchers (Ané *et al.*, 2008). In our studies we used the accession A17, which is a descendant line from the Jemalong cultivar, the most used in pastures and agricultural practices above all in Southern Australia (Crawford *et al.*, 1989). This accession is, in addition, the primary reference for the

development of many contemporary tools and resources for molecular, genetic, structural and functional genomic studies (Kamphuis *et al.*, 2007), making it a prime option for field and laboratory experiments (**Fig. 1**).

Figure 1. *Medicago truncatula* plants. *Left*, *M. truncatula* plant in the field. [Source: Beller, D (2020)]. ***Right***, *M. truncatula* plants growing in Petri dishes for their use in research. [Source: Oelkers *et al.* (2008)].

B. ROOT SYSTEM – THE HIDDEN HALF

Since high yield and growth are visible in the shoots, a high number of studies have focused on the analysis of the aerial part, neglecting the importance of the root tissue. However, while great progress has been done in improving plant yield through the manipulation of above-ground traits, this is not enough since more than 2,000 million people still suffer from food insecurity and more than 800 million suffer from hunger (FAO, 2019). Hence, the root tissue emerges as a potential source of improvement of plant productivity, especially in this context of rapid climate change (Khan *et al.*, 2016). Even though the shoot is important for plant growth because it provides plants with carbon compounds through photosynthesis and drives water uptake through transpiration, is the root system which ultimately determines the plant access to water, which is the most limiting factor for plant growth (Sperry *et al.*, 2002). In addition, roots are responsible for the uptake of nutrients and serve as anchorage, even though they have many other functions such as storage or synthesis of various hormones (Fitter, 2002).

It should be taken into account that the root system is actually comprised of four basic classes of roots attending to their site of origin: tap (embryonic first root), lateral (branch of another root), basal (hypocotyl-borne root) and shoot-borne roots (Zobel, 2011; Zobel and Waisel, 2010). These classes are also functionally and genetically different, and thus the International Society for Root Research encourages to differentiate them in separate entities when designing experiments (Zobel and Waisel, 2010). On one hand, coarse roots such as the taproot serve as anchorage and root architecture definition and are capable of exploring deep and compacted soil layers, being sometimes used as storage of nutrients. On the contrary, lateral roots are the most responsible for water uptake, comprising most of the surface area of the root system. There are two main kinds of root systems in plants (**Fig. 2**): 1) the taproot system, typical of dicots such as arabidopsis or legumes, composed of a single primary root growing vertically exploring the soil and lateral roots emerging from it (in addition to basal/anchor roots arising from the root–shoot junction); and 2) the fibrous root system, typical of monocots such as maize or rice, which is comprised of a shorter primary root and may also include seminal and shoot-borne roots, creating a network of roots close to the soil surface.

The root system architecture describes the shape and spatial arrangement of a root system within the soil (or growth medium) and is gaining interest in regard to stress tolerance (Rogers and Benfey, 2015). In fact, several root traits have been found to increase productivity under drought, such as the number of root tips, root hair density, aquaporin activity, the diameter of the fine roots, root depth and plant allometry (metrics of root-to-shoot relationships). Since water is stored in deeper soil layers and the topsoil dries more quickly, plants with deeper root systems such as those with a taproot system are usually more drought tolerant (Koevoets *et al.*, 2016). For a more in-depth perspective, please refer to previous reviews in this topic (Comas *et al.*, 2013; Meister *et al.*, 2014; Vadez, 2014). Hence, a better understanding of the different root types` function and physiology could be crucial for the development and selection of more stress-resistant varieties, thereby maintaining yield and ensuring global food security.

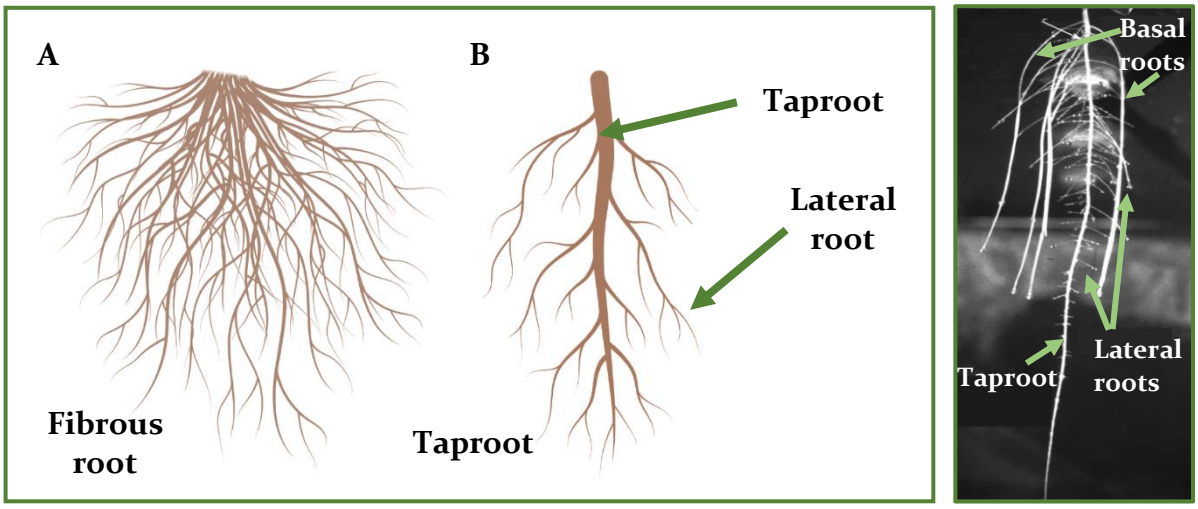

Figure 2. The root system. ***Left***, a fibrous root system typical of grasses (**A**) and a taproot system (**B**). [Created with BioRender.com]. ***Right***, a soybean seedling grown in aeroponics displaying three classes of roots. [Adapted from Zobel and Waisel (2010)].

C. PHLOEM TRANSPORT – HIGHWAY TO ROOTS

The physical communication between plant organs is of utmost importance not only for allowing the mobilization of nutrients and water from sources to sinks but also of hormones and signaling molecules. This is achieved by the xylem and phloem, which are the tissues that link the root and shoot and, thus, become fast lanes for plant communication, allowing the proper development of the plant and its optimal response to endogenous and exogenous factors.

Phloem's main (but not only) role is the translocation of photosynthesis products (mainly sucrose) from mature leaves to growing and heterotrophic tissues such as roots (**Fig. 3**) and is comprised of water and water-soluble molecules above all carbohydrates, but also amino acids, hormones, RNAs, proteins, inorganic ions and some secondary compounds related to defense (Turnbull and López-Cobollo, 2013). The cells that conform the phloem conducts are called sieve elements (SE), while the companion cells have a role in the transport of photosynthetic products from the source cells to the SE and in the aid at some critical metabolic functions such as protein synthesis. SE are living cells without nucleus, and even though they lack some subcellular elements they differ from the dead tracheary elements of the xylem.

The phloem sap is transported from supply areas such as mature leaves (sources) to growing and storage areas such as heterotrophic organs (sinks), even though the specific transport pathways are very complex (**Fig. 4**). This flow is driven by the source and sink strengths, the latter being defined as the competitive ability of a sink organ to import assimilates, depending on both its physical (size) and physiological (activity) capabilities (Bihmidine *et al.*, 2013). Assimilates move into the phloem through a symplastic (cytoplasmic) pathway or are first exported to the apoplast (i.e., cell wall space) surrounding the phloem and then are imported into the phloem companion cells and/or SE using energy-driven transport (Lalonde *et al.*, 2003). Unloading of sucrose into sink organs can occur either symplastically (via plasmodesmata) or apoplastically, depending on the species, organ or tissue. In the apoplastic route, sucrose is cleaved by acid invertase (acidINV) into glucose and fructose, which are then taken up by the sink cell by hexose transporters. Alternatively, apoplastic sucrose can be taken up by specific sucrose transporters or by a sucrose-induced endocytic process, being then metabolized by sucrose synthase (SuSy) and/or alkaline/neutral invertase (AlkINV) (Bahaji *et al.*, 2014, Hennion *et al.*, 2019). On the other hand, phloem unloading of amino acids is more straightforward, usually involving a symplastic route and amino acid transporters (Yang *et al.*, 2020).

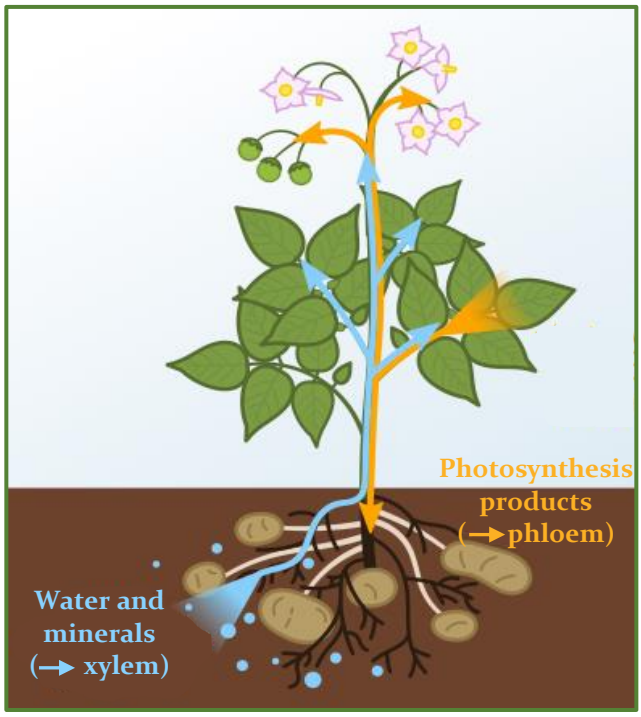

Figure 3. Nutrient transport in plants. Diagram of the phloem transport of photoassimilates from mature leaves to heterotrophic tissues, and of water and minerals from the roots to the rest of the plant through the xylem. [Adapted from Nefronus (2020)].

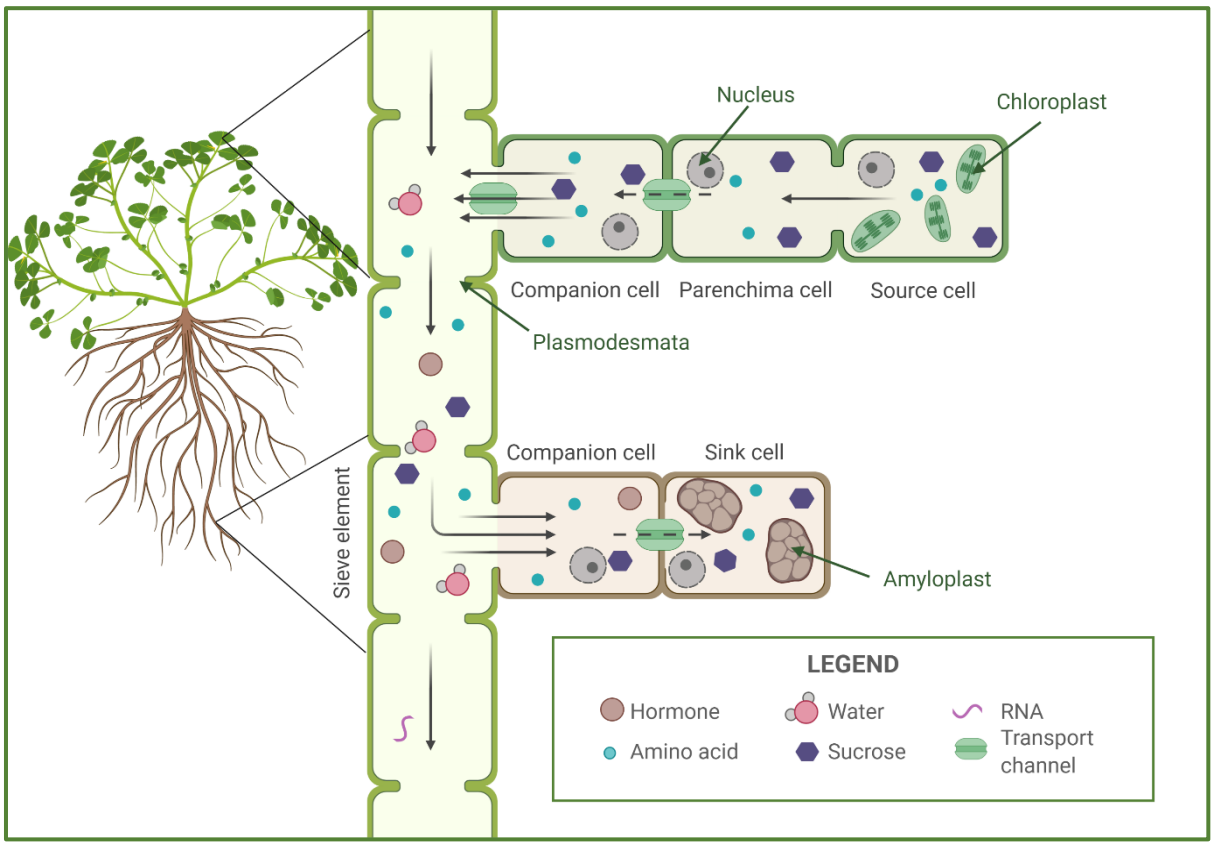

Figure 4. Phloem loading and unloading of metabolites. Diagram of the mass flow in the phloem, depicting the flow of sugars from source leaves to roots. Sugars are "loaded" into the sieve elements from the source cells (usually mature leaves), which sequesters water from the xylem due to osmosis, and are unloaded in sink cells (such as roots), allowing water to return to the xylem (Taiz and Zeiger, 2010). In the symplastic route sugars move from source cells to sieve elements via plasmodesmata. However, in the apoplastic route sugars move from the source cell to the apoplast and are actively transported into the companion cells via transporters, then moving to sieve elements via transporter proteins and plasmodesmata. [Created with BioRender.com].

D. SHOOTS AND ROOTS – THE FIGHT FOR THE PHOTOASSIMILATES

As mentioned before, while shoots are essentially involved in photosynthesis, the roots' main role is the water and nutrient uptake from the soil (see **section B**). Sucrose is synthesized in leaves, travels through the phloem sap and reaches sink organs such as roots and developing leaves, where it is broken down as described in the above sections. On the contrary, nitrogen compounds can be synthesized in the roots and be sent to the shoots for further use (Taiz and Zeiger, 2010). In addition, there are many secondary metabolite-synthesis routes that are tissue specific, highlighting the different nature of

shoots and roots. Hence, while shoots are considered organic carbon source organs, roots are inorganic nutrient sources (Bais *et al.*, 2001). These different roles in plant physiology may imply that shoots and roots compete for the resources that the plant acquires. Indeed, plants continuously adapt to the resource availability by differentially allocating the available resources to shoots and roots in order to optimize their use. Hence these tissues commonly show opposing behaviors, especially under stressful conditions (Chang *et al.*, 2017). Carbohydrate partitioning involves the processes of assimilating, transporting and distributing sugars from sources to sinks, being fundamental for plant growth and development and even for plant tolerance to biotic and abiotic stresses (Gargallo-Garriga *et al.*, 2014). Thus, understanding plant shoots and roots` response to water-deficit stress, including metabolite partitioning between them, is essential to allow research directed to increasing crop yield under these conditions (Julius *et al.*, 2017).

Under changing environmental conditions, plants can respond by altering tissue-specific metabolic activities, as well as by adjusting the resource allocation patterns depending on their availability in order to optimize their use (Julius *et al.*, 2017). For example, under low-light high-water conditions plants preferentially reallocate their resources to the shoots in order to increase light absorption (Cruz, 1997), while the opposite is usually observed under high-light low-water conditions to increase water absorption capacity of the roots (Gargallo-Garriga *et al.*, 2014). Plants, however, not only alter their biomass allocation but also change their metabolic activities as well as antioxidant and other metabolites' profile or abundance in response to stress (Ågren and Franklin, 2003). Indeed, several authors have reported different or even opposite behaviors of shoots and roots to various plant stresses including salinity (Sobhanian *et al.*, 2010) and drought (Gargallo-Garriga *et al.*, 2014). For example, Gargallo-Garriga *et al.* (2014) observed that both organs have different sets of metabolomes and nutrient and elemental stoichiometries, with the shoot metabolome being much more variable among species and seasons than the root metabolome in *Alopecurus pratensis* and *Holcus lanatus.* In salt-stressed cowpea plants, Cavalcanti *et al.* (2007) observed distinct response mechanisms regarding lipid peroxidation and catalase and superoxide dismutase activities, while wild and cultivated barley showed different sets of metabolites involved in salt-tolerance enhancement in both tissues (Wu *et al.*, 2013).

E. WATER-DEFICIT STRESS

E.1. Drought impacts on plant physiology

It has been estimated that two-thirds of the potential yield of major crops are usually lost due to adverse growing environments (Wu *et al.*, 2013). Abiotic stresses, above all soil water deficit, are the most important factors limiting crop productivity, with a growing importance due to the increase in climate alterations such as reduced rainfall (Bajaj *et al.*, 1999; Daryanto *et al.*, 2016). Indeed, most climate change studies predict an increase in arid areas worldwide due to the increased frequency (22% to 123%), intensity, spatial extend (between 23% and 46%) and length of droughts (Lesk *et al.*, 2016; Seager *et al.*, 2007). This is aggravated by the rapidly increasing world population, which puts pressure in food and water demands (Grillakis, 2019). This not only makes the limiting nature of water supplies more apparent, but also leads to an improper management of agricultural lands. For example, most crops are cultivated in lands and regions to which they are not optimally adapted, yielding up to only 22% of their genetic potential due to improper climatic and soil conditions (Somerville and Briscoe, 2001). Therefore, the understanding of plant drought stress tolerance has become an urgent matter, since it can allow us a better management of crops under stress and to minimize its harmful effects. Indeed, the integration of breeding and biotechnological approaches can lead to the development of drought-resistant plants (Boyer, 1982).

Drought is defined as "the decrease in water inputs into an agro/ecosystem over time that is sufficient to result in soil water deficit (i.e., decrease in the available soil water)" (Khan *et al.*, 2016). This stress interferes with the optimal plant growth, physiology and reproduction, ultimately causing a significant reduction in plant productivity and even death (**Fig. 5**). Water deficit in the soil causes *primary effects* such as reduced water potential, cellular dehydration or increased hydraulic resistance, directly altering the optimal functioning of cells and leading to *secondary effects* [e.g., stomatal closure, ion cytotoxicity, reduced cellular and metabolic activities, reactive oxygen species (ROS) production, altered carbon partitioning and photosynthetic inhibition] (Farooq *et al.*, 2009). These negative factors damage cells and can ultimately lead to their death. In order to cope with adverse conditions and avoid these negative impacts, plants have

evolved two major kinds of drought resistance mechanisms: drought-stress avoidance and tolerance. Stress avoidance includes inherited mechanisms that delay or prevent the negative impact of a stress in the plant such as the modified stems and leaves (needles) in cacti or the exploration of deeper soils and is characterized by the maintenance of high plant water potentials under water shortage conditions. On the other hand, plant tolerance is the ability of a plant to grow and acclimate to adverse conditions. Plant acclimation is plastic and reverted once the stressor disappears, and some examples could be the accumulation of various osmoprotectants, the onset of antioxidant systems or the regulation of stomatal conductivity under water stress (Taiz and Zeiger, 2010). Additional drought-stress resistance mechanisms are drought escape and drought recovery, which will not be discussed here.

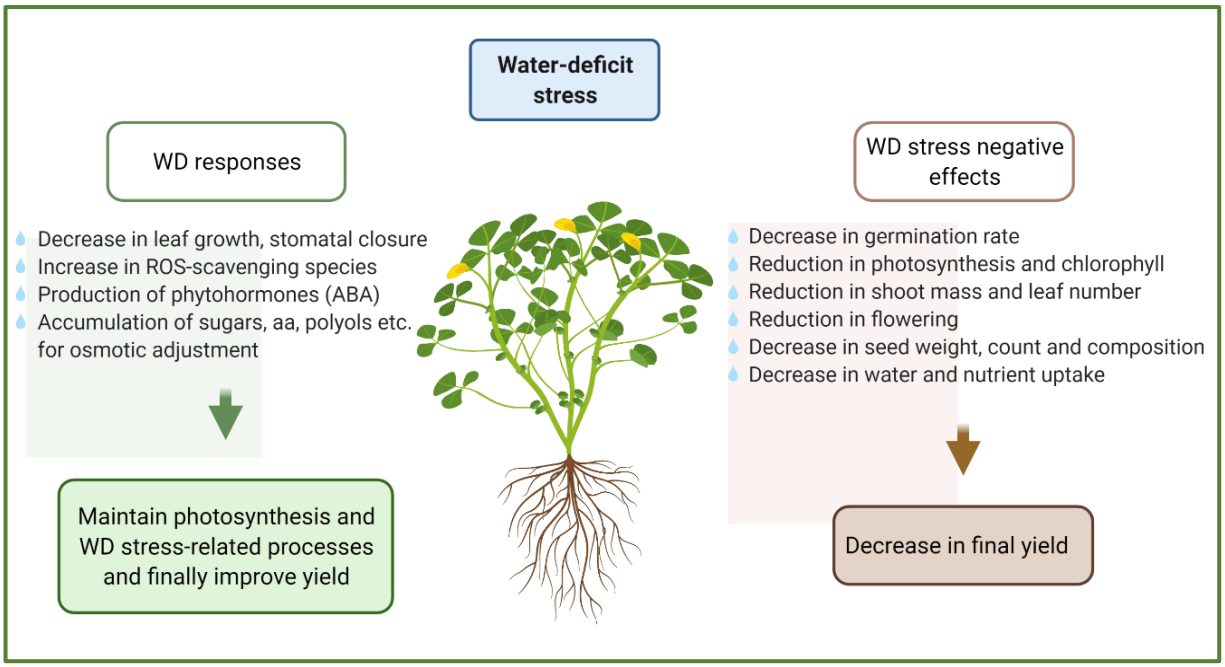

Figure 5. Effects of water-deficit on plants and their response. *aa*, amino acids; *ABA*, abscisic acid; *ROS*, reactive oxygen species; *WD*, water deficit. [Adapted with BioRender.com from Nadeem *et al.* (2019a)].

E.2. Salinity and drought stress

Water deficit not only occurs under drought conditions, but also under freezing and high-salinity conditions, due to the lower availability of free water in these circumstances (Aroca *et al.*, 2012). Regarding drought, it is estimated that 45% of the agricultural lands are subjected to continuous or frequent episodes of water scarcity (Butcher *et al.*, 2016). In addition to the inherent negative effects of drought, the reduced rainfall or irrigation accentuates the accumulation of soluble salts in the soil, both directly due to the reduced available water to leach ions and indirectly by increasing the need of artificial irrigation, which often leads to secondary salinization of land and water resources. The percentage of salinity-affected soils varies depending on the consulted source, but the Food and Agriculture Organization of the United Nations' (FAO) 2011 assessment showed that around 34 Mha of soil worldwide (11% of the irrigated land) could be affected (FAO, 2011). This problem is of special relevance in the Mediterranean countries, where it is one of the major causes of desertification. Soil salinity is increasing due to the scarcity of precipitation, low-quality water irrigation and seawater infiltration into the groundwater layer due to poor irrigation techniques. Thus, 25% of the Mediterranean croplands are affected by salinity, while 3% of Spain's irrigated land is severely affected and another 15% at serious risk of salinization (Stolte *et al.*, 2016).

Low water availability through irrigation as well as salinity exert osmotic stress (i.e., situations where insufficient water availability limits plant growth and development), the latter due to the increase in the solute concentration of the soil or growing medium. Thus, both stresses share many common reactions in plants due to their osmotic dehydrating nature (which causes the removal of water from the cytoplasm to the extracellular space) such as the increased production of ROS, stomatal closure and increased synthesis of osmolytes (Munns, 2011; Zhu *et al.*, 1997). However, salinity-induced osmotic stress differs from that exerted by drought by the later onset of ion toxicity as a result of the ionic component of salinity stress.

During the initial phases of salinity stress, the osmotic component of salinity leads to responses also present under drought stress conditions such as cell membrane alter-

ation or decreased photosynthesis rates and stomatal conductance (Munns, 2011). However, as Na^+ and Cl^- ions start to accumulate in the older transpiring leaves, senescence processes are activated, thus reducing the amount of assimilates available for growth and new leaves formation. This phase, related to ion toxicity, is the one that separates genotypes that differ in their salt tolerance (Munns and Tester, 2008). Thus, while plant growth is limited by osmotic stress, salt-sensitive species that have a high rate of salt uptake (do not minimize its entry through the roots) or are not able to effectively compartmentalize salt in the vacuoles develop salt-specific effects that further affect plant growth and metabolism (Munns, 2002). Since many salts are also plant nutrients and compete for their uptake and transportation with others, as will be discussed in s**ection E.3.6**, the increased salt levels in the soil can disrupt nutrient balance and/or nutrient uptake. Indeed, one of the most important consequences for plant health is the inhibition of K^+ uptake, which can result in lower productivity or even death (Munns, 2011).

Thus, both drought and soil salinity are the major causes of crop productivity reduction. Sustainable agriculture requires that plants growing in the increasing arid and semi-arid regions do so with less input of fresh water, a decreasing precious resource as a consequence of the climate change and growing population pressure. The development of drought-resistant plants could allow their growth in arid and semi-arid regions without depending, or at least not so much, on artificial irrigation. Additionally, salt-tolerant plants could additionally allow irrigation with poor-quality water, which could further save valuable good-quality fresh water for human consumption and other uses (Schroeder *et al.*, 1994). In order to better understand and improve water-deficit stress tolerance in these regions it is very important to study the physiological and biochemical responses to this stress in genetically-tractable model plants such as *M. truncatula*, which offers the additional benefit of being a species native of semi-arid regions, and applying them to an efficient crop production (Fita *et al.*, 2015). In the next section we will discuss the plant responses to water-deficit stress in detail.

E.3. Plant water-deficit stress responses

The plant response to abiotic stress occurs at all levels of organization. At the molecular level, stress conditions exert changes in gene expression, above all in those genes involved in the protection against stress such as detoxifying enzymes, as well as in those encoding regulatory proteins such as transcription factors. At the cellular level, water and salinity stress lead to adjustments in the membrane system, modification of the cell wall as well as changes in the cell cycle, while changes in plant metabolism can also involve protective mechanisms such as the increased production of compatible solutes and the activation of the redox metabolism (Shao *et al.*, 2009). The alteration of key physiological processes like photosynthesis, respiration, water relations and antioxidant and hormone metabolism helps plants cope with limiting environmental conditions (Krasensky and Jonak, 2012), and the understanding of all these processes and their importance under abiotic stress may contribute to the development of plants resistant to water deficit.

E.3.1. Growth and water relations

One of the most readily affected processes by water-deficit stress is growth, particularly the shoot's (**Fig. 6**). This reduces the needs of this tissue for metabolites, energy and reducing power, which can be redirected to other processes such as the synthesis of protective compounds related to osmotic adjustment (Bhargava and Sawant, 2012). This growth inhibition is primarily driven by the lack of cell turgor in the growing cells derived from the lack of available water. Conversely, the reduced water availability is due to the poor hydraulic conductance from roots to leaves derived from the closure of stomata as a fast response to the decreased leaf turgor and chemical signals generated in roots, such as increased abscisic acid (ABA) (Bhargava and Sawant, 2012). The reduction of stomatal conductance (stomatal opening) is an adaptive mechanism to water-deficit stress in order to avoid water loss through transpiration and is governed mostly, but not only, by ABA (Bhargava and Sawant, 2012). Even though growth arrest usually happens in roots also, it is to a lower extent or occurs later than that of shoots`possibly thanks to the faster osmoprotectant accumulation in this tissue, being considered an adaptation to water-deficit stress rather than a physiological constraint (Daszkowska-Golec and

Szarejko, 2013; Pandey and Shukla, 2015). Indeed, the increase in the root-to-shoot ratio has been extensively reported in plants subjected to drought stress, allowing a better water uptake and growth towards deeper soil layers with higher humidity levels (Comas *et al.*, 2013).

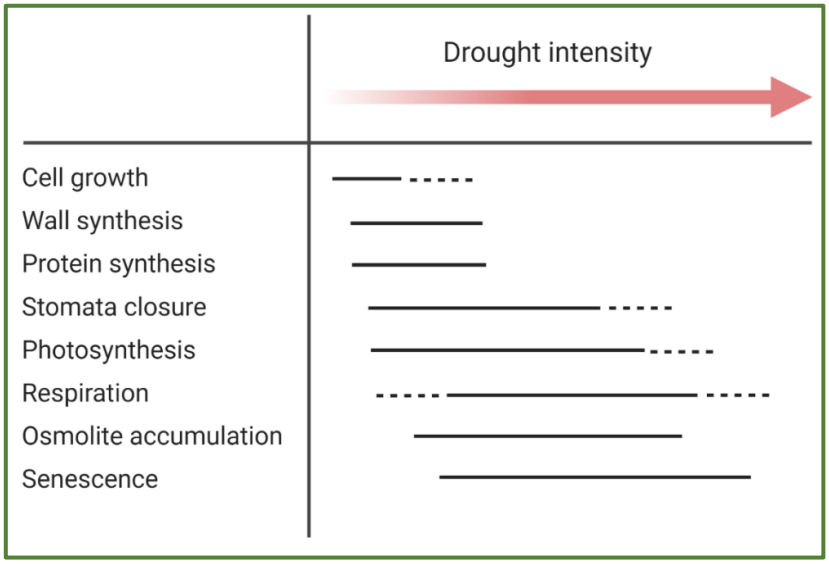

Figure 6. Metabolic processes affected by different levels of drought stress. While cell growth is the most sensitive process to drought stress, others such as osmolyte accumulation are activated at higher drought intensities. [Adapted with BioRender.com from Taiz and Zeiger (2010)].

Water potential governs the transport of water across cell membranes and is very commonly used to assess the water status of a plant, since it depends on the relative fluxes of water through the plant (Parihar *et al.*, 2015; Taiz and Zeiger, 2010). When the soil water potential decreases moderately due to water deficit (such as that caused by drought or salinity), plants can adjust osmotically (as explained in **section E.3.4**) and achieve a lower water potential than that of the soil, thus maintaining a potential gradient that allows the influx of water into the plant. However, when the soil reaches very low water potentials, the plant cannot keep up this adaptive mechanism and loses its ability to extract water from the soil, which can lead to plant death (Parihar *et al.*, 2015; Taiz and Zeiger, 2010). This parameter, together with tissue water content, transpiration rate and stomatal conductance are important attributes describing plant water relations (Parihar *et al.*, 2015), and all are usually negatively affected by water-deficit stress, with important effects on the plant's physiology and metabolism (Farooq *et al.*, 2009).

E.3.2. Alteration of electron transport processes

Photosynthesis and respiration are the two main carbon and energy metabolism pathways in plants, and while the first one uses light, CO_2 and H_2O in order to synthesize carbohydrates, the second uses them to support plant growth and maintenance by providing carbon intermediates, reducing equivalents and ATP (Taiz and Zeiger, 2010). However, both processes are affected by water-deficit stress, with major impacts on plant metabolism.

Photosynthesis

Photosynthesis is a process in which plants use light energy to convert atmospheric carbon into carbohydrates. The photosynthetic electron transport is the first stage of photosynthesis and is responsible for the production of ATP and NADPH (light reactions), which will be used later for the synthesis of carbohydrates in the Calvin-Benson cycle (dark reactions). For this first step an electron transport chain (ETC) localized in the chloroplast thylakoid membrane is used, consisting of the proteins and complexes photosystem II (PSII), the cytochrome b_6f complex, photosystem I (PSI) and the free-electron carriers plastoquinone and plastocyanin (Vanlerberghe, 2013). However, water-deficit stress not only affects the light reactions responsible for ATP and NADPH synthesis, but also the assimilation efficiency of the dark reactions, leading to an overall reduction in the production of photoassimilates (Rochaix, 2011).

As we have previously described, the stomatal closure in response to water-deficit stress is an adaptive mechanism that prevents water loss through transpiration (Fang and Xiong, 2014). However, this leads to excess light energy in the photosynthetic ETC, since the decrease in CO_2 availability inside the leaf leads to a reduction in the Calvin-Benson cycle and, thus, a reduction in energy consumption (Pandey and Shukla, 2015). This excess energy leads to an over-reduction of the ETC, with electrons being transferred to O_2 causing the generation of ROS such as superoxide (O_2^-), hydrogen peroxide (H_2O_2) and hydroxyl radicals ($^{\bullet}OH$) in a process known as photo-oxidation (Lawlor and Tezara, 2009). The over-accumulation of ROS can cause irreversible damage to the pho-

tosynthetic apparatus, which further decreases photophosphorylation and ATP generation in a negative feedback manner. Thus photosynthesis is decreased under water-deficit conditions by stomatal (low CO_2 availability) and non-stomatal limitations such as the alteration of the photosynthetic machinery (decrease in the maximum quantum efficiency of PSII, synthesis of photosynthetic pigments, regeneration of ribulose-1,5-bisphosphate and in the decrease in the activity of enzymes related to CO_2 assimilation) or the deleterious effects derived from ROS accumulation and protein aggregation (Fang and Xiong, 2014; Feller, 2016; Mahajan and Tuteja, 2005). Under salinity stress, the presence of excessive amounts of Na^+ and/or Cl^- ions in the cells has also been linked to a decrease in the net photosynthesis rate due to a decreased chlorophyll content, PSII efficiency and assimilation rate of CO_2, together with the dehydration of cellular membranes (which reduces their permeability to CO_2), salt toxicity (resulting from the replacement of K^+ by Na^+ in biochemical reactions and Na^+ and Cl^--induced conformational changes in proteins), enhanced senescence and reduced sink activity, amongst others (Rao and Chaitanya, 2016; Thapa *et al.*, 2011).

Respiration

Plant growth is determined by the ratio of CO_2 assimilated by photosynthesis and CO_2 lost in respiration (Bhargava and Sawant, 2012; Chaves *et al.*, 2009). Plant mitochondrial respiration is a process that oxidizes organic substrates in order to generate ATP needed for plant maintenance and growth. Indeed, nutrient uptake and assimilation by roots as well as sucrose synthesis and translocation of assimilates to sink issues are important processes employing ATP, while the biosynthetic processes are the most important pathways for NADH and tricarboxylic acid (TCA) cycle intermediates usage (Bhargava and Sawant, 2012). Plant respiration involves several metabolic pathways such as glycolysis, the oxidative pentose phosphate (OPP) pathway and the mitochondrial TCA cycle, which couple carbon oxidation with the generation of reducing equivalents that can either be used to support biosynthetic reactions or be regenerated by their oxidation in the mitochondrial ETC. The electrons resulting from NAD(P)H or $FADH_2$ oxidation travel through the mitochondrial ETC to a final cytochromic oxidase, which uses them to reduce O_2 to H_2O (**Fig. 7**). This electron flow is coupled to proton pumping

towards the intermembrane space, being the resulting proton-motive force used by a terminal ATPase to generate ATP (Bhargava and Sawant, 2012). In addition, several dehydrogenases in the mitochondrial matrix and intermembrane space such as glutamate (GDH), isocitrate (IDH), proline (ProDH), malate (MDH) and α-ketoglutatarate (α-KGDH) dehydrogenases can also provide electrons for the ETC, being all these pathways highly regulated according to the metabolic plant status and environmental factors (Millar *et al.*, 2011).

Usually, respiration is believed to decrease when plants are subjected to water-deficit stress (Schertl and Braun, 2014). However, an increased net respiration has also been observed under water-deficit conditions in some studies at different desiccation stages (Bhargava and Sawant, 2012). Thus, at initial stages of water-deficit stress a drop in respiration is usually observed, with the evidence pointing towards the inhibition of growth as its main cause rather than being due to a decreased availability of photoassimilates derived from the inhibition of photosynthesis (Bhargava and Sawant, 2012). However, at more advanced levels of water-deficit stress, respiration could be activated by the change in the metabolism related to the increased synthesis of compatible solutes such as proline (see **section E.3.4**). In addition, the increased respiration also helps dissipate the excessive reducing equivalents (NADPH) generated by the limitation of CO_2 fixation (Flexas *et al.*, 2005). Thus, plant respiration can be regarded as a means to cope with the metabolic dysregulation that occurs under water-deficit stress.

Additionally, the plant mitochondrial ETC has another terminal oxidase called alternative oxidase (AOX), which introduces a branch in the ETC making the electrons divert between both pathways, stabilizing the ubiquinone reduction level and preventing the production of excessive ROS (**Fig. 7**). However, the AOX pathway bypasses most proton-pumping sites, hence yielding much less ATP (Bhargava and Sawant, 2012; Flexas *et al.*, 2005). Even though this pathway leads to a waste of energy it is useful under certain circumstances such as floral development in certain plants (volatilization of pollinator-attracting compounds) and, most notably, under biotic and abiotic stresses (Vanlerberghe, 2013). Thus, the potential negative effects of AOX in reducing ATP and reductant availability for growth is compensated by the increased metabolic flexibility

that allows the maintenance of respiration in light, improving chloroplast energy balance and photosynthesis (Vanlerberghe, 2013). Accordingly, several studies indicate that AOX respiration is of higher relevance under abiotic stresses such as temperature, drought, nutrient limitation, salt stress, hypoxia or metal toxicity (Vanlerberghe *et al.*, 2016, 2020). Is actually the stress-induced ROS accumulation one of the signals for the activation of the AOX expression, whose activity prevents the over-reduction of the ETC and the generation of destructive ROS such as hydroxyl radicals (**Fig. 7**). Thus, in addition to the AOX's role in maintaining metabolic homeostasis, it also has a role in maintaining signaling homeostasis when reactive oxygen and nitrogen species are regarded as signaling molecules. Moreover, AOX can also contribute to stress tolerance through the oxidation of "excess" reducing power that is not used in the Calvin cycle, contributing to NAD(P)$^+$ recycling (del Saz *et al.*, 2016; Vanlerberghe, 2013).

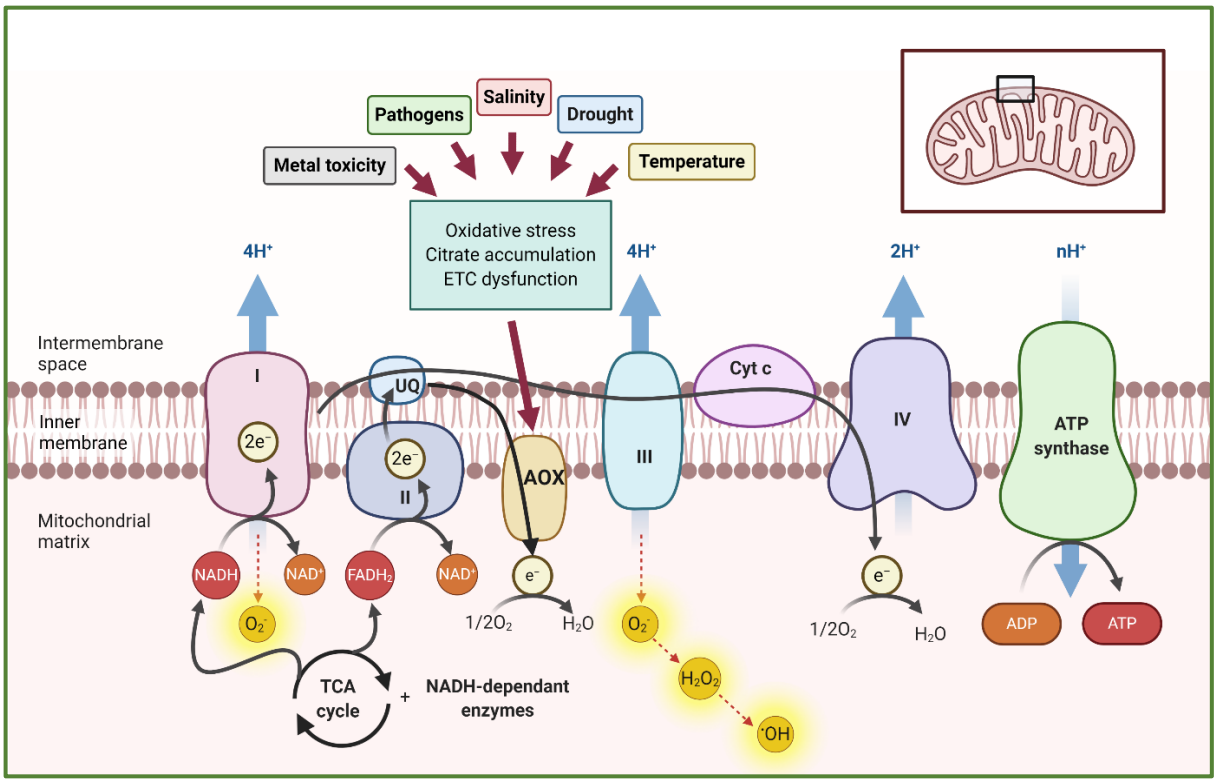

Figure 7. Regulation of alternative oxidase's expression and activity. Several stresses such as drought, salinity or metal toxicity lead to an increase in reactive oxygen and nitrogen species as well as citrate levels which, together with the dysfunction of the mitochondrial ETC complexes, lead to an induction of the expression of AOX. The increased activity of AOX diverts electrons bypassing complexes III and IV of the cytochrome pathway, reducing ATP generation and thus helping maintain the metabolic homeostasis and signaling dynamics in mitochondria. The reducing power that feeds

the ETC comes from diverse sources such as the TCA cycle and several enzymatic reactions. *AOX*, alternative oxidase; *cyt*, cytochrome; *ETC*, electron transport chain; *I-IV*, complexes I-IV; *TCA*, tricarboxylic acid; *UQ*, ubiquinone. [Created with BioRender.com, inspired by Saha *et al.* (2016)].

E.3.3. Alteration in the carbon metabolism

The rapid inhibition of plant growth, especially in the shoots, as well as the reduction in photosynthesis in response to water-deficit stress lead to an important alteration in carbon partitioning between source and sink tissues. Thus, carbohydrates usually employed in growth become now available for selective growth of roots or the synthesis of compounds related to stress tolerance such as antioxidants or solutes for osmotic adjustment (Bhargava and Sawant, 2012).

The study of carbon metabolism is quite complex due to the multigenic nature of the enzymes involved and their varying role depending on the tissue and developmental stage of the plant (Bhargava and Sawant, 2012). During the day, sucrose phosphate synthase (SPS) catalyzes the synthesis of sucrose in autotrophic tissues (leaves) (**Fig. 8**) to be sent to the heterotrophic sink tissues (roots) through the vascular tissue (phloem), and is this source-to-sink communication what modulates carbon partitioning between these tissues. On the other hand, glucose and fructose are formed in the first steps of glycolysis through two enzymatic reactions, both taking part in the unloading of sucrose from the phloem. Invertase (INV) irreversibly splits sucrose into fructose and glucose, while SuSy generates fructose and UDP-glucose using sucrose and UDP as substrates (**Fig. 8**). Even though SuSy can use other nucleotides such as ADP, UDP is the preferred one (Stein and Granot, 2019). In most cases, INV seems to play regulatory roles in plant growth and development, while SuSy is mainly involved in biosynthetic processes (including starch and cellulose synthesis) as well as in the generation of energy in the form of ATP (Stitt, 2013). In addition, hexose signaling regulates plant growth and development, with high concentration of these molecules inhibiting growth and vice versa (Singh *et al.*, 2015).

Starch is synthesized during the day from excess sucrose in the leaf chloroplasts and is mobilized at night in order to guarantee a supply of carbon and energy when photosynthesis is not working. However, it can also be stored long term or serve other functions such as aiding in the origination of organic acids and sugars in the guard cells bordering the stomatal pores, which increases cell turgor and allows stomatal opening (Braun *et al.*, 2014; Thalmann and Santelia, 2017). Starch synthesis, degradation and translocation of its precursors require the activity of specialized enzymes in different cell types, which explains the vast number of existing starch-related enzymes. Starch synthesis is linked to the Calvin-Benson cycle through the conversion of fructose-6-phosphate (F6P) to glucose-1-phosphate (G1P) by the sequential action of phosphoglucoisomerase (PGI) and phosphoglucomutase (PGM). Then, ADP-glucose pyrophosphorylase (AGPase), the main enzyme involved in starch synthesis, uses ATP to convert G1P to ADP-glucose, which is used to build starch by the action of starch synthases and branching and debranching enzymes (Horrer *et al.*, 2016). On the other hand, starch degradation occurs via a network of reactions rather than through a linear pathway, involving glucan phosphorylation followed by the action of β-amylases and debranching enzymes (**Fig. 8**, Stitt and Zeeman, 2012).

It has been shown that under various abiotic stresses many plants remobilize their starch reserves in order to obtain energy, sugars and derivatives to help mitigate the stress (Stitt and Zeeman, 2012; Thalmann and Santelia, 2017). The remobilization of starch provides plants with carbon and energy when photosynthesis is inhibited, and the released components can then sustain growth, function as osmoprotectants or even as signaling molecules, for example. This increased starch degradation could be due, at least partly, by an increase in ABA, but the knowledge of starch metabolism regulation is in its infancy (Thalmann and Santelia, 2017). However, research points towards a coordination between starch degradation rates and carbon utilization for growth, achieved by the integration of circadian signals with environmental and metabolic signals (Thalmann and Santelia, 2017). Curiously, several studies have reported an increase in the starch content under stress, mainly high-salinity or cold stress conditions (Stitt and Zeeman, 2012). The reason for this discrepancy is unclear, but it has been suggested that plants might use starch to scavenge sodium under salinity stress (Thalmann and

Santelia, 2017). Nonetheless, these different responses in starch content in different growing conditions, plant species or even tissues highlight the plasticity of starch metabolism and its further roles in plant biology than as a mere storage compound.

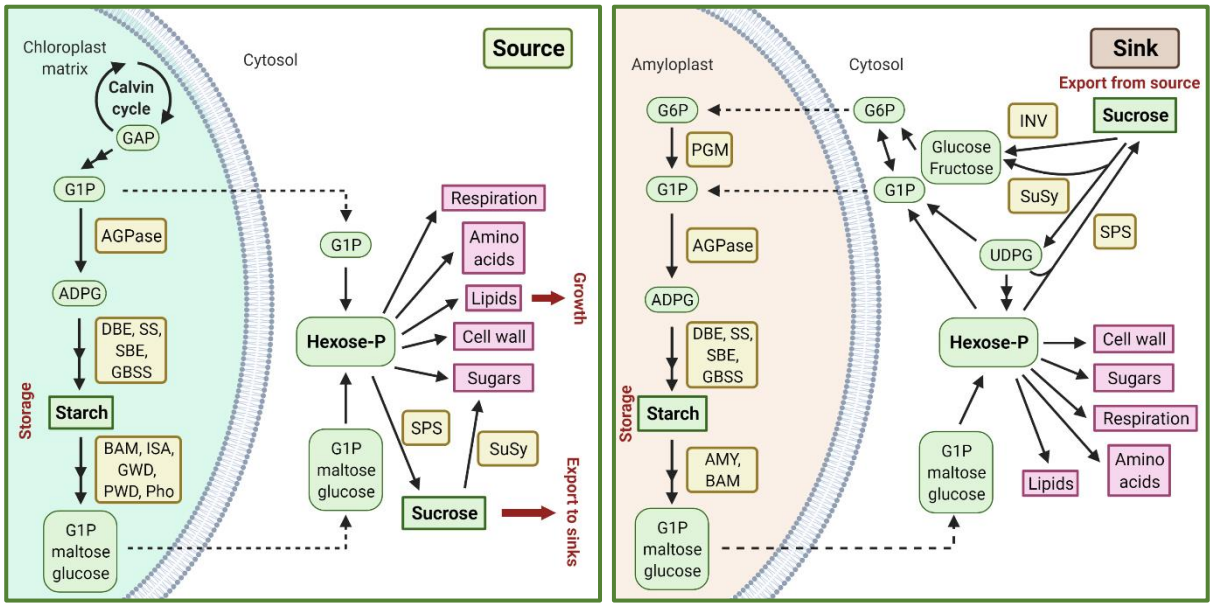

Figure 8. Starch and sucrose biosynthetic and degradation pathways in source and sink tissues. ***Left***, starch metabolism in photosynthetic tissues. In the chloroplast the GAP formed in the Calvin cycle is converted to G1P, which serves as substrate for AGPase to generate ADPG, considered the first step of the starch biosynthetic pathway. The degradation products of starch catabolism are exported to the cytosol, where they are converted to hexose phosphates to be used for several metabolic processes or for sucrose synthesis through SPS. This formed sucrose can then be stored in the vacuole or loaded to the phloem and travel to sink tissues. ***Right***, starch metabolism in non-photosynthetic sink tissues. Imported sucrose can be stored in vacuoles or be degraded by INV or SuSy. In the first pathway, glucose and fructose are formed, while SuSy produces fructose and UDPG. These hexoses can then be converted to ADPG to form starch or be used for other cellular processes. Note that several routes and molecules have been omitted and the chloroplast inner and outer membranes are depicted as a one-only membrane for clarity. *ADPG*, ADP-glucose; *AGPase*, ADP-glucose pyrophosphorylase; *AMY*, α-amylase; *BAM*, β-amylase; *GAP*, glyceraldehyde-3-phosphate; *GBSS*, ground bound starch synthase; *G1P*, glucose-1-phosphate; *G6P*, glucose-6-phosphate; *GWD*, glucan, water dikinase; *INV*, invertase; *ISA*, isoamylase; *PGM*, phosphoglucomutase; *Pho*, starch phosphorylase; *PWD*, phosphoglucan, water dikinase; *SBE*, starch branching enzyme; *SPS*, sucrose phosphate synthase; *SS*, starch synthase; SuSy, sucrose synthase; *UDPG*, UDP-glucose. *Key*: green boxes, carbohydrates; yellow boxes, enzymes; pink boxes, cellular processes; dashed lines indicate membrane transport. [Adapted with BioRender.com from Dong and Beckles (2019) and MacNeill *et al.* (2017)].

While starch synthesis is usually highly inhibited under water-deficit conditions, a maintenance or even increase in the concentration of soluble sugars is usually observed under stress conditions. Soluble sugars (sucrose, glucose and fructose) are used as carbon and energy sources in plant cells, but they also act as regulators of metabolism and stress response (Mahajan and Tuteja, 2005). It has been shown that the accumulation of soluble sugars in leaves and roots enhances plant tolerance against several abiotic stresses such as drought, salinity and cold, and this protection could be linked to their capacity to increase proline content, stimulate antioxidant enzymes and act as osmoprotectants upon water-deficit stress, amongst others (Sami *et al.*, 2016). Indeed, soluble sugars can keep proteins and membrane surfaces "hydrated", stabilizing these important macromolecules under desiccation stress (Hoekstra *et al.*, 2001). Hence, their accumulation is often observed in response to water-deficit stress, conferring tolerance to drought (Abid *et al.*, 2018) and salinity (Nemati *et al.*, 2011). It should be noted that the commonly observed increase in sucrose is mainly derived from starch degradation, since both fructose-1,6 bisphosphatase and SPS activities decline in response to reduced water potential (Mahajan and Tuteja, 2005).

E.3.4. Compatible solute accumulation

As previously stated, one common response to water-deficit stress is the increased accumulation of compatible solutes. These metabolites, also known as osmoprotectants, are small neutral molecules that act like osmolytes, protecting cells against osmotic stress without being toxic even at high concentrations. This protection is achieved through the stabilization of proteins and cellular structures such as membranes, scavenging ROS and/or maintaining cell turgor (Stitt, 2013). They comprise amino acids (e.g., proline, asparagine, glutamate, carnitine or GABA), sugars (glucose, trehalose or sucrose), polyols (mannitol, sorbitol or pinitol), some methylated relatives of proline and proline analogues as well as quaternary ammonium compounds such as glycine-betaine. On the other hand, there are other species that can contribute to osmotic adjustment but are not considered osmoprotectants such as Na^+, Cl^- or K^+ ions. Since the metabolic

pathways of soluble sugars and their role as osmoprotectants have already been discussed in the previous section, only proline and other amino acids as well as inorganic ions will be discussed in this section.

Proline and other amino acids

One example of osmoprotectant is the amino acid proline, whose accumulation in response to various stresses has been widely correlated to stress tolerance. However, proline not only acts as an osmolyte, but has many roles that protect cells against stress such as molecular chaperone, cryoprotectant, or buffering cytosolic pH and the cellular redox status, as well as influencing cell cycle and altering gene expression and signaling to modulate mitochondrial function (Singh *et al.*, 2015). One key aspect of proline that makes it an excellent molecular chaperone is that it has very strong hydration abilities: while its hydrophobic side binds to proteins, its hydrophilic part binds to water molecules, allowing proteins and other macromolecules to attract more water, thus enhancing their solubility and preventing protein denaturation under cellular desiccation conditions (Fang and Xiong, 2014; Kaur and Asthir, 2015; Rao and Chaitanya, 2016; Szabados and Savouré, 2010).

Two routes have been proposed for proline biosynthesis: via glutamate or via ornithine (**Fig. 9**). Under normal conditions, ornithine is converted by ornithine aminotransferase (OAT) to Δ^1-1-pyrroline-5-carboxylate (P5C) in mitochondria, being further reduced by P5C reductase (P5CR). However, under osmotic stress P5C is mainly produced from glutamate by P5C synthetase (P5CS, the rate limiting enzyme in the Pro biosynthetic pathway) in the cytosol and plastids (Fang and Xiong, 2014). The importance of the ornithine pathway in proline biosynthesis is unclear and it has been suggested that OAT only has a role in N-recycling from Arg through P5C, which is then converted to Glu by P5C dehydrogenase (P5CDH) (Zarattini and Forlani, 2017). Nonetheless, the activity of OAT seems to be important during seedling development and in some plants and/or organs under stress (Funck *et al.*, 2008). Up to date, the regulation of P5CR and P5CS gene expression is not well understood and both ABA-dependent and independent signaling networks have been shown to lead to proline synthesis induction (Funck *et al.*, 2008; Roosens *et al.*, 1998; Verdoy *et al.*, 2006; Xue *et al.*, 2009).

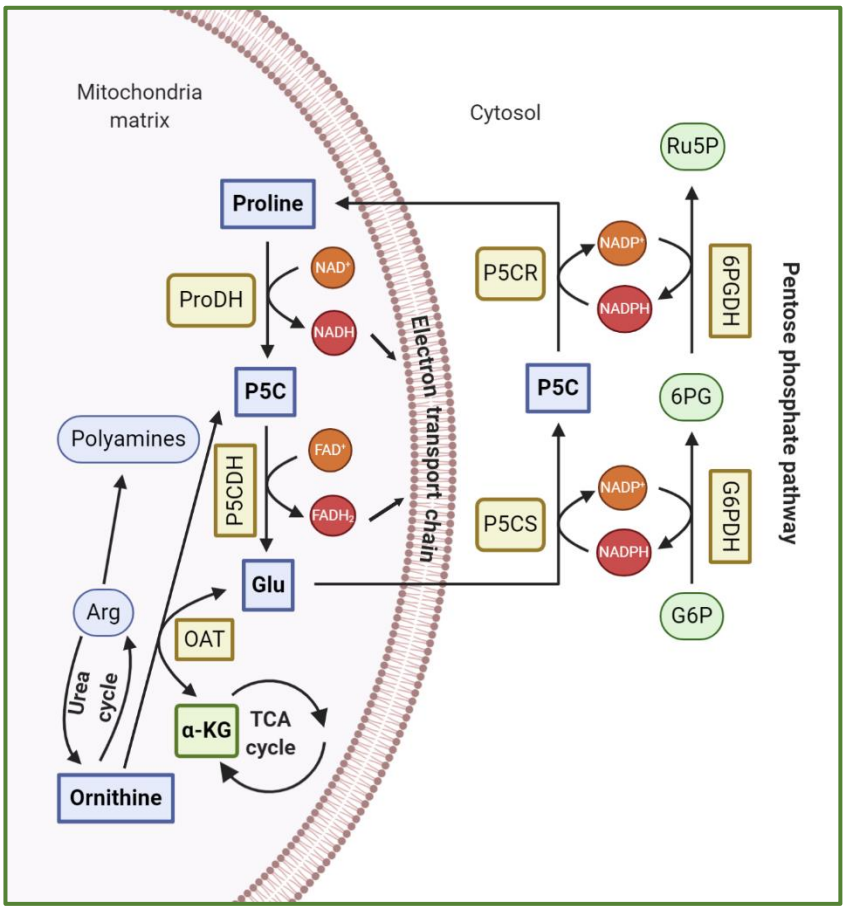

Figure 9. Proline synthesis and degradation pathways. While proline synthesis via P5CS occurs in the cytoplasm or the chloroplast matrix, linking the reducing-power regeneration with the pentose phosphate pathway, the OAT pathway occurs in the mitochondria, involving α-KG generated in the TCA cycle. On the other hand, proline degradation takes place in mitochondria as well, where the generated reducing power can feed the electron transport chain. Note that several routes and molecules have been omitted and the mitochondrial inner and outer membranes are depicted as a one-only membrane for clarity. *G6P*, glucose-6-phosphate; *G6PDH*, glucose-6-phosphate dehydrogenase; *α-KG*, α-ketoglutarate; *OAT*, ornithine aminotransferase; *P5C*, Δ^1-1-pyrroline-5-carboxylate; *P5CDH*, Δ^1-1-pyrroline-5-carboxylate dehydrogenase; *P5CR*, Δ^1-1-pyrroline-5-carboxylate reductase; *P5CS*, Δ^1-1-pyrroline-5-carboxylate synthase; *6PG*, 6-phosphogluconate; *6PGDH*, 6-phosphogluconate dehydrogenase; *ProDH*, proline dehydrogenase; *Ru5P*, ribulose-5-phosphate; *TCA*, tricarboxylic acid. *Key*: green boxes, carbohydrates; blue boxes, amino acids; yellow boxes, enzymes. [Created with BioRender.com, inspired by Shetty (2004)].

Proline catabolism is even less understood and is catalyzed by proline dehydrogenase (ProDH) [also known as proline oxidase (POX)] and P5CDH, which catalyze the reverse action of P5CR and P5CS in the mitochondria, respectively (**Fig. 9**). ProDH and P5CDH regenerate NADH and $FADH_2$, respectively, and deliver electrons to the mitochondrial respiration electron chain, thus being useful in the generation of energy and reducing equivalents for the TCA cycle (Zarattini and Forlani, 2017). Under environmental stress, proline content is regulated through the balance of its anabolism and catabolism (Cabassa-Hourton *et al.*, 2016; Deuschle *et al.*, 2004; Kishor *et al.*, 2005). Indeed, in response to many stresses proline accumulation seems to be the result of the increased activity of P5CS and the decreased proline catabolism (Per *et al.*, 2017). Accordingly, ProDH gene expression is usually down-regulated by osmotic stress (thus preventing proline degradation during abiotic stress) and increased by proline, hypo-osmolarity and during osmotic-stress recovery. Under the latter conditions, an increase in the activity of ProDH uses accumulated proline to generate Glu, thus serving as energy and nitrogen source (Verbruggen and Hermans, 2008). However, it is not clear that this reciprocal mechanism controlling proline accumulation is common to all plants or organs (Fujita *et al.*, 1998; Verdoy *et al.*, 2006).

In addition to osmoprotection, proline is very often considered to exert a protective role under water-deficit conditions as ROS scavenger. However, some authors argue that proline accumulation might exert beneficial aspects as a consequence of its metabolism rather than due to its inherent properties (Sharma *et al.*, 2011). Indeed, recent studies show that proline is unable to scavenge peroxynitrite ($ONOO^-$), nitric oxide ($^{\bullet}NO$), superoxide ($^{\bullet}O_2^-$) or nitrogen dioxide ($^{\bullet}NO_2$) and that its antioxidant capacity is limited to reduce hydroxyl radical ($^{\bullet}OH$) toxicity (Signorelli *et al.*, 2016). Nonetheless, proline can attenuate oxidative damage through other mechanisms such as the maintenance of an adequate redox balance. As we have described, proline biosynthesis regenerates $NADP^+$, which can be used in the photosynthetic ETC, thus reducing ROS generation by photosynthetic electron leakage. Overall, this results in a lower damage of the photosynthetic machinery and, hence, a higher tolerance to stress. Also the Pro-Pro cycle, produced in the scavenging of $^{\bullet}OH$ by Pro, contributes to $NADP^+$ regeneration (Signorelli *et al.*, 2014). In this cycle, $^{\bullet}OH$ attacks proline twice (first in the carboxylic group and then in the

amine group) resulting in the formation of P5C, which is then reconverted to proline by P5CS using NADPH. In addition, proline can enhance the activity of antioxidant enzymes and molecules, thus indirectly decreasing ROS (Signorelli *et al.*, 2016). Gill and Tuteja (2010) also suggest that, due to the high levels of Pro accumulation under stress, the selectivity of this molecule to $^{\bullet}OH$ could be beneficial, since if the high levels of proline reacted with, for example, $^{\bullet}NO$ (required for the optimal establishment of symbiotic interactions in legumes) it could impose a deleterious effect, since these symbiotic interactions positively affect plant status and stress tolerance (Hichri *et al.*, 2015). We must remember that ROS and RNS are signaling molecules too, so a dramatic decrease in their levels could attenuate responses mediated by their signaling such as stomatal closure or root elongation, with important negative effects on the plant stress tolerance (Signorelli *et al.*, 2016).

Not only proline but a general accumulation of amino acids in leaves and roots has been related to abiotic stress tolerance. Thus, depending on the studied species, various amino acids other than proline have been linked to stress tolerance such as asparagine, serine glycine, aspartic acid, alanine or GABA (Signorelli *et al.*, 2016).

Inorganic ions

As mentioned before, due to their toxicity at high concentrations, inorganic ions such as K^+ and Cl^- are not considered compatible solutes but can act as osmolytes, attracting water molecules and thus preserving cell turgor. For example, under water-shortage stress there is a rapid osmotic adjustment derived from the accumulation of K^+ and Cl^- ions in the vacuole (Nieves-Cordones *et al.*, 2019). Upon salinity conditions, plants can also sequester Na^+ and Cl^- inside vacuoles to avoid salt toxicity within the cells but also to serve as osmolytes, allowing the maintenance of cell turgor pressure (Rai, 2002). On the other hand, K^+ is a major osmoticum that contributes greatly to the cell's osmotic potential (Shabala and Pottosin, 2014). When Na^+ and Cl^- ions are sequestered in the vacuole, this requires a mirrored increase in the cytosolic osmotic potential, for which K^+ ions seem to be essential. However, when not enough K^+ can be taken up, which is a common phenomenon under high NaCl conditions, plants must incur high carbon cost in the production of organic osmolytes such as those above described, which

involves yield penalties. This could explain why salt-tolerant barley varieties had higher levels of root K^+ and lower levels of organic osmolytes compared to salt-sensitive plants (Chen *et al.*, 2007) and could be one of the reasons why plants that are capable of retaining more K^+ have fewer symptoms of salinity stress (Sun *et al.*, 2015). This will be discussed in more detail in **section E.3.6**.

E.3.5. Antioxidant metabolism

ROS include a variety of radicals such as singlet oxygen ($^1O_2$), superoxide ($^{\bullet}O_2^-$), hydroxyl radical ($^{\bullet}OH$), and hydrogen peroxide (H_2O_2) and are continuously generated as a consequence of plant metabolic processes due to the incomplete reduction of oxygen. However, their production is enhanced under salinity and drought stress due to an increased imbalance between the generation and utilization of electrons under these conditions (Fang and Xiong, 2014). This stress-induced ROS formation can lead to oxidative damages in various cellular components such as proteins, lipids and DNA, interrupting vital cellular functions of plants. For example, membrane lipids can be peroxydated, while the spatial configuration of membrane proteins can change due to ROS damage, leading to increased membrane permeability and ion leakage, chlorophyll destruction, metabolism perturbation and even severe injury or death (Parihar *et al.*, 2015). However, as recently discussed, ROS molecules can also act as intracellular signaling molecules that trigger the acclimation ability of plants to stressful conditions, for instance inducing proline accumulation or being involved in hormone-mediated events (Parihar *et al.*, 2015).

Plants have developed several antioxidant strategies to scavenge these toxic compounds and maintain the homeostasis of the intracellular redox state, thus enhancing tolerance to stressful conditions (Shao *et al.*, 2009). As stated in **section E.3.4**, Pro can prevent ROS-induced oxidative damage as $^{\bullet}OH$ scavenger, but, in addition, stress-induced Pro synthesis from Glu requires the oxidation of NAD(P)H, allowing for a $NAD(P)^+$ recycling process, otherwise compromised due to a stress-induced down-regulation of the Calvin cycle (Blum, 2017). In addition, Pro can also indirectly help in ROS scavenging trough enhancing plant antioxidant enzymes such as superoxide dismutase (SOD), catalase, peroxidase, ascorbate peroxidase (APX) or glutathione reductase (GR),

as well as non-enzymatic antioxidants such as ascorbate or glutathione (Gill and Tuteja, 2010). Other molecules such as carotenoids, anthocyanins, osmolytes, proteins (e.g., peroxiredoxin) and amphiphilic molecules (e.g., α-tocopherol) can also function as ROS scavengers (Wang *et al.*, 2003). These non-enzymatic antioxidants have multiple physiological functions involved in the maintenance of intracellular redox homeostasis and defense reactions, as well as other important functions involved in growth, development and metabolism (Anjum *et al.*, 2010).

Ascorbate occurs in all plant tissues except for seeds, being able to react with $^1O_2$, $^{\bullet}O_2^-$ and $^{\bullet}OH$. In addition, it is a key co-substrate of important antioxidant enzymes such as APX, who detoxifies H_2O_2, and 2-oxoacid-dependent dioxygenase, involved in the synthesis of ABA (Rao and Chaitanya, 2016). Ascorbate is connected to another important non-enzymatic antioxidant, glutathione, through the ascorbate-glutathione cycle (also known as the Halliwell-Asada cycle) (**Fig. 10**, Foyer and Noctor, 2011), which is highly activated under stress conditions such as drought and salinity (Sofo *et al.*, 2010). Glutathione (L-γ-glutamyl-L-cysteinyl-glycine) is also a low-molecular-weight antioxidant occurring in virtually all cellular components with multiple functions. Thus, this molecule serves as storage and transport of reduced sulfur, detoxicant of xenobiotics through glutathione-S-transferase and is involved in the synthesis of phytochelatins and, the function we want to address here, in the regulation of redox homeostasis of the cell. It directly scavenges $^1O_2$ and H_2O_2, but indirectly reacts with other ROS as well since it helps regenerate ascorbate through the ascorbate-glutathione cycle. Homoglutathione (L-γ-glutamyl-L-cysteinyl-β-alanine) is a glutathione homologue unique to the *Leguminosae* family with similar functions (Asthir *et al.*, 2020). The accumulation of these antioxidant molecules is linked to stress tolerance against drought and salinity (Cheng *et al.*, 2015).

In addition to being an integral component of osmotic adjustment, soluble sugars have been reported to be closely associated with the cellular antioxidation system. Indeed, sugar metabolism and signaling are involved in the metabolism, signaling and scavenging systems of various hormones and ROS. For example, hexokinase (HK) seems to regulate mitochondrial ROS levels, stimulating antioxidant defense mechanisms and phenolic compounds synthesis. Glucose-6-phosphate dehydrogenase (G6PDH) may

also be crucial for the regulation of redox homeostasis and ROS detoxification in chloroplasts, while sucrose has been reported to increase ascorbate synthesis and recycling (Bolouri-Moghaddam *et al.*, 2010). Soluble sugars can also feed $NADP^+$-reducing pathways such as the OPP pathway, thus producing NADPH to be used as cofactor of ROS-scavenging pathways such as the Halliwell-Asada cycle (Couée *et al.*, 2006). Sugar variations have been reported to also affect the expression SOD, heat shock proteins and glutathione-S-transferase genes, involved in redox metabolism (Keunen *et al.*, 2013). Additionally, while at low concentrations soluble sugars might function as substrates or signals for ROS levels regulation, at high concentrations they can directly scavenge ROS. Indeed, sucrose has been reported to scavenge $^{\bullet}OH$ (van den Ende and Valluru, 2009).

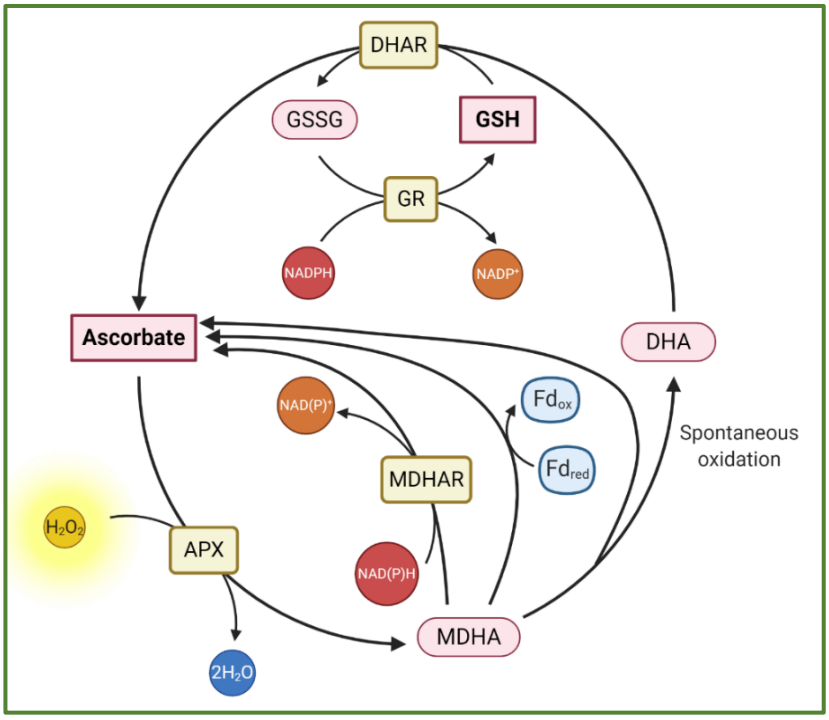

Figure 10. The plant ascorbate-glutathione cycle. The ascorbate-glutathione pathway detoxifies H_2O_2, a reactive oxygen species generated as a waste metabolic product. In this cycle NADPH is employed in a series of reactions that lead to the recovery of the reduced ascorbate and glutathione species through several enzymatic and non-enzymatic reactions. Ascorbate is oxidized to the radical MDHA which, if not reduced back to ascorbate through MDHAR or Fd, disproportionates spontaneously into DHA and ascorbate. DHA is then reduced back to ascorbate through the oxidation of glutathione, which is reduced back by GR employing NADPH. *APX*, ascorbate peroxidase; *DHA*, dehydroascorbate; *Fd*, ferredoxin; *GR*, glutathione reductase; *GSH*, reduced glutathione; *GSSG*, oxidized glutathione; *MDHA*, monodehydroascorbate; *MDHAR*, monodehydroascorbate reductase. [Created with BioRender.com, inspired by Anjum *et al.* (2010)].

E.3.6. Mineral nutrient deficiencies

One of the consequences of decreased rainfall is its direct impact on the physico-chemical properties of the soil, which reduces the diffusion of nutrients to the roots and their uptake by the plant (He and Dijkstra, 2014). Hence, even though a plant might be growing in a nutrient-rich soil, it might suffer from water-deficit-derived nutrient deficiency since it cannot take them. In addition, drought stress induces stomatal closure, which reduces the translocation of water and nutrients to the leaves due to the reduced transpiration, while microorganisms and enzymes involved in the mineralization process can also be negatively affected by stress. Hence, drought stress might cause nutrient deficiencies due to low nutrient availability and transport in plants (Ahanger *et al.*, 2016; Nieves-Cordones *et al.*, 2019). Apart from K^+ and Ca^{2+}, essential for plant survival, all macronutrients are integrated into vital organic compounds such as amino acids and proteins (nitrogen and sulfur), nucleic acids (nitrogen and phosphorous), phospholipids (phosphorous) and chlorophyll (Mg^{2+}), so nutrient deficiencies have major impacts on plant health and development (Ciríaco-da Silva *et al.*, 2011; Taiz and Zeiger, 2010). However, this nutrient deficiency is not always observed, and some studies even suggest that mild drought positively affects the nutrient content of crops (Fischer *et al.*, 2019).

In addition to these effects, the high levels of Na^+ and Cl^- ions in saline soils lead to additional nutritional imbalances due to the competition of these ions with other nutrients (Parihar *et al.*, 2015). Indeed, Na^+, K^+, Mg^{2+}, Ca^{2+} and NH_4^+ as well as Cl^-, SO_4^-, PO_4^{3-} and NO_3^- compete with each other for the ion transporters during root uptake and translocation, as well as during their use in biochemical processes such as enzymatic reactions (Hauser and Horie, 2010). This is of special relevance in the case of K^+, whose homeostasis is crucial due to its implication in multiple essential roles in the plant and the activation of caspase-like proteases that lead to cell death upon low cytosolic levels of this ion (Shabala, 2009; Shabala and Pottosin, 2014). On the other hand, Cl^- has antagonistic effects on NO_3^- uptake and transport, which can result in a reduction of N-uptake and storage (Wu and Li, 2019). Overall, multiple studies have reported salinity-derived nutrient deficiencies and imbalances, being one of the most important causes of reduced growth and even plant death under stressful conditions (Hu and Schmidhalter, 2005).

› GENERAL AIM

The decreased water reserves available for irrigation due to the increasing world population together with the altered rainfall regimes (i.e., less rainy days, longer drought periods between events, higher frequencies of extreme precipitation) are leading to an increase in the frequency and intensity of water-deficit conditions to which plants must adapt in order to survive. However, plant response to water-deficit stress is still not completely understood, even though it is needed to improve crop management and breeding techniques. Since plant yield and growth are visible in the shoots, a high number of studies have focused on the analysis of the aerial part, neglecting the importance of the plant root system not only for normal plant growth and development, but also for abiotic stress tolerance. Indeed, this organ is the first to encounter water-deficit stress and the responsible for water uptake from the soil, among other functions, making the understanding of root physiology of utmost importance, above all under low-water-availability conditions. **Hence, the aim of this work was to better understand the plant response to water-deficit conditions, focusing on the importance of the root tissue but with an integrated view of the whole-plant system using biochemical, physiological and metabolic approaches in the model legume *Medicago truncatula*.**

In order to do so, two different but interrelated objectives were set, which have been expounded on two different chapters:

1. To gain further insights into the different role and strategy to cope with low water availability stress of different root types by studying the taproot and fibrous root's physiology and biochemistry under well-watered and low-water conditions.
2. To ascertain the specific strategies exerted by the different plant tissues to face water-deficit stress by evaluating the leaf, root and phloem sap response to different but iso-osmotical conditions (NaCl, KCl, PEG-6000 or no-irrigation) of water-deficit stress.

› CHAPTER 1

Functional analysis of the taproot and fibrous roots of *Medicago truncatula*: sucrose and proline catabolism primary response to water deficit

Published in *Agric. Water Manag.* (2019) 216: 473-83

1.1. INTRODUCTION

Legumes are characterized by their high nutritional value for humans and livestock and by their ecological value as nitrate suppliers through their symbiosis with N-fixing bacteria (Graham and Vance, 2003). These advantages are however compromised by their low ability to adapt to adverse environmental conditions such as drought (Zahran, 1999). Within a climate change context, it is of great importance to maintain/increase their yield in stressful growth conditions to meet the requirements of the increasing world population. In order to achieve this, it is mandatory to further understand the adaptive response of these plants to water-deficit stress and select particular traits that allow them to better cope with the lack of water in the soil. *Medicago truncatula* is a model legume cultivated as an annual forage in several regions worldwide (see **section A**, Michaud *et al.*, 1988) and is phylogenetically related to some of the most relevant European legume crops (Aubert *et al.*, 2006; Phan *et al.*, 2007). While grain legumes are generally described as drought sensitive (González *et al.*, 1995; González *et al.*, 1998; Ramos *et al.*, 1999), forage legumes such as *M. truncatula* exhibit a higher tolerance to dry environments (Araújo *et al.*, 2015).

Plant roots are essential for plant productivity and serve a variety of functions such as anchorage and water and nutrient absorption. Tap or primary roots are those formed in the embryo growing directly downwards, whilst lateral roots are those formed post-embryonically emerging from the pericycle (see **section B**). In general, cultivated legumes develop a taproot system with a strongly developed primary root with branches. Indeed, in the perennial alfalfa the taproot has been described as the main underground storage organ, acting as a carbon and nitrogen reservoir to drive the regrowth after cutting (Erice *et al.*, 2011). Despite being a close relative of alfalfa, the root system of the model legume *M. truncatula* consists of numerous branches emerging from a short taproot located at the upper side, appearing similar to the fibrous root system of monocots. Hence, in this work we used the terms taproot (tapR) and fibrous root (FibR) in order to differentiate both root types.

Despite the importance of the root system as the first organ encountering soil water deficit, its response to drought stress has not been as extensively studied as the green parts. Besides, the vast majority of studies focused on the root system regard it as a whole without distinguishing root types that emerge from it, not taking into account their particular anatomical and physiological characteristics (Tian *et al.*, 2014). However, plant roots are starting to gain interest regarding their role in drought stress tolerance (Sutka *et al.*, 2016; Zhan *et al.*, 2015). Indeed, the identification of root mechanisms improving drought tolerance is essential to design drought-tolerant crops, with factors related to anatomo-morphological characteristics of the different root types having a high relevance (Gewin, 2010; Lynch *et al.*, 2014). Studies conducted during the last decade show a clear interaction between environmental conditions (such as drought) and legume taproot development, which responds by trapping the vegetative storage proteins and avoiding their export towards the shoot to allow regrowth production when the stress disappears (Erice *et al.*, 2007). Physiological differences between the taproot and lateral roots have also been suggested in faba bean related to lipid metabolism (Waisel and Radunz, 2006). In addition, an increased taproot diameter has been identified as key component in providing a deeper root system in white clover under drought-prone environments (Woodfield *et al.*, 1996). In *M. truncatula*, scarce information is available regarding the characteristics of its root system (Echeverria and González, 2021; Moreau, 2006). However, the relevance of different root properties has been demonstrated in other species when comparing the response of tolerant and sensitive cultivars to drought stress. Some examples are the increase in the osmoregulating properties of the root cells of durum wheat (Bajji *et al.*, 2000), an improved efficiency of water absorption in tall fescue (Huang and Gao, 2000) or the synthesis of protective molecules in *Brasica juncea* (Phutela *et al.*, 2000).

Osmotic adjustment has been proven to be a prime adaptive trait in support of crop yield under drought conditions (see **section E.3.4**, Blum, 2017). Amino acids are key players in this osmotic adjustment, but proline stands out by its role in cellular homeostasis, including redox balance and energy status, amongst others (Szabados and

Savouré, 2010). It has been shown that proline pools supply a reducing potential for mitochondria through its degradation/oxidation, which provides electrons for the respiratory chain and therefore contributes to energy supply for growth (Kishor *et al.*, 2005). In addition, carbohydrates often accumulate in the form of soluble sugars such as hexoses and sucrose, dismissing the prediction of a carbon starvation provoked by a reduced photosynthesis rate under water deficit (Muller *et al.*, 2011). Although in this context an osmoprotective role has been associated to carbohydrates (Gil *et al.*, 2013), the growth and development of sink organs is known to be, at least partly, under the control of carbon availability (Muller *et al.*, 2011). However, carbon partitioning to roots has been a long-time described response to drought stress, which could allow root integrity and even growth for the maintenance of efficient water uptake when this is limited (Gargallo-Garriga *et al.*, 2014). In this regard, the sucrose-degrading enzymes sucrose synthase (SuSy) and invertase (INV) play key roles in sugar partitioning to the roots and determining sink strength (see **section E.3.3**, Sturm and Tang, 1999).

1.2. OBJECTIVE

We hypothesize that the behavior of the main root types in *M. truncatula* is different under both control and drought conditions. In the current study, we aim to characterize the physiology and metabolism of the taproot and fibrous root under control, moderate and severe water-deficit stress conditions, with a special attention to sucrose and proline metabolism.

1.3. MATERIALS AND METHODS

1.3.1. Plant material and stress treatments

Medicago truncatula seeds were scarified with sulfuric acid 98% for 7 min, washed and then sterilized with 3.5% sodium hypochlorite for 90 s. After a thorough wash, the seeds were soaked in water and left shaking in the dark for 6 h. When the seeds were hydrated, they were transferred to 7‰ agar plates at 4 °C for one day in the dark and then incubated at 20 °C for two days. The seedlings were then planted 1-L brown plastic pots with perlite/vermiculite (1/3, *v*/*v*) and grown under controlled conditions [22/18 °C day/night temperature, 70% relative humidity, 500 µmol m^{-2} s^{-1} (PPFD), 12 h photoperiod] and irrigated with Evans medium supplemented with 5 mM NH_4NO_3 (Evans, 1981).

Six-week-old plants were randomly separated into three sets containing ten biological replicates each. Water-deficit stress was then imposed by withdrawing irrigation, and the hydric status of the water-deprived and control (well-watered) plants was monitored daily by measuring the water potential of the leaves (Ψ_{leaf}). During the water-deficit study, control (C) plants were irrigated with $_dH_2O$ to avoid nutritional differences. When the Ψ_{leaf} of the water-deficit-stressed plants reached the desired value [for moderate deficit (MD) $\Psi_{leaf} \approx$ -1.5 MPa, after 6-8 days treatment, and for severe deficit (SD) $\Psi_{leaf} \approx$ -2.5 MPa, after 7-9 days], plants were harvested by separating the primary root (tapR) from the lateral fibrous roots (FibR) with a scalpel and flash-freezing both in liquid N_2, except for the samples used in respiration measurements, which were analysed *in situ*. Control plants were harvested from day 5 to day 9 of treatment, showing an average Ψ_{leaf}= -0.37 ± 0.01 MPa. Samples were stored at -80 °C for further analysis. The number of biological replicates employed for each analysis is indicated in each figure/table.

1.3.2. Plant water status

Plant transpiration was gravimetrically determined on a daily basis by weighting the pots one hour after the beginning of the photoperiod. Ψ_{leaf} was measured in the second fully expanded leaf at this time point using a pressure chamber (Soilmoisture Equipment, Santa Barbara, CA, USA) as earlier described (Scholander *et al.*, 1965). Leaf and roots water content (WC) was determined on the basis of the fresh weight (FW) and the dry weight (DW), obtained after 48 h drying at 70 °C, using the following formula (1):

$$\mathrm{WC}\ (\%) = [100 \times (\mathrm{FW} - \mathrm{DW})] \times (\mathrm{FW})^{-1} \qquad (1)$$

1.3.3. Respiration measurements

Root respiration (O_2 consumption at 21 °C) was measured using a Clark-type O_2 electrode (Hansatech Oxygraph, H. Saur Laborbedarf, Reutlingen, Germany) connected to constant-temperature circulating water baths at 25 °C. For each plant, two root aliquots (≈0.05 g FW) were placed into two tightly closed oxygraph chambers containing 1 mL reaction buffer (25 mM imidazole-HCl pH 6.5) under stirring. After a constant rate of O_2 uptake was attained, 10 µL of 0.01 M cyanide (KCN) in 20 mM HEPES pH 8 or 20 µL of 1 M salicylhydroxamic acid (SHAM) in 2-methoxyethanol were added to each chamber. About 5 min after the application of the first respiration inhibitor the other inhibitor was added. Total respiration (totalR) was determined as the rate of O_2 consumption before the addition of any inhibitor, while the residual respiration (residualR) was determined as the O_2 consumption in the presence of both SHAM and KCN. The alternative pathway (AlternatP) capacity was calculated by subtracting the residualR from the O_2 consumption rate obtained after inhibiting the cytochromic pathway with KCN, while the cytochrome pathway (CytocP) capacity was calculated in a similar way but after inhibiting the alternative pathway with SHAM.

1.3.4. Determination of soluble sugar and starch content

Soluble sugars were extracted as detailed by Gálvez *et al.* (2005). Frozen material was exhaustively extracted three times in boiling ethanol (80%, *v/v*) for 30 s and one more time at RT. The aqueous phase of the ethanol extract was evaporated at 40 °C using a Turbovap LV evaporator (Zymark Corp., Hopkinton, MA, USA) for soluble sugar determination. After the evaporation cycle, the dry residue was resuspended in $_{dd}H_2O$ by vigorous vortexing. A sample cleaning was then performed by centrifugation for 10 min, and the supernatants were then stored at -20 °C for further analysis.

The remaining tissue after ethanol-soluble compound extraction was dried at 70 °C for 48 h. Then, the dry samples were homogenized with $_{dd}H_2O$ using mortar and pestle and further boiled for one hour for starch grain breakage. After cooling down, 1 mL of desalted amyloglucosidase solution (EC 3.2.1.3, 0.5 units mL^{-1} acetate buffer pH 4.5) was added to each tube and incubated under shaking at 55 °C for starch digestion. Extractions were centrifuged at 2,330 × *g* for 10 min, and the supernatants were stored at -20 °C for further glucose quantification. Sucrose, glucose and fructose were determined by capillary electrophoresis (CE) in a Coulter P/ACE system 5500 (Beckman Coulter Inc., Fullerton, CA, USA) coupled to a diode array detector (Marino *et al.*, 2006). Concentrations were calculated from peak heights using commercial standards (Sigma-Aldrich, Steinheim, Germany).

1.3.5. Determination of free amino acid content

Frozen samples were ground to powder under liquid N_2 and subsequently homogenized using a mortar and pestle with 1 M HCl (≈10 mL g FW^{-1}) and incubated on ice for 10 min. Subsequently, extracts were centrifuged at 20,000 × *g* and 4 °C for 10 min. Supernatants were neutralized using NaOH, and internal standards norvaline and homoglutamic acid were spiked. Then, samples were derivatized with 1 mM fluorescein isothiocyanate (FITC) dissolved in acetone for 15 h at RT in 20 mM borate buffer pH 10. The content of free amino acids was determined using a Beckman Coulter CE PA-800 (Beckman Coulter Inc., Brea, CA, USA) coupled to laser-induced fluorescence detection (argon laser at 488 nm), as described previously (Arlt *et al.*, 2001; Takizawa and

Nakamura, 1998), with minor modifications. A fused-silica capillary, 43/53.2 cm long and 50 µm internal diameter (Beckman Coulter Inc., Brea, CA, USA), was employed. For amino acid separation, 45 mM α-cyclodextrin in 80 mM borax buffer pH 9.2 was used. Analyses were performed at 20 °C and at a voltage of 30 kV (110 µA). Total amino acid content is presented as the summation of all the measured single amino acids for each sample and expressed on a DW basis.

1.3.6. Determination of total soluble proteins and enzymatic activities

Aliquots of frozen roots (≈1 g) were ground to powder under liquid N_2 and homogenized with extraction buffer [50 mM MOPS pH 7.5, 0.1% (*v*/*v*) Triton X-100, 10 mM $MgCl_2$, 1 mM EDTA, 20 mM KCl, 10 mM DTT, 10 mM β-mercaptoethanol, 2.5% (*w*/*v*) PVPP, 2 mM PMSF and a protease inhibitor cocktail tablet] and centrifuged at 24,000 × *g* and 4 °C for 20 min. The protein content of the supernatant was determined by the Bradford assay in the crude extract using bovine serum albumin as protein standard.

Additionally, the crude protein extract was also employed to determine the activity of glutamate synthase (GOGAT, EC 1.4.1.14), proline dehydrogenase (ProDH, EC 1.5.5.2), Δ^1-1-pyrroline-5-carboxylate synthase (P5CS, EC EC 1.2.1.88), ADP-glucose pyrophosphorylase (AGPase, EC 2.7.7.27) and pyruvate decarboxylase (PDC, EC 4.1.1.1). An aliquot of this extract was desalted through BioGel P-6 Desalting Gel (Bio-Rad Laboratories, Inc., Hercules, CA, USA) equilibrated with desalting buffer (250 mM MOPS pH 7.5, 50 mM $MgCl_2$, 100 mM KCl) to be used for the determination of alcohol dehydrogenase (ADH, EC 1.1.1.1), UDP- and ADP-sucrose synthase (SuSy, EC 2.4.1.13), UDP-glucose pyrophosphorylase (UGPase, EC 2.7.7.9), malate dehydrogenase (MDH, EC 1.1.1.37), soluble alkaline/neutral invertase (INV, EC 3.2.1.26), aspartate aminotransferase (AAT, EC 2.6.1.1), alanine aminotransferase (AlaAT, EC 2.6.1.2), glucose-6-phosphate dehydrogenase (G6PDH, EC 1.1.1.49), NADH-glutamate dehydrogenase (GDH, EC 1.4.1.2), fructose-1,6-bisphosphatase (FBPase, EC 3.1.3.11), glyceraldehyde-3-phosphate dehydrogenase (GAPDH, EC 1.2.1.12), isocitrate dehydrogenase (IDH, EC 1.1.1.41), malic enzyme (ME, EC 1.1.1.40), glycerol-3-phosphate dehydrogenase (GPDH, EC 1.1.5.3), pyruvate kinase (PK, EC 2.7.1.40) and hexokinase (HK, EC 2.7.1.1) activities. The pellet fraction was employed

to assay cell wall acid invertase (acidINV). Enzymatic activities were assayed spectrophotometrically as the oxidation or reduction of NAD(P)(H) nucleotides at 30 °C and 340 nm for 15 min after an initial incubation of 5 min at RT before the substrate addition. For an overview of the metabolic pathways in which the studied enzymes are involved refer to **Fig. 1.1**.

PDC, ADH, SuSy, acid and alkaline/neutral INV, UGPase, MDH and GOGAT were assayed as González *et al.* (1998); AAT and AlaAT as Hatch and Mau (1973); ProDH and P5CS as Rouached *et al.* (2013); G6PDH, GDH (in the aminating direction), FBPase, GAPDH and IDH as Gibon *et al.* (2004); ME as Ryšlavá *et al.* (2003); GPDH as Shen *et al.* (2006); AGPase as Baroja-Fernandez *et al.* (2003); PK as Wood (1968) and HK as Sigma protocols. Enzymatic activities were expressed on a protein basis in order to visualize possible regulation mechanisms in response to water-deficit stress.

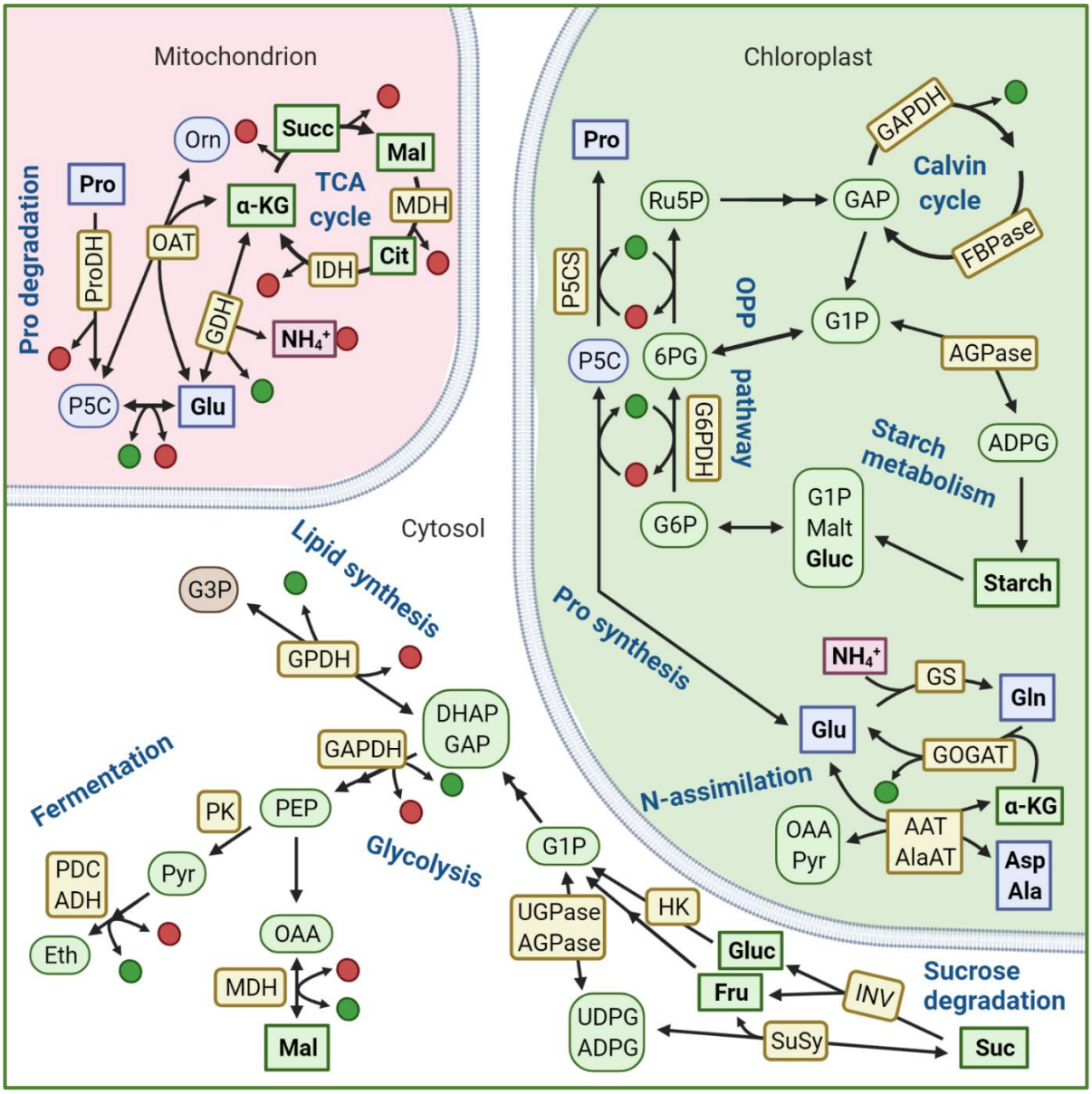

Figure 1.1. Main metabolic routes and enzymatic activities involved in this study. *AAT*, aspartate aminotransferase; *ADH*, alcohol dehydrogenase; *ADPG*, ADP-glucose; *AGPase*, ADP-glucose pyrophosphorylase; *AlaAT*, alanine aminotransferase; *Cit*, citrate; *DHAP*, dihydroxyacetone phosphate; *Eth*, ethanol; *FBP*ase, fructose-1,6-bisphosphatase; *Fru*, fructose; *GAP*, glyceraldehyde-3-phosphate; *GAPDH*, glyceraldehyde-3-phosphate dehydrogenase; *GDH*, glutamate dehydrogenase; *Gluc*, glucose; *G1P*, glucose-1-phosphate; *G3P*, glycerol-3-phosphate; *G6P*, glucose-6-phosphate; *GPDH*, glycerol-3-phosphate dehydrogenase; *G6PDH*, glucose-6-phosphate dehydrogenase; *GOGAT*, glutamate synthase; *GS*, glutamine synthase; *HK*, hexokinase; *IDH*, isocitrate dehydrogenase; *INV*, invertase; *α-KG*, α-ketoglutarate; *Mal*, malate; *Malt*, maltose; *MDH*, malate dehydrogenase; *ME*, malic enzyme; *OAA*, oxaloacetate; *OAT*, ornithine aminotransferase; *OPP*, oxidative pentose phosphate; *Orn*, ornithine; *P5C*, Δ^1-1-pyrroline-5-carboxylate; *P5CS*, Δ^1-1-

pyrroline-5-carboxylate synthase; *PDC*, pyruvate decarboxylase; *PEP*, phosphoenolpyruvate; *6PG*, 6-phosphogluconate; *PK*, pyruvate kinase; *ProDH*, proline dehydrogenase; *Pyr*, pyruvate; *Ru5P*, ribulose-5-phosphate; *Suc*, sucrose; *Succ*, succinate; *SuSy*, sucrose synthase; *TCA*, tricarboxylic acid; *UDPG*, UDP-glucose; *UGPase*, UDP-glucose pyrophosphorylase. Several routes and molecules have been omitted and membranes are depicted as a one-only membrane for clarity. Note that enzymes can have more than one subcellular localization, like in the case of GPDH, AAT and AlaAT, amongst others. *Key*: yellow boxes, enzymes; green boxes, carbohydrates; blue boxes, amino acids; red and green circles, reduced and oxidized reducing power, respectively. Measured carbohydrates and amino acids in both chapters are in bold. [Created with BioRender.com].

1.3.7. Statistical analysis

All data are reported as the mean ± standard error (SE) of n = 5-10 independent measurements. For all studied parameters, a two-way analysis of variance (ANOVA) was performed in order to test the influence of the measured organ and the drought treatment as well as their possible interactions using SPSS v27.0. Statistical significance among averages was evaluated using Bonferroni *post hoc* test $p < 0.05$, while Student's t-test was performed when only comparing treatment and control. Before statistical analyses, data were checked for normality and homogeneity of variances, being log-transformed when needed.

1.4. RESULTS

For this study, watering was stopped for drought-stressed plants, while control plants were watered daily. Upon the beginning of the treatment, leaf water potential (Ψ_{leaf}) was not significantly affected until the fourth day, exhibiting afterwards a continuous drop (**Fig. 1.2**). Plants entered a moderate level of water-deficit stress (MD) 6-8 days after water-deficit stress imposition and were harvested when their Ψ_{leaf} reached -1.51 ± 0.02 MPa. On the other hand, the severely stressed plants (SD) were harvested after 7-9 days of treatment with an average Ψ_{leaf} of -2.51 ± 0.04 MPa. Plant transpiration (measured as plant evapotranspiration) gradually decreased from the second day after the beginning of the water-deficit treatment (**Fig. 1.2**). Significant differences in the shoot and root DW biomass were not observed, although an increase in the root-to-shoot trend could be observed (data not shown). A visual loss of turgor correlated well with the general decline in the leaf water content (WC), with significant differences in the leaf, taproot (tapR) and fibrous root (FibR) WC response to water-deficit stress (**Fig. 1.3**). Indeed, the WC of leaves and tapR decreased around 15% under SD, while the FibR WC decreased 30 and 65% under MD and SD, respectively.

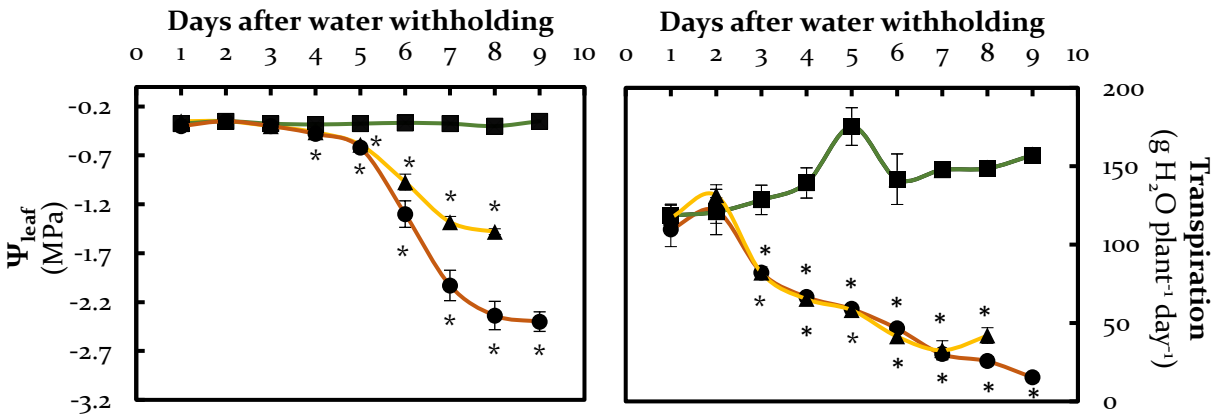

Figure 1.2. Leaf water potential and transpiration changes upon water-deficit stress. Changes in the leaf water potential (Ψ_{leaf}) (**left**) and transpiration (**right**) under control (squares, green), moderate (triangles, yellow) and severe (circles, orange) drought stress conditions. Each value represents the mean (n = 2-10) ± SE. Asterisks indicate statistical differences between control and treatment according to Student's t-test ($p < 0.05$).

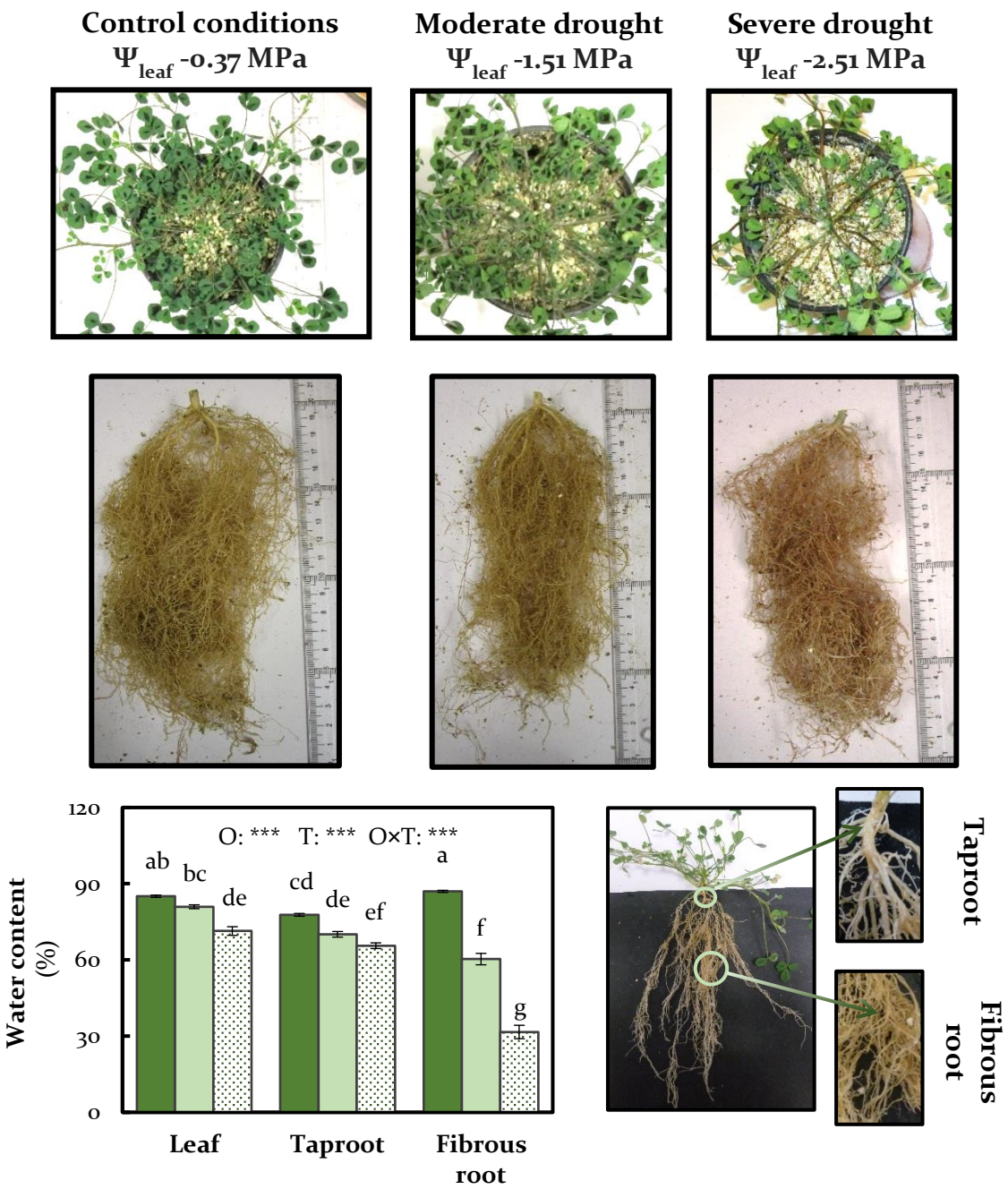

Figure 1.3. Visual and physiological response of *M. truncatula* plants to water-deficit stress. ***Above***, visual appearance of shoots and roots of 6-week-old plants subjected to control (C, Ψ_{leaf} = -0.37 ± 0.01 MPa), moderate (MD, Ψ_{leaf} = -1.51 ± 0.02 MPa) and severe drought (SD, Ψ_{leaf} = -2.51 ± 0.04 MPa) conditions. ***Below left***, water content of the leaf, taproot and fibrous roots under C (dark green), MD (light green) and SD (dots) conditions. Bars represent the mean ± SE (n = 10). A two-way ANOVA was performed and the *p*-values of the effects of organ (O), treatment (T) and their interaction (O×T) are indicated: *** $p < 0.001$. Different letters indicate significantly different averages according to the Bonferroni *post hoc* test ($p < 0.05$). ***Below right***, detail of the taproot and fibrous roots of *M. truncatula* plants.

Regarding root respiration, while the most relevant results are shown in **Fig. 1.4**, all data and its statistical analysis can be consulted in **Tables S1.1 and S1.2**. Water-deficit stress led to a decline in the total root respiration of both tapR and FibR, with the response of the latter being more abrupt than that of the tapR (**Fig. 1.4A**): in the tapR, the total respiration rate declined 2-fold in SD compared to C, while the respiration drop for the FibR was 4-fold. The residual respiration (residualR), measured after inhibiting both the alternative and cytochrome pathways, was similar in both root types under control conditions (**Fig. 1.4B**), accounting for the 28% and 24% of the total measured respiration for the tapR and FibR, respectively. Water-deficit stress did not significantly affect the residualR in the tapR, while abruptly decreasing to half the value under moderate conditions and remaining low under severe conditions in the FibR. However, when residualR values were relativized for the total root respiration, a statistically significant increase was observed for both root types under water-deficit stress conditions (**Fig. 1.4B**).

Under control conditions, as it has been observed for the total respiration rate, the alternative (AlternatP) and cytochrome pathway (CytocP) capacities were higher in the FibR than the tapR (**Fig. 1.4C, D; Table S1.1**). Both respiration capacities declined in response to water-deficit stress, being CytocP the most affected one with a 4- and 15-fold decrease in the tapR and FibR, respectively. The AlternatP capacity declined significantly in the FibR under both stress conditions, but in the taproot this effect was only significant under severe water deficit. In addition, not only the decline in both capacities was different for each root type, but also the AlternatP/CytocP ratio differed from one root type to the other. In both cases, despite the decrease in the measured AlternatP and CytocP capacities, water-deficit stress led to a similar increase in the relative AlternatP capacity in detriment of the CytocP, with these changes being already statistically significant under MD in the case of the FibR (**Fig. 1.4C, D**).

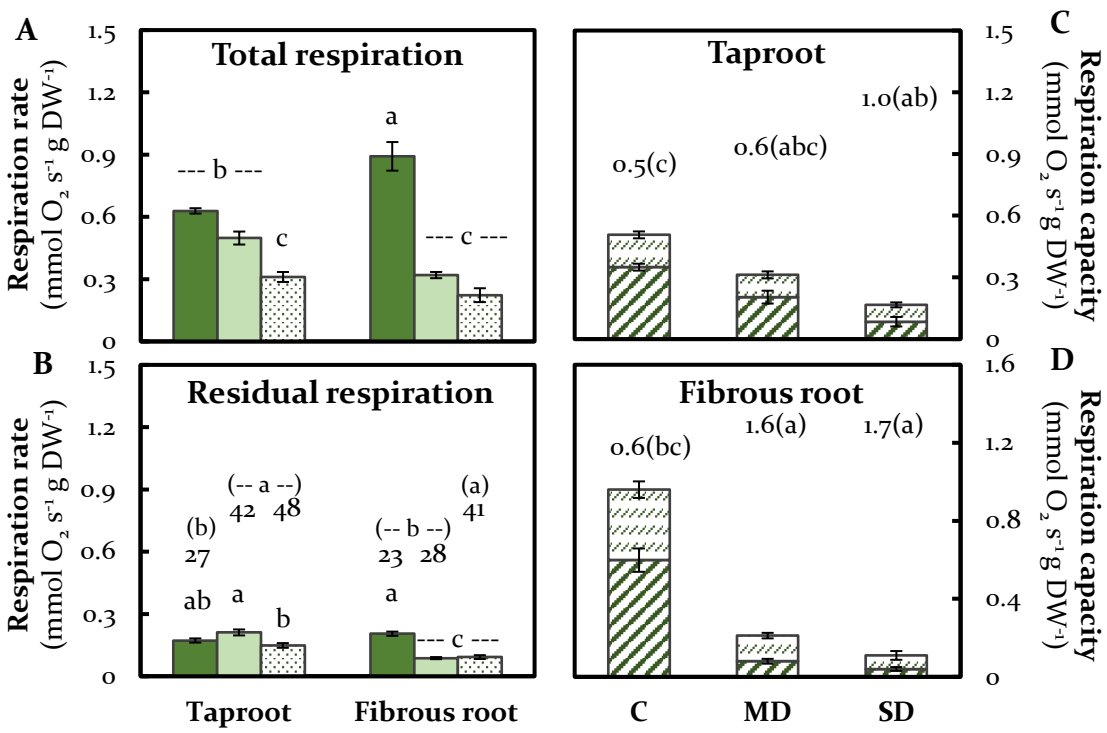

Figure 1.4. Effect of water-deficit stress on root respiration. Total (**A**) and residual root respiration (**B**) of the taproot and fibrous roots under control (C, dark green), moderate (MD, light green) and severe (SD, dots) water-deficit stress conditions. In B, the values above the bars represent the contribution of residual respiration (as %) to the total respiration. Graphs **C** and **D** represent the changes in cytochrome (CytocP, strips) and alternative (AlternatP, dashes) pathway capacities in the taproot and fibrous root, respectively. The values above the bars represent the AlternatP/CytocP ratios under the different water regimes. Bars represent the mean ± SE (n = 10). Different letters indicate statistically significant different averages [two-way ANOVA followed by the Bonferroni *post hoc* test ($p < 0.05$). See **Table S1.2.2** for the two-way ANOVA results]. See **Table S1.1** for detailed values and statistical analysis of measured respiration parameters.

Regarding carbohydrates, under control conditions sucrose and starch were more abundant in the tapR than in the FibR, even though the differences were not statistically significant in the latter (**Fig. 1.5**). On the other hand, glucose and fructose were more abundant in the FibR. Upon water-deficit stress, the sucrose content increased 3- and 8-fold in the tapR and FibR, respectively, while only the FibR showed a significant accumulation of glucose and fructose upon water-deficit stress **(Fig. 1.5).** On the other hand, water-deficit stress led to a significant decline in the starch content in both root types, being this decrease more abrupt in the FibR.

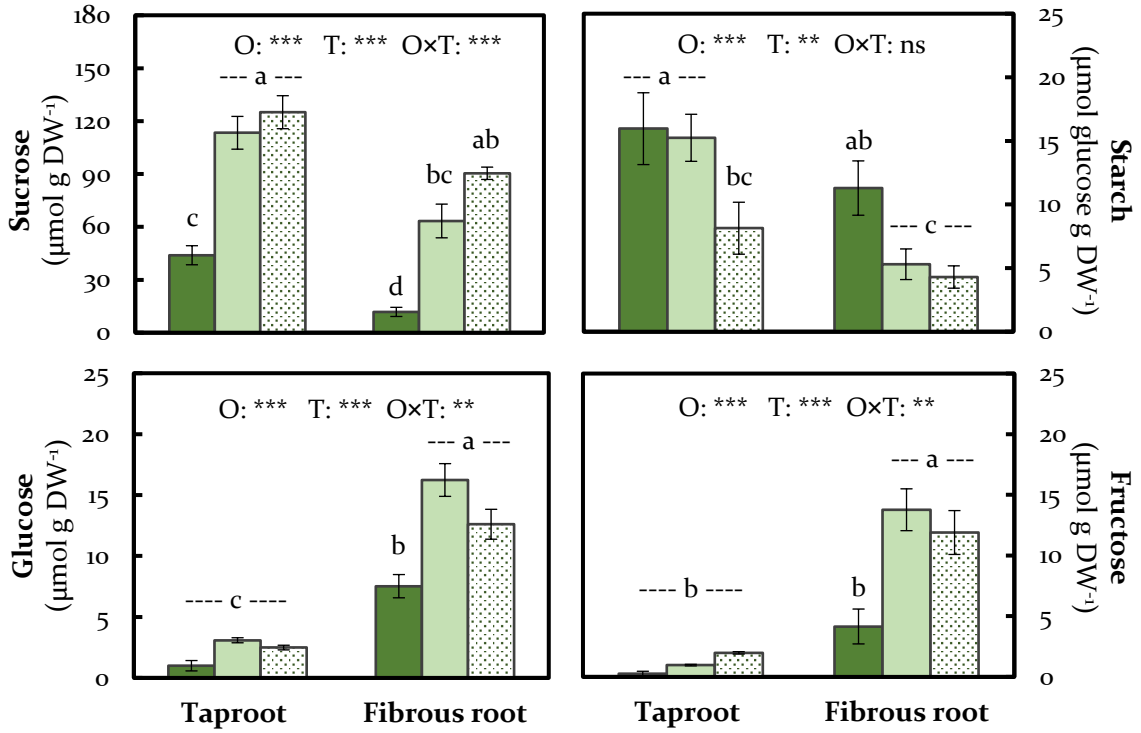

Figure 1.5. Soluble sugars and starch content of water-deficit stressed roots. Changes in sucrose, starch (measured as glucose released after starch enzymatic breakdown), fructose and glucose contents of *M. truncatula* taproot and fibrous roots under control (C, dark green), moderate (MD, light green) and severe (SD, dots) water-deficit stress conditions. Bars represent the mean ± SE (n = 6). A two-way ANOVA was performed and the *p*-values of the effects of organ (O), treatment (T) and their interaction (O×T) are indicated: ns > 0.05; $^{**}p < 0.01$; $^{***}p < 0.001$. Different letters indicate significantly different averages according to the Bonferroni *post hoc* test ($p < 0.05$).

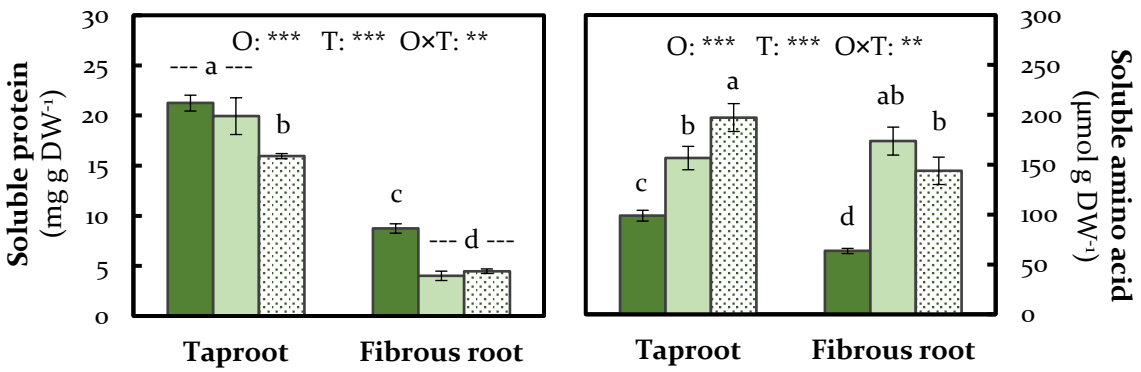

Figure 1.6. Water-deficit stress effect on the nitrogen status of roots. Soluble protein and amino acid content of the taproot and fibrous roots under control (C, dark green), moderate (MD, light green) and severe (SD, dots) water-deficit stress conditions. Bars represent the mean ± SE (n = 10). A two-way ANOVA was performed and the *p*-values of the effects of organ (O), treatment (T) and their interaction (O×T) are indicated: $^{**}p < 0.01$; $^{***}p < 0.001$. Different letters indicate significantly different averages according to the Bonferroni *post hoc* test ($p < 0.05$).

Water-deficit stress provoked a reduction in the soluble protein content of both root tissues, being the effect more pronounced in the FibR (**Fig. 1.6**). However, the soluble amino acid levels increased in response to water deficit in both root types even under moderate stress. Regarding control conditions, there was a higher total amino acid content in the tapR compared to the FibR (**Fig. 1.6**). In these conditions there was a clear supremacy of Asn in the fibrous root (74%) contrasting with the more diverse composition of the taproot, which held significant amounts of Asn (47%), GABA (11%), Ser (11%) and Pro (6%) (**Fig. 1.7A**). **Fig. 1.7B** represents the fold change of each amino acid in the tapR and FibR in response to MD and SD regarding their relative content. In the FibR, the only significant changes (≥ 2-fold) in response to water-deficit stress were the accumulation of Pro, His, and Trp together with the decrease in Gly content. Conversely, in the tapR water-deficit stress provoked a more marked effect at amino acid level. Thus, in addition to Pro and His, a significant increase of the branched-chain amino acids and a decrease of Gln, GABA, Glu and Asp were observed in the tapR (**Fig. 1.7B**).

Regarding the effects of water-deficit stress on the absolute content of individual amino acids, the most common pattern was a progressive increase in the tapR amino acid content under MD and SD, together with the increase under MD and no further increment upon SD in the FibR, like in the case of Val, Leu, Ile, Pro, Phe, Trp and Lys (**Fig. 1.8**). Thr and Tyr responded in a similar way, but their increase in the tapR was only significant upon SD. In the case of Arg, Met and Gly, their levels did not increase in the FibR in response to water-deficit stress but did so in the tapR. Another common response was the decline in the tapR under MD and no further decrease under SD, while increasing in the FibR in response to MD and declining halfway between MD and control conditions under SD, as it was seen for Ala, Ser, Gln, GABA and Asp. Glu showed a similar response but with the decline in the tapR being apparent under SD. Asn and His were the amino acids which showed the biggest resemblance between the tapR and FibR, showing a similar increasing trend in response to MD and similar concentrations between both root types under most conditions.

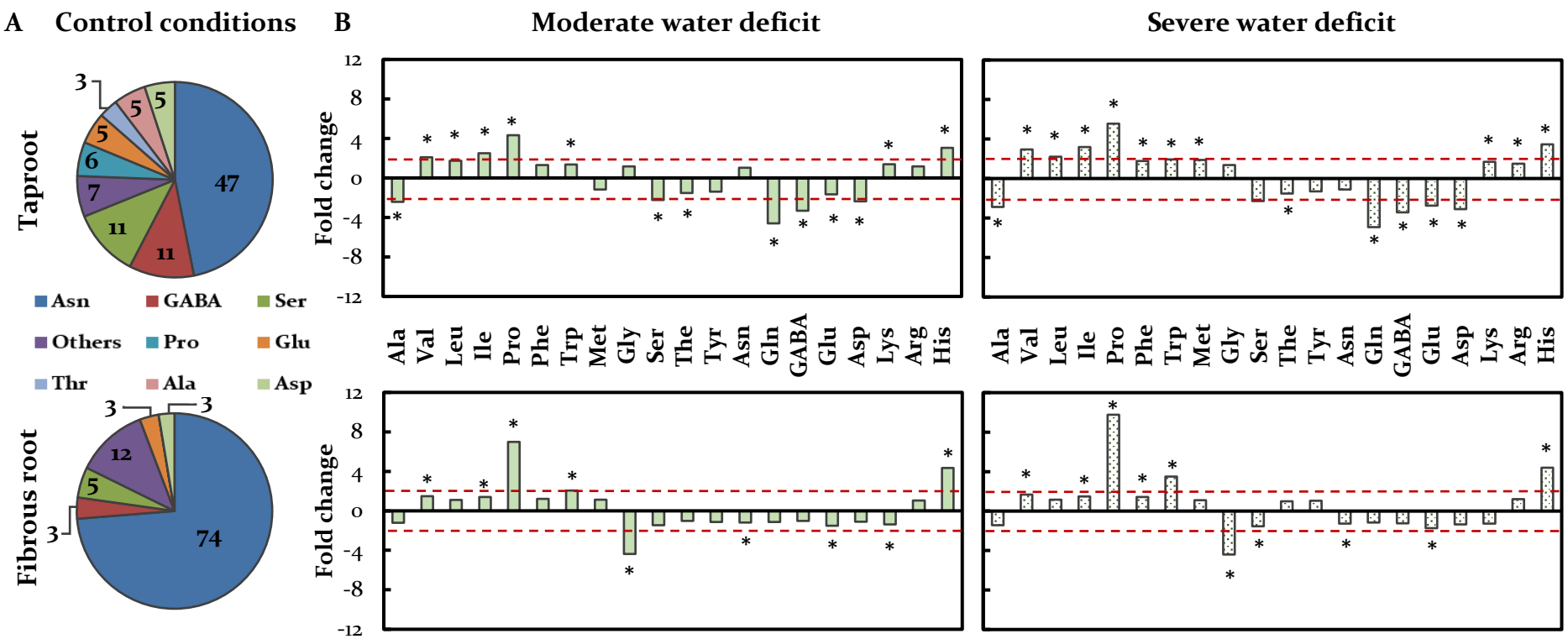

Figure 1.7. Relative amino acid composition of the roots under control and water-deficit stress conditions. A), soluble amino acid composition of the taproot and fibrous roots under control conditions. Values represent the relative amount (as %) of each individual amino acid. Those representing less than 3% of the total amino acid pool are pooled together in the pie chart tagged as "others". **B**), bars represent the mean (n = 5) fold change of the individual amino acid's relative content in response to moderate and severe water-deficit conditions. Asterisks indicate significant differences between control and drought treatments (Student's t-test, $p < 0.05$).

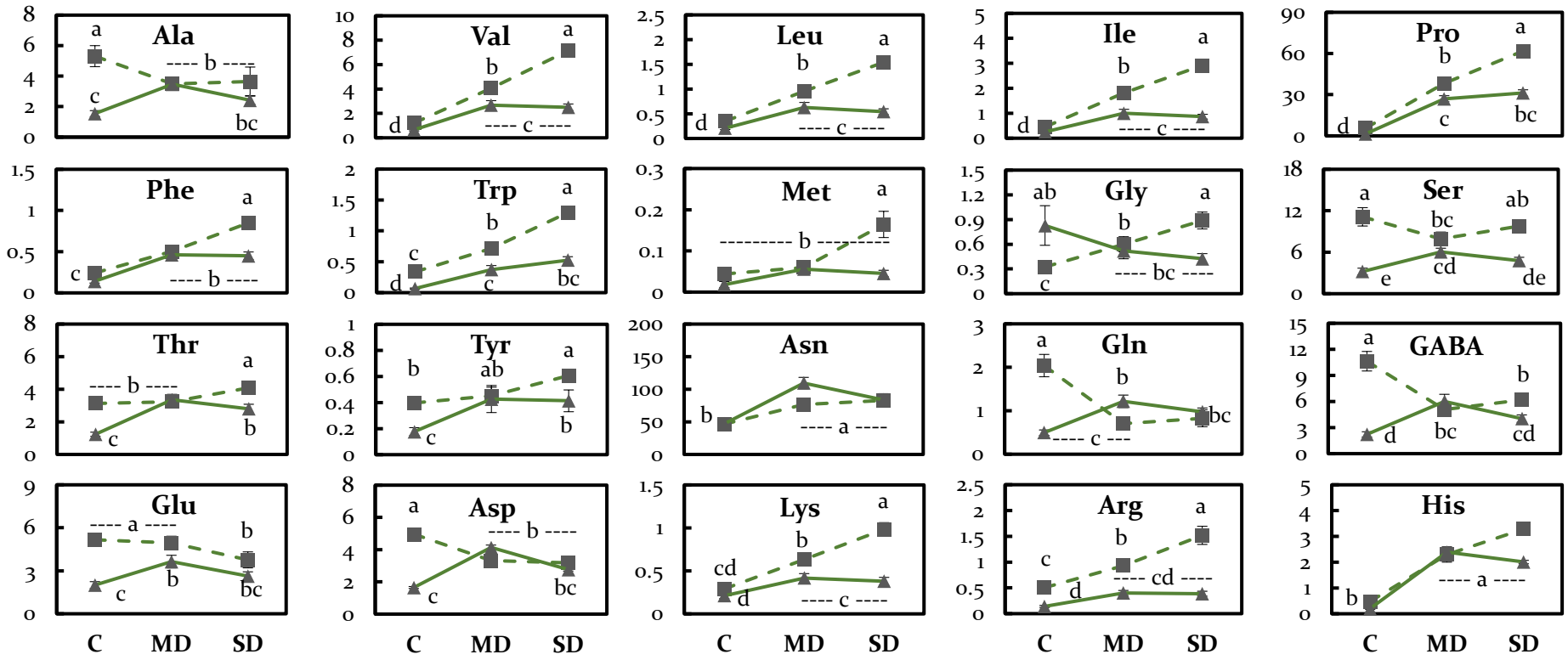

Figure 1.8. Absolute soluble amino acid content in drought-stressed roots. Absolute amino acid content (as µmol g DW^{-1}) in the taproot (dotted line, squares) and fibrous roots (continuous line, triangles) of *M. truncatula* under control (C), moderate (MD) and severe (SD) water-deficit stress conditions. Values are the mean ± SE (n = 5). Different letters indicate statistically significant different averages [two-way ANOVA followed by the Bonferroni *post hoc* test ($p < 0.05$). See **Table S1.2** for the two-way ANOVA results].

Among the measured enzymatic activities, only those whose activity was significantly affected by water-deficit stress are shown in **Fig. 1.9 and 1.10**, while those enzymatic activities showing non-significant differences are represented in **Fig. S1.1**. Amongst the enzymes related to carbon metabolism (**Fig. 1.9**), UDP-SuSy activity was as much as 40 times higher than that of ADP-SuSy in both root types and under all conditions. In addition, while both UDP- and ADP-SuSy decreased in response to water deficit, UDP-SuSy activity decreased significantly in both root tissues even at moderate water deficit, while the response of ADP-SuSy, although showing a similar trend, was less pronounced. Acid INV (acidINV) and alkaline/neutral INV (AlkINV) are also involved in the sucrose degradation route in the cell wall and cytosol, respectively, producing glucose and fructose in an irreversible manner. Cell wall acidINV showed similar activities in both root types under control conditions, declining significantly only under SD in the FibR. However, AlkINV was up to 4-fold more active than the acidINV and with a higher relevance in the FibR, specially upon water-deficit stress. GPDH, a major link between the carbon and lipid metabolism, and G6PDH, a key enzyme of the OPP pathway, were both unaltered in the tapR when roots were subjected to water-deficit stress. However, they both exhibited a clear response in the FibR: GPDH activity increased 3- and 5.5-fold under MD and SD, respectively, while G6PDH showed a loss of activity concomitant with the water-deficit stress level increment.

Regarding root N-assimilation, neither GOGAT nor GDH were significantly affected, while AAT and AlaAT were down-regulated in the FibR upon water-deficit stress (**Fig. 1.10**). P5CS and ProDH catalyze the synthesis and degradation of proline, respectively. Water-deficit stress did not affect P5CS in the tapR but led to a 2.4-fold increase in the case of the FibR. However, ProDH activity was induced by water deficit in both root types, exhibiting a higher basal activity in the tapR than in the FibR.

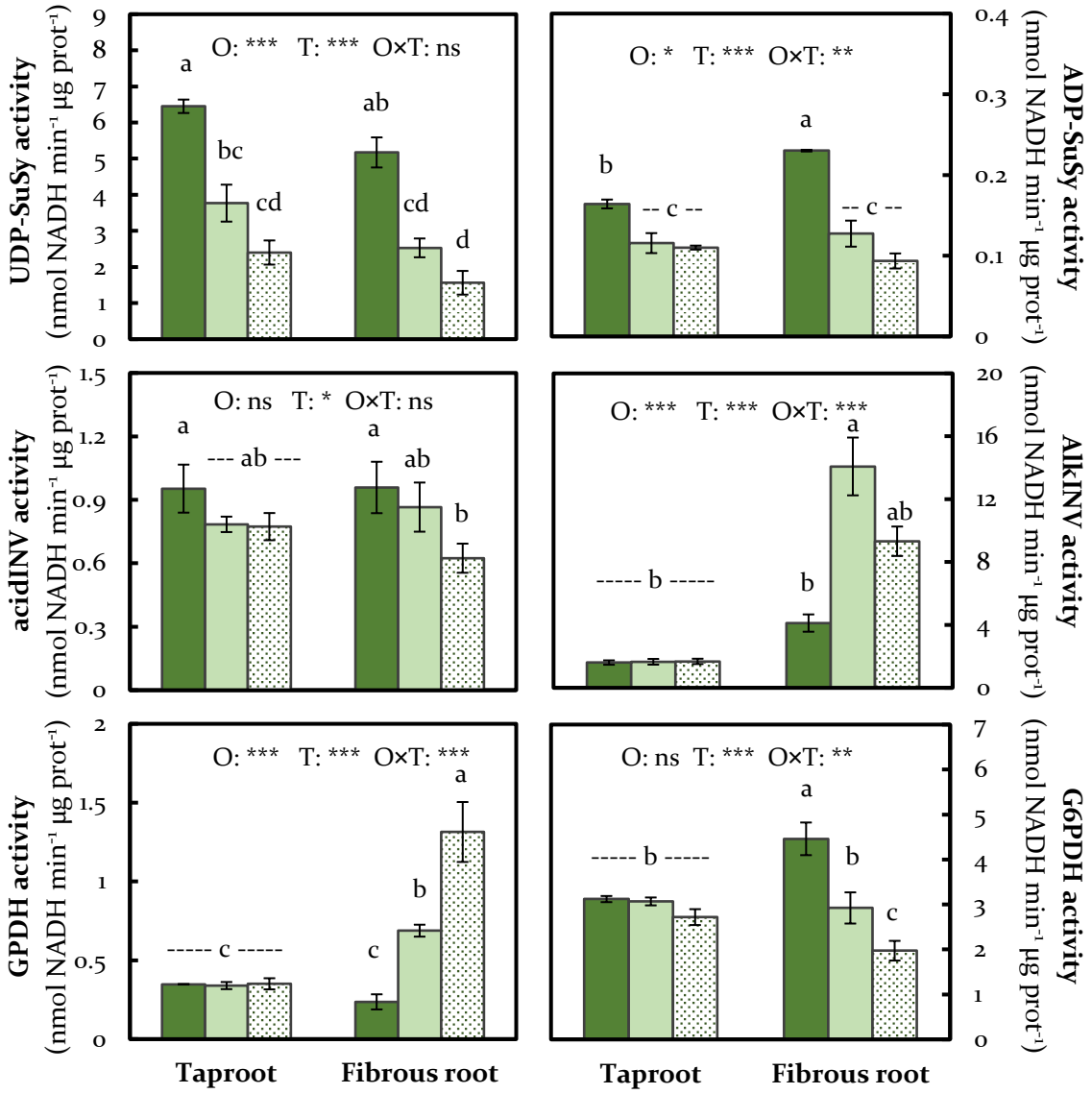

Figure 1.9. Carbon metabolism-related enzymatic activities' response to water-deficit stress in the root tissue. Enzymatic activities related to the carbon metabolism measured in the taproot and fibrous roots of *M. truncatula* under control (C, dark green), moderate (MD, light green) and severe (SD, dots) water-deficit stress conditions. Bars represent the mean ± SE (n = 4-10). A two-way ANOVA was performed and the *p*-values of the effects of organ (O), treatment (T) and their interaction (O×T) are indicated: ns > 0.05; $^{*}p < 0.05$; $^{**}p < 0.01$; $^{***}p < 0.001$. Different letters indicate significant different averages according to the Bonferroni *post hoc* test ($p < 0.05$). *acidINV*, acid invertase; *ADP-SuSy*, ADP-sucrose synthase; *AlkINV*, alkaline/neutral invertase; *G6PDH*, glucose-6-phosphate dehydrogenase; *GPDH*, glycerol-3-phosphate dehydrogenase; *UDP-SuSy*, UDP-sucrose synthase.

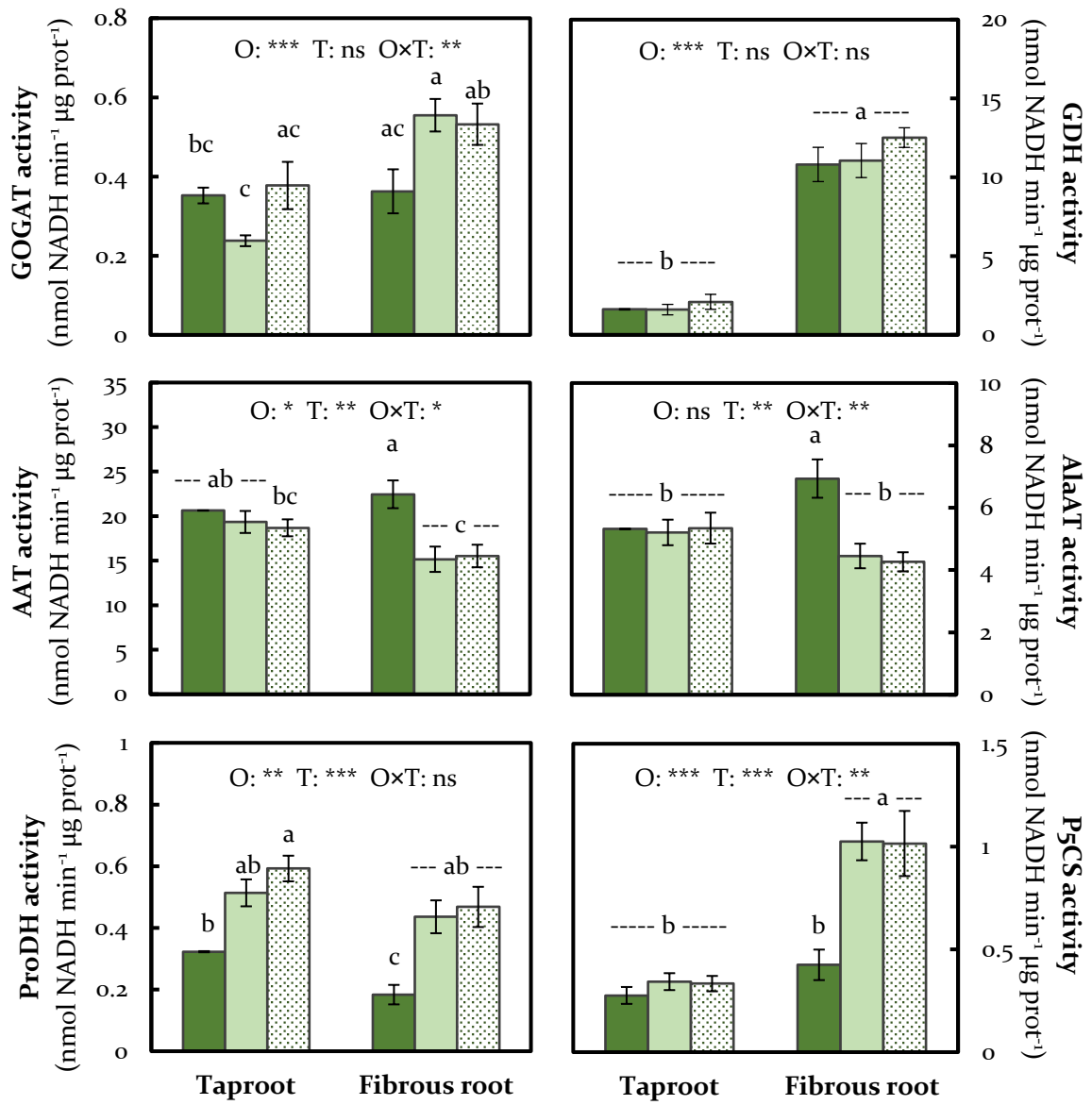

Figure 1.10. Nitrogen metabolism-related enzymatic activities' response to water-deficit stress in the root tissue. Enzymatic activities related to the nitrogen metabolism measured in the taproot and fibrous roots of *M. truncatula* under control (C, dark green), moderate (MD, light green) and severe (SD, dots) water-deficit stress conditions. Bars represent the mean ± SE (n = 4-10). A two-way ANOVA was performed and the *p*-values of the effects of organ (O), treatment (T) and their interaction (O×T) are indicated: ns > 0.05; $^{*}p < 0.05$; $^{**}p < 0.01$; $^{***}p < .001$. Different letters indicate significant different averages according to the Bonferroni *post hoc* test ($p < 0.05$). *AAT*, aspartate aminotransferase; *AlaAT*, alanine aminotransferase; *GDH*, glutamate dehydrogenase; *GOGAT*, glutamine oxoglutarate aminotransferase/glutamate synthase; *P5CS*, Δ^1-1-pyrroline-5-carboxylate synthase; *ProDH*, proline dehydrogenase.

Fig. 1.11 represents the ratio tapR/FibR expressed on a logarithmic basis for different enzyme activities, metabolites and physiological measurements under control conditions. Several enzymatic activities showed significant differences between both root types such as ADH, ProDH and UGPase, which were 2-fold more active in the tapR than in the FibR (**Fig. 1.11A**). Conversely, GDH, AGPase and AlkINV were around 7, 4 and 2.5-fold more represented in the FibR than the tapR, respectively (**Fig. 1.11A**). The tapR was enriched in sucrose, proteins and amino acids whilst glucose and fructose were more abundant in the FibR, in agreement with a higher respiratory activity in this root type (**Fig. 1.11B, C**).

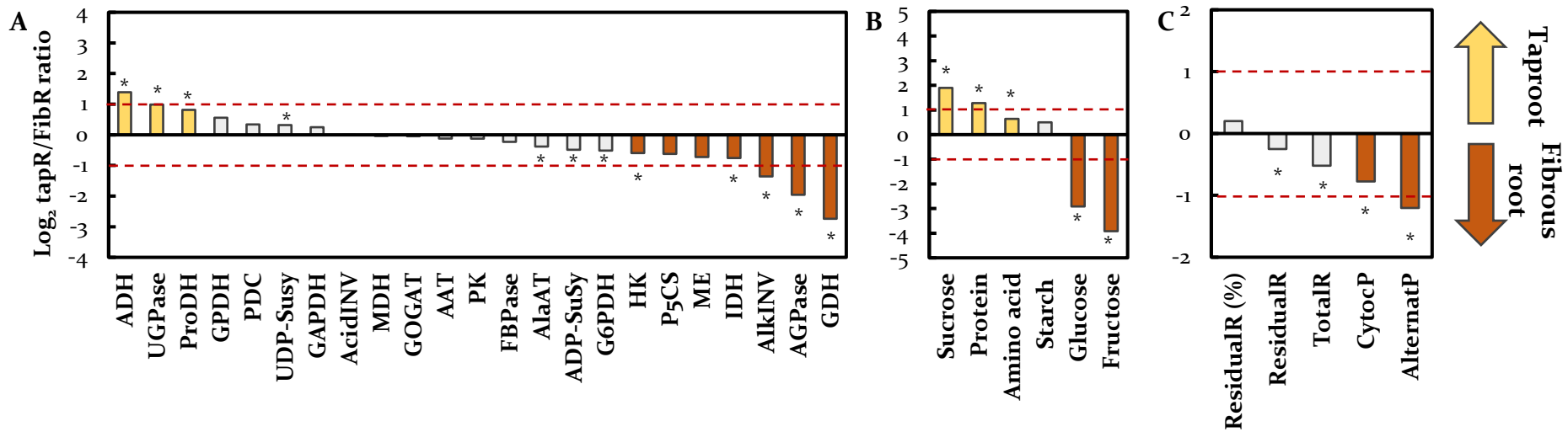

Figure 1.11. Distribution of enzymatic activities, metabolite contents and respiration rates between both root types. Bars represent the $\log_2$ of the taproot (tapR)/fibrous root (FibR) ratio for enzymatic activities (**A**), metabolites (**B**) and respiration rates (**C**) under control conditions. Yellow and brown bars represent ratios higher than 1.5-fold (more present in the taproot) or lower than -1.5-fold (more present in the fibrous root), respectively, while grey bars represent less significant changes. Asterisks indicate significant differences for a given parameter between the values of the taproot and the fibrous root (Student's t-test, $p < 0.05$). *AAT*, aspartate aminotransferase; *acidINV*, acid invertase; *ADH*, alcohol dehydrogenase; *AGPase*, ADP-glucose pyrophosphorylase; *AlaAT*, alanine aminotransferase; *AlkINV*, alkaline/neutral invertase; *AlternatP*, alternative pathway capacity; *CytocP*, cytochrome pathway capacity; *FBPase*, fructose-1,6-bisphosphatase; *GAPDH*, glyceraldehyde-3-phosphate dehydrogenase; *GDH*, glutamate dehydrogenase; *GOGAT*, glutamine oxoglutarate aminotransferase/glutamate synthase; *G6PDH*, glucose-6-phosphate dehydrogenase; *GPDH*, glycerol-3-phosphate dehydrogenase; *HK*, hexokinase; *IDH*, isocitrate dehydrogenase; *MDH*, malate dehydrogenase; *ME*, malic enzyme; *P5CS*, Δ^1-1-pyrroline-5-carboxylate synthase; *PDC*, pyruvate decarboxylase; *PK*, pyruvate kinase; *ProDH*, proline dehydrogenase; *residualR*, residual respiration; *SuSy*, sucrose synthase; *totalR*, total respiration; *UGPase*, UDP-glucose pyrophosphorylase.

1.5. DISCUSSION

1.5.1. Is the primary metabolism homogeneous in the whole root system?

In barrel medic, the primary root or taproot (tapR) is restricted to the top of the root system, while the lateral or fibrous roots (FibR) emerging from it account (volume and weight-wise) for most of the root system (**Fig. 1.3**). This study addresses the differences between the tapR and FibR of *M. truncatula* to better describe their role at the whole-plant level by examining the distribution of the different enzymatic activities, metabolites and physiological measurements (**Fig. 1.3-10**) under control conditions. **Fig. 1.11** summarizes all the measured parameters in this study as the tapR/FibR ratio on a logarithmic basis, allowing to see how the different parameters are represented in the different root types.

Attending to metabolic features, the tapR exhibited a remarkably high ADH activity which may be related to its thicker anatomy (**Fig. 1.11A**). ADH is related to the fermentative respiratory metabolism and maintenance of a constant NAD^+ supply (**Fig. 1.1**, Päpke *et al.*, 2013) and is usually reported to increase under hypoxic conditions (Fox *et al.*, 1994). Therefore, this high activity of ADH exhibited by the tapR suggests a role in carbon metabolism for this root type. Similarly, the high content of sucrose, the enhancement of UDP-SuSy and UGPase activities and the limited accumulation of starch in the tapR in comparison to the FibR (**Fig. 1.11A, B**) reinforce its active role on carbon partitioning rather than just on reserve storage. In addition, a role on starch storage is also dismissed attending to the activity of the enzyme AGPase, involved in the synthesis of ADP-glucose for starch synthesis (Geigenberger, 2011), which is 5-times less active in the tapR than in the FibR. Similarly, ADP-SuSy, which has also been related to ADP-glucose synthesis in the cytosol (Baroja-Fernández *et al.*, 2003), is also less active in the tapR (**Fig. 1.11A**). The distribution of sucrose-degrading enzymes between both root types was also remarkable: AlkINV activity was more abundant in the FibR than in tapR whereas UPD-SuSy behaved in the opposite way, although in the latter the difference between both root types was not so important (**Fig. 1.11A**). Indeed, sucrose degraded via

INV requires two molecules of ATP to be converted into hexose-phosphates, while the SuSy pathway linked to UGPase requires only one molecule of PPi (Stitt, 1998), and therefore this different strategy for sucrose metabolization in each root type could be related to the higher respiration rate exhibited by the FibR compared to the tapR (**Fig. 1.4A, 1.11C**). Even though the role of these sucrose-degrading enzymes in the plant's metabolism is still a matter of debate (Vargas and Salerno, 2010), while SuSy has been traditionally assigned to the role of sucrose cleavage, this role has also been assigned to INV in arabidopsis roots (Lou *et al.*, 2007), with some authors even declaring INV as the most important enzyme supplying carbon from sucrose to non-photosynthetic cells (Barrat *et al.*, 2009). On the other hand, the high level of glucose and fructose in the FibR (**Fig. 1.11B**) suggests a high rate of sucrose metabolization in the FibR, which is also in agreement with a higher activity of AlkINV and the pentose phosphate pathway, as suggested by the enhancement of G6PDH (**Fig. 1.9, 1.11A**). These results are in agreement with those reported in the most recent research conducted on *M. truncatula* roots (Echeverria and González, 2021).

Regarding N-metabolism, an important percentage of the soluble protein pool (around 40%) has been related to N-storage in alfalfa taproots (Staswick, 1994). In agreement with this, the soluble protein content pool of the tapR was more than 2-fold higher than that of the FibR (**Fig. 1.11**). In addition, the soluble amino acid pool was also more abundant in the tapR, suggesting a N-storage role in this root type. This is also the case for proline, postulated to function as nitrogen reservoir under stress (Albert *et al.*, 2012). Accordingly, ProDH, a mitochondrial enzyme activated by proline and responsible for its degradation, exhibited a high activity in the tapR (**Fig. 1.11A**) suggesting that Pro catabolism may have a role on N-partitioning. On the other hand, Asn, the most abundant amino acid and associated to N-transport in the plant, exhibited a similar concentration in both root tissues (≈50 µmols g DW^{-1}; **Fig. 1.8**). Nevertheless, when expressed in relative values, Asn accounted for the 74% of the bulk amino acid content of the FibR, which could be linked to the nutrient assimilation role of this root type (**Fig. 1.7A**). This

is supported by the high IDH and GDH activities detected in the FibR (**Fig. 1.11A**), enzymes mainly related to the supply of α-ketoglutarate for ammonium assimilation (Fontaine *et al.*, 2012; Hodges *et al.*, 2003).

In summary, specific features are present in each root type that suggest that they exert a different role in the physiology of the whole plant root system. However, in addition to nitrogen storage, the tapR seems to have a particular metabolic endowment to deal with carbon and nitrogen partitioning as well.

1.5.2. Common responses to water-deficit stress in the whole root system

Even though drought is one of the most important factors that inhibit photosynthesis, this decline occurs late during the onset of water-deficit stress whilst other processes such as cell growth and biosynthetic processes are rapidly affected at very moderate water potentials (see **sectionE.3.1**, Hsiao, 1973). Gargallo-Garriga *et al.* (2014) showed that the shoots and roots exhibit an opposite metabolic response to water deficit, playing the root a more active role in facing the effects of water-deficit stress. Through CO_2 assimilation, the shoot provides carbohydrates (mainly in the form of sucrose) to roots where they are mainly delivered to sustain root growth and respiration. However, most of the studies on the response of the respiratory process to water deficit have been focused on shoots (Flexas *et al.*, 2006), being scarce the results available at root level. Respiration is the main source of ATP needed for the uptake, transport and assimilation of nutrients and provides root cells with carbon skeletons for the biosynthesis of cellular components. Water-deficit stress is often reported to reduce respiration as a consequence of reduced carbon demand for growth, even though this inhibition can also be the consequence of a reduced carbon supply due to inhibited photosynthesis or damage in the root cell integrity derived from soil drying (Flexas *et al.*, 2006; Hasibeder *et al.*, 2015). In our study, root respiration was also negatively affected in both root tissues, with an increase in the contribution of the alternative pathway and residual respiration to the total respiration rate (**Fig. 1.4**). In our case, the increase in soluble sugars (**Fig. 1.5**) rules out a carbon deficiency state under drought stress, as previously observed (Muller *et al.*,

2011), while the decline in the respiration of the thicker tapR despite the lower alteration of other parameters such as WC and several enzymatic activities suggests a reduced carbon demand as the main cause of respiration inhibition.

As described in **section E.3.2**, the respiratory alternative pathway, which involves an alternative oxidase that directly reduces oxygen bypassing complexes III and IV, has been reported to confer tolerance to various stresses including salinity and drought (del Saz *et al.*, 2016; del Saz *et al.*, 2020; Saha *et al.*, 2016; Vanlerberghe, 2013; Vanlerberghe *et al.*, 2020). This is achieved thanks to its role in regulating ROS generation and, thus, all ROS-signaling pathways involved in plant response to stress, maintaining the homeostasis of mitochondrial energetics and function (Saha *et al.*, 2016). On the other hand, residual respiration, which is insensitive to KCN and SHAM and, thus, is not mediated either by the cytochromic nor the alternative pathways, increased its contribution to total respiration upon water-deficit stress, especially in the tapR (**Fig. 1.4B**). Even though the nature of this respiration is still under debate, with a possible origin in the fatty acid oxidation in peroxisomes/glyoxisomes and/or supplementary terminal oxidases, amongst others (Shugaeva *et al.*, 2007), it could also play an important role in plant stress tolerance (Chocobar-Ponce *et al.*, 2014). Hence, the increase in the alternative and residual respiration observed in our study is in agreement with previous observations and could have a key role in the regulation of ROS production and signaling, as well as in the regulation of intracellular soluble carbohydrates and the redirection of carbon metabolites for the enhancement of cellular defense against stress (Chocobar-Ponce *et al.*, 2014). Additionally, there was a a general and early decline of SuSy activity, dismissing a role of this enzyme on carbon supply for respiratory activity at this point (**Fig. 1.9**). The response of this enzyme to stress has also been reported to decrease in salted maize (Hütsch *et al.*, 2016), non-irrigated sorghum roots (Goche *et al.*, 2020) and drought-stressed nodules of soybean (González *et al.*, 1995) and *M. truncatula* (Arrese-Igor *et al.*, 1999), where it is an essential enzyme for N-fixation (Gordon *et al.*, 1999). No reports on the response of this enzyme in drought-stressed *M. truncatula* roots had been published at the time this work was done, but similar results in recent works in our group (Castañeda *et al.*, 2021; Echeverria and Gonzalez, 2021; Echeverria *et al.*,

2021) further suggest that SuSy could be an interesting marker of early water-deficit stress in this plant.

Regarding amino acids, the observed overall accumulation (**Fig. 1.6**) is a common response towards water-deficit stress amongst various plant species and organs (Gil-Quintana *et al.*, 2013; Rouached *et al.*, 2013;). It is well known that protein biosynthesis is early hampered under drought stress in harmony with plant cell growth (Sharma and Dubey, 2019). On the other hand, the accumulation of free amino acids is a commonly observed phenomenon under drought stress due to the osmoprotectant nature of these compounds (Signorelli *et al.*, 2016), being the cause for this increment their reduced incorporation into new proteins, *de novo* synthesis (especially in the case of proline), or increased proteolysis (like in the case of BCAAs) (Hildebrandt, 2018; Huang and Jander, 2017). Our study showed how Pro and His were the two amino acids that were accumulated to the largest extent in both root types, even at moderate water-deficit stress (**Fig. 1.7B, 1.8**). Proline has been described to act as a compatible compound for osmotic adjustment. More specifically, this amino acid has been described to retain water and protect and stabilize macromolecules and structures from stress-induced damage (Rouached *et al.*, 2013). In plants, proline is synthesized mainly from glutamate by the P5CS enzyme, whilst its catabolism occurs via the sequential action of ProDH (producing P5C) and P5C dehydrogenase, which converts P5C to glutamate (see **section E.3.4**, reviewed in Szabados and Savouré, 2010). Although P5CS activity was only induced in the FibR (**Fig. 1.10**), ProDH activity increased in both tissues in response to water-deficit stress. ProDH has been described to be down-regulated in other plant systems exposed to different water-deficit stresses (Miller *et al.*, 2005; Phutela *et al.*, 2000; Rouached *et al.*, 2013). Nevertheless, Verdoy *et al.* (2006) also observed a ProDH up-regulation in roots and nodules of salt-stressed *M. truncatula* plants, suggesting that the induction exerted by the high proline concentration surpasses the down-regulation effect of dehydration under moderate stress conditions. Indeed, the proline catabolism pathway can be used to generate energy and reducing equivalents for the TCA cycle when the respiratory flux is blocked, being considered a tolerance mechanism to water-deficit stress (Kaur and Asthir, 2015; Kishor *et al.*, 2005).

Summarizing, both root types exhibited a similar strategy to face water deficit: respiration decreased despite the over-accumulation of sucrose and simple sugars, indicating a lower carbon demand. On the other hand, the increase in the alternative and residual respiration observed in our study could have a key role in the regulation of ROS production and signaling, as well as in the regulation of intracellular soluble carbohydrates and the redirection of carbon metabolites towards the enhancement of cellular defense against stress. Even though the increase in soluble sugars and has been widely reported as a common response to water-deficit stress, we suggest an important role of proline catabolism in the tolerance of *M. truncatula* to drought.

1.5.3. The taproot is more resilient to water deficit than the fibrous root: SuSy and ProDH are first affected by water-deficit stress

Despite the physiological and metabolic similarities under control conditions and the common responses to water deficit observed in the tapR and FibR discussed in **sections 1.5.1 and 1.5.2**, several specific features in both root types were noticeable. The tapR was able to keep a higher water content (> 65%) than the FibR upon water-deficit stress, responding similarly to the aerial part (**Fig. 1.3**). Accordingly, all measured parameters showed a better resilience towards stress in the tapR. The totalR rate decreased less markedly in the tapR than in the FibR, and the AlternatP/CytocP capacity ratio was not affected in the tapR under MD whilst it increased almost 3-fold in the FibR at this water stress level (**Fig. 1.4C, D**). Starch degradation was unaffected in the tapR under MD whilst a 50% reduction in starch content was observed in the FibR (**Fig. 1.5**). In addition, most of the analysed enzymes were fully unaffected in the tapR, while actively responding in the FibR upon water-deficit stress (**Fig. 1.9, 1.10**).

However, despite the higher resilience exhibited by the tapR, some responses were readily activated in this tissue, which may be interpreted as a primary response to water deficit at the root level. The more marked effects observed in the tapR under MD concerned UDP-Susy and ProDH activities (**Fig. 1.9, 1.10**). UDP-SuSy was rapidly inhibited in accordance with a marked accumulation of sucrose (**Fig. 1.5**). Attending to primary metabolism, both SuSy and INV can catalyse the cleavage reaction of sucrose. However,

SuSy might be more involved in the biosynthesis of sugar polymers such as starch and cellulose and ATP generation, while INV might have a wider range of regulatory functions additional to its role in primary carbon metabolism (Ruan *et al.*, 2010). In arabidopsis roots, cytosolic INV has been shown to be essential for normal plant development, being capable of compensating the loss of SuSy activity but not vice-versa (Barratt *et al.*, 2009). However, this compensation mechanism did not work in other sinks as maize seeds (Cheng and Chourey, 1999). In the present study, as observed by Echeverria and González (2021), the compensatory role of AlkINV worked exclusively in the FibR (**Fig. 1.9**) which may suggest a higher need of this root type for maintenance of the sink strength through sucrose unloading from the phloem. Accordingly, the higher starch levels in the tapR (**Fig. 1.5**) suggest a lower need for shoot carbohydrate import and a lower level of water-deficit stress in this root type. In the last decade, new roles are being explored in relation to INV besides sucrose metabolization in primary metabolism (Ruan *et al.*, 2010). Indeed, INV is emerging as a key regulator of assimilate partitioning and plant response to the environment and its increase upon drought suggests a key role in sucrose unloading and degradation in roots which could support growth under these conditions (Xu *et al.*, 2015).

Similarly, ProDH activity also exhibited an early increase in the tapR (**Fig. 1.10**) accompanied by a rapid accumulation of proline in this root part (**Fig. 1.8**). ProDH transcript-level response to water deficit is quite controversial and its up-regulation (Verdoy *et al.*, 2006) and down-regulation (Miller *et al.*, 2005) have been already documented in *Medicago* species. Recently, a role in oxidizing excess proline and transferring electrons to the respiratory chain has been indicated for ProDH in arabidopsis (Cabassa-Hourton *et al.*, 2016), which may act as an alternative source of energy when carbon metabolism is being impaired (**Fig. 1.4, 1.9**). In addition, the BCAAs Leu, Ile and Val had a higher absolute and relative presence under control conditions and increased linearly upon water-deficit stress in the tapR (**Fig. 1.7, 1.8**). Accordingly, Virlouvet *et al.* (2011) observed that BCAA biosynthesis was enhanced under water-limited conditions and contributed to maintaining kernel yield in maize. Pires *et al.* (2016) have recently shown in arabidop-

sis plants that BCAAs can also be used as alternative electron donors to the mitochondrial ETC, reinforcing their role on water-deficit tolerance most likely delaying the onset of stress. Hence, this increase proline oxidation and higher BCAA content could suggest a change of respiration substrate from sucrose, allowing sucrose and starch build-up in the tapR for regrowth after the water-deficit stress disappears.

In addition to the INV increase, another distinct response to water-deficit stress in the FibR root type was the increase in glycerol-3-phosphate dehydrogenase (GPDH) activity (**Fig. 1.9**). This enzyme catalyzes the reversible formation of glycerol-3-phosphate (G3P) from dihydroxyacetone phosphate and NADH, playing a key role in glycerol and lipid synthesis and in modulating NADH/NAD^+ ratio. In addition to being an important link between lipid and carbohydrate metabolism, it is a major contributor of electrons to the mitochondrial respiratory chain and has been reported to confer tolerance to water-deficit stress (Shen *et al.*, 2006; Zhao *et al.*, 2018). This could be due to the compatible solute nature of glycerol (Bahieldin *et al.*, 2013; Casais-Molina *et al.*, 2016; Chen *et al.*, 2009), but other mechanisms have also been suggested such as increased unsaturation of membranes (e.g., protecting photosystems from photoinhibition) (Sui *et al.*, 2017), the involvement of G3P in lipid defense-signals generation (Kachroo *et al.*, 2004) and, perhaps more importantly, the high relevance of this enzyme in maintaining cellular redox homeostasis (Shen *et al.*, 2006). Actually, this enzyme was reported to increase its expression upon fluctuations in the NADH/NAD^+ ratio while also being affected by O_2 availability, suggesting a link with mitochondrial respiration (Shen *et al.*, 2006).

In summary, the response of the tapR to water-deficit stress was milder to that of the FibR in regard to the lower response of the WC as well as several metabolites and enzymatic activities in this root type. However, UDP-SuSy and ProDH were readily affected even in the tapR, suggesting a higher sensitivity to stress and hence becoming potential good markers of water-deficit stress. In addition, the increase in proline catabolism and BCAA accumulation could be used as potential additional substrates for root respiration under adverse conditions. On the other hand, the induction of GPDH and AlkINV in the FibR could offer additional means to avoid drought negative effects in this root type.

1.6. CONCLUSIONS

In conclusion, specific metabolic features were present in each root type that suggest that they exert a different role in the physiology of the whole-plant root system. The taproot (tapR) seemed to have a particular metabolic endowment to deal with carbon and nitrogen partitioning, in addition to its role in nitrogen storage. Overall, both root types exhibited a similar strategy to face water deficit, although the tapR exhibited a higher resilience to this stress than the fibrous root (FibR). An early blockage of sucrose metabolism occurred at the level of sucrose synthase (SuSy) activity leading to a marked accumulation of sucrose in the root. The overall accumulation of amino acids dismissed any nitrogen limitation, while the enhancement of proline catabolism may contribute to counterbalance the deficiencies in carbon metabolism throughout the respiratory pathway. In addition, the higher resilience of the tapR than the FibR towards water-deficit stress made this root type an interesting target of breeding programs improving plant tolerance towards stress focusing on the different functionality of the root system. Lastly, the enhancement of root invertase (AlkINV) and glycerol-3-phosphate dehydrogenase (GPDH) in the FibR suggest key roles in the drought tolerance of this plant, opening the doors to future studies that confirm their relevance.

› CHAPTER 2

Strategies to apply water-deficit stress: similarities and disparities at the whole-plant metabolism level in *Medicago truncatula*

Published in *Int. J. Mol. Sci.* (2021) 22: 2813

2.1. INTRODUCTION

Plant growth, development and productivity are adversely affected by various abiotic stress factors, being drought and soil salinity the major problems reducing crop productivity by more than 50% (Mahajan and Tuteja, 2005). It is then of outmost importance to breed crops capable of tolerating or resisting these stresses without a significant impact on their yield. However, the knowledge about drought and salinity stress resistance is still limited (Luo *et al.*, 2019) partly due to the complexity of the trait, which involves important metabolic and physiological changes at the whole-plant level. Water deficit can be defined as any water content of a tissue or cell below the highest water content exhibited in the most hydrated state. Hence, although the terms "drought stress" and "water-deficit stress" are usually employed indistinctively, water does not only become limiting for plant communities as a result of inadequate rainfall but also due to other environmental conditions like excessive salinity in the soil solution. Both drought and salinity cause osmotic stress by lowering the water potential of plant cells, which can lead to cell turgor loss, membrane disorganization, protein denaturation, inhibition of photosynthesis and oxidative damage and, thus, both stresses share many plant responses (Krasensky and Jonak, 2012). However, in addition to the cellular water deficit provoked by the presence of salts, salinity stress also has an ionic component that further alters plant ion homeostasis through Na^+ and Cl^- toxicity.

Both water-deficit stresses affect plant growth and development through changes in the plant biochemistry, physiology and morphology which have been investigated independently in many plant species, including *Medicago truncatula* (Castañeda *et al.*, 2021; Larrainzar *et al.*, 2014; Nunes *et al.*, 2008). Studies comparing different osmotic stresses are much less common, with a few done in some crop plants such as *M. falcate* (Miao *et al.*, 2015) and rice (Do *et al.*, 2014). In *M. truncatula*, Staudinger *et al.* (2012) observed significant differences in the degree and strategy of early drought, as compared to salt stress response, concluding that N-nutrition seems of crucial importance for plant stress acclimation. However, more studies are needed in order to better understand plant response to different water-deficit stresses.

In general, water-deficit stress implies a negative effect in almost all metabolic processes in the plant, with major detrimental impacts on the cellular energy supply and redox homeostasis, which requires a global reprogramming of the plant primary metabolism (see **section E.3**, Golldack *et al.*, 2014). Amongst the most readily and profoundly altered functions are photosynthesis and cell growth. The growth of both shoots and roots are in competition for the available assimilates, water and minerals and, hence, are coordinated and vary depending on the environmental conditions in order to optimize the use of these valuable nutrients with the least penalty on plant yield. However, it is leaf growth the first to be inhibited by a reduced water potential in the medium or tissue due to its slower ability to adjust osmotically and recover its turgor compared to the root (Hsiao and Xu, 2000). On the other hand, the alteration of photosynthesis usually derives in the formation of ROS, whose accumulation leads to oxidative damage. However, plants have evolved diverse mechanisms to reduce their formation and/or impact such as the activation of antioxidant enzymes and molecules or the accumulation of compatible solutes such as proline (see **sections E.3.4 and E.3.5**, Upadhyaya *et al.*, 2013). The accumulation of amino acids and soluble sugars is also a means to facilitate water uptake by decreasing the water potential of the plant to a higher extent than that of the soil, in a process called osmoregulation. Inorganic ions can also be used for this purpose, but their accumulation is restricted to the vacuole, where they do not denature proteins or destabilize the membrane. In addition to osmotic adjustment, some of these solutes have other functions that improve plant tolerance towards stress, such as membrane and protein stabilization or carbon, nitrogen and energy storage (Singh *et al.*, 2015).

It is not surprising that no-irrigation and salinity stress lead to a severe alteration of the carbon and nitrogen metabolism of the plant, which are the main providers of energy and nutrients of the plant (Cui *et al.*, 2019a). Carbon metabolism, including photosynthesis, sucrose and starch metabolism or carbohydrate utilization, provides carbon skeletons, energy and reducing power that can be used in nitrogen metabolism-related processes such as nitrogen assimilation and amino acid and protein synthesis. On the other hand, nitrogen compounds include amino acids, proteins (including Rubisco and light-harvesting complexes), nucleotides and chlorophyll, amongst others, being thus very

important for photosynthesis, amongst other processes (Nunes-Nesi *et al.*, 2010). Inorganic nitrogen is taken up by roots and can be assimilated in this organ thanks to the energy and carbon provided by the respiration of sucrose imported from shoots, or can be transported to the leaves and be assimilated there with the support of photosynthesis (Nunes-Nesi *et al.*, 2010). Thus, both metabolisms are highly integrated and depend on one another, requiring a complex regulatory machine that coordinates them, involving signals derived from NO_3^- and NH_4^+, nitrogen-containing metabolites such as amino acids, availability of reducing power and metabolites related to the carbon metabolism (Nunes-Nesi *et al.*, 2010). The coordination of carbon and nitrogen assimilation ensures the availability of amino acids and carbon skeletons, building blocks of biomass production and important compounds associated with increased water-stress tolerance, at the required amounts and moment (Nunes-Nesi *et al.*, 2010). Due to their essential roles in plant metabolism, the maintenance of carbon and nitrogen assimilation is very important to maintain source/sink relationships and improve water-deficit stress tolerance, thus minimizing stress-induced yield losses (Ren *et al.*, 2020). However, despite their high relevance on plant growth and stress tolerance, their response to water-deficit stress is still not fully understood (Cui *et al.*, 2019a).

Once the nitrogen is assimilated into amino acids, their transport occurs in both the xylem and the phloem sap. However, the transport of carbon assimilates mostly occurs in the phloem, a part of the vascular system that connects all plant parts and directs the movement of these metabolites from their sites of synthesis ("sources", such as mature leaves) to the sites of utilization or "sinks" (heterotrophic organs such as roots or growing leaves) (Griffiths *et al.*, 2016). Carbon transport is thus influenced by source and sink activities, so the phloem transport integrates the whole plant metabolism and affects aspects such as growth, stress tolerance and reproduction (Savage *et al.*, 2016). The most accepted mechanism for phloem transport drive is explained by an osmotic pressure differential between the source and sink tissues. This implies that changes in the sink and/or source tissues such as those triggered by abiotic stresses can alter phloem transport (Lemoine *et al.*, 2013; Pommerrenig *et al.*, 2007; Sevanto, 2014, 2018). Despite the crucial role of the phloem as essential metabolite transporter and its impact on

plant-environment interactions, little research has been done on how its potential function alteration influences plant response to stress (Savage *et al.*, 2016). However, compelling studies suggest that the response of the phloem sap to stress conditions such as drought might predict plant survival and recovery capacity and can, in any case, help us better understand the response to stress at a whole-plant level (Sevanto, 2018).

The lack of research on the phloem sap can be partly attributed to the challenges involved in its recollection such as the high turgor pressure in the sieve elements, its small volume, the wounding protection mechanisms or the potential contamination derived from the sudden pressure release when collected, which can disrupt organelles and pull substances from surrounding cells such as companion cells. In addition, the sap composition greatly depends on the chosen collection method (Turnbull and López-Cobollo, 2013). Among the different methods to extract phloem sap a highly used one is based on its exudation from cut petioles or stems in the presence of EDTA, which chelates calcium and thus inhibits callose synthesis and the consequent sealing of the cut petiole, allowing exudation to occur for extended periods (King and Zeevaart, 1974). To our knowledge and up to this date, only one study has been conducted in *M. truncatula* considering the phloem sap and its response to water-deficit stress (Castañeda *et al.*, 2021). In this proteomics study, Castañeda *et al.* described the existence of a core stress responsive proteome in *M. truncatula* across different tissues including the phloem sap, suggesting a major role of the phloem in stress protection and antioxidant activity, especially by linking below- and above-ground communication in order to fine-tune the stress response. Other studies considering the phloem sap and different water-deficit stresses have been made in tomato (Ogden *et al.*, 2020; Pérez-Alfocea *et al.*, 2000), *Plantago major* (Pommerrenig *et al.*, 2007), white clover (Lee *et al.*, 2009), *Ricinus communis* (Jeschke and Pate, 1991), maize (Lohaus *et al.*, 2000) and alfalfa (Girousse *et al.*, 1996).

Different experimental systems are usually employed to tackle the strategies to face abiotic stress by plants. In order to mimic drought stress conditions, the media or nutrient solutions used for plant growth are usually supplemented with polyethylene glycol (PEG), mannitol or sorbitol. Mannitol and sorbitol are naturally occurring sugar alcohols

which accumulate in some plants, and not surprisingly they are taken up from the growing medium when present, interfering in the plant metabolism (Osmolovskaya *et al.*, 2018). On the other hand, the highly viscous PEG-containing nutrient solutions might lead to root hypoxia and, even though some authors believe that the high molecular size of PEG-6000 impedes it from entering the roots, it has been reported to penetrate and accumulate in various plants, which can lead to changes in plant growth additional to those inherent to osmotic stress (Osmolovskaya *et al.*, 2018). However, PEG is still the most used osmoticum to mimic drought stress, obviating the possibility of tissue contamination and generating conclusions that aim to be relevant to this stress (Peng *et al.*, 2017; Zhang and Shi, 2018). Regarding salinity, NaCl is the most common chemical formula used to mimic salt stress *in vitro*. However, other salts are commonly included in comparison experiments to discern among the toxicity of the different ions, with KCl being one of the most frequently employed (Jung *et al.*, 2017).

Many authors have studied the effect of water-deficit stress in leaves (Luo *et al.*, 2016) or roots (Echeverria and González, 2021; Long *et al.*, 2016), but not many have simultaneously addressed the response in both organs (Lyon *et al.*, 2016; Zhang *et al.*, 2014) and even fewer at the whole-plant level including the phloem sap (Castañeda *et al.*, 2021; Lee *et al.*, 2009), even though the study of a plant as a whole can give us a unique and valuable information and understanding of its response to stress. Hence, the study of several water-deficit treatments at various organs simultaneously and from various perspectives in this work provides us invaluable information that can be used in research focused on the improvement of the selection and breeding of genotypes under water-deficit stress.

2.2. OBJECTIVE

We hypothesize that the impact of different osmotic treatments frequently applied to simulate water-deficit stress is markedly different at the whole-plant level. In the present study, different stresses modifying the cell water status (water-deficit stress) are compared in order to identify the similarities and differences in the mechanisms involved at the whole-plant level in the response to each stress. PEG-6000 and no-irrigation (No-W) are employed to induce drought stress, while NaCl and KCl provoke salt stress. The whole plant physiology and metabolism is explored by characterizing the stress responses at root, phloem sap and leaf levels.

2.3. MATERIALS AND METHODS

2.3.1. Plant material and stress treatments

M. truncatula seeds were scarified with sulfuric acid 98% for 7 min, washed and then sterilized with 3.5% sodium hypochloride for 90 s. After a thorough wash, the seeds were soaked in water and left shaking in the dark for 6 h. When the seeds were hydrated, they were transferred to 7‰ agar plates at 4 °C for one day in the dark and then incubated at 20 °C for two days. The seedlings were then planted in 1-L brown plastic pots with perlite/vermiculite (1/3, *v/v*) and grown for 11 weeks in a controlled chamber [22/18 °C day/night temperature, 70% relative humidity, 500 µmol m^{-2} s^{-1} (PPFD), 12-h photoperiod] and irrigated with Evans medium supplemented with 5 mM NH_4NO_3 (Evans, 1981).

KCl, NaCl, no-watering (No-W) and PEG-6000 stress were applied to provoke a drop of the leaf water potential (Ψ_{leaf}) similar to a moderate water-deficit level. Ψ_{leaf} was around -0.5 MPa in field-capacity irrigated plants and it was brought to ≈-1.7 MPa after the application of the different stresses. Salt stresses were applied by watering plants with 0.25 M KCl or NaCl (after a daily $_dH_2O$ pre-wash), which generated an osmolarity of 450 mmol Kg^{-1} in the solution. The No-W treatment was applied by limiting water irrigation to 2/3 of the daily transpired water. Lastly, 250 g L^{-1} PEG-6000 were dissolved in water to reach the same osmolarity than the above-described salt solutions. Control plants were watered daily with $_dH_2O$. All treatments were applied for 7 days, and then plant physiology parameters were determined one hour after the beginning of the photoperiod. In addition, different aliquots of leaf and lateral-root tissue were collected and stored at -80 °C for further analysis. In the case of PEG-treated plants a large variation in the Ψ_{leaf} response was observed and only the ones with Ψ_{leaf} ≈ -1.7 MPa were selected for further experiments.

2.3.2. Physiological measurements

Plant transpiration was gravimetrically determined on a daily basis by weighting the pots one hour after the beginning of the photoperiod. Ψ_{leaf} was measured at this time

point in the second fully expanded leaf using a pressure chamber (Soilmoisture Equipment, Santa Barbara, CA, USA) as earlier described (Scholander *et al.*, 1965). Stomatal conductance was measured with a dynamic diffusion porometer (AP4; Delta-T devices, Cambridge, UK) in leaflets of the second fully expanded leaf. Chlorophyll content was measured in five leaves per plant using a SPAD-502 meter (Konica-Minolta, Osaka, Japan) in leaflets of the second fully expanded leaf. Leaf and root water content (WC) was determined on the basis of the fresh weight (FW) and the dry weight (DW) obtained after 48 h drying at 70 °C using the previously described formula (1).

2.3.3. Phloem sap exudation

Phloem sap exudation was performed as indicated by Rahmat and Turnbull (2013) with minor modifications (**Fig. 2.1**). Petioles were cut with razor blades in buffer containing 10 mM EDTA, 10 mM HEPES pH 7. After gently drying the cut with paper, 10 leaves per plant were arranged and soaked in Eppendorf tubes containing 1.5 mL of the above-mentioned buffer. The phloem sap was exudated in the dark at 21 °C with the opening of the tube sealed with parafilm tape and in saturated humidity conditions. After exudating for 22 h, the leaves were carefully removed from the tube, and exudated extracts were frozen in liquid N_2 and stored at -80 °C for further use.

Figure 2.1. Arrangement of the EDTA-facilitated phloem exudation system. A) 10 *Medicago truncatula* leaves were soaked in 10 mM EDTA buffer and left overnight in the dark in saturated humidity conditions. This setup was based on the one used by Rahmat and Turnbull (2013) (**B**) but, additionally, parafilm tape covering the remaining Eppendorf tube opening in order to avoid evaporation was included (not shown).

2.3.4. PEG uptake measurement

The following procedure was adapted from the method described by Hyden (1956). Frozen leaves and roots aliquots (≈0.15 g) of all PEG-treated plants were homogenized in 1 mL extraction buffer (50 mM MOPS pH 7.5, 10 mM $MgCl_2$, 20 mM KCl), and samples were centrifuged for 5 min at 11,500 × *g*. The supernatant was then pipetted into a centrifuge tube and 0.6 mL of 10% (*w*/*v*) $BaCl{\cdot}2H_20$, 0.6 mL of saturated $Ba(OH)_2$ and 0.6 mL of 5% (*w*/*v*) $ZnSO_4{\cdot}7H_2O$ were added with shaking between each addition. The tubes were allowed to stand for at least 5 min and then were centrifuged at 7,600 × *g*. The supernatant was mixed with 3 mL TCA solution (450 g TCA and 50 g $BaCl_2{\cdot}2H_2O$ in 1 L $_{dd}H_2O$) and left for 5 min. The turbidity was then measured as the percentage of light absorbed at 600 nm, and the PEG content was calculated using a calibration curve (Janes, 1974). The measured turbidity value in control plants was considered as zero.

2.3.5. Determination of soluble sugar and starch content

The determination of the soluble sugars as well as starch contents was performed as described in **section 1.3.4**. The soluble sugar analysis in the phloem sap was performed directly using the exudates.

2.3.6. Determination of organic acids and inorganic ions

Frozen samples (≈100 mg) were homogenized to a fine powder in liquid N_2 using a mortar and pestle. For organic and inorganic anions, 1.5 mL of 10% (*w*/*v*) TCA were added, and the homogenate was centrifuged for 10 min at 1,750 × *g* and 4 °C. The aqueous phase was washed three times with ethyl ether saturated with $_{dd}H_2O$. The upper ether solution was discarded, and the aqueous phase was purged with N_2 gas for 2 min and subsequently filtered (0.45 nm pore size). For cations, finely ground leaf and root material was extracted with 1 mL $_{dd}H_2O$ for 30 min at 90 °C. After centrifugation (12,500 × *g*, 10 min), the supernatant was collected and centrifuged again for 5 min. Ion levels were determined by ion chromatography in a DX-500 system (Dionex Ltd., Sunnvale, CA, USA). Cations were analysed by isocratic separation (CS12A columns) and anions by gradient separation (AS11 column; 2.5 mM NaOH/18% methanol to 45 mM NaOH/18% methanol in 13 min) according to the manufacturer's instructions.

2.3.7. Determination of free amino acid content

Frozen leaves (≈70 mg FW) and roots (≈150 mg FW) were ground to powder under liquid N_2 and subsequently homogenized using a mortar and pestle with 3 mL 1 M HCl. The determination of the free amino acid content was then performed as described in **section 1.3.5**. In the case of the phloem sap, internal standards were directly added to the exudates.

2.3.8. Determination of small antioxidants

Frozen samples (≈130 mg FW leaves and ≈180 mg FW roots) were ground to powder in liquid N_2 and subsequently homogenized with 1 mL of ice-cold 2% (*w*/*v*) metaphosphoric acid (*w*/*v*). The homogenate was centrifuged at 4,400 × *g* and 4 °C for 2 min. Antioxidants were analysed by high-performance CE in a Beckman Coulter P/ACE system 5500 (Beckman coulter Inc., Fullerton, CA, USA) associated with a diode array detector, as described by Herrero-Martínez *et al.* (2000). The CE instrument was equipped with the P/ACE station software for instrument control and data handling. The background buffer was 60 mM NaH_2PO_4 pH 7 containing 60 mM NaCl and 0.0001% hexadimethrine bromide. The applied potential was 15 kV, and the capillary tubing (50 µM) was 30/37 cm long. The indirect UV detection wavelength was set at 200 and 265 nm. Reduced ascorbate (ASC), glutathione (GSH) and homoglutathione (hGSH) were determined directly by injecting a plant extract aliquot in the CE as described above. Dehydroascorbate (DHA) and oxidized glutathione (GSSG) and homoglutathione (hGSSG) were reduced with DTT, and then total ascorbate and glutathione were directly analysed by CE. DHA, GSSG and hGSSG levels were determined as the difference between total ascorbate, glutathione and homoglutathione and their respective reduced form levels.

2.3.9. Determination of total soluble proteins and enzymatic activities

Leaf and root samples were ground into a fine powder with liquid N_2 and homogenized with extraction buffer [50 mM MOPS pH 7.5, 0.1% (*v*/*v*) Triton X-100, 10 mM $MgCl_2$, 1 mM EDTA, 20 mM KCl, 10 mM DTT, 10 mM β-mercaptoethanol, 2.5% (*w*/*v*) PVPP, 2 mM PMSF and a protease inhibitor cocktail tablet] and centrifuged at 24,000 × *g* and 4 °C for 20 min. The protein content of the supernatant was determined by the Bradford assay in the crude extract, while an aliquot was desalted through BioGel P-6 Desalting Gel (Bio-Rad Laboratories, Inc., Hercules, CA, USA) for some enzymatic determinations. Enzymatic activities for aspartate aminotransferase (AAT), glutamate synthase (GOGAT), glucose-6-phospate dehydrogenase (G6PDH), sucrose synthase (SuSy), NADP-isocitrate dehydrogenase (IDH), glutamate dehydrogenase (GDH), alkaline/neutral invertase (AlkINV), Δ^1-1-pyrroline-5-carboxylate synthase (P5CS), ornithine aminotransferase (OAT) and proline dehydrogenase (ProDH) were performed as described in **section 1.3.6**. Glutamine synthase (GS) activity was performed as described in González *et al*. (1998). For a comprehensive view of the metabolic pathways in which these enzymes are involved please refer to **Fig. 1.1**.

2.3.10. Statistical analysis

All data are reported as the mean ± SE of 5 to 10 independent biological replicates, as indicated in each figure/table. Multiple comparison analyses were performed with SPSS v27.0 using ANOVA and Tukey's HSD *post hoc* test ($p < 0.05$), while comparisons between treatment and control (when needed) were analyzed by Student's t-test ($p < 0.05$). All mentioned correlations were statistically tested with XLSTAT 2020.5 (https://www.xlstat.com/en/) using Pearson's correlation coefficient. Principal Component Analyses (PCA) were performed in log-transformed data using MetaboAnalyst 5.0 (https://www.metaboanalyst.ca/) and MetaGeneAlyse v1.7.1 (https://metagenealyse.mpimp-golm.mpg.de/). Before statistical analyses, data were checked for normality and homogeneity of variances, being log-transformed when needed.

2.4. RESULTS

2.4.1. Physiological measurements

KCl, NaCl, no-watering (No-W) and PEG-6000 stress were applied to provoke a drop of the leaf water potential similar to a moderate water-deficit level. Selected treatments were based on results from previous studies, in which the addition of 250 mM NaCl led to an average drop to Ψ_{leaf} -1.7 MPa after 7 days. Visually, salt-treated and No-W plants showed a vigorous and turgid appearance in the shoots, but some yellowing could be observed in the oldest leaves of salt-treated plants, above all under KCl stress. On the other hand, PEG-treated plants showed a less leafy appearance and a whitish discoloration in the leaves (**Fig. 2.2**). Regarding plant biomass, the imposition of water-deficit stress did not significantly impact total, shoot or root dry biomasses except for a higher root-to-shoot ratio observed in No-W plants compared to the other treatments (**Table 2.1**).

Control plants exhibited a Ψ_{leaf} value of -0.50 ± 0.00 MPa, while the NaCl, PEG and No-W stress led to drops in the Ψ_{leaf} to an average value of -1.70 ± 0.02 MPa (**Fig. 2.3**). Although the KCl treatment contained the same salt concentration than that of NaCl, it led to the highest drop in Ψ_{leaf}, reaching an average value of -2.04 ± 0.04 MPa. The stomatal conductance was severely reduced under NaCl and KCl stress, while this parameter reached values close to zero in No-W and PEG-treated plants, suggesting a higher degree of stomatal closure under these conditions (**Fig. 2.3**). Accordingly, transpiration rates were also markedly decreased under all stress treatments, with no significant differences among them (**Fig. 2.3**). On the other hand, the chlorophyll content, measured in the second fully expanded leaf, decreased only slightly in the PEG treatment (**Fig. 2.3**). It should be noted that no measurements were made in the oldest leaves. Leaf water content (WC) did not significantly decrease in neither salt nor No-W treatments, while dropping around 16% in the PEG treatment. Conversely, the No-W stress was the only treatment significantly reducing from 82.5% to around 65% the root WC (**Fig. 2.4**). On the other hand, the average PEG concentration measured in leaves and roots of PEG-treated plants was 8.24 ± 1.33 and 152.88 ± 16.49 mg g DW^{-1}, respectively.

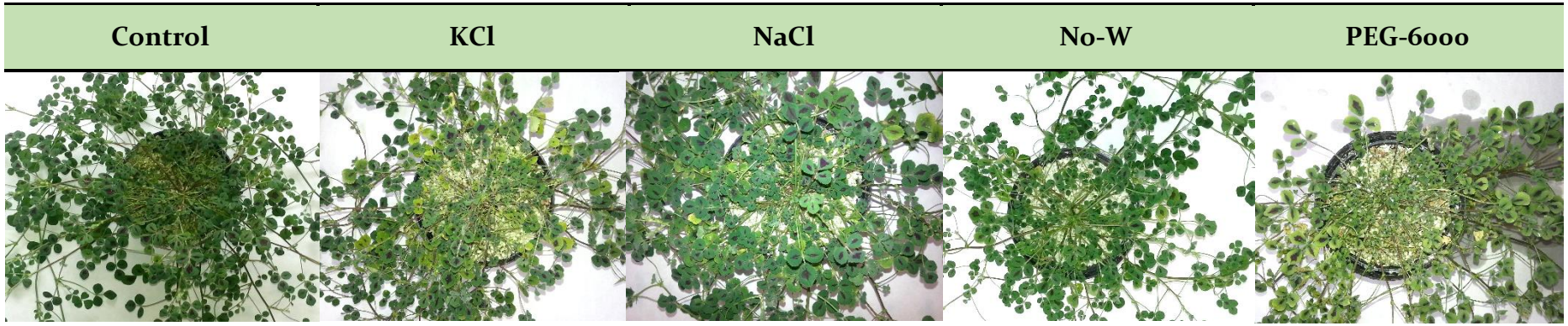

Figure 2.2. Appearance of *M. truncatula* plants under different stress treatments. Twelve-week-old plants were subjected to iso-osmotical conditions of salinity and drought. The addition of 0.25 M KCl and NaCl lead to a slight yellowing of the oldest leaves, especially under KCl stress. No-watering (No-W) treatment consisted of limiting water irrigation to 2/3 of the daily transpired water and did not provoke noticeable changes in the shoot, except for a slight turgor loss. On the other hand, the addition of 250 g L^{-1} PEG-6000 to the irrigation solution lead to a less leafy appearance and the slight whitening of the leaves.

Table 2.1. Growth parameters under different iso-osmotical conditions. Total, shoot and root dry biomasses (g DW^{-1}) and root-to-shoot ratios (on a DW basis) for the different treatments are displayed. Values represent the means ± SE (n = 5). Letters represent statistical differences (Tukey`s test, $p < 0.05$) between treatments. *No-W*, no-watering.

	Total biomass	Shoot biomass	Root biomass	Root/Shoot ratio
Control	16.7 ± 0.72 [a]	8.8 ± 0.32 [a]	7.5 ± 0.38 [a]	0.81 ± 0.03 [b]
KCl	15.3 ± 0.58 [a]	8.2 ± 0.28 [a]	7.0 ± 0.23 [a]	0.85 ± 0.00 [b]
NaCl	15.6 ± 0.89 [a]	8.4 ± 0.52 [a]	7.3 ± 0.36 [a]	0.88 ± 0.03 [b]
No-W	17.0 ± 1.44 [a]	8.2 ± 0.63 [a]	8.8 ± 0.81 [a]	1.07 ± 0.02 [a]
PEG	14.8 ± 0.88 [a]	7.8 ± 0.69 [a]	7.0 ± 0.34 [a]	0.92 ± 0.08 [ab]

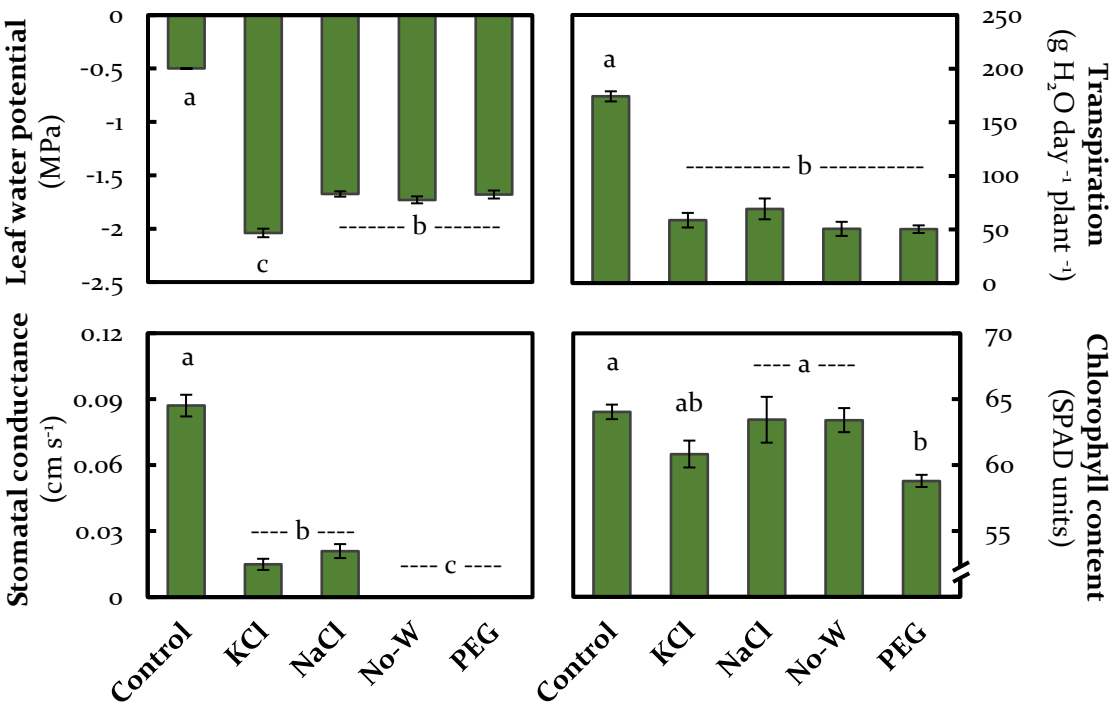

Figure 2.3. Effect of the different water-deficit stress treatments on plant water status. The effect of KCl, NaCl, no-watering (No-W) and PEG treatments was evaluated in the leaf water potential, plant transpiration, leaf stomatal conductance and leaf chlorophyll content. Bars represent the means ± SE (n = 5 for chlorophyll content, n=10 for other measurements). Letters represent statistical differences (Tukey`s test, $p < 0.05$) between treatments.

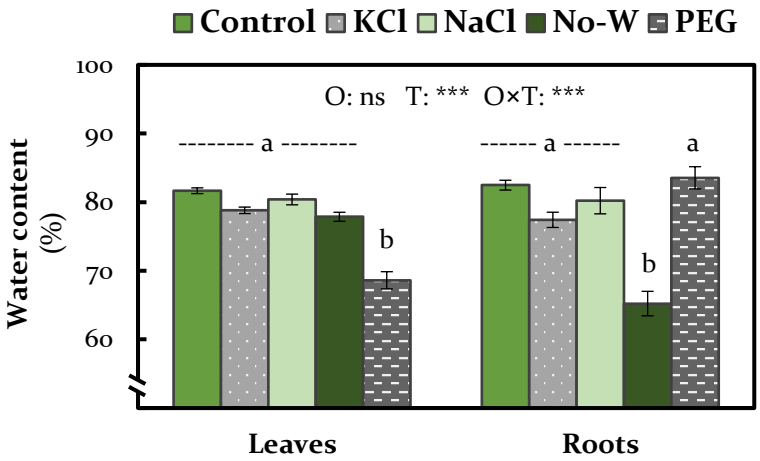

Figure 2.4. Effect of the different water-deficit stress treatments on leaf and root water contents. Bars represent the means ± SE (n = 10). A two-way ANOVA was performed and the *p*-values of the effects of organ (O), treatment (T) and their interaction (O×T) are indicated: ns > 0.05; *** $p < 0.001$. Different letters indicate significantly different averages according to the Bonferroni *post hoc* test ($p < 0.05$). *No-W*, no-watering.

2.4.2. Carbon metabolites

The concentration of starch and soluble sugars was differently affected by the stress treatments in the leaf, root and phloem sap of *Medicago truncatula* (**Fig. 2.5**). Both salt treatments exhibited a similar pattern: starch and sucrose accumulated markedly in leaves, being mostly unaffected or slightly modified in roots and phloem. However, in PEG-treated plants starch was fully depleted in leaves and significantly reduced in roots, while sucrose accumulated markedly in leaves and roots without any change at phloem sap level. A significant decrease in starch was observed in the No-W-treated plants concomitant with a moderate accumulation of sucrose. Both salt stresses and PEG treatment led to a depletion of glucose and fructose at root level, being unaffected at the leaf level. Conversely, No-W treatment showed a marked hexose increase in leaves and roots.

Regarding organic acids (**Fig. 2.6**), none of the salt stresses significantly affected malate, citrate and succinate content in leaves, while provoking an overall decrease in the malate content on the root tissue. In salt-stressed plants, the α-KG levels also decreased in the root tissue, whilst it accumulated significantly in leaves. No-W stress had a minor impact on organic acids (**Fig. 2.6**): the more abundant organic acids, malate and citrate, were not significantly affected in either leaves or roots, while α-KG increased slightly in the latter. PEG treatment led to a decline in citrate and succinate levels in the shoots, while a significant decrease in citrate was observed in roots together with an up to 6-fold accumulation of succinate levels.

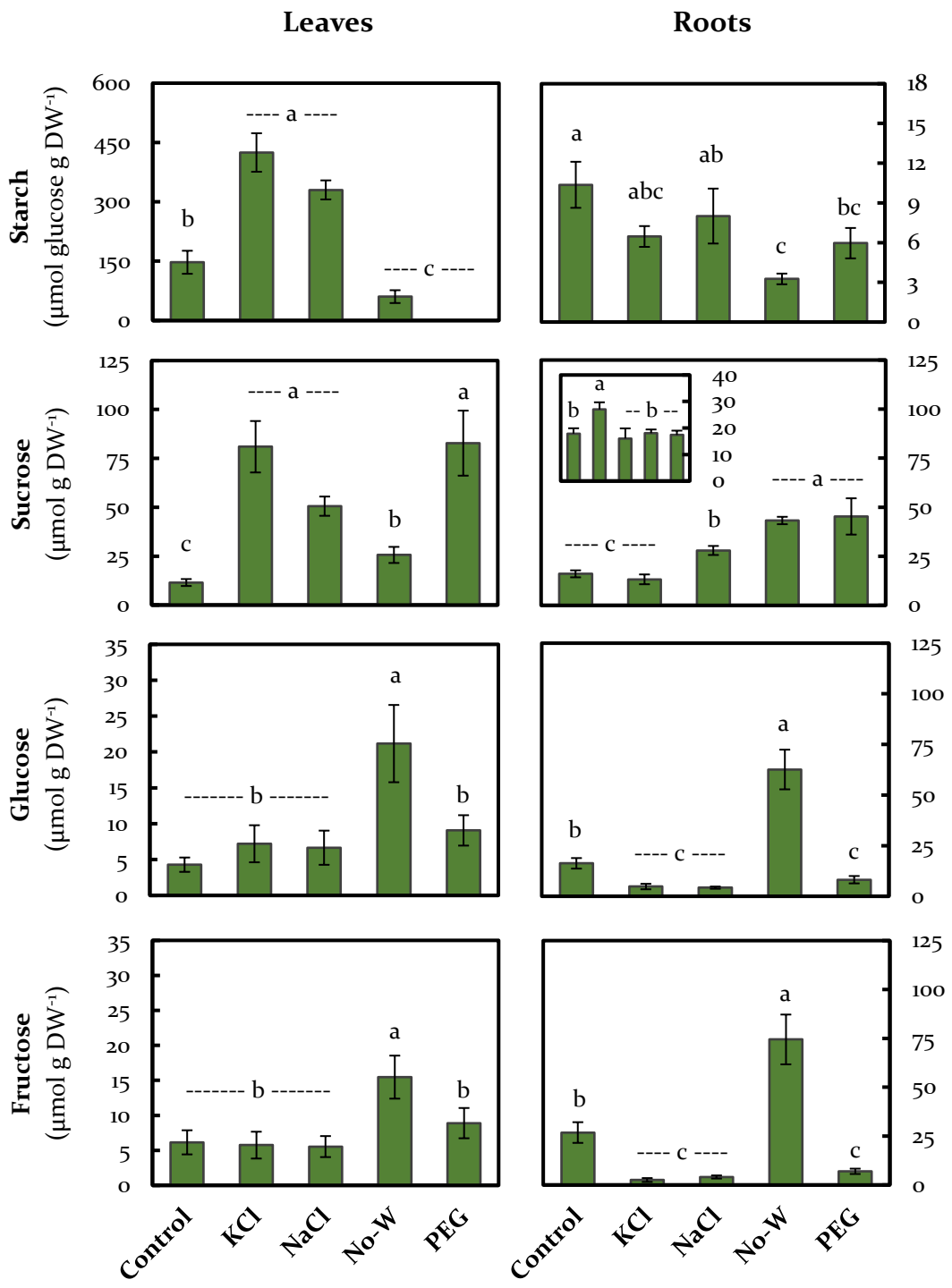

Figure 2.5. Effect of the different water-deficit stress treatments on the carbohydrate content. Effect of different treatments on the starch (measured as glucose units released after starch enzymatic breakdown), sucrose, glucose and fructose contents in leaf, root and phloem sap (as inserted figure) of *M. truncatula* plants. Bars represent the means ± SE (n = 5). Letters represent statistical differences (Tukey`s test, $p < 0.05$) between treatments. *No-W*, no-watering.

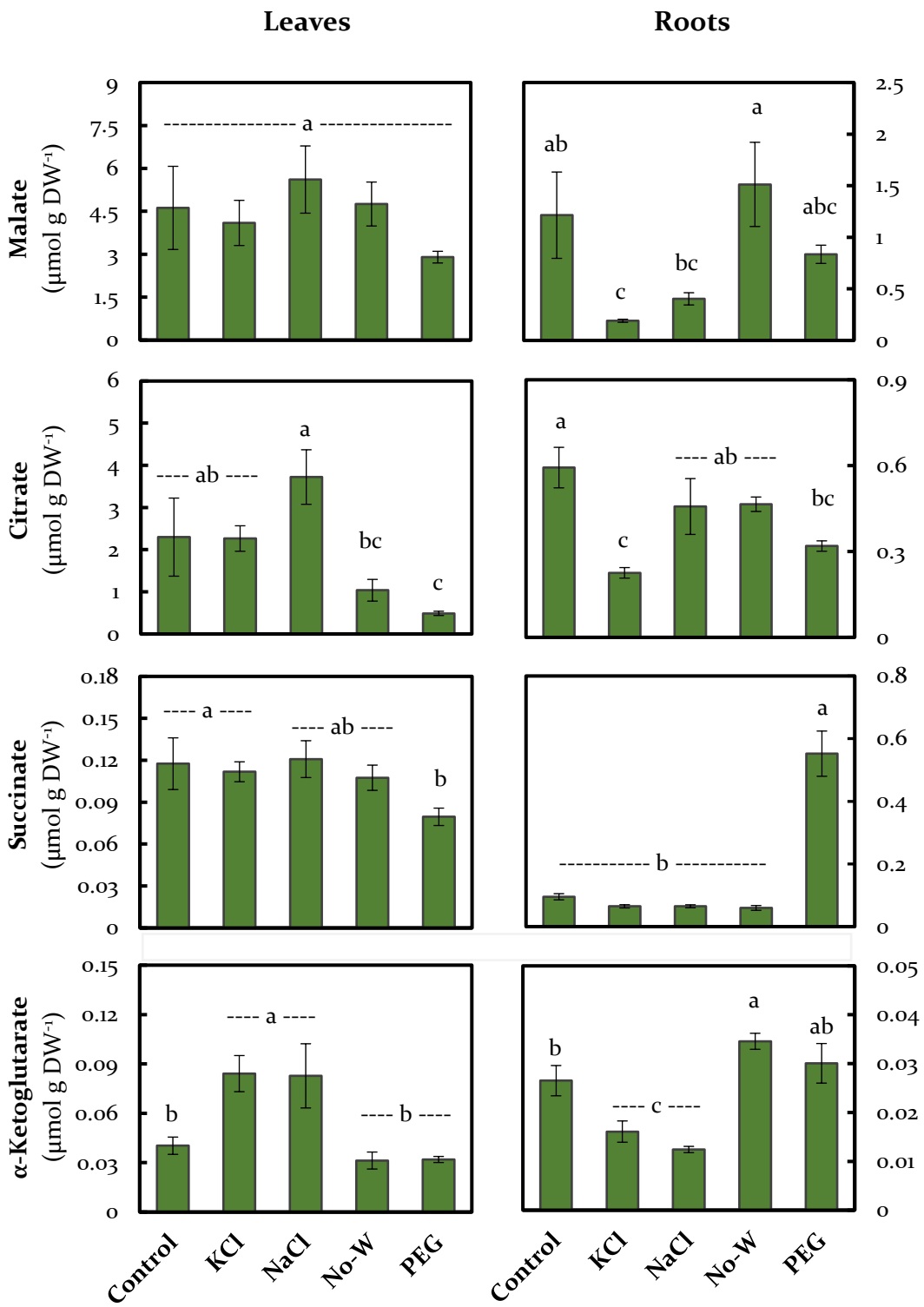

Figure 2.6. Effect of the different water-deficit stress treatments on the organic acids content of *M. truncatula*. Effect of different treatments on the malate, citrate, succinate and α-ketoglutarate contents in leaves and roots of *M. truncatula* plants. Bars represent the means ± SE (n = 5). Letters represent statistical differences (Tukey`s test, $p < 0.05$) between treatments. *No-W*, no-watering.

2.4.3. Nitrogen status

The soluble protein content (**Fig. 2.7**) was not significantly affected by any treatment in leaves while it showed a decreasing trend in roots, above all in response to KCl stress. A significant increase of total free amino acid concentration was found in leaves and roots of the PEG and No-W treatments whilst this parameter was not significantly affected in any of the salt stresses (**Fig. 2.7**). The amino acid content of the phloem sap exhibited a marked accumulation of up to 4-folds in the KCl-treated plants, but a more moderate increase was observed in NaCl and PEG treatments. Although the No-W treatment significantly altered the total amino acid concentration of leaves and, above all, roots, it did not show any changes at phloem level.

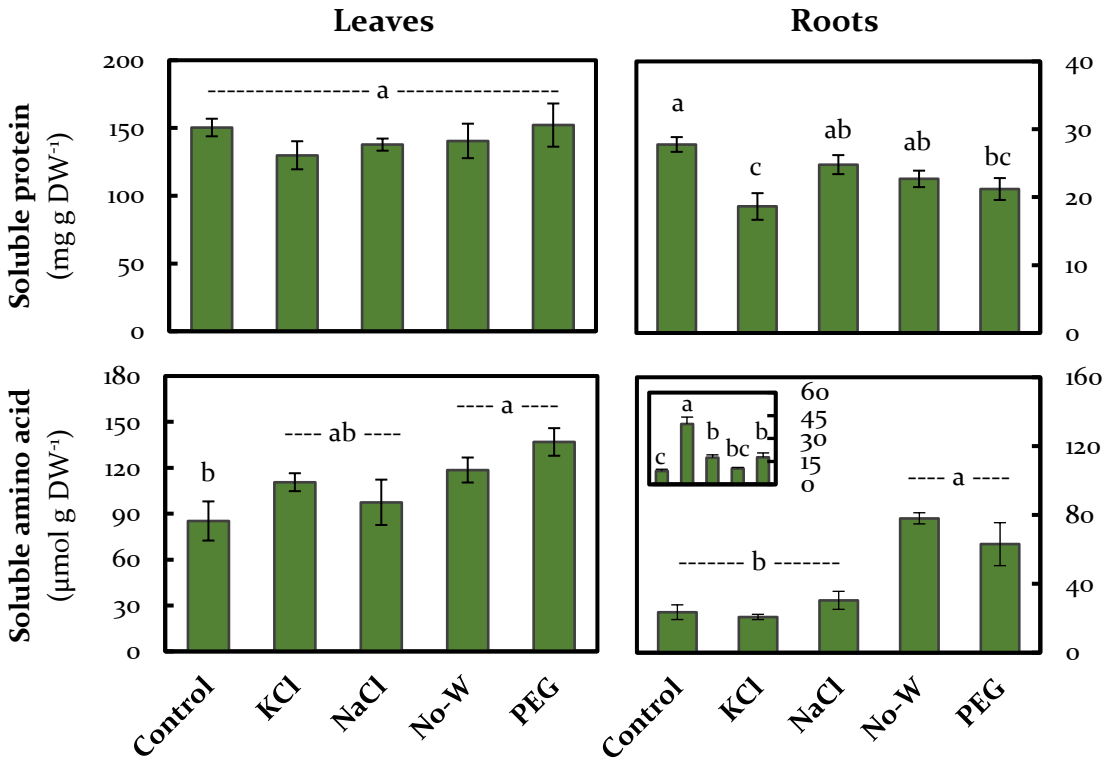

Figure 2.7. Effect of the different water-deficit stress treatments on soluble protein and amino acid contents. Effect of KCl, NaCl, no-watering (No-W) and PEG treatments on the protein and amino acid contents in leaves, roots and phloem sap (as inserted figure) of *M. truncatula* plants. Bars represent the means ± SE (n = 5). Letters represent statistical differences (Tukey`s test, $p < 0.05$) between treatments.

Regarding individual amino acids, only statistically significant changes higher than 2-fold are discussed (**Table 2.2**). Pro accumulated in all the treatments and organs, including the phloem sap. In salt treatments, Pro increased around 15-fold in leaves and roots with a remarkable accumulation at the phloem level (24-63-fold). Pro accumulation was much less marked in the leaves of No-W-treated plants, while the highest increase (29-fold) was observed at the root level. PEG provoked a similar Pro accumulation in leaves and roots (30-fold) with a more moderate increase at the phloem level.

Regarding Asn, the most abundant amino acid under control conditions in all plant organs, only roots of No-W treatment showed an accumulation of up to 3-folds. The phloem sap of KCl and PEG-treated plants showed also a significant accumulation of Asn. In general, the concentration of leaf amino acids, except for Pro, was not markedly affected by any stress, being the leaves of No-W-treated plants the most affected tissue, showing an accumulation of His, Trp, Phe, Val, Ile, Lys and Met. No-W also showed the most altered root amino acid content, with the exception of GABA, Gly, Gln and Thr. PEG-treated plant roots also showed an accumulation of several amino acids with a remarkable increase of Arg, His, GABA, Gly, Val, Ala, Leu and Ile. No-W treatment did not remarkably affect the phloem sap amino acid levels, while the primary amino acids Gln, Asn and Asp were significantly affected in the PEG treatment. Conversely, the main accumulation at the phloem sap level occurred under salt stress, where Arg, GABA, Ser and Gln showed significant increments in both treatments, while several additional amino acids were modulated in KCl plants.

Table 2.2. Effect of the different stress treatments on the absolute content of individual amino acids. Individual amino acid absolute content (as µmol g DW^{-1}) in leaves, roots and phloem sap in response to KCl, NaCl, no-watering (No-W) and PEG treatments. Values represent the means ± SE (n = 5), while values in brackets represent the fold change *versus* control conditions when higher than 4. Letters represent statistical differences (Tukey`s test, $p < 0.05$) between treatments. Those amino acids showing more than a ± two-fold change and significant differences between control and treatments are highlighted in red and blue, respectively.

		Ala	Val	Leu	Ile	Pro	Phe	Trp	Met	Gly	Ser
Leaf	Control	2.1±0.4 ^{a}	2.2±0.4 ^{b}	0.83±0.09 ^{b}	0.8±0.1 ^{b}	1.9±0.1 ^{d}	0.8±0.1 ^{c}	0.5±0.0 ^{d}	0.13±0.01 ^{c}	0.29±0.0 ^{b}	4.6±1.2 ^{b}
	KCl	1.9±0.3 ^{a}	3.0±0.5 ^{b}	0.84±0.05 ^{b}	1.0±0.1 ^{b}	32.1±2.1(17) ^{b}	1.2±0.2 ^{c}	1.0±0.2 ^{bc}	0.22±0.01 ^{ab}	0.40±0.1 ^{ab}	13.7±1.6 ^{a}
	NaCl	2.2±0.5 ^{a}	2.2±0.3 ^{b}	0.62±0.10 ^{b}	0.8±0.1 ^{b}	24.5±0.9(13) ^{bc}	1.1±0.2 ^{c}	0.9±0.2 ^{cd}	0.15±0.02 ^{bc}	0.28±0.0 ^{b}	15.3±3.6 ^{a}
	No-W	2.6±0.2 ^{a}	5.0±0.2 ^{a}	1.41±0.05 ^{a}	1.7±0.1 ^{a}	16.1±0.8(9) ^{c}	2.1±0.1 ^{b}	1.4±0.1 ^{ab}	0.31±0.02 ^{a}	0.42±0.0 ^{ab}	3.6±0.6 ^{b}
	PEG	2.0±0.1 ^{a}	5.1±0.5 ^{a}	0.82±0.10 ^{b}	1.0±0.1 ^{b}	56.7±7.3(30) ^{a}	2.9±0.3 ^{a}	1.7±0.2 ^{a}	0.22±0.03 ^{abc}	0.50±0.0 ^{a}	5.7±0.4 ^{b}
Phloem	Control	0.3±0.0 ^{b}	0.7±0.1 ^{b}	0.17±0.03 ^{ab}	0.23±0.04 ^{ab}	0.2±0.03 ^{d}	0.10±0.02 ^{b}	0.02±0.01 ^{a}	0.02±0.00 ^{b}	0.05±0.01 ^{b}	0.5±0.1 ^{b}
	KCl	1.1±0.1(4) ^{a}	1.1±0.1 ^{a}	0.27±0.03 ^{a}	0.27±0.03 ^{a}	10.6±1.5(63) ^{a}	0.20±0.03 ^{a}	0.02±0.01 ^{a}	0.10±0.02(6) ^{a}	0.14±0.02 ^{a}	1.5±0.5 ^{a}
	NaCl	0.5±0.1 ^{b}	0.4±0.0 ^{c}	0.15±0.02 ^{b}	0.12±0.01 ^{c}	4.1±0.7(24) ^{b}	0.09±0.01 ^{b}	0.01±0.00 ^{a}	0.02±0.00 ^{b}	0.07±0.01 ^{b}	1.3±0.2 ^{a}
	No-W	0.3±0.0 ^{b}	0.5±0.0 ^{bc}	0.08±0.00 ^{c}	0.14±0.00 ^{bc}	1.3±0.1(8) ^{c}	0.07±0.01 ^{b}	0.01±0.00 ^{a}	0.01±0.00 ^{b}	0.05±0.00 ^{b}	0.3±0.1 ^{b}
	PEG	0.4±0.1 ^{b}	0.5±0.1 ^{bc}	0.09±0.02 ^{bc}	0.10±0.02 ^{c}	2.2±0.5(13) ^{c}	0.09±0.02 ^{b}	0.01±0.00 ^{a}	0.02±0.00 ^{b}	0.07±0.01 ^{b}	0.5±0.1 ^{b}
Root	Control	0.7±0.1 ^{c}	0.7±0.1 ^{b}	0.22±0.03 ^{b}	0.26±0.03 ^{b}	0.5±0.1 ^{c}	0.17±0.02 ^{b}	0.32±0.04 ^{bc}	0.06±0.00 ^{b}	0.25±0.03 ^{b}	2.1±0.2 ^{b}
	KCl	0.7±0.1 ^{c}	0.5±0.1 ^{b}	0.18±0.01 ^{b}	0.19±0.01 ^{b}	7.0±0.7(15) ^{b}	0.16±0.02 ^{b}	0.20±0.03 ^{c}	0.04±0.00 ^{b}	0.28±0.01 ^{b}	1.6±0.1 ^{b}
	NaCl	0.6±0.1 ^{c}	0.6±0.1 ^{b}	0.19±0.03 ^{b}	0.24±0.03 ^{b}	6.9±1.2(14) ^{b}	0.19±0.02 ^{b}	0.29±0.05 ^{bc}	0.04±0.01 ^{b}	0.24±0.03 ^{b}	1.8±0.2 ^{b}
	No-W	1.2±0.1 ^{b}	2.2±0.1 ^{a}	0.52±0.09 ^{a}	0.96±0.09 ^{a}	13.6±0.9(29) ^{a}	0.51±0.05 ^{a}	0.89±0.08 ^{a}	0.11±0.01 ^{a}	0.50±0.04 ^{ab}	3.5±0.1 ^{a}
	PEG	3.5±1.1(5) ^{a}	2.0±0.3 ^{a}	0.53±0.17 ^{a}	0.99±0.17 ^{a}	14.3±3.1(30) ^{a}	0.36±0.08 ^{ab}	0.60±0.13 ^{ab}	0.10±0.01 ^{a}	0.76±0.12 ^{a}	3.2±0.4 ^{a}

Table 2.2. Effect of the different stress treatments on the absolute content of individual soluble amino acids (continued).

		Thr	Tyr	Asn	Gln	GABA	Glu	Asp	Lys	Arg	His
Leaf	Control	2.6±0.2 [b]	0.51±0.06 [ab]	48.3±11.4 [a]	0.8±0.0 [bc]	0.6±0.1 [a]	11.3±1.5 [ab]	5.1±0.7 [a]	0.55±0.10 [b]	0.68±0.17 [ab]	0.6±0.0 [c]
	KCl	1.9±0.1 [bc]	0.31±0.02 [c]	37.3±6.6 [a]	0.6±0.0 [c]	0.4±0.0 [a]	10.1±0.8 [ab]	2.2±0.3 [c]	0.52±0.04 [b]	0.38±0.03 [b]	1.4±0.2 [b]
	NaCl	2.0±0.2 [bc]	0.37±0.04 [bc]	30.2±10.5 [a]	0.6±0.1 [c]	0.5±0.1 [a]	10.7±1.4 [ab]	3.4±0.7 [bc]	0.61±0.06 [b]	0.31±0.06 [b]	0.9±0.2 [bc]
	No-W	3.8±0.2 [a]	0.72±0.06 [a]	57.2±6.8 [a]	1.4±0.1 [a]	0.7±0.1 [a]	13.0±1.0 [a]	3.7±0.2 [ab]	1.24±0.12 [a]	0.87±0.12 [ab]	1.3±0.2 [b]
	PEG	1.4±0.1 [c]	0.60±0.07 [a]	42.4±4.3 [a]	1.2±0.3 [ab]	0.7±0.1 [a]	7.4±0.5 [b]	2.0±0.1 [c]	0.90±0.08 [ab]	1.17±0.22 [a]	2.4±0.3 [a]
Phloem	Control	0.2±0.0 [b]	0.08±0.01 [b]	3.8±0.7 [c]	0.14±0.03 [d]	0.6±0.1 [d]	0.4±0.0 [b]	0.8±0.2 [d]	0.30±0.03 [ab]	0.06±0.01 [c]	0.10±0.02 [a]
	KCl	0.6±0.1 [a]	0.19±0.03 [a]	11.8±2.0 [a]	1.16±0.05(8) [a]	3.9±0.6(6) [a]	1.6±0.1 [a]	4.2±0.5(5) [a]	0.43±0.04 [a]	0.21±0.02 [a]	0.10±0.01 [a]
	NaCl	0.3±0.0 [b]	0.10±0.01 [b]	5.4±1.0 [bc]	0.68±0.14(4) [b]	1.9±0.4 [b]	0.7±0.1 [b]	1.5±0.4 [cd]	0.23±0.02 [b]	0.12±0.01 [ab]	0.06±0.01 [a]
	No-W	0.2±0.0 [b]	0.06±0.00 [b]	3.52±0.3 [c]	0.17±0.01 [d]	0.7±0.0 [cd]	0.7±0.1 [b]	1.9±0.2 [c]	0.23±0.02 [b]	0.05±0.01 [c]	0.06±0.01 [a]
	PEG	0.3±0.0 [b]	0.10±0.02 [b]	7.9±1.2 [b]	0.38±0.03 [c]	1.4±0.3 [bc]	0.7±0.2 [b]	2.5±0.6 [b]	0.19±0.04 [b]	0.07±0.02 [bc]	0.08±0.02 [a]
Root	Control	1.7±0.3 [ab]	0.15±0.03 [b]	12.8±3.3 [c]	0.45±0.08 [a]	1.2±0.2 [b]	0.7±0.2 [b]	0.4±0.1 [b]	0.22±0.05 [b]	0.13±0.02 [b]	0.6±0.1 [c]
	KCl	0.7±0.1 [c]	0.14±0.01 [b]	5.2±0.7 [c]	0.85±0.07 [a]	0.8±0.1 [b]	0.9±0.1 [b]	0.4±0.1 [b]	0.25±0.03 [b]	0.11±0.01 [b]	0.6±0.0 [c]
	NaCl	0.9±0.0 [bc]	0.10±0.02 [b]	14.2±3.6 [c]	0.57±0.09 [a]	0.9±0.1 [b]	1.0±0.1 [ab]	0.4±0.0 [b]	0.27±0.04 [b]	0.21±0.05 [b]	0.8±0.2 [bc]
	No-W	2.3±0.2 [a]	0.27±0.03 [a]	44.1±2.7 [a]	0.78±0.26 [a]	1.2±0.1 [b]	1.4±0.1 [a]	1.0±0.1 [a]	0.69±0.06 [a]	0.41±0.04 [a]	2.0±0.2 [ab]
	PEG	2.1±0.4 [a]	0.28±0.07 [a]	24.9±5.1 [b]	0.49±0.16 [a]	3.3±0.8 [a]	1.1±0.2 [ab]	0.6±0.1 [b]	0.55±0.15 [ab]	0.43±0.09 [a]	3.1±0.6(5) [a]

2.4.4. Inorganic ions

Under control conditions K^+ was the most abundant ion in leaves and roots and both tissues showed a similar ion profile, with a higher relative abundance of SO_4^{2-} and Na^+ ions in detriment of Mg^{2+} in the roots compared to leaves (**Fig. 2.8A**). **Fig. 2.8B and C** show the treatment/control fold change for each ion in leaves and roots in response to the different treatments. KCl stress provoked a marked accumulation of Cl^- in both tissues (10-17-fold). However, K^+ only accumulated around 2-3 times in both tissues compared to control plants. It needs to be remarked that under control conditions, the K^+ concentration in both leaves and roots was around 10-fold higher than the Cl^- concentration (**Fig. 2.8A**) and therefore 2-fold changes of K^+ imply an important net accumulation of this ion. NaCl stress provoked a marked accumulation of both ions in leaves and roots, being Na^+ preferentially accumulated in leaves and Cl^- in roots. A decrease in Mg^{2+}, Ca^{2+} and SO_4^{2-} levels was observed in roots of both salt stresses, with an additional decrease in Na^+ and K^+ ions under KCl and NaCl conditions, respectively. PEG provoked a marked ion alteration mostly at the root level, leading to a decline in the Na^+, K^+, Cl^-, Mg^{2+}, Ca^{2+} and SO_4^{2-} concentrations. Lastly, No-W did not significantly modify the inorganic ions levels in any tissue, and only NO_3^- exhibited a significant accumulation in roots. The absolute ion content under all stresses and both leaves and roots can be found in **Table 2.3**. In addition to the already stated changes in the ionic content, a remarkable increase in the total ion content could be observed in both tissues in response to salinity stress, especially in KCl roots, while the total ion content was decreased under PEG-6000, specially in roots.

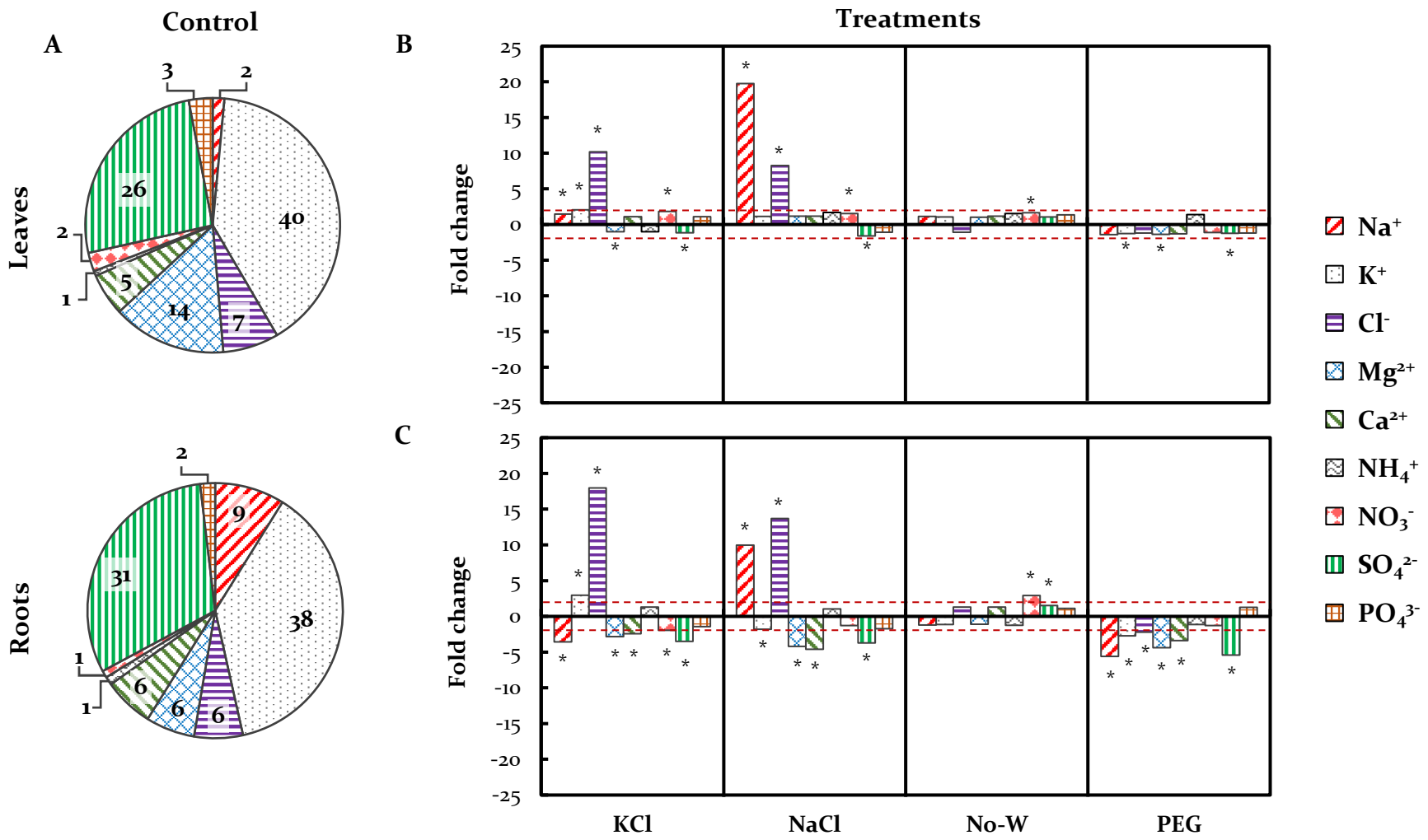

Figure 2.8. Inorganic ion content under control conditions and its response upon water-deficit stress. In **A**, the ion composition expressed as a percentage in leaves and roots under control conditions is shown. In **B** and **C** bars represent the means (n = 5) of the treatment/control ratios` fold change in leaves and roots, respectively. Asterisks represent statistical differences (Student's t-test, $p < 0.05$) between control and treatments. *No-W*, no-watering.

Table 2.3. Effect of the different treatments on the individual and total inorganic ions in *M truncatula*. Absolute content of individual (as µmol g DW^{-1}) and total (as mmol g DW^{-1}) inorganic ions in leaves and roots under control and water-deficit stress conditions. Values represent the means ± SE (n = 5). Letters represent statistical differences (Tukey`s test, $p < 0.05$) between treatments. Those inorganic ions showing more than a ± two-fold change and significant differences between control and treatments are highlighted in red and blue, respectively. *No-W*, no-watering.

		Na^+	K^+	Cl^-	Mg^{2+}	Ca^{2+}	NH_4^+	NO_3^-	SO_4^{2-}	PO_4^{3-}	TOTAL
Leaf	Control	19.1±3.3 ^{bc}	516.5±20.9 ^{b}	91.4±6.1 ^{c}	186.0±8.3 ^{a}	69.4±8.6 ^{ab}	8.1±0.9^{a}	30.7±1.9 ^{bc}	327.9±13.9^{a}	39.0±3.6^{ab}	1.29±0.05^{b}
	KCl	28.3±1.3 ^{b}	1065.7±40.8 ^{a}	929.7±19.2 ^{a}	181.7±9.7 ^{a}	77.2±5.4 ^{ab}	7.9±0.4^{a}	56.8±4.7 ^{a}	285.8±9.1 ^{a}	42.0±2.7^{ab}	2.68±0.07^{a}
	NaCl	376.8±66.3^{a}	578.2±35.4 ^{b}	757.0±58.7^{b}	217.9±12.3^{a}	81.3±3.0 ^{a}	13.7±4.6^{a}	47.4±3.7 ^{ab}	206.7±17.4^{b}	35.5±3.3^{ab}	2.29±0.15 ^{a}
	No-W	21.3±1.2 ^{bc}	542.2±16.3 ^{b}	84.6±4.8 ^{c}	190.1±6.6 ^{a}	80.9±6.2 ^{a}	12.3±2.8^{a}	50.1±4.4 ^{a}	343.0±19.0^{a}	53.0±6.2^{a}	1.37±0.02^{b}
	PEG	13.5±2.0 ^{c}	401.7±18.8 ^{c}	77.3±5.3 ^{c}	133.7±4.1 ^{b}	52.6±7.0 ^{b}	11.2±3.1 ^{a}	27.8±3.1 ^{c}	266.1±22.1^{ab}	32.4±3.2^{b}	1.02±0.04^{c}
Root	Control	78.0±13.1 ^{b}	332.1±30.8 ^{b}	54.4±5.9 ^{c}	54.7±4.9 ^{a}	56.0±10.9^{a}	9.3±0.9^{a}	7.9±1.7 ^{b}	273.0±33.3^{b}	16.6±3.1 ^{ab}	0.88±0.06^{c}
	KCl	21.8±3.6 ^{c}	981.2±109.2^{a}	975.6±47.4^{a}	19.2±2.2 ^{b}	22.9±1.9 ^{b}	12.1±1.7 ^{a}	4.0±0.4 ^{b}	78.4±3.9 ^{c}	11.5±1.4^{b}	2.13±0.12 ^{a}
	NaCl	776.7±42.6^{a}	183.5±13.4 ^{bc}	744.8±38.8^{b}	13.1±0.6 ^{b}	12.1±1.1 ^{b}	9.7±1.1 ^{a}	6.2±1.0 ^{b}	73.1±7.9 ^{cd}	9.7±1.4^{b}	1.78±0.12 ^{b}
	No-W	63.6±13.4 ^{b}	292.9±56.4 ^{b}	70.3±5.2 ^{c}	50.1±5.0 ^{a}	74.4±15.7^{a}	7.5±2.7^{a}	23.1±3.7 ^{a}	413.9±15.9^{a}	18.5±0.5^{a}	1.02±0.09^{c}
	PEG	13.9±2.1 ^{c}	121.9±12.1 ^{c}	24.8±1.9 ^{d}	13.1±1.5 ^{b}	16.6±3.8 ^{b}	8.2±1.7 ^{a}	6.1±0.7 ^{b}	50.3±5.1 ^{d}	20.9±1.6^{a}	0.28±0.02^{d}

Fold change

>4 3 2 -2 -3 <-4

2.4.5. Antioxidant content

Ascorbate, glutathione and homoglutathione contents, in both oxidized and reduced forms, were analyzed in the different tissues and treatments (**Fig. 2.9, 2.10**). The antioxidant metabolites` concentration in the phloem sap was below the detection limit of our analytical system (5 ppm), so no values could be obtained in this tissue. The total antioxidant level was higher in leaves than roots in the case of glutathione and, above all, ascorbate, while homoglutathione was more present in the root tissue (**Fig. 2.9A, B**). Salt stress did not significantly modify the total glutathione or homoglutathione pools but provoked a significant decrease in the total ascorbate pool (**Fig. 2.9A, B**). This decrease was due to a decline in the reduced form (ASC) in leaves but to a decline in both the oxidized (DHA) and reduced forms in roots (**Fig. 2.10A, B**). However, in leaves of No-W-treated plants total antioxidant levels remained unaffected (**Fig. 2.9A**). Conversely, in No-W roots total glutathione and homoglutathione increased significantly in both forms concomitantly with the decrease of the ascorbate pool (**Fig. 2.9B; 2.10D, F**). Since the total ascorbate level was near the detection level of our analytical method in the root tissue, it was not possible to discern between both antioxidant forms in this tissue in those treatments provoking a decrease of the ascorbate pool such as No-W or PEG. This metabolite could then only be measured as the whole pool **(Fig. 2.10B)**. PEG provoked an overall decrease of the ascorbate pool in leaves and roots, while the glutathione and homoglutathione pools remained unaffected. Regarding the ratio reduced form/total pool for each metabolite (**Fig. 2.9C, D**), only PEG led to a significant reduction in the ascorbate and glutathione ratios in the leaf. Conversely, in roots, the glutathione ratio was the only negatively affected in all the stresses, with the ascorbate and homoglutathione ratios remaining unaffected (**Fig. 2.9D**).

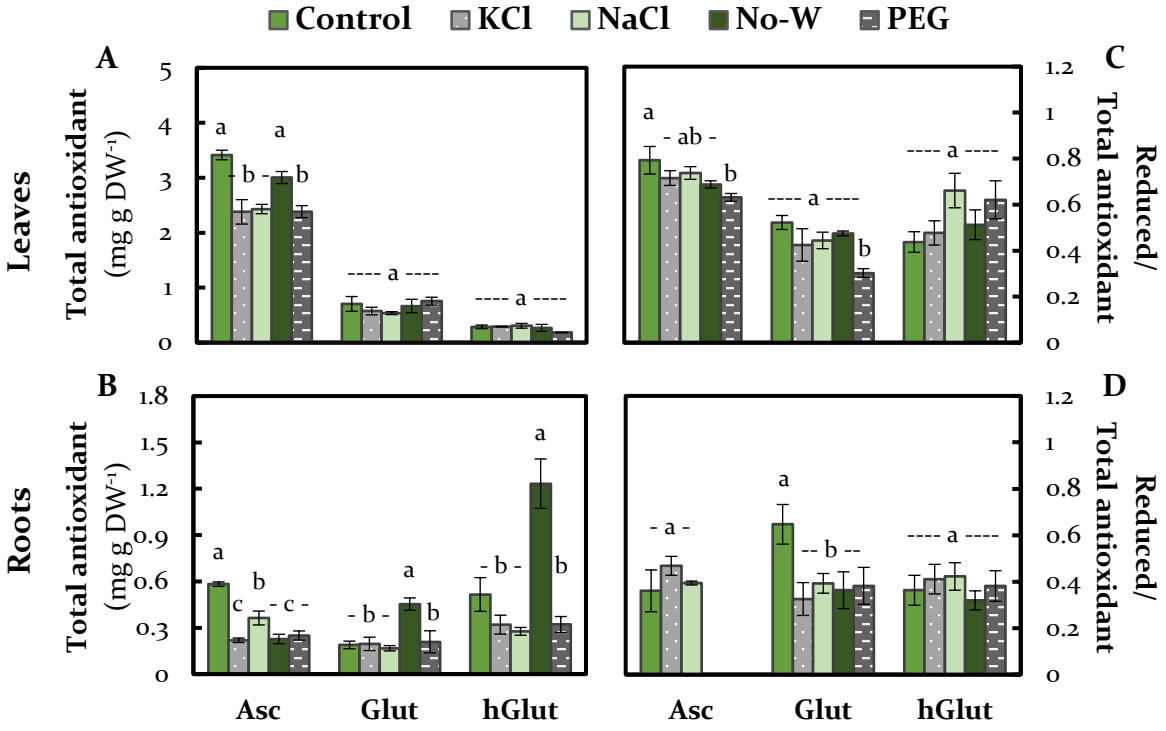

Figure 2.9. Effect of the different water-deficit stress treatments on the total antioxidant content and the reduced/total antioxidant ratio in *M. truncatula*. Total ascorbate (Asc), glutathione (Glut) and homoglutathione (hGlut) contents in leaves (**A**) and roots (**B**) and the ratio between the reduced form and their total content (**C, D**). Bars represent the means ± SE (n = 5). Letters represent statistical differences (Tukey`s test, $p < 0.05$) between treatments for each parameter. No reduced ascorbate could be measured in the root tissue under No-W or PEG conditions. *No-W*, no-watering.

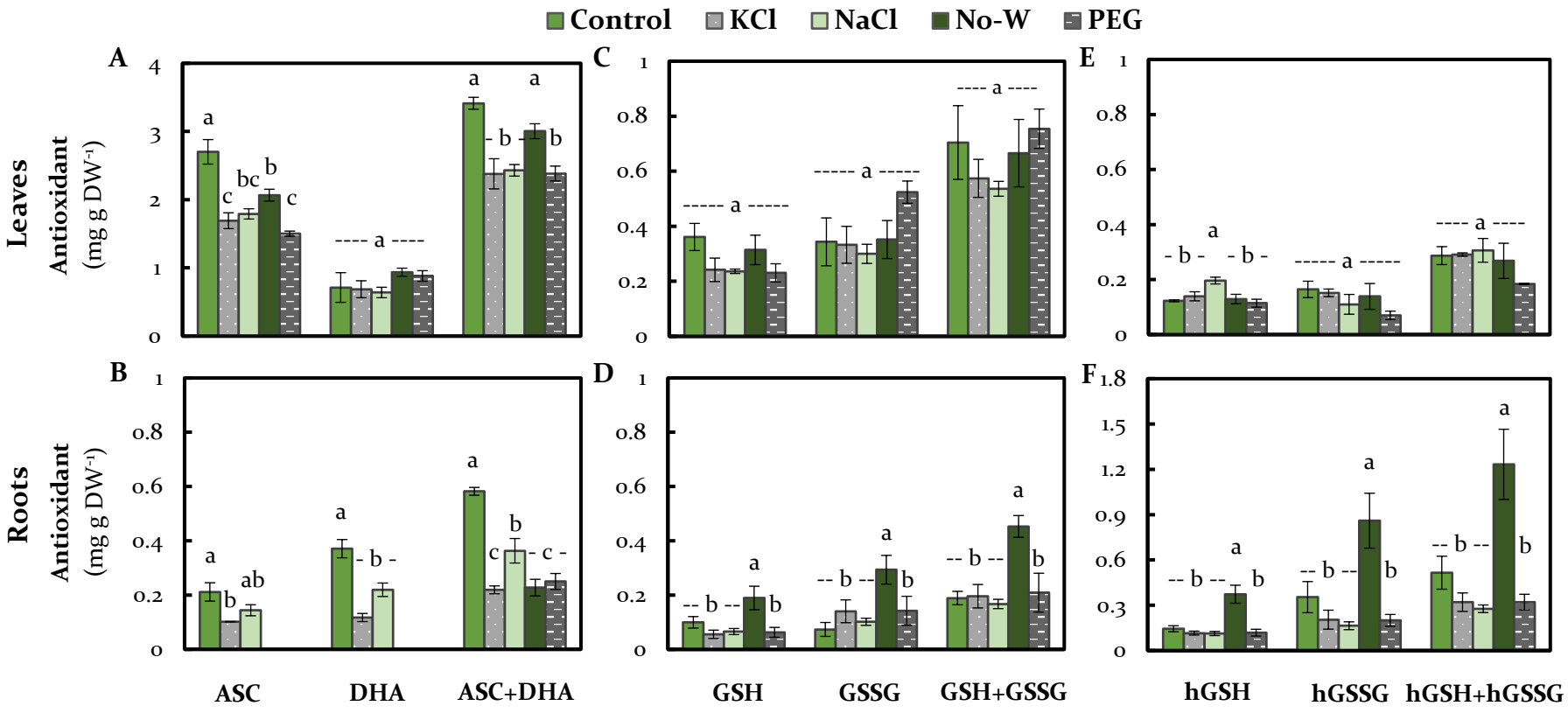

Figure 2.10. Effect of the different water-deficit stress treatments on the antioxidant composition in leaves and roots. Antioxidant composition in leaves (**A, C, E**) and roots (**B, D, F**) of *M. truncatula* plants under various water-deficit stresses. Bars represent the means ± SE (n = 5). Letters represent statistical differences (Tukey`s test, $p < 0.05$) between treatments for each parameter. In B, no reduced ascorbate nor DHA data could be under No-W or PEG conditions. *ASC*, reduced ascorbate; *DHA*, dehydroascorbate; *GSH*, reduced glutathione; *GSSG*, oxidized glutathione; *hGSH*, reduced homoglutathione; *hGSSG*, oxidized homoglutathione; *No-W*, no-watering.

2.4.6. Carbon and nitrogen enzymatic activities

Several enzymatic activities related to the carbon (AlkINV, G6PDH, IDH and SuSy), nitrogen (AAT, GDH, GOGAT and GS) and proline (OAT, P5CS and ProDH) metabolism were measured in leaves and roots of *M. truncatula* (**Fig. 2.11-13, S2.1**).

Overall, the measured carbon and nitrogen-related enzyme activities (G6PDH, AAT and GDH) were not significantly affected in leaves, except for an increase in the IDH activity under salinity stress (**Fig. 2.11**). On the contrary, the root tissue showed a generalized response at the enzymatic activity level: AAT and SuSy activities showed a general down-regulation in all treatments (**Fig. 2.12**). Conversely, AlkINV showed a significant enhancement in the No-W, while it decreased in the PEG-treated roots. On the other hand, G6PDH, the first enzyme of the OPP pathway, increased its activity under NaCl irrigation by 1.5-fold, while decreasing significantly under No-W and PEG treatments. Root GDH and IDH activities did not significantly change in response to any treatment, except for a decline in IDH under KCl conditions (**Fig. 2.12**). GOGAT and GS activities were not significantly altered in either roots or shoots under either treatment (**Fig. S2.1**).

Proline synthesis-related P5CS and OAT enzymes increased significantly in leaves and roots of salt-stressed plants, while the proline-degrading ProDH was slightly inhibited in the leaves (**Fig. 2.13**). However, in leaves of No-W-treated plants proline metabolism was not affected while the three enzymatic activities increased significantly in roots. This Pro metabolism activation occurred also in roots of PEG-treated plants, while OAT was negatively affected in leaves under this treatment (**Fig. 2.13**).

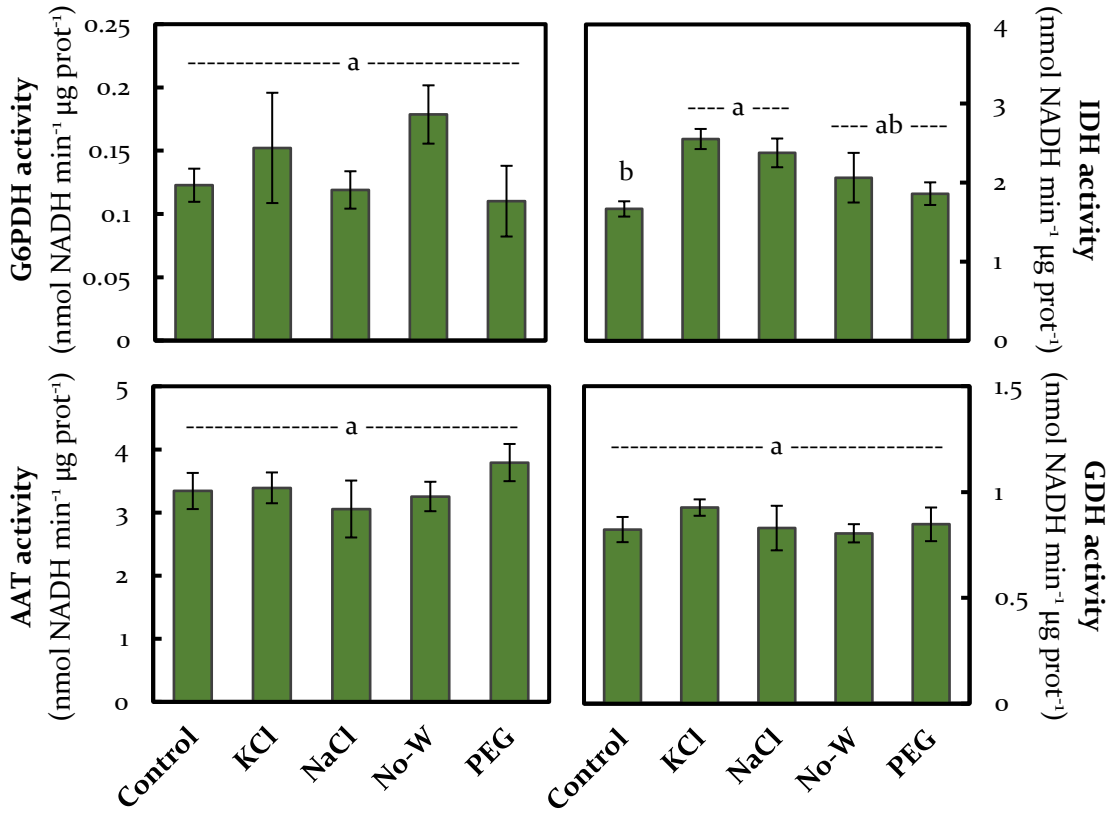

Figure 2.11. Effect of the different treatments in the carbon- and nitrogen-related enzymatic activities of the leaf tissue. Enzymatic activities of glucose-6-phosphate dehydrogenase (G6PDH), isocitrate dehydrogenase (IDH), aspartate aminotransferase (AAT) and glutamate dehydrogenase (GDH) under KCl, NaCl, no-irrigation (No-W) and PEG stress in leaves. Bars represent the means ± SE (n = 5). Letters represent statistical differences (Tukey`s test, $p < 0.05$) between treatments.

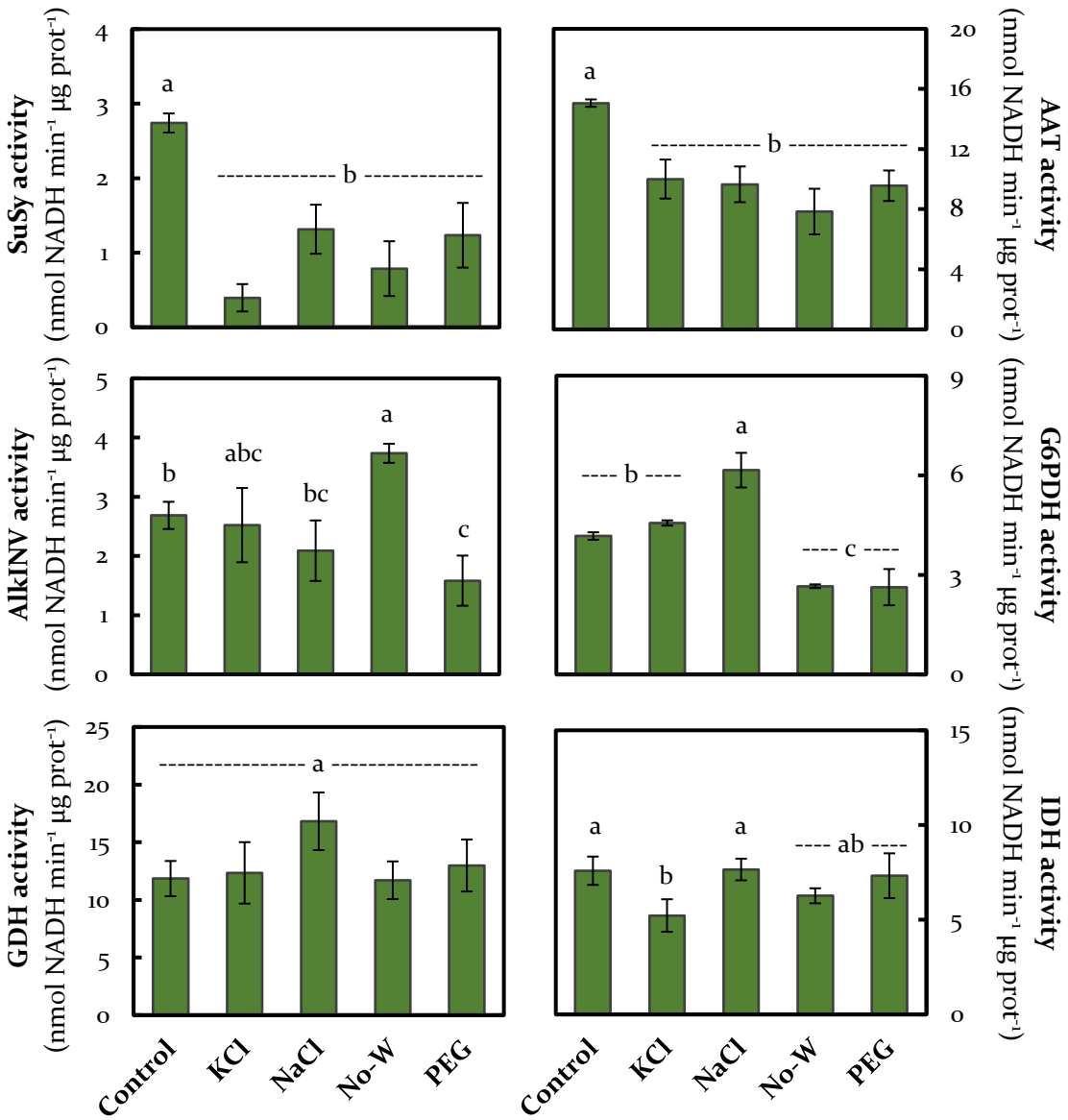

Figure 2.12. Effect of the different treatments in several carbon- and nitrogen-related enzymatic activities in the root tissue. Enzymatic activities of sucrose synthase (SuSy), aspartate aminotransferase (AAT), alkaline invertase (AlkINV), glucose-6-phosphate dehydrogenase (G6PDH), glutamate dehydrogenase (GDH) and isocitrate dehydrogenase (IDH) in response to KCl, NaCl, no-watering (No-W) and PEG treatments. Bars represent the means ± SE (n = 5). Letters represent statistical differences (Tukey`s test, $p < 0.05$) between treatments.

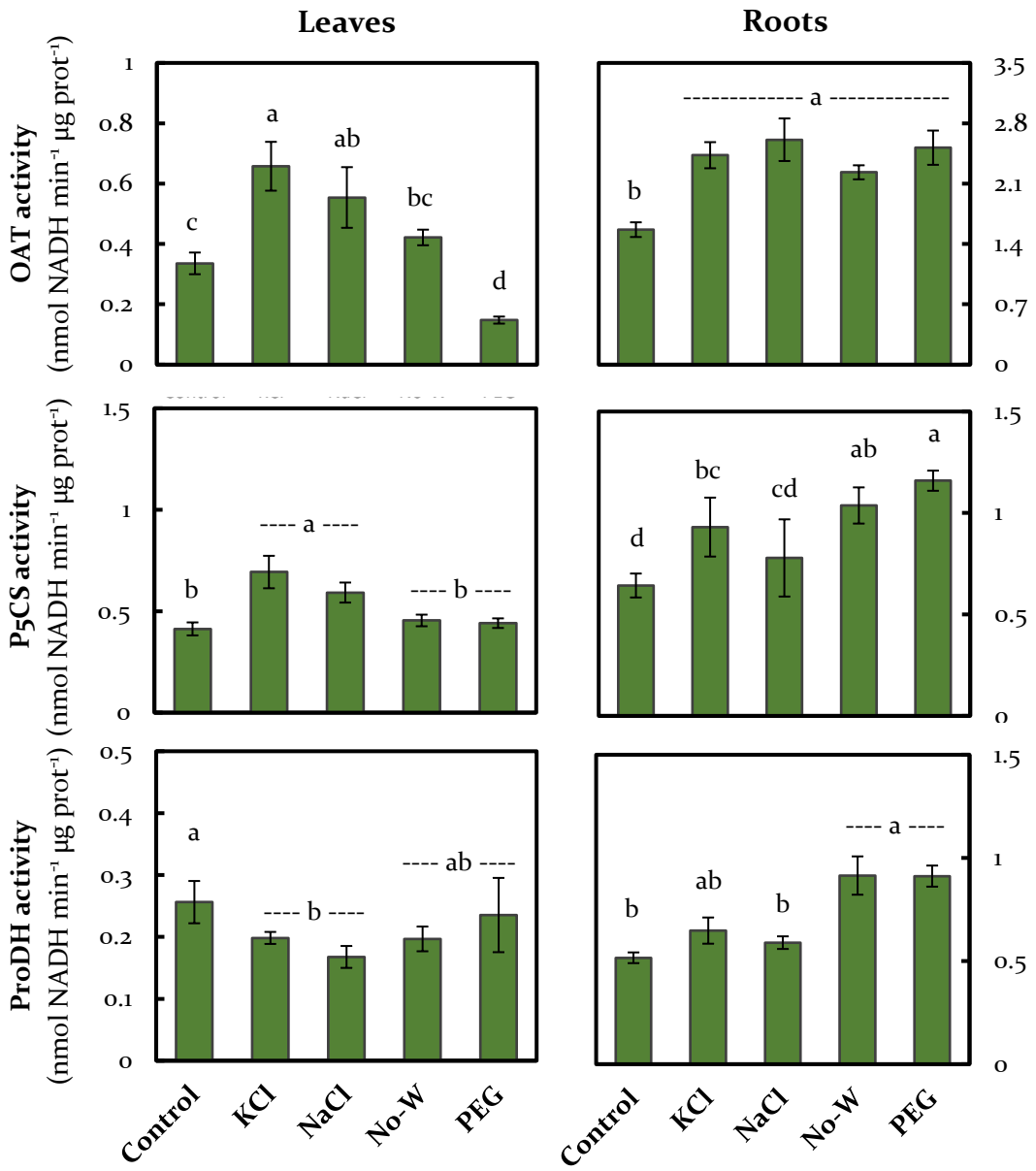

Figure 2.13. Effect of the different treatments in proline metabolism-related enzymatic activities. Enzymatic activities of ornithine aminotransferase (OAT), Δ^1-1-pyrroline-5-carboxylate synthase (P5CS) and proline dehydrogenase (ProDH) in response to KCl, NaCl, no-watering (No-W) and PEG treatments. Bars represent the means ± SE (n = 5). Letters represent statistical differences (Tukey`s test, $p < 0.05$) between treatments.

2.4.7. Principal Component Analyses

Several Principal Component Analyses (PCA) were performed with all measured parameters in order to further confirm the differences between the treatments. All treatments were compared in **Fig. S2.2** in which a clear differentiation between samples, above all between control and drought treatments, could be observed. Indeed, when compared as a pair, No-W and PEG-treated plants showed different scores along the first PC axis (**Fig. 14A**), with the variables with the most weight responsible for the separation of both treatments being leaf starch and proline, root fructose, glucose and succinate contents, root Na^+, Ca^{2+}, Mg^{2+}, NO_3^-, SO_4^{2-} and total ion contents, as well as root reduced glutathione and reduced, oxidized and total homoglutathione contents (**Fig. 14B**). A very obvious sample separation occurred too when NaCl and No-W-treated plants were analyzed (**Fig. 15A**), with the most responsible variables being leaf stomatal conductance, root fructose and glucose contents, leaf starch and citrate, leaf and root Na^+ and Cl^- contents, root SO_4^{2-}, NO_3^- and Ca^{2+}, root Ile content and root oxidized and total homoglutathione contents (**Fig. 15B**). Regarding NaCl and KCl samples, which showed a less marked but still significant separation in the PCA (**Fig. 16A**), the parameters most responsible for their separation in the PC1 were leaf and root Na^+ contents, root K^+ and Asn contents, SuSy activity and many phloem individual amino acids, including the total phloem amino acid content (**Fig. 16B**). The statistical significance of the cited parameters was further acknowledged by Student's t-test ($p < 0.05$), while the complete list of loading values for each PCA is shown in **Table S2.1**.

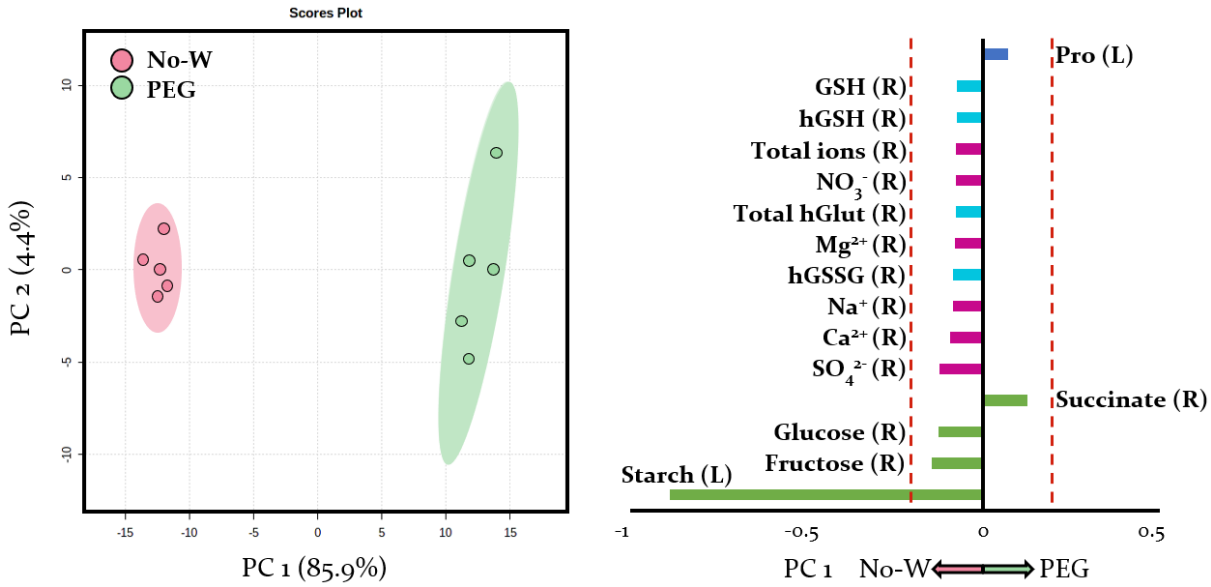

Figure 2.14. Principal Component Analysis (PCA) conducted with all measured parameters in No-W and PEG-6000-treated plants. ***Left***, PCA scores plot showing the non-irrigated (No-W) and PEG-6000 cases. ***Right,*** loading values of all variables in PC1 separating both treatments. *GSH*, reduced glutathione; *hGlut*, homoglutathione; *hGSH*, reduced homoglutathione; *hGSSG*, oxidized homoglutathione; *L*, leaves; *R*, roots. *Bar key*: dark blue, amino acids; green, carbohydrates; light blue, antioxidants; pink, inorganic ions.

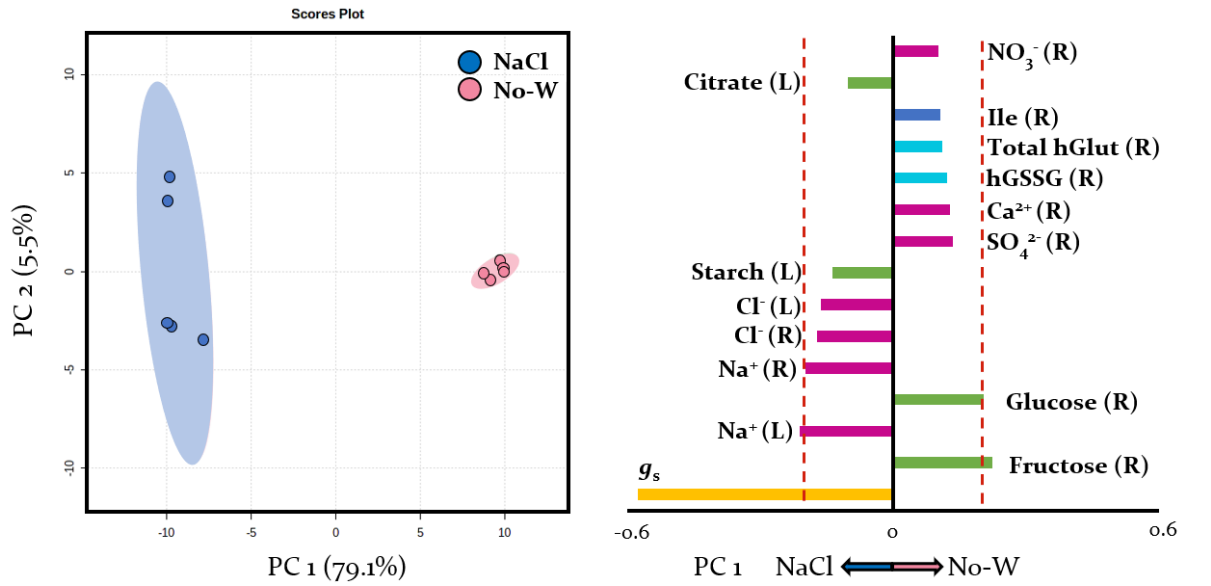

Figure 2.15. Principal Component Analysis conducted with all measured parameters in NaCl and No-W-treated plants. ***Left***, PCA scores plot showing the salted (NaCl) and non-irrigated (No-W) cases. ***Right***, loading values of all variables in PC1 separating both treatments. g_s, stomatal conductance; *hGlut,* homoglutathione; *hGSSG,* oxidized homoglutathione; *L*, leaves; *R*, roots. *Bar key:* dark blue, amino acids; green, carbohydrates; light blue, antioxidants; pink, inorganic ions; yellow, physiological measurements.

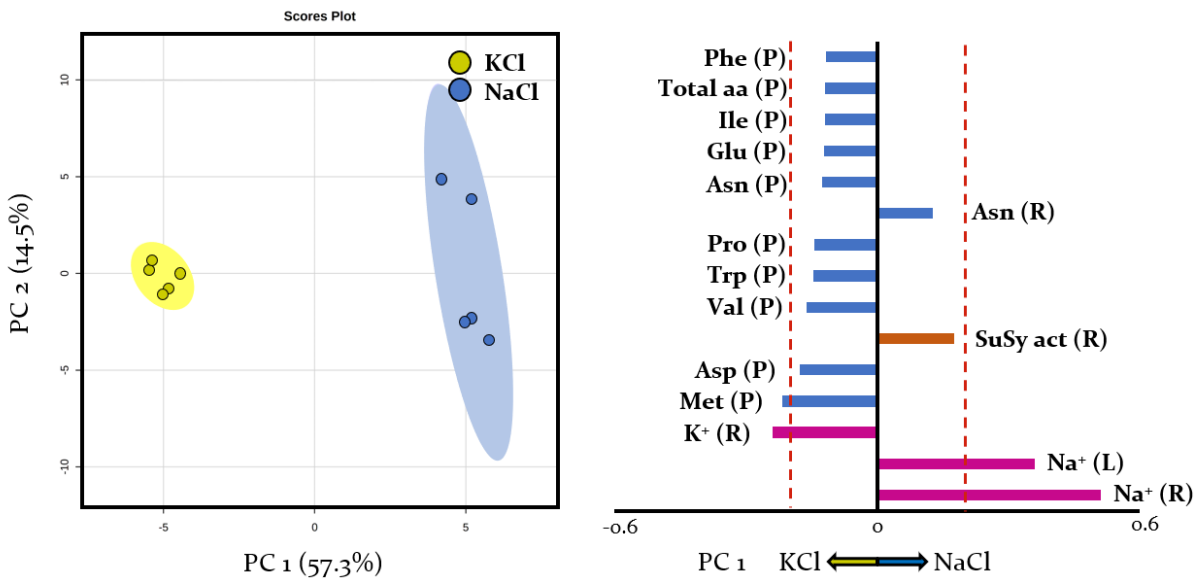

Figure 2.16. Principal Component Analysis conducted with all measured parameters in NaCl and KCl-treated plants. ***Left***, PCA scores plot showing the NaCl and KCl cases. ***Right***, loading values of all variables in PC1 separating both treatments. *aa*, amino acids; *act*, activity; *L*, leaves; *P*, phloem sap; *R*, roots; *SuSy*, sucrose synthase. *Bar key*: blue, amino acids; orange, enzymatic activities; pink, inorganic ions.

2.5. DISCUSSION

2.5.1. PEG: a false mimicker of drought

PEG is a polymer widely employed to mimic drought stress (Peng *et al.*, 2017; Zhang and Shi, 2018). One of the advantages of using this osmotic agent *versus* water-deficit imposition through withholding irrigation is the possibility to adjust precisely the stress level in the hydroponic solution, yielding a more uniform and controlled stress, which is of outmost relevance to study very early responses to water-deficit stress (Dubois and Inzé, 2020). However, even though PEG-6000 molecules are usually described as too large to be taken up by intact roots, several studies have observed PEG uptake by both leaves and roots which, together with the hypoxic nature of the highly-viscous PEG solution, can lead to additional stresses in plants subjected to PEG irrigation (Osmolovskaya *et al.*, 2018). Despite this potential problem and the simplicity of the procedure, PEG uptake by plants is not routinely assessed, which makes the determination of its effect and the comparison of the results with other drought studies even more difficult.

For this study, PEG-treated plants exhibiting a $\Psi_{leaf} \approx -1.7$ MPa were selected in order to perform a comparative analysis among the different stresses at an equal level of water-deficit stress. In this context, when comparing PEG and No-W-treated plants we found some common physiological and metabolic responses such as the reduced transpiration and stomatal conductance (**Fig. 2.3**) and root soluble protein content, as well as the general amino acid accumulation (**Fig. 2.7**), especially proline (**Table 2.2**). These responses are in agreement with previous studies with plants subjected to drought stress as part of their stress response (Fang and Xiong, 2014). However, PEG-treated plants' WC behaved in an opposite way compared to No-W-treated plants, with a lower WC in PEG-treated leaves and non-irrigated roots (**Fig. 2.4**). This is in agreement with Fan and Blake (1997), who observed a higher decline in leaf WC of 5-month-old seedlings of jack pine, black spruce and flooded gum treated with PEG-3350 compared to those subjected to no irrigation at similar Ψ_{leaf}. This phenomenon could be a consequence of the reduced root water flow due to the high viscosity of high-molecular weight PEG solutions (Chazen *et*

al., 1995). Indeed, PEG treatment has been reported to exert deleterious effects on plants due to the hypoxia of the highly viscous PEG medium but also due to the presence of contaminants as well as of different PEG sizes, which could explain the batch-dependent toxicity response observed by Janes (1974). Additionally, the decrease in leaf WC in PEG-treated plants could be a sign of PEG uptake and toxicity, which has been reported to disturb leaf water relations by blocking the water-conducting channels and possibly exert a toxic response (Fan and Blake, 1997; Lawlor, 1970). On the other hand, Forner-Giner *et al.* (2011) observed that citrus seedlings treated with 10% PEG-6000 compared to those subjected to lack of irrigation exhibited similar leaf WC values and the same Ψ_{leaf} around -1.5 MPa. However, the much higher leaf and root ABA levels and lower stomatal conductance under PEG stress compared to those under no-irrigation conditions could suggest a higher degree of stress under PEG exposure. Former studies reported an active high-molecular weight PEG uptake by intact plants (Fan and Blake, 1997; Jacomini *et al.*, 1988; Yaniv and Werker, 1983), highly dependent on PEG size, concentration and exposure time, as well as on the studied species (Janes, 1974; Lawlor, 1970). The short duration (48 h) of the PEG exposition in citrus seedlings compared to the 12-day-long study performed by Fan and Blake (1997) or our 7-day-long exposure could explain some of the differences observed between these studies.

One of the most divergent aspects differentiating no-irrigation and PEG treatment was the carbohydrate content (**Fig. 2.5, 2.14**). Indeed, even though starch depletion has been a long time described phenomenon under drought stress that serves as energy and carbon supply when photosynthesis may be limited (Thalmann and Santelia, 2017), its decline was more dramatic in leaves subjected to PEG irrigation. In addition, root sucrose levels were similarly increased under both stresses, correlating well with the inhibition of root SuSy (**Fig. 2.12**), a key enzyme involved in sucrose degradation. However, sucrose accumulation was especially remarkable in PEG leaves, while hexoses concentration only increased under No-W (**Fig. 2.5, 2.14**). This increase in leaf soluble sugars was also observed in alfalfa plants subjected to -1.2 MPa PEG-6000 for 15 days (Zhang and Shi, 2018) and has been described as a common behaviour in drought-stressed plants due to their role in osmoregulation, amongst others (see **section E.3.3,** Fang and Xiong,

2015). Darko *et al.* (2019) also reported a different pattern of soluble sugars accumulation in leaves and roots of wheat seedlings depending on the studied stress (PEG-6000, mannitol, sorbitol and NaCl). This suggests that the soluble sugar accumulation profile is highly dependent on the imposed stress, which could have a role in the signalling process of the regulation of plant metabolism and development (Darko *et al.*, 2019; Rosa *et al.*, 2009). In our study, while both treatments led to an overall increase in leaf soluble sugars, PEG-treated plants showed a more pronounced accumulation, which is in agreement with previous studies that observed a higher photosynthesis inhibition under PEG conditions (Fan and Blake, 1997). Indeed, an increase in soluble sugars has been linked to a decrease in the photosynthesis rate (Rosa *et al.*, 2009). Overall, these results suggest that carbon metabolism is being differentially regulated under both stresses. This is in agreement with Cui *et al.* (2019b), who observed a differential modulation of carbon metabolism-related enzymes under PEG-6000 and soil drought treatments in leaves of wheat seedlings.

Proline accumulation is another drought stress response that is observed early in the onset of osmotic stress (Fang and Xiong, 2014). In our study, both PEG and No-W-treated plants showed a marked increase in this compatible solute, with a much higher accumulation in PEG-treated leaves and phloem sap (**Table 2.2; Fig. 2.14**). However, these results are in disagreement with the higher leaf proline accumulation of drought-treated apple seedlings compared to those exposed to either 5 or 10% PEG-6000 (Kautz *et al.*, 2015). Yang *et al.*(2017) also observed a higher proline accumulation in three strains of tobacco plants subjected to up to 20 days of limited watering compared to those under 15% PEG-6000 for 16 or 24 h. This was explained as a consequence of the immediate stress provoked by PEG compared to the progressive effect of the cessation of irrigation, which allows a continuous proline accumulation in the time course of the experiment. On the other hand, Cui *et al.* observed a similar accumulation of proline under both treatments, which was consistent with the increases in the content of key enzymes involved in proline metabolism (Cui *et al.*, 2019b). However, like in our study, a differential activation of proline metabolism-related enzymes was observed (**Fig. 2.13**), suggesting that PEG and No-W affect proline metabolism through different mechanisms.

An additional and very marked difference between both water-deficit treatments was the depletion of inorganic nutrients under PEG treatment (**Fig. 2.8, 2.14; Table 2.3**). The decrease in leaf ions was also observed in wheat leaves subjected to PEG stress (Filek *et al.*, 2012; Pei *et al.*, 2010). However,water withholding did not alter the leaf ion content in *Limonium* species either (González-Orenga *et al.*, 2019), suggesting a lack of nutrient deficiency under these conditions. Maintaining appropriate nutrient levels is key for plant function and growth, and it is of special relevance under drought stress, where the decrease in transpiration and water uptake can lower K^+ influx to the roots (see **section E.3.6**). K^+ is an essential nutrient with a key role in drought resistance due to its implication in osmotic adjustment, water uptake, cell membrane stability, stomatal regulation and ROS detoxification, among others (Shabala and Pottosin, 2014; Wang *et al.*, 2013). Considering the special importance of this nutrient, its decline, together with the decline in other essential nutrients under PEG exposure compared to no-irrigation stress suggests a higher plant metabolic and physiologic alteration and lower tolerance towards PEG treatment. These lower nutrient levels upon PEG exposure could be another consequence of low oxygen availability due to the highly viscous nature of the PEG solution (Munns *et al.*, 2010; Osmolovskaya *et al.*, 2018). Indeed, hypoxic conditions cause a low energy status that can impair ion transport processes and the uptake of essential ions such as K^+, NH_4^+ or Mg^{2+} (Wang *et al.*, 2013). The presence of hypoxic conditions in PEG-treated plants could also explain the vast increase in succinate and alanine levels in PEG-treated roots (**Fig. 2.6; Table 2.2**) due to a shift in the primary carbon metabolism under these conditions (António *et al.*, 2016).

Based on the observed results, even though at a physiological level a similar response to water withdrawal can be observed and the presence of typical drought stress markers such as proline accumulation could suggest PEG as an adequate mimicker of drought, the important impairment on nutrient uptake and the differential regulation of carbon and proline metabolism exerted by PEG discourage to believe that conclusions based on PEG studies may be directly extrapolated to the understanding of drought stress responses.

2.5.2. Salinity and drought: differences in the metabolic response at the whole-plant level

Drought, salt and cold stress share in common a water-deficit stress at the cellular level, and therefore several studies analyse and compare the effect of these stresses in the plant metabolism to better understand the particularities of each one. Some of the studies are focused exclusively on drought/no-irrigation and salt stress (Fita *et al.*, 2015) due to the higher impact of these stresses on crop productivity. Indeed, salinity and drought are two of the major abiotic stresses affecting plant yield, and it is estimated that up to 45% of the agricultural lands are subjected to continuous or frequent drought and that 50% of all arable land will become impacted by salinity by 2050 (Butcher *et al.*, 2016). Although salt and drought stress trigger some common responses in plants, especially at early stages, salinity implies an important ionic stress by high intracellular sodium and chloride concentrations (Munns, 2011), thus affecting plant metabolism in a different way than no-irrigation stress.

In this study, salt (NaCl) and drought (no-irrigation) stress were imposed to provoke a drop to Ψ_{leaf} -1.7 MPa in order to elucidate the different effects that both stresses exerted at a whole-plant level. The closure of stomata is a common phenomenon under water-deficit stress as previously observed in this plant (Filippou *et al.*, 2011), aimed at decreasing water loss through transpiration. It has long been thought that the main driver of stomatal closure in response to soil drought was ABA synthetised in roots and transported to leaves in the xylem. However, evidence now points towards a "hydroactive feedback" mechanism (the regulation of the osmotic pressure in the guard cell in relation to the leaf water status), which would possibly involve ABA synthetised in leaves (Buckley, 2019). This could explain why, despite the similar Ψ_{leaf} achieved by No-W and NaCl-stressed plants, drought stress led to a lower stomatal conductance, which correlated well with the lower leaf WC in the soil-drying experiment (**Fig. 2.3, 2.4, 2.15**). On the other hand, while salt stress did not significantly affect the roots` WC, No-W conditions led to a significant decrease in this parameter (**Fig. 2.4**). This could mean that, while the lack of irrigation led to an obvious decrease in the soil water content, the presence of NaCl and consequent increase in the soil osmotic potential was not enough to

fully inhibit root water absorption under these conditions. Despite these physiological differences, it was at the metabolism level where the disparities between both treatments became more evident.

Drought stress modulates carbon metabolism in the roots, while salinity does so in the shoots

The differential response exerted by both water-deficit treatments was also visible when analysing the carbohydrate content (**Fig. 2.5, 2.15**). In leaves the starch content increased in response to salt stress but decreased dramatically upon No-W stress, while sucrose accumulated under both stresses, above all in response to NaCl. This behaviour was also observed in rice leaves (Amirjani, 2011) and would be in agreement with the higher hexose content in No-W stressed leaves compared to the NaCl-treated ones, in which the inhibition of starch synthesis would allow for glucose and fructose build-up (**Fig. 2.5**). On the other hand, the leaf sucrose accumulation under salinity stress despite this starch accumulation implies a sucrose *de novo* synthesis derived from photosynthesis, which is in agreement with the better stomatal conductance observed under these conditions (**Fig. 2.3**). This sugar partitioning into starch is often observed in salinity experiments and could be a means to scavenge excess sodium and/or to avoid metabolic alterations derived from an excessive accumulation of sucrose, which can act as a feedback inhibitor of processes such as photosynthesis (Dong and Beckles, 2019; Thalmann and Santelia, 2017). In agreement with this statement, sucrose levels correlated well with starch levels in *M. truncatula* leaves under salt and No-W treatments (**Fig. 2.5**). Additionally, the higher starch content in the NaCl- than No-W-treated roots (**Fig. 2.5**) could increase starch statoliths and gravitropic response, aiding in root depth perception and directing root growth for the proper acquisition of nutrients, minerals and/or water (Dong and Beckles, 2019). The decrease in starch content in response to water-deficit conditions has been previously described as a common behaviour in response to drought stress in order to provide energy and carbon when photosynthesis is limited (Krasensky and Jonak, 2012; Thalmann and Santelia, 2017).

Soluble sugars, including fructose and, especially, sucrose and glucose, play a crucial role in plant metabolism and in the defence of plants against stress, serving as osmoprotectants, source of energy and carbon, as well as signaling molecules involved in the up-regulation of genes involved in plant defense (see **section E.3.3**, Dong and Beckles, 2019; Gibson, 2000; Rosa *et al.*, 2009; Ruan *et al.*, 2010). Hence, the accumulation of these molecules under abiotic stress has been widely reported in the literature (Singh *et al.*, 2015), usually linked to the increased synthesis from starch or the decreased demand as a consequence of growth limitation (Dong and Beckles, 2019; Hummel *et al.*, 2010; Thalmann and Santelia, 2017). In our study, the differential regulation of hexoses, sucrose and starch levels in salinity and drought-stressed leaves suggests a different mechanism for stress tolerance, in which the tight control of sucrose levels through activation of starch synthesis would avoid photosynthesis inhibition under salinity stress. On the other hand, the higher stomatal closure under No-W stress (**Fig. 2.3**) would make this mechanism redundant, allowing starch degradation and soluble sugars accumulation to be available for abiotic stress tolerance.

The phloem sap is the fluid transported by the phloem sieve tubes, translocating the products of photosynthesis from mature leaves to growing and storage organs, including the roots (see **section C**, Savage *et al.*, 2016). It is currently believed that the local osmotic gradients in each tissue generate a pressure difference between the source and the sink driving the phloem transport, which implies that changes in tissues, such as those driven by drought and salt stress, may alter this transport (Sevanto, 2014). Despite the high relevance to plant growth and interaction with the environment, there are not many works studying the phloem sap because of the challenges involved in its obtaining, above all under drought conditions. The EDTA-facilitated phloem exudation technique employs low concentrations (10-20 mM) of EDTA to prevent Ca^{2+} ions from sealing the phloem. This protocol has been extensively used in plants such as arabidopsis (Rahmat and Turnbull, 2013), allowing an easy, quick and cheap study of the phloem sap even in plant species with thin petioles and under water-deficit conditions such as those that are addressed here.

In this study, phloem sucrose concentration was not altered under NaCl or No-W conditions (**Fig. 2.5 insert**). It must be taken into account that the phloem collection took place one hour after the beginning of the photoperiod, which might imply a lower photosynthesis rate and sugar translocation compared to mid-day values (Dong *et al.*, 2018). However, these results suggest that plant metabolism was not severely affected by these stresses, with enough starch available to sustain plant metabolism even at night (Dong *et al.*, 2018). Considering the fact that phloem translocation depends on source and sink strengths, the maintenance of the sucrose phloem transport despite the inhibition of photosynthesis under No-W conditions (**Fig. 2.3**) suggests an increased sink strength. This is in agreement with the significant increase in the root-to-shoot ratio under No-W and increased AlkINV activity in the root (**Table 2.1; Fig.2.12**). Indeed, the significant increase in the root/shoot ratio is a commonly observed phenomenon under drought stress, linked to the change in carbon partitioning under these conditions derived from the lower growth inhibition of the root compared to the shoots, allowing better water uptake from the soil (see **section E.3.1**). This increase in root strength under No-W could be linked to the increase in AlkINV observed in this organ, which could compensate for the decrease in the SuSy activity (**Fig. 2.12**), as observed previously in arabidopsis (Barratt *et al.*, 2009), rice (Xu *et al.*, 2015) and, just recently, *M. truncatula* (Echeverria and González, 2021, Echeverria *et al.*, 2021). The decrease in root SuSy activity in response to abiotic stress has also been reported in maize (Hütsch *et al.*, 2016) and in the roots of drought-tolerant and sensitive cultivars of sorghum (Goche *et al.*, 2020), as well as in *M. truncatula* nodules (Gil-Quintana *et al.*, 2015), while increasing in the roots of drought sensitive grapevine (Prinsi *et al.*, 2018). In our study, the decrease in root sink strength under salinity due to a decrease in both SuSy and INV might indicate a preferential redistribution of assimilates to the shoots rather than to the roots in NaCl stressed *M. truncatula* plants. On the other hand, these responses suggest a key role of AlkINV in the regulation of assimilate partitioning and plant response to drought stress, allowing sucrose transportation, unloading and degradation in the root tissue for its use in root growth and/or osmoprotection under adverse conditions. Indeed, various authors have reported a key role of INV in the positive regulation of root growth and root-to-shoot ratio in arabidopsis (Lou *et al.*, 2007; Meng *et al.*, 2020; Sergeeva *et al.*, 2006).

The increase in root soluble sugar content under No-W (**Fig. 2.5, 2.15**) was also observed in drought-tolerant wheat cultivars, where the maintenance or even increase in the levels of root soluble sugars, amino acids and TCA cycle-involved organic acids allowed the maintenance of the intracellular ionic balance and nutrient uptake (Guo *et al.*, 2018). The increase in root sucrose and hexose content was also evident in droughted mountain grassland and was attributed to a decrease in the carbon demand linked to the decrease in root respiration (Hasibeder *et al.*, 2015). This increase in soluble sugar content together with the decrease in root respiration was previously reported in drought-stressed *M. truncatula* plants, being a commonly described response to osmotic stress linked to drought tolerance (see **sections E.3.2 and 1.5.2**). However, the effect of salinity on root respiration is highly variable, with no agreement between the different studies that address it (Jacoby *et al.*, 2011). In our study, even though no measurements of respiration under NaCl stress were made, the higher root starch and soluble protein levels (**Fig. 2.5, 2.7**), higher G6PDH activity, lower inhibition of SuSy and lower activation of root AlkINV under NaCl stress (**Fig. 2.12**) suggest a more active root metabolism under salinity conditions than drought.

In our study, the levels of leaf organic acids remained constant under No-W stress, while α-KG and citrate increased significantly under salinity stress, reflecting the subtle differences in the management of the different osmotic stresses (**Fig. 2.6**). The α-KG accumulation observed in salt-stressed leaves could be a result of a decreased breakdown through ketoglutarate dehydrogenase (α-KGDH) inhibition due to salinity-derived oxidative stress, an increased translocation from roots to shoots and/or an increased formation through $NADP^+$-IDH activation, as observed in our study (**Fig. 2.11**). α-KGDH, which catalyses the oxidation of α-KG into succinate with the generation of NADH, is very sensitive to oxidative stress and is a rate limiting step for NADH production, thus controlling mitochondrial electron transport and ATP production (Araújo *et al.*, 2008). On the other hand, the observed activation of IDH in salt-treated leaves, as previously observed (Naliwajski and Skłodowska, 2018), not only could allow for this α-KG build-up, but also for net glutamate biosynthesis via the GS/GOGAT cycle, thus playing a key role in the synthesis of amino acids as well as in the linkage between carbon

and nitrogen metabolism (Foyer *et al.*, 2011). In addition, the reaction catalysed by IDH provides the cytosol with NADPH, which can be used in the reduction of NO_3^- and many other biosynthetic processes such as proline biosynthesis or glutathione regeneration, allowing ROS scavenging (Corpas and Barroso, 2014). This could explain why its over-expression increased salt tolerance in transgenic *A. thaliana* plants (Liu *et al.*, 2010) and its activity decreased in salt-sensitive durum wheat (Bouthour *et al.*, 2015), hence suggesting an important role in *M. truncatula* tolerance to NaCl.

Overall, the marked soluble root sugar accumulation in No-W plants and increased AlkINV activity indicates a reduced root respiration linked to an increased sink strength under drought conditions. However, this response seems to be absent or less relevant under NaCl conditions, where the accumulation of starch in leaves could be a means to avoid photosynthesis inhibition and/or scavenge excess ions. On the other hand, starch and IDH emerge as potential important players in salinity stress response.

Drought elicits an overall accumulation of amino acids in roots while only proline metabolism is modulated under salt stress

Attending to nitrogen compounds, the response of salt and drought stress was also different. Protein degradation is a common phenomenon observed under stress conditions, being more prevalent under severe stress and/or in sensitive plants and contributing to the amino acid pool build-up (Krasensky and Jonak, 2012). In addition, the increased protein catabolism could also be linked to the provision of carbon sources for respiration as a mechanism linked to drought stress tolerance (Araújo *et al.*, 2011). In our study, soluble protein and total amino acid contents were not relevantly affected at either shoot or root level under salt stress. However, the lack of irrigation provoked a significant accumulation of amino acids in roots accompanied by a non-significant decrease in the protein content in No-W stressed roots (**Fig. 2.7**) in agreement with previous studies (Akhzari and Pessarakli, 2016; Lyon *et al.*, 2016). In addition, the lack of phloem amino acid accumulation under drought stress (**Fig. 2.7 insert**) opposed to the increase in leaves and roots suggests an *in situ* root amino acid synthesis or protein recycling rather than import from the shoots. This is in agreement with the observed proteomic changes in *M. truncatula* (Lyon *et al.*, 2016), where drought stress provoked an

accumulation of protein degradation and amino acid synthesis-related proteins in roots while decreasing in shoots, as suggested by our enzymatic studies (**Fig. 2.13**). As observed in the previous chapter, the BCAAs Leu, Ile and Val increased upon water-deficit stress, which could be used as alternative electron donors for respiration, reinforcing their role on water-deficit tolerance (Pires *et al.*, 2016).

Even though drought stress did not increase the phloem sap total amino acid content, Pro was significantly increased in agreement with studies in white clover (Lee *et al.*, 2009) and arabidopsis (Mewis *et al.*, 2012). Lee *et al.* (2009) concluded that Pro loading to the phloem sap has a significant influence on the down-regulation of N-uptake and assimilation, which could imply a means of avoiding further NH_4^+ build-up due to the down-regulation of growth and protein synthesis (Kim *et al.*, 2004). Indeed, the increased proline phloem loading in white clover was closely related to the decrease in nitrogen reductase in roots, nitrogen uptake and its assimilation (Lee *et al.*, 2009). Thus, an increased proline phloem transport is a common phenomenon observed under drought and salinity stress (Gilbert *et al.*, 1998; Girousse *et al.*, 1996; Hasanuzzaman *et al.*, 2019), suggesting an important abiotic stress tolerance mechanism and a wider array of roles than merely serving as an osmoticum (Kishor and Sreenivasulu, 2014).

Contrary to drought, salt stress did exert significant changes in the phloem sap amino acid content, with a significant increase in total and several individual amino acid contents, above all Pro and less significantly Gln, Ser, Arg and GABA (**Table 2.2**). The increase in total phloem sap amino acids was also observed in tomato plants (Pérez-Alfocea *et al.*, 2000), but the lack of increase in NaCl roots suggests their redistribution in the shoots. In addition, the increase in amino acid flow in the phloem could also be considered a nitrogen source, correlating well with the decrease in the NO_3^- levels in the roots of NaCl plants (**Fig. 2.8C**), which further highlights the different response and adaptations of *M. truncatula* to both stresses. On the other hand, Cuin and Shabala suggested that certain amino acids such as GABA, Pro, Gln, Ser and Arg can mitigate the NaCl-induced K^+ efflux, while others such as Val can enhance the detrimental effects of salinity on K^+ homeostasis (Cuin and Shabala, 2007). This is in agreement with the amino acid changes observed in the salt-stressed phloem sap, indicating that increases

in free amino acids under abiotic stress might have a key role in plant salinity tolerance and are far from merely being a symptom of damage (Cuin and Shabala, 2007).

It is remarkable the overall accumulation of proline at the whole-plant level in response to both stresses (**Table 2.2**), which is a widely accepted response of plants to abiotic stress. Proline is a compatible solute which acts as osmolyte, molecular chaperone and hydroxyl radical scavenger, protecting cells from stress-induced damage (Krasensky and Jonak, 2012; Sharma *et al.*, 2011). Two routes have been proposed for proline biosynthesis: via glutamate (involving P5CS) or via ornithine (through OAT, see **section E.3.4**). Even though there is some controversy regarding the relevance of each route, it has been suggested that the ornithine pathway would have a more important role under normal conditions, while the P5CS route would take more relevance under N-limitation or osmotic stress conditions (Zarattini and Forlani, 2017). However, the importance of the ornithine pathway in proline biosynthesis is unclear and it has also been proven to be important in some plants and/or organs under stress as well (Anwar *et al.*, 2018). In our study, Pro synthesis was increased in both leaves and roots in NaCl-treated plants, while no-irrigation only altered Pro synthesis-related enzymes in the root tissue (**Fig. 2.13**). This is in agreement with the higher Pro content in the leaves and phloem sap under salt than no-irrigation conditions (**Table 2.2**). On the contrary, Pro root degradation was only activated upon drought stress, possibly as a mechanism for energy and reducing equivalents generation under stressful conditions (Kaur and Asthir, 2015), highlighting again the need of root metabolism maintenance under No-W. In these conditions, Pro synthesis took place mainly in the roots as shown by the increase in both P5CS and OAT activity (**Fig. 2.13**), as needed for supporting Pro degradation and a possible Pro translocation to the shoots. These results are in agreement with Verdoy *et al.* (2006), who observed an increased Pro degradation and activation of OAT activity in osmotic stressed *M. truncatula* roots, thus remarking the importance of the ornithine pathway under stressful conditions in this plant species. These results, together with the differential Pro accumulation under both stresses and organs (**Table 2.2**) highlight the organ and stress-dependant Pro metabolism regulation in *M. truncatula*.

As mentioned above, despite the higher total amino acid accumulation in No-W than NaCl treatments, Pro and Ser accumulated more in salt-treated than drought-stressed leaves, while the opposite was observed for roots (**Table 2.2**). This was also observed in another study using *M. truncatula* drought- and salt-stressed plants (Staudinger *et al.*, 2012). A higher shoot amino acid accumulation compared to roots was also observed in different wheat and barley genotypes and addition lines in response to salinity stress (Darko *et al.*, 2017). Due to the compatible solute nature of both amino acids, their higher accumulation in leaves under salt stress, together with the higher sucrose accumulation in this tissue (**Fig. 2.5**) could be linked to a higher effort of the plant for preserving shoot integrity under salinity conditions. However, the opposite situation was observed for drought-stressed roots, where a higher sucrose and amino acids, above all proline, accumulation was observed. Together, these results highlight the importance of root integrity maintenance under drought conditions, where water uptake from the soil is crucial to overcome stress injury.

Salt stress provokes a nutrient deficiency which does not occur in drought-stressed plants

The most notorious differential effect of both stresses was observed in the *M. truncatula* ionome (**Fig.2.8, 2.15; Table 2.3**). Thus, while drought stress did not significantly alter the ion content of leaves and roots, salt stress led to massive ion alterations in both tissues, especially roots. NaCl irrigation led to a very important Na^+ and Cl^- ion accumulation in both organs, as previously reported for alfalfa plants (Sun *et al.*, 2016). These ions' transport to the shoot and vacuole sequestration is an extensively described salt-tolerance mechanism for the maintenance of a healthy high cytosolic K^+/Na^+ ratio (Nadeem *et al.*, 2019b). The decrease in Ca^{2+} ions in the root tissue has also been previously observed in alfalfa plants under salinity stress (Ashrafi *et al.*, 2018), possibly related to a decreased uptake due to a reduced Ca^{2+} activity in NaCl-rich soil solutions. Indeed, Na^+ and Cl^- ions compete with other ions such as K^+, Ca^{2+}, Mg^{2+} and NH_4^+ as well as SO_4^{2-} ,PO_4^{3-} and NO_3^- , respectively, for the ion transporters during root uptake and translocation in plant shoots, as well as during their use in biochemical processes such as enzymatic reactions (see **section E.3.6**, Hauser and Horie, 2010; Parihar *et al.*, 2015). This ion

competition was especially relevant in the root tissue, where the accumulation of Na^+ and Cl^- ions was accompanied by the concomitant decrease in the K^+, Mg^{2+}, Ca^{2+} and SO_4^{2-} contents (**Fig. 2.8; Table 2.3**).

The only significant effect of drought stress in the plant ionome was the accumulation of NO_3^- and, to a lesser extent, SO_4^{2-} in the root tissue (**Fig. 2.8C**). Nitrate is the main nitrogen source in agricultural soils and the mineral nutrient that most frequently limits plant growth. This NO_3^- accumulation has been previously observed in *Spartina alterniflora* plants under drought stress (Hessini *et al.*, 2009) and could be due to a reduction in the nitrate reductase activity, the first and rate-limiting strep enzyme in the nitrate assimilation pathway, which has been observed to decline in many species even under mild-water stress (Correia *et al.*, 2005). The decline in root AAT activity (**Fig. 2.12**), another nitrogen metabolism-related enzyme, also agrees with this decrease in root nitrogen metabolism under water-deficit conditions. However, despite the decrease in the primary assimilation of nitrogen, the increase in nitrogen compounds such as amino acids rules out a deficit in nitrogen under this stress, possibly due to the reduced N-demand derived from halted protein synthesis upon drought stress (Castañeda *et al.*, 2018).

Overall, salt stress led to the accumulation of Na^+ and Cl^- ions in both leaves and roots, but only the latter exerted ion balance mechanisms through the decrease in K^+, Ca^{2+}, Mg^{2+} and SO_4^{2-} contents, suggesting an important nutrient deficit in this tissue compared to the seemingly efficient Na^+ and Cl^- vacuole sequestration in the shoots. However, no nutrient deficiency was observed in neither leaves nor roots of drought-stressed plants and even an increase in nitrate levels was observed in the roots, suggesting a lower N-assimilation under these conditions.

α-KG metabolism might be involved in modulating the cellular redox environment in salt-treated leaves

Water-deficit stress has been long known to increase the generation of ROS, which can serve as a signalling mechanism to activate the defence responses of the plant to stress, but can also lead to cellular damage and even death when reaching excessive concentrations (Czarnocka and Karpiński, 2018). In order to modulate ROS levels, several metabolites which serve as antioxidant molecules work in a coordinated manner, being a key process their conversion back to their reduced state using NAD(P)H in order to be able to maintain their function (see **section E.3.5**, Xiao and Loscalzo, 2020).

Interestingly, total glutathione and homoglutathione levels were lower in salt-stressed roots compared to those of No-W-treated plants (**Fig. 2.9B; 2.15**). Glutathione is one of the main plant polar antioxidants and plays a central role in ROS scavenging through the glutathione-ascorbate cycle and as an electron donor to glutathione peroxidase, while homoglutathione is a glutathione homologue with similar functions and characteristic of legumes, being usually accumulated under various stresses, including drought (Zagorchev *et al.*, 2013). On the other hand, even though the total glutathione and homoglutathione levels remained unchanged in salt-treated leaves, the reduced homoglutathione/total homoglutathione ratio was increased under salinity stress, even though without statistical significance (**Fig. 2.9A, C**). A higher reduced/oxidized ratio is linked to plant tolerance to stress (Hasanuzzaman *et al.*, 2019), which might indicate a higher effort and/or ability of salt-exposed plants to protect the shoots from oxidative stress.

In addition, as discussed previously, while most citric acid cycle-related organic acids were not significantly affected by either stress, α-KG contents increased in NaCl-stressed leaves (**Fig. 2.6**). The inherent ROS detoxifying properties of α-KG and its accumulation under NaCl stress, together with the decreased ROS formation as a result of inhibited respiration due to lower NADH availability (through the potential inhibition of α-KGDH) confer a unique strategy to modulate the cellular redox environment (Mailloux *et al.*, 2007). The increase in sucrose and starch contents without the decrease in the leaf organic acid content in NaCl leaves also suggest a reduced respiration rate in

this tissue (**Fig. 2.5, 2.6**), as previously reported (Che-Othman *et al.*, 2017; Henry *et al.*, 2015). Hence, the higher accumulation of α-KG in salt-treated leaves and drought-stressed roots may reflect the higher need of these tissues for a ROS detoxification. This apparently higher sensitivity of leaves to NaCl stress than roots was also reported for maize plants and switchgrass, with one of the responses being a higher antioxidant content in leaves than roots (Qing *et al.*, 2009; Wang *et al.*, 2012). Overall, results suggest a higher protection through diverse antioxidant mechanisms of NaCl shoots and non-irrigated roots.

Generally, *M. truncatula* is considered a relatively drought-tolerant legume compared to others like pea or soybean (Limami *et al.*, 2007). However, regarding salinity stress *M. truncatula* Jemalong A17 cultivar is considered salt sensitive by some authors (Long *et al.*, 2016) and salt-tolerant by others (de Bruijn, 2020). Our study suggests a similar tolerance to both drought and salt stress, with even some parameters such as higher stomatal conductance and leaf WC suggesting a slightly better coping with NaCl at similar leaf water potentials. Nonetheless, *M. truncatula* responses to both stresses differed notably (**Fig. 2.17**), with a marked defensive response of NaCl shoots and droughted roots through the accumulation of soluble sugars and amino acids under both stresses. In addition, the most relevant differences in the plant's response to stress was the increased starch content in plants under NaCl, possibly as a mechanism of ion sequestration and avoidance of photosynthesis inhibition, as well as the increase in IDH activity and α-KG content. The distinct amino acid profile in the phloem sap of salt-stressed plants could also be linked to salinity tolerance rather than merely being a symptom of damage. On the other hand, root proline catabolism, BCAA accumulation as well as the increased root sink strength via INV could play key roles in *M. truncatula* response to no-irrigation stress.

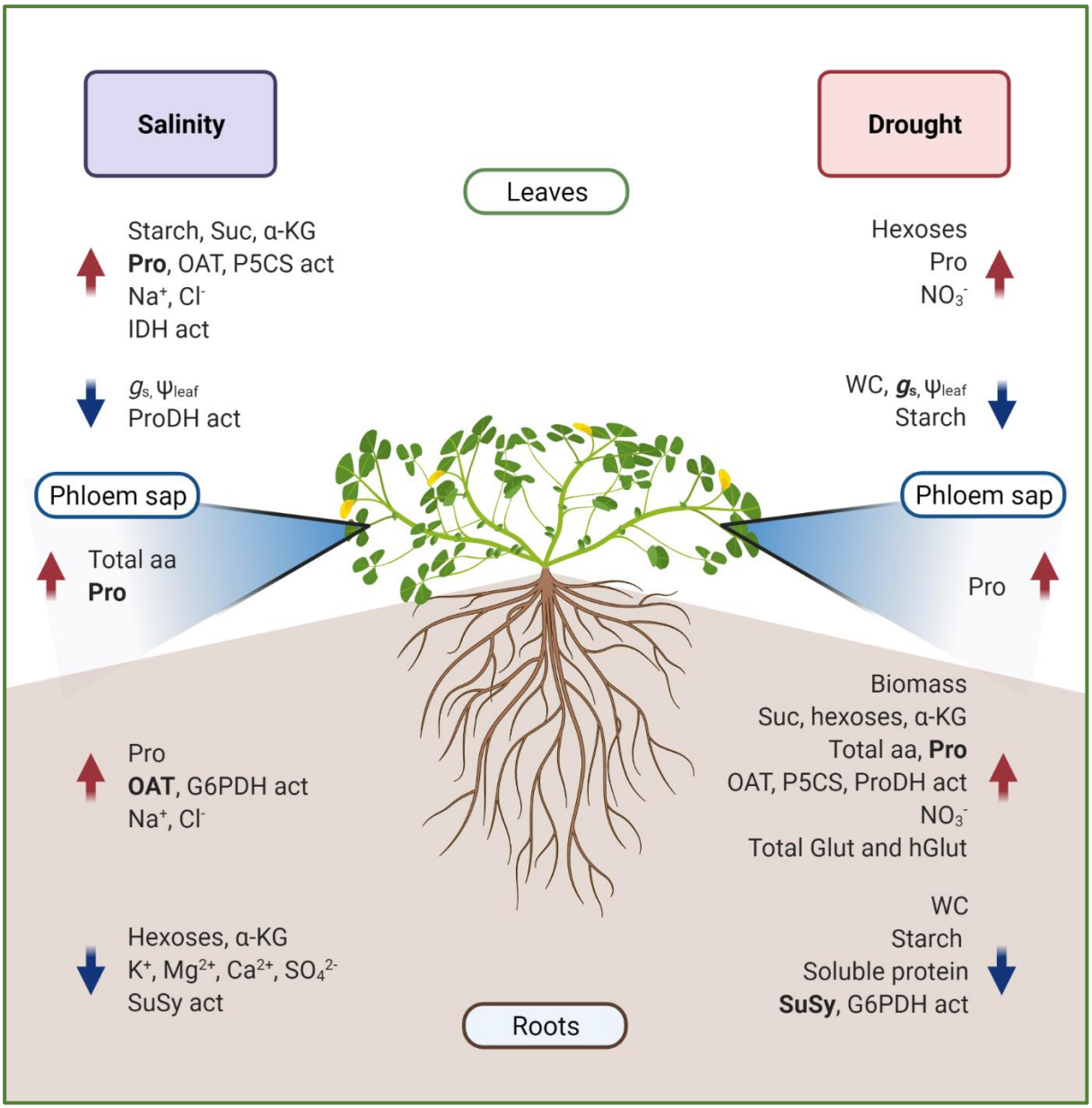

Figure 2.17. Summary of the most relevant *M. truncatula* responses to salinity and drought stress. This image depicts the increases and decreases in physiological parameters as well as enzymatic activities and metabolite and nutrient concentrations in leaves, roots and phloem sap under NaCl/salinity and no-irrigation/drought conditions. Parameters in bold represent more significant changes compared to the other stress. *aa*, amino acids; *act*, activity; *Glut*, glutathione; *G6PDH*, glucose-6-phosphate dehydrogenase; g_s, stomatal conductance; *hGlut*, homoglutathione; *IDH*, isocitrate dehydrogenase; *α-KG*, α-ketoglutarate; *OAT*, ornithine aminotransferase; *P5CS*, Δ^1-1-pyrroline-5-carboxylate synthase; *ProDH*, proline dehydrogenase; *Suc*, sucrose; *SuSy*, sucrose synthase; *WC*, water content; Ψ_{leaf}, leaf water potential. [Created with BioRender.com].

2.5.3. Sodium *versus* potassium salinity: similarities and disparities

Soil salinity derives from the accumulation of an excessive amount of ions such as calcium, sodium, sulphates or chlorides in the soil, leading to plant growth and function inhibition mainly through the interference of nutrient and water uptake (Munns, 2011). As a result, salinization is one of the major plant abiotic stresses reducing crop yield, affecting between 11 and 20% of the world's irrigated lands (Butcher *et al.*, 2016; FAO, 2011). Saline soils are often associated with high NaCl concentrations, which exert both osmotic stress (linked to the decrease in the medium's osmotic potential) and ion cyto-toxicity (mainly due to Na^+ ion accumulation and its effect on protein denaturation and membrane destabilization). However, the over-accumulation of Cl^- ions under stress conditions can also lead to chloride toxicity (Li *et al.*, 2017). The induction of salt stress using KCl in addition to NaCl has been used in previous studies for a better understanding of the toxic effect of NaCl in the plants (Dao and Hirai, 2018; Richter *et al.*, 2019), being this salt a common component in fertilized and saline soils as well (Kafkafi *et al.*, 2001). While various reports observe a more deleterious effect of KCl irrigation than NaCl (Ramos *et al.*, 2004; Slabu *et al.*, 2009; Yao *et al.*, 2010) the opposite behaviour has also been observed (Sima *et al.*, 2013) but, to our knowledge, no studies comparing NaCl and KCl effects have been performed in *M. truncatula* plants.

In this study, the physiological response to both salt stresses was similar in *M. truncatula*, with a similar reduction in transpiration and stomatal conductance (**Fig. 2.3**). The reduction in Ψ_{leaf}, transpiration and stomatal conductance is a common response of plants to osmotic and ionic stresses such as the exerted by the presence of high NaCl and KCl concentrations. However, KCl plants reached a lower Ψ_{leaf} than NaCl plants after the same 7–day treatment period and same salt concentration (**Fig. 2.3**), suggesting a more deleterious effect of KCl than NaCl on plant physiology. On the other hand, while the total dry biomass was not significantly altered in response to either stress (**Table 2.1**), KCl-treated plants showed a higher level of chlorosis in the oldest leaves (**Fig. 2.2**), even though this was not significantly detected when measuring chlorophyll content in the second fully expanded leaves (**Fig. 2.3**). The KCl-induced chlorosis in older leaves will be discussed in the next paragraphs.

Similarly, the carbon-metabolism response under KCl resembled that of under NaCl stress, but changes occurred at a different degree: starch and sucrose only accumulated in leaves, while hexoses and several organics acids were significantly reduced in roots under both salt stresses, with a more notorious response under KCl conditions in most cases (**Fig. 2.5, 2.6**). As discussed for drought, sucrose accumulation in response to salinity stress has been widely reported, with a role in the maintenance of cell turgor pressure and protection of molecules, allowing an active osmotic adjustment which facilitates the plant adaptation to salinity stress (Singh *et al.*, 2015). In agreement with our study, the exposure of a salt-tolerant rice cultivar to 200 mM NaCl lead to an increase in the leaf starch and soluble sugar contents generated from photosynthesis and starch degradation, respectively (Theerawitaya *et al.*, 2012). A higher increase in leaf sucrose levels under KCl despite the higher alteration of carbon metabolism and physiological parameters than NaCl-treated plants suggests a higher need for plant protection against the deleterious effects of this salt. Indeed, even though the extent of K^+ accumulation in KCl shoots was smaller than that of Na^+ ions under NaCl stress (**Fig. 2.8B**), the absolute total ion content accumulation was higher under KCl (**Table 2.3**), which would imply a higher disturbance of plant metabolism and ion homeostasis. On the other hand, the lower activity of SuSy in KCl-treated roots compared to NaCl (**Fig. 2.12, 2.16**) together with the lower root sucrose levels suggest that the efforts of the plant are focused on the preservation of the shoot integrity. In addition to this, the increased sucrose levels in the KCl-treated phloem despite the lower root sucrose mirrors the higher sucrose levels in the shoots under KCl stress (**Fig. 2.5**) and suggests a more important redistribution of sucrose between leaves in order to optimize osmotic adjustment. Indeed, excess ions under salinity stress are usually accumulated in the oldest leaves, as suggested in our study from the higher chlorosis level in these tissues, where they comprise most of the leaf osmolality. However, younger leaves usually increase their soluble sugar content in a higher extent than the older leaves in an effort to decrease leaf osmotic potential in a more carbon-dependent manner (Khelil *et al.*, 2007; Puniran-Hartley *et al.*, 2014). On the other hand, the main organic acids, citrate and malate, were decreased in KCl roots compared to control conditions. This, together with the lower IDH (a key enzyme in the TCA cycle) and G6PDH (a key enzyme of the OPP pathway) activities compared to NaCl

(**Fig. 2.12**) suggests a higher root respiration inhibition, which could be linked to the higher Cl^- ion accumulation in these plants (Geilfus, 2018). Additionally, the decrease in root organic acids in KCl roots could also be linked to their use as substrates for amino acid biosynthesis (Hill *et al.*, 2013).

Regarding nitrogen metabolism, a decrease in the root soluble protein content was observed, only statistically significant under KCl, while the amino acid content increased without statistical significance in the shoot, especially under KCl stress (**Fig. 2.7**). The increase in the total amino acid content in the shoot was mostly due to the significant increase in proline, even though serine also significantly increased its content (**Table 2.2**). This increase in amino acid content, especially proline, has been extensively described as a mechanism to cope with osmotic and salinity stress (Munns, 2011) and could mirror the higher damage of the shoots under KCl stress. Indeed, Pro accumulation is a great indicator of tissue damage, being considered a stress-tolerance mechanism in some studies but a mere marker of the level of stress affecting the plant in others (Arteaga *et al.*, 2020; Poustini *et al.*, 2007). However, this increase in the amino acid content in KCl plants was most obvious when analyzing the phloem sap (**Fig. 2.7 insert, 2.16**). The lack of correlation between this elevated amino acid concentration in the phloem sap compared to that of the roots suggests their redistribution in the shoots such as old transpiring leaves (Khelil *et al.*, 2007; Puniran-Hartley *et al.*, 2014).

The most relevant differences between both salt treatments were observed in the plant ionome (**Fig. 2.8, 2.16**). K^+ ions were moderately accumulated in KCl-treated plants compared to the Na^+ ion accumulation under NaCl stress, whilst Cl^- was readily accumulated under both salt stresses, above all in response to KCl stress. Ramos *et al.* (2004) reported similar results for NaCl and KCl-treated *Atriplex nummularia* plants, with an up to two-fold accumulation of K^+ ions under KCl treatment compared to the more than ten-fold accumulation observed for Na^+ ions under NaCl irrigation, while Cl^- ions were slightly more accumulated under KCl than NaCl stress. In addition to these three ions, their accumulation was accompanied by the decrease in other ions such as Mg^{2+}, Ca^{2+}, NO_3^- and SO_4^{2-}, especially in the roots (**Fig. 2.8**). The disturbance of the plant ionome, especially that of the root, is a widely reported effect of this stress, deriving in nutrient

imbalances as observed in our experiment (see **section E.3.6**, Hill *et al.*, 2013; Wang and Han, 2007). Salt stress is usually linked to toxicity derived from Na^+ over-accumulation, which plants avoid through several mechanisms such as cellular restricted Na^+ uptake, active Na^+ exclusion back to the soil or ion sequestration in the vacuole, in addition to whole-plant level mechanisms such as Na^+ loading into senescing leaves or leaf epidermis compartmentation (Jha *et al.*, 2019). One of the main consequences of excess Na^+ ions is the interference with plant mineral nutrition, especially K^+ (Hauser and Horie, 2010; Parihar *et al.*, 2015). K^+ is an essential ion involved in key metabolic processes such as osmotic adjustment and turgor generation, regulation of membrane electric potential, cytoplasmic pH homeostasis and enzyme activation. There are more than 50 cytoplasmic enzymes activated by this ion such as those related to protein synthesis and ribosomes, so since many plant enzymes are selective to K^+ ions, their replacement by Na^+ or the perturbance of the cytoplasmic Na^+/K^+ ratio can lead to important alterations in the plant biochemistry (Page and Cera, 2006; Vašák and Schnabl, 2016). In addition to this, K^+ is the most abundant inorganic cation in plants and, hence, plants keep its concentration within narrow limits, leading its over-accumulation to toxic effects in plants.

Less attention has been paid to Cl^- over-accumulation, even though it is the most common anion in saline soils. Cl^- is an essential anion that regulates enzymatic activities and the cellular membrane potential, while it is also involved in cell turgor and pH regulation. However, as happens with the other ions, Cl^- can be toxic to plants at high concentrations, mainly by its effect on inorganic anions' nutrient balance (Wu and Li, 2019). Tavakkoli *et al.* (2010) applied NaCl, Na^+ and Cl^- ions to faba bean plants and could distinguish the specific effects of both ions: Cl^- lead to chlorophyll degradation possibly due to a structural impact on PSII, while Na^+ ions interfered with K^+ and Ca^{2+} nutrition and disturbed the stomatal regulation. Hence, they concluded that both Na^+ and Cl^- ions were simultaneously responsible of the growth limitation of the plants but through different mechanisms. In our study, even though K^+ accumulation in the KCl treatment was of a lesser extent than that of Na^+ under NaCl (**Fig. 2.8B, C**), the high levels of constitutive K^+ in *M. truncatula* cells (**Fig. 2.8A**) imply a very important net accumulation of this ion even at low fold changes (**Table 2.3**). This factor could be one explanation for

the slightly higher plant damage [observed as lower Ψ_{leaf} (**Fig. 2.3**) and other markers above mentioned] under KCl conditions. In addition, the higher Cl^- accumulation in these plants might also cause a higher ion toxicity under KCl than NaCl irrigation and be responsible for the higher chlorosis observed in KCl plants (**Fig. 2.2**). This is in agreement with the higher deleterious effect of KCl salts than NaCl salts observed by other authors. For example, Yao *et al.* (2010) investigated the effects of NaCl and KCl exposure in the growth and leaf antioxidative responses of the salt-resistant *Chenopodium album* by submitting the 1-month-old seedlings to 0, 50 and 300 mM NaCl or KCl for 2 months and observed a higher growth inhibition and oxidative stress under KCl conditions. Ramos *et al.* (2004) subjected *Atriplex nummularia* plants to 100, 350 and 500mM NaCl or KCl for 28 days, and in all salt concentrations they observed a higher growth inhibition of KCl than NaCl salts. In our study, the lower ionome alteration under NaCl stress suggests more effective salinity avoidance mechanisms for this salt than KCl, which could be explained by the more common presence of NaCl than KCl salts in saline soils, having made *M. truncatula* plants evolve and better adapt to its presence compared to KCl, as explained for *A. nummularia* (Ramos *et al.*, 2004).

In summary, NaCl and KCl iso-osmotical solutions were used as salt stressors in order to better differentiate the individual ion contribution to plant salt stress. However, the higher Cl^- uptake by KCl-treated plants did not allow us to clearly attribute the negative effects to each ion. *M. truncatula* plants did not show significant differences between both treatments when several physiological and metabolic parameters were measured, indicating that not only Na^+ and Cl^- but also K^+ ions can elicit plant toxicity when over-accumulated. The lower leaf water potential, together with the usually observed higher response of certain physiological and biochemical parameters and the indications of a higher inhibition of root respiration under KCl suggest a slightly higher sensitivity of *M. truncatula* to this salt. Nevertheless, these differences did not make a substantial alteration in the carbon metabolite pattern amongst both stresses and, thus, we conclude that both treatments provoked a similar effect on carbon and nitrogen primary metabolism despite the different nature of the accumulated ion in each case.

2.6. CONCLUSIONS

In summary, in this study iso-osmotical conditions of salinity [NaCl and KCl] and drought [PEG-6000 and no-irrigation (No-W)] were used to analyse the water-deficit responses of *M. truncatula* plants. Even though PEG is widely used as desiccation mimicker, the important impairment on nutrient uptake and the differential regulation of carbon and proline metabolism together with the observed PEG-6000 uptake do not suggest that conclusions based on PEG studies may be directly extrapolated to the understanding of drought stress responses. On the other hand, there were no significant differences between NaCl and KCl-salt treatments, even though some markers such as the lower leaf water potential, higher chlorosis in older leaves and lower organic acid levels, amongst others, suggest a higher sensitivity of this plant to high KCl soil concentrations. When No-W and NaCl stress treatments were compared in order to differentiate the ionic component of the latter stress, some remarkable differences were observed, with a marked defensive response of NaCl shoots and droughted-roots through the accumulation of soluble sugars, antioxidants and amino acids under both stresses. In addition, the most relevant differences in the plant's response to stress was the increased starch content under NaCl, possibly as a mechanism of ion sequestration and avoidance of photosynthesis inhibition, as well as the increase in IDH activity and α-KG content. On the other hand, root proline catabolism, BCAA accumulation as well as the increased root sink strength via INV could play key roles in *M. truncatula* response to no-irrigation stress. It is remarkable that, despite the much higher nutrient imbalance in the roots of salt-stressed plants compared to No-W, more compatible solutes and antioxidants were accumulated in the roots of non-irrigated plants. This highlights the higher relevance of root growth and integrity preservation under drought stress, and the importance of the inorganic ions' component in the decrease in plant water potential under salinity stress. The specific phloem accumulation of amino acids under salinity conditions also suggests additional roles such as signalling, regulation of nitrogen uptake, nitrogen source or even their redistribution to young growing or NaCl-accumulating mature leaves. The conclusions derived from this work highlight the importance of the study of the response to abiotic stress in plants as whole systems and open the doors to future studies that research the relevance of the analysed traits for water-deficit tolerance.

› GENERAL CONCLUSIONS

Within a climate change and growing world population context, it is of great importance to maintain/increase plant yield under stressful growth conditions, for which the understanding of the adaptive responses of plants to water-deficit stress becomes mandatory. Indeed, much research is being focused on identifying biomarkers responding to water deficit for genetic engineering and smart breeding that improve plant tolerance to this stress. In this work *Medicago truncatula*, a model legume plant, has been subjected to water-deficit stress conditions for this purpose.

Being the root system the first organ to encounter soil water deficit, the taproot (tapR) and lateral or fibrous roots (FibR) physiology was analysed. Under well-watered conditions the tapR showed higher levels of sucrose and soluble proteins as well as alcohol dehydrogenase and sucrose synthase (SuSy) activities with a limited content of starch compared to the FibR, suggesting a role of tapR in C and N-partitioning as well as N-storage. The higher respiration levels as well as the increased enzymatic activities related to N-assimilation together with the higher levels of the N-assimilation-related amino acid Asn suggested a more important role of the FibR in this nutrient assimilation.

Upon water-deficit stress, there was a general activation of plant defence mechanisms against stress like the accumulation of compatible solutes (including soluble sugars and amino acids such as Pro and BCAAs) or the activation of the alternative oxidase pathway and the residual respiration, linked to redox homeostasis. On the other hand, the FibR showed additional mechanisms to cope with the higher levels of water-deficit stress such as the induction of glycerol-3-phosphate dehydrogenase (GPDH) and invertase (INV) enzymatic activities. The tapR showed a more resilient nature than the FibR to water-deficit stress, but the ready response of SuSy and proline dehydrogenase (ProDH) in both root types converts them in potential good markers of water-deficit stress. The increase in proline catabolism could be a means to generate energy and reducing equivalents upon respiration inhibition and could play a key role in *M. truncatula* root tolerance to drought. In addition, the differential resilience of the tapR and FibR

towards water-deficit stress makes it an interesting target of breeding programs improving plant tolerance towards stress by focusing on the different functionality of the root system.

Water-deficit stress does not only derive from inadequate rainfall but can also appear due to other environmental conditions like excessive salinity in the soil solution. However, even though salinity and drought share many plant responses due to the osmotic stress they exert, salinity also has an ionic component that further alters plant ion homeostasis through Na^+ and Cl^- toxicity. When *M. truncatula* plants were subjected to iso-osmotic conditions of salinity (NaCl and KCl), no-irrigation (No-W) and osmotic stress (PEG-6000) to provoke a drop in the leaf water potential (Ψ_{leaf}) similar to a moderate water-deficit level, several common and distinct responses could be observed. PEG treatment lead to its uptake by roots and leaves and caused a dramatic nutrient deficiency in both organs that was not present under No-W conditions, probably as a consequence of the perturbation of leaf water relations due to PEG accumulation and the hypoxic nature of the PEG solution. This, together with the distinct carbon and proline metabolism regulation between both treatments lead us to discard PEG as a safe mimicker of drought stress.

NaCl treatment led to an increase in leaf starch that could be linked to the sequestration of toxic ions and the avoidance of photosynthesis inhibition. On the other hand, No-W plants degraded starch allowing the accumulation of soluble sugars in the roots as a mechanism of tolerance to stress. The higher protection of roots than shoots under No-W was also apparent in the form of a higher root-to-shoot ratio, glutathione and homoglutathione, Pro and BCAAs levels as well as increased INV activity (allowing the maintenance of sink strength), or the activation of proline catabolism, which could become an important source of energy and reducing equivalents. On the other hand, the higher shoot relevance under salinity stress was apparent through the higher sucrose and proline accumulation in this tissue, together with the higher α-KG content and isocitrate dehydrogenase (IDH) activity, possibly involved in the generation of NADPH for other tolerance mechanisms such as proline synthesis or glutathione regeneration. Even though *M. truncatula* plants did not seem to be dramatically affected by either stress, a

very important root nutrient deficiency could be observed under NaCl irrigation. On the other hand, the decline in root aspartate aminotransferase and the accumulation of NO_3^- suggesting an inhibition of nitrate reductase pointed towards a decrease in the primary assimilation of nitrogen upon No-W, even though the increase in nitrogen compounds such as amino acids ruled out a nitrogen deficit under this stress. The study of the phloem sap response to salinity stress suggested a preferential diversion of assimilates to the shoots rather than roots. However, the increase in the amino acid content in the phloem sap could have a key role in plant salinity-tolerance more linked to the role of specific amino acids in stress signalling and regulation of nitrogen uptake.

KCl treatment was employed as a means to better understand the toxic effects of NaCl in *M. truncatula* plants, but the higher Cl^- accumulation under these conditions did not allow a clear conclusion of the negative effect of each ion in the plant status. The lower leaf water potential, higher older leaves` chlorosis and slightly more pronounced responses of several parameters to stress suggested a slightly more deleterious effect of this salt compared to NaCl. Even though K^+ ions accumulated less under KCl than Na^+ ions under NaCl irrigation, the higher constitutive K^+ levels together with the higher Cl^- accumulation could be the cause of the more negative effect of this salt.

Considering all results, INV and proline catabolism seem to be key players in the *M. truncatula response* to no irrigation, highlighting the relevance of the root tissue for understanding the whole-plant response to stress and as a key trait for drought tolerance. However, studies using PEG as drought mimicker should be taken with caution, due to the important consequences that its uptake by the plant and the hypoxic nature of the solution have in plant metabolism. On the other hand, even when the plant is still able to maintain a correct functioning without showing serious effects at any level, there are important differences between the osmotic stress derived from no irrigation and the presence of high salt levels. Thus, while plants under NaCl irrigation focus on preserving the shoot integrity, non-irrigated plants focus their efforts on the maintenance of root functioning. On the contrary to the mentioned root ProDH and INV activation under no-irrigation, starch accumulation and IDH seem to play key roles in NaCl tolerance.

The conclusions derived from this work open the doors to future studies that research the relevance of the analysed traits for drought tolerance. Indeed, future studies are needed to investigate how *M. truncatula* plants with a higher proportion of tapR *versus* FibR perform upon well-watered and water-deficit stress conditions, as well as the relevance of proline metabolism, especially the catabolism, and INV in drought tolerance. Whether or not IDH can confer salinity tolerance is also a non-explored worthy pursuit, while the role of phloem sap amino acids under NaCl conditions is another interesting research topic with potential broad implications. The comparison of *M. truncatula* cultivars differing in water-deficit tolerance as well as the employment of different developmental stages as well as time points during water-deficit stress and even recovery could provide unvaluable information regarding *M. truncatula* response to this stress.

› BIBLIOGRAPHY

Abid M, Ali S, Kang QL, Zahoor R, Tian Z, Jiang D, *et al.* (2018) Physiological and biochemical changes during drought and recovery periods at tillering and jointing stages in wheat (*Triticum aestivum* L.). *Sci. Rep.* 8: 4615.

Ågren GI, Franklin O. (2003) Root:shoot ratios, optimization and nitrogen productivity. *Ann. Bot.* 92: 795–800.

Ahanger MA, Morad-Talab N, Abd-Allah EF, Ahmad P, Hajiboland R. (2016) Plant growth under drought stress: significance of mineral nutrients. In: Ahmad P (ed). *Water stress and crop plants: a sustainable approach,* Vol 1. 1st ed. West Sussex: Wiley, pp. 649–668.

Akhzari D, Pessarakli M. (2016) Effect of drought stress on total protein, essential oil content, and physiological traits of *Levisticum officinale* Koch. *J. Plant Nutr.* 39: 1365–1371.

Albert B, Le-Cahérec F, Niogret MF, Faes P, Avice JC, Leport L, *et al.* (2012) Nitrogen availability impacts oilseed rape (*Brassica napus* L.) plant water status and proline production efficiency under water-limited conditions. *Planta*. 236: 659–676.

Amirjani MR. (2011) Effect of salinity stress on growth, sugar content, pigments and enzyme activity of rice. *Int. J. Bot.* 7: 73–81.

Ané JM, Zhu H, Frugoli J. (2008) Recent advances in *Medicago truncatula* genomics. *Int. J. Plant Genomics*. 2008: 256597.

Anjum NA, Chan MT, Umar S (eds) (2010) Ascorbate-glutathione pathway and stress tolerance in plants. 1st ed. Netherlands: Springer.

António C, Päpke C, Rocha M, Diab H, Limami A, Obata T, *et al.* (2016) Regulation of primary metabolism in response to low oxygen availability as revealed by carbon and nitrogen isotope redistribution. *Plant Physiol*. 170: 43–56.

Anwar A, She M, Wang K, Riaz B, Ye X. (2018) Biological roles of ornithine aminotransferase (OAT) in plant stress tolerance: present progress and future perspectives. *Int. J. Mol. Sci.* 19: 3681.

Araújo SS, Beebe S, Crespi M, Delbreil B, González EM, Gruber V, *et al.* (2015) Abiotic stress responses in legumes: strategies used to cope with environmental challenges. *Crit. Rev. Plant Sci.* 34: 237–280.

Araújo WL, Nunes-Nesi A, Trenkamp S, Bunik VI, Fernie AR. (2008) Inhibition of 2-oxoglutarate dehydrogenase in potato tuber suggests the enzyme is limiting for respiration and confirms its importance in nitrogen assimilation. *Plant Physiol.* 148: 1782–1796.

Araújo WL, Tohge T, Ishizaki K, Leaver CJ, Fernie AR. (2011) Protein degradation - an alternative respiratory substrate for stressed plants. *Trends Plant Sci.* 16: 489–498.

Arlt K, Brandt S, Kehr J. (2001) Amino acid analysis in five pooled single plant cell samples using capillary electrophoresis coupled to laser-induced fluorescence detection. *J. Chromatogr. A*. 926: 319–325.

Arrese-Igor C, González E, Gordon A, Minchin F, Gálvez L, Royuela M, *et al.* (1999) Sucrose synthase and nodule nitrogen fixation under drought and other environmental stresses. *Symbiosis*. 27: 189–202.

Arteaga S, Yabor L, Díez MJ, Prohens J, Boscaiu M, Vicente O. (2020) The use of proline in screening for tolerance to drought and salinity in common bean (*Phaseolus vulgaris* L.) genotypes. *Agronomy*. 10: 817.

Ashrafi E, Razmjoo J, Zahedi M. (2018) Effect of salt stress on growth and ion accumulation of alfalfa (*Medicago sativa* L.) cultivars. *J. Plant Nutr.* 41: 818–831.

Asthir B, Kaur G, Kaur B. (2020) Convergence of pathways towards ascorbate–glutathione for stress mitigation. *J. Plant Biol.* 63: 243–257.

Aubert G, Morin J, Jacquin F, Loridon K, Quillet MC, Petit A, *et al.* (2006) Functional mapping in pea, as an aid to the candidate gene selection and for investigating synteny with the model legume *Medicago truncatula*. *Theor. Appl. Genet.* 112: 1024–1041.

Bahaji A, Li J, Sánchez-López ÁM, Baroja-Fernández E, Muñoz FJ, Ovecka M, *et al.* (2014) Starch biosynthesis, its regulation and biotechnological approaches to improve crop yields. *Biotechnol. Adv.* 32: 87–106.

Bahieldin A, Sabir JSM, Ramadan A, Alzohairy AM, Younis RA, Shokry AM, *et al.* (2013) Control of glycerol biosynthesis under high salt stress in arabidopsis. *Funct. Plant Biol.* 41: 87–95.

Bais HP, Loyola-Vargas VM, Flores HE, Vivanco JM. (2001) Root-specific metabolism: the biology and biochemistry of underground organs. *Vitr. Cell. Dev. Biol. - Plant*. 37: 730–741.

Bajaj S, Targolli J, Liu LF, David-Ho TH, Wu R. (1999) Transgenic approaches to increase dehydration-stress tolerance in plants. *Mol. Breed.* 5: 493–503.

Bajji M, Lutts S, Kinet J. (2000) Physiological changes after exposure to and recovery from polyethylene glycol-induced water deficit in roots and leaves of durum wheat (*Triticum durum* Desf.) cultivars differing in drought resistance. *J. Plant Physiol.* 157: 100–108.

Barker DG, Bianchi S, Blondon F, Dattée Y, Duc G, Essad S, *et al.* (1990) *Medicago truncatula*, a model plant for studying the molecular genetics of the *Rhizobium*-legume symbiosis. *Plant Mol. Biol. Report.* 8: 40–49.

Baroja-Fernández E, Muñoz FJ, Saikusa T, Rodríguez-López M, Akazawa T, Pozueta-Romero J. (2003) Sucrose synthase catalyzes the *de novo* production of ADP-glucose linked to starch biosynthesis in heterotrophic tissues of plants. *Plant Cell Physiol.* 44: 500–509.

Barratt DHP, Derbyshire P, Findlay K, Pike M, Wellner N, Lunn J, *et al.* (2009) Normal growth of arabidopsis requires cytosolic invertase but not sucrose synthase. *Proc. Natl. Acad. Sci. U. S. A.* 106: 13124–13129.

Beller, D. (2018) *Medicago truncatula* [Image]. California: Calflora [Accessed 25th October 2020]. Available at: https://www.calflora.org//cgi-bin/species_query.cgi?where-calrecnum=11827.

Bhargava S, Sawant K. (2012) Drought stress adaptation: metabolic adjustment and regulation of gene expression. *Plant Breed.* 132: 21–32.

Bihmidine S, Hunter CT, Johns CE, Koch KE, Braun DM. (2013) Regulation of assimilate import into sink organs: update on molecular drivers of sink strength. *Front. Plant Sci.* 4: 177.

Blum A. (2017) Osmotic adjustment is a prime drought stress adaptive engine in support of plant production. *Plant. Cell Environ.* 40: 4–10.

Bolouri-Moghaddam MR, Le-Roy K, Xiang L, Rolland F, van den Ende W. (2010) Sugar signalling and antioxidant network connections in plant cells. *FEBS J.* 277: 2022–2037.

Bouthour D, Kalai T, Chaffei HC, Gouia H, Corpas FJ. (2015) Differential response of NADP-dehydrogenases and carbon metabolism in leaves and roots of two durum wheat (*Triticum durum* Desf.) cultivars (Karim and Azizi) with different sensitivities to salt stress. *J. Plant Physiol.* 179: 56–63.

Boyer JS. (1982) Plant productivity and environment. *Science.* 218: 443–448.

Braun DM, Wang L, Ruan YL. (2014) Understanding and manipulating sucrose phloem loading, unloading, metabolism, and signalling to enhance crop yield and food security. *J. Exp. Bot.* 65: 1713–35.

Buckley TN. (2019) How do stomata respond to water status? *New Phytol.* 224: 21–36.

Butcher K, Wick AF, DeSutter T, Chatterjee A, Harmon J. (2016) Soil salinity: a threat to global food security. *Agron. J.* 108: 2189.

Cabassa-Hourton C, Schertl P, Bordenave-Jacquemin M, Saadallah K, Guivarc'h A, Lebreton S, *et al.* (2016) Proteomic and functional analysis of proline dehydrogenase 1 link proline catabolism to mitochondrial electron transport in *Arabidopsis thaliana*. *Biochem. J.* 473: 2623–2634.

Casais-Molina ML, Peraza-Echeverria S, Echevarría-Machado I, Herrera-Valencia VA. (2016) Expression of *Chlamydomonas reinhardtii CrGPDH2* and *CrGPDH3* cDNAs in yeast reveals that they encode functional glycerol-3-phosphate dehydrogenases involved in glycerol production and osmotic-stress tolerance. *J. Appl. Phycol.* 28: 219–226.

Castañeda V, Gil-Quintana E, Echeverria A, González E. (2018) Legume nitrogen utilization under drought stress. In: Shrawat A, Zayed A, Lightfoot DA (eds). *Engineering nitrogen utilization in crop plants*, Vol 1. 1st ed. Cham, Switzerland: Springer.

Castañeda V, González EM, Wienkoop S. (2021) Phloem sap proteins are part of a core stress responsive proteome involved in drought-stress adjustment. *Front. Plant Sci.* 12: 55.

Cavalcanti FR, Santos-Lima JPM, Ferreira-Silva SL, Viegas RA, Silveira JAG. (2007) Roots and leaves display contrasting oxidative response during salt stress and recovery in cowpea. *J. Plant Physiol.* 164: 591–600.

Chang TG, Zhu XG, Raines C. (2017) Source–sink interaction: a century-old concept under the light of modern molecular systems biology. *J. Exp. Bot.* 68: 4417–4431.

Chaves MM, Flexas J, Pinheiro C. (2009) Photosynthesis under drought and salt stress: regulation mechanisms from whole plant to cell. *Ann. Bot.* 103: 551–560.

Chazen O, Hartung W, Neumann PM. (1995) The different effects of PEG-6000 and NaCl on leaf development are associated with differential inhibition of root water transport. *Plant, Cell Environ.* 18: 727–735.

Che-Othman MH, Millar AH, Taylor NL. (2017) Connecting salt stress signalling pathways with salinity-induced changes in mitochondrial metabolic processes in C3 plants. *Plant. Cell Environ.* 40: 2875–2905.

Chen H, Jiang JG, Wu GH. (2009) Effects of salinity changes on the growth of *Dunallella salina* and its isozyme activities of glycerol-3-phosphate dehydrogenase. *J. Agric. Food Chem.* 57: 6178–6182.

Chen Z, Cuin TA, Zhou M, Twomey A, Naidu BP, Shabala S. (2007) Compatible solute accumulation and stress-mitigating effects in barley genotypes contrasting in their salt tolerance. *J. Exp. Bot.* 58: 4245–4255.

Cheng MC, Ko K, Chang WL, Kuo WC, Chen GH, Lin TP. (2015) Increased glutathione contributes to stress tolerance and global translational changes in arabidopsis. *Plant J.* 83: 926–939.

Cheng WH, Chourey PS. (1999) Genetic evidence that invertase-mediated release of hexoses is critical for appropriate carbon partitioning and normal seed development in maize. *Theor. Appl. Genet.* 98: 485–495.

Chocobar-Ponce S, Prado C, González R, Rosa M, Prado FE. (2014) Mitochondrial respiration: involvement of the alternative respiratory pathway and residual respiration in abiotic stress responses. In: Ahmad P, Wani M (eds). *Physiological mechanisms and adaptation strategies in plants under changing environment,* Vol 2. 1st ed. New York, NY: Springer, pp. 321–364.

Ciríaco-da Silva E, Nogueira RJMC, da Silva MA, de Albuquerque MB. (2011) Drought stress and plant nutrition. *Plant Stress*. 5: 32–41.

Comas LH, Becker SR, Cruz VMV, Byrne PF, Dierig DA. (2013) Root traits contributing to plant productivity under drought. *Front. Plant Sci.* 4: 442.

Corpas FJ, Barroso JB. (2014) NADPH-generating dehydrogenases: their role in the mechanism of protection against nitro-oxidative stress induced by adverse environmental conditions. *Front. Environ. Sci.* 2: 55.

Correia MJ, Fonseca F, Azedo-Silva J, Dias C, David MM, Barrote I, *et al.* (2005) Effects of water deficit on the activity of nitrate reductase and content of sugars, nitrate and free amino acids in the leaves and roots of sunflower and white lupin plants growing under two nutrient supply regimes. *Physiol. Plant.* 124: 61–70.

Couée I, Sulmon C, Gouesbet G, El-Amrani A. (2006) Involvement of soluble sugars in reactive oxygen species balance and responses to oxidative stress in plants. *J. Exp. Bot.* 57: 449–459.

Crawford EJ, Lake AWH, Boyce KG. (1989) Breeding annual *Medicago* species for semiarid conditions in Southern Australia. *Adv. Agron.* 42: 399–437.

Cruz P. (1997) Effect of shade on the carbon and nitrogen allocation in a perennial tropical grass, *Dichanthium aristatum*. *J. Exp. Bot.* 48: 15–24.

Cui G, Zhang Y, Zhang W, Lang D, Zhang X, Li Z, *et al.* (2019a) Response of carbon and nitrogen metabolism and secondary metabolites to drought stress and salt stress in plants. *J. Plant Biol.* 62: 387–399.

Cui G, Zhao Y, Zhang J, Chao M, Xie K, Zhang C, *et al.* (2019b) Proteomic analysis of the similarities and differences of soil drought and polyethylene glycol-stress responses in wheat (*Triticum aestivum* L.). *Plant Mol. Biol.* 100: 391–410.

Cuin TA, Shabala S. (2007) Amino acids regulate salinity-induced potassium efflux in barley root epidermis. *Planta*. 225: 753–761.

Czarnocka W, Karpiński S. (2018) Friend or foe? Reactive oxygen species production, scavenging and signaling in plant response to environmental stresses. *Free Radic. Biol. Med.* 122: 4–20.

Dao HD, Hirai Y. (2018) Cl^- more detrimental than Na^+ in rice under long-term saline conditions. *J. Agric. Sci.* 10: 66.

Darko E, Gierczik K, Hudák O, Forgó P, Pál M, Türkösi E, *et al.* (2017) Differing metabolic responses to salt stress in wheat-barley addition lines containing different 7H chromosomal fragments. *PLoS One*. 12: e0174170.

Darko E, Végh B, Khalil R, Marček T, Szalai G, Pál M, *et al.* (2019) Metabolic responses of wheat seedlings to osmotic stress induced by various osmolytes under iso-osmotic conditions. *PLoS One*. 14: e0226151.

Daryanto S, Wang L, Jacinthe PA, Yu X, Luo L, Cui K. (2016) Global synthesis of drought effects on maize and wheat production. *PLoS One*. 11: e0156362.

Daszkowska-Golec A, Szarejko I. (2013) Open or close the gate - Stomata action under the control of phytohormones in drought-stress conditions. *Front. Plant Sci.* 4: 138.

de Bruijn FJ. (2020) Genetic map of *Medicago truncatula*. In: de Bruijn FJ (ed). *The model legume* Medicago truncatula, Vol 1. 1st ed.Weinheim: Wiley, pp. 817–820.

del Saz NF, Florez-Sarasa I, Clemente-Moreno MJ, Mhadhbi H, Flexas J, Fernie AR, *et al.* (2016) Salinity tolerance is related to cyanide-resistant alternative respiration in *Medicago truncatula* under sudden severe stress. *Plant. Cell Environ.* 39: 2361–2369.

del Saz NF, Palma F, Herrera-Cervera JA, Ribas-Carbo M. (2020) Deciphering the role of the alternative respiration under salt stress in *Medicago truncatula*. In: de Bruijn FJ (ed). *The model legume* Medicago truncatula, Vol 1. 1st ed. Weinheim: Wiley, pp. 261–267.

Deuschle K, Funck D, Forlani G, Stransky H, Biehl A, Leister D, *et al.* (2004) The role of Δ1-pyrroline-5-carboxylate dehydrogenase in proline degradation. *Plant Cell*. 16: 3413–3425.

Do PT, Drechsel O, Heyer AG, Hincha DK, Zuther E. (2014) Changes in free polyamine levels, expression of polyamine biosynthesis genes, and performance of rice cultivars under salt stress: a comparison with responses to drought. *Front. Plant Sci.* 5: 182.

Dong S, Beckles DM. (2019) Dynamic changes in the starch-sugar interconversion within plant source and sink tissues promote a better abiotic stress response. *J. Plant Physiol.* 234–235: 80–93.

Dong S, Zhang J, Beckles DM. (2018) A pivotal role for starch in the reconfiguration of 14C-partitioning and allocation in *Arabidopsis thaliana* under short-term abiotic stress. *Sci. Rep.* 8: 9314.

Dubois M, Inzé D. (2020) Plant growth under suboptimal water conditions: early responses and methods to study them. *J. Exp. Bot.* 71: 1706–1722.

Echeverria A, González EM. (2021) Root system of *Medicago sativa* and *Medicago truncatula*: drought effects on carbon metabolism. *Plant Soil*. 3: 1–15.

Echeverria A, Larrainzar E, Li W, Watanabe Y, Sato M, Tran CD, et al. (2021) *Medicago sativa* and *Medicago truncatula* show contrasting root metabolic responses to drought. *Front. Plant Sci.* 12: 612.

Erice G, Irigoyen JJ, Sánchez-Díaz M, Avice JC, Ourry A. (2007) Effect of drought, elevated CO_2 and temperature on accumulation of N and vegetative storage proteins (VSP) in taproot of nodulated alfalfa before and after cutting. *Plant Sci.* 172: 903–912.

Erice G, Sanz-Sáez A, Aranjuelo I, Irigoyen JJ, Aguirreolea J, Avice JC, *et al.* (2011) Photosynthesis, N_2 fixation and taproot reserves during the cutting-regrowth cycle of alfalfa under elevated CO_2 and temperature. *J. Plant Physiol.* 168: 2007–2014.

Evans HJ. (1981) Symbiotic nitrogen fixation in legume nodules. In: Moore T (ed). *Research experiences in plant physiology*, Vol. 1. 1st ed. New York, NY: Springer-Verlag, pp. 294–310.

Fan S, Blake TJ. (1997) Comparison of polyethylene glycol-3350-induced osmotic stress and soil drying for drought simulation in three woody species. *Trees*. 11: 342.

Fang Y, Xiong L. (2014) General mechanisms of drought response and their application in drought resistance improvement in plants. *Cell. Mol. Life Sci.* 72: 673–689.

FAO. (2019) State of food security and nutrition. Rome: Food and Agriculture Organization of the United Nations (ed). *http://www.fao.org/state-of-food-security-nutrition*.

FAO. (2011) The state of the world's land and water resources for food and agriculture (SOLAW) – Managing systems at risk. Rome: Food and Agriculture Organization of the United Nations and Earthscan (eds). http://www.fao.org/3/i1688e/i1688e00.htm.

Farooq M, Wahid A, Kobayashi N, Fujita D, Basra SMA. (2009) Plant drought stress: effects, mechanisms and management. *Sustain. Agric.* 29: 153–188.

Feller U. (2016) Drought stress and carbon assimilation in a warming climate: reversible and irreversible impacts. *J. Plant Physiol.* 203: 84–94.

Filek M, Walas S, Mrowiec H, Rudolphy-Skórska E, Sieprawska A, Biesaga-Kościelniak J. (2012) Membrane permeability and micro- and macroelement accumulation in spring wheat cultivars during the short-term effect of salinity- and PEG-induced water stress. *Acta Physiol. Plant.* 34: 985–995.

Filippou P, Antoniou C, Fotopoulos V. (2011) Effect of drought and rewatering on the cellular status and antioxidant response of *Medicago truncatula* plants. *Plant Signal. Behav.* 6: 270–7.

Fischer S, Hilger T, Piepho HP, Jordan I, Cadisch, G. (2019) Do we need more drought for better nutrition? The effect of precipitation on nutrient concentration in East African food crops. *Sci. Total Environ*. 658: 405–415.

Fita A, Rodríguez-Burruezo A, Boscaiu M, Prohens J, Vicente O. (2015) Breeding and domesticating crops adapted to drought and salinity: a new paradigm for increasing food production. *Front. Plant Sci.* 6: 978.

Fitter A. (2002) Characteristics and functions of root systems. In: Waisel Y, Eshel A, Beeckman T, Kafkafi U (eds). *Plant roots: the hidden half,* Vol 1. 4th ed. Boca Ratón, FL: CRC Press, pp. 15–32.

Flexas J, Bota J, Galmés J, Medrano H, Ribas-Carbó M. (2006) Keeping a positive carbon balance under adverse conditions: responses of photosynthesis and respiration to water stress. *Physiol. Plant*. 127: 343–352.

Flexas J, Galmes J, Ribas-Carbo M, Medrano H. (2005) The effects of water stress on plant respiration. In: Lambers H, Ribas-Carbo M (eds). *Plant respiration: from cell to ecosystem. Advances in photosynthesis and respiration,* Vol 18. 1st ed. Berlin: Springer, pp. 85–94.

Fontaine JX, Tercé-Laforgue T, Armengaud P, Clément G, Renou JP, Pelletier S, *et al.* (2012) Characterization of a NADH-dependent glutamate dehydrogenase mutant of arabidopsis demonstrates the key role of this enzyme in root carbon and nitrogen metabolism. *Plant Cell*. 24: 4044–4065.

Forner-Giner MÁ, Rodríguez-Gamir J, Primo-Millo E, Iglesias DJ. (2011) Hydraulic and chemical responses of citrus seedlings to drought and osmotic stress. *J. Plant Growth Regul.* 30: 353–366.

Fox TC, Kennedy RA, Rumpho ME. (1994) Energetics of plant growth under anoxia: metabolic adaptations of *Oryza sativa* and *Echinochloa phyllopogon*. *Ann. Bot.* 74: 445–455.

Foyer CH, Noctor G. (2011) Ascorbate and glutathione: the heart of the redox hub. *Plant Physiol.* 155: 2–18.

Foyer CH, Noctor G, Hodges M. (2011) Respiration and nitrogen assimilation: targeting mitochondria-associated metabolism as a means to enhance nitrogen use efficiency. *J. Exp. Bot.* 62: 1467–1482.

Fujita T, Maggio A, García-Ríos M, Bressan RA, Csonka LN. (1998) Comparative analysis of the regulation of expression and structures of two evolutionary divergent genes for Δ1-pyrroline-5-carboxylate synthetase from tomato. *Plant Physiol.* 118: 661–674.

Funck D, Stadelhofer B, Koch W. (2008) Ornithine-δ-aminotransferase is essential for arginine catabolism but not for proline biosynthesis. *BMC Plant Biol.* 8: 40.

Galibert F, Finan TM, Long SR, Puhler A, Abola P, Ampe F, *et al.* (2001) The composite genome of the legume symbiont *Sinorhizobium meliloti*. *Science.* 293: 668–672.

Gálvez L, González EM, Arrese-Igor C. (2005) Evidence for carbon flux shortage and strong carbon/nitrogen interactions in pea nodules at early stages of water stress. *J. Exp. Bot.* 56: 2551–2561.

Gargallo-Garriga A, Sardans J, Pérez-Trujillo M, Rivas-Ubach A, Oravec M, Vecerova K, *et al.* (2014) Opposite metabolic responses of shoots and roots to drought. *Sci. Rep.* 4: 6829.

Geigenberger P. (2011) Regulation of starch biosynthesis in response to a fluctuating environment. *Plant Physiol.* 155: 1566–1577.

Geilfus CM. (2018) Chloride: from nutrient to toxicant. *Plant Cell Physiol.* 59: 877–886.

Gepts P, Beavis WD, Brummer EC, Shoemaker RC, Stalker HT, Weeden NE, *et al.* (2005) Legumes as a model plant family. Genomics for food and feed report of the cross-legume advances through genomics conference. *Plant Physiol.* 137: 1228–1235.

Gewin V. (2010) Food: an underground revolution. *Nature*. 466: 552–553.

Gibon Y, Blaesing OE, Hannemann J, Carillo P, Höhne M, Hendriks JHM, *et al.* (2004) A robot-based platform to measure multiple enzyme activities in arabidopsis using a set of cycling assays: comparison of changes of enzyme activities and transcript levels during diurnal cycles and in prolonged darkness. *Plant Cell*. 16: 3304–3325.

Gibson SI. (2000) Plant sugar-response pathways. Part of a complex regulatory web. *Plant Physiol.* 124: 1532–1539.

Gil-Quintana E, Larrainzar E, Arrese-Igor C, González EM. (2013) Is N-feedback involved in the inhibition of nitrogen fixation in drought-stressed *Medicago truncatula*? *J. Exp. Bot.* 64: 281–292.

Gil-Quintana E, Lyon D, Staudinger C, Wienkoop S, González EM. (2015) *Medicago truncatula* and *Glycine max*: different drought tolerance and similar local response of the root nodule proteome. *J. Proteome Res.* 14: 5240–51.

Gil R, Boscaiu M, Lull C, Bautista I, Lidón A, Vicente O. (2013) Are soluble carbohydrates ecologically relevant for salt tolerance in halophytes? *Funct. Plant Biol.* 40: 805–818.

Gilbert GA, Gadush MV, Wilson C, Madore MA. (1998) Amino acid accumulation in sink and source tissues of *Coleus blumei* Benth. during salinity stress. *J. Exp. Bot.* 49: 107–114.

Gill SS, Tuteja N. (2010) Reactive oxygen species and antioxidant machinery in abiotic-stress tolerance in crop plants. *Plant Physiol. Biochem.* 48: 909–930.

Girousse C, Bournoville R, Bonnemain JL. (1996) Water deficit-induced changes in concentrations in proline and some other amino acids in the phloem sap of alfalfa. *Plant Physiol.* 111: 109–113.

Goche T, Shargie NG, Cummins I, Brown AP, Chivasa S, Ngara R. (2020) Comparative physiological and root proteome analyses of two sorghum varieties responding to water limitation. *Sci. Rep.* 10: 11835.

Golldack D, Li C, Mohan H, Probst N. (2014) Tolerance to drought and salt stress in plants: unraveling the signaling networks. *Front. Plant Sci.* 5: 151.

González-Orenga S, Alhassan M, Llinares JV, Lisón P, López-Gresa MP, Verdeguer M, *et al.* (2019) Qualitative and quantitative differences in osmolytes accumulation and antioxidant activities in response to water deficit in four Mediterranean *Limonium* species. *Plants*. 8: 506.

González EM, Aparicio-Tejo PM, Gordon AJ, Minchin FR, Royuela M, Arrese-Igor C. (1998) Water-deficit effects on carbon and nitrogen metabolism of pea nodules. *J. Exp. Bot.* 49: 1705–1714.

González EM, Gordon AJ, James CL, Arrese-Igor C. (1995) The role of sucrose synthase in the response of soybean nodules to drought. *J. Exp. Bot.* 46: 1515–1523.

Gordon AJ, Minchin FR, James CL, Komina O. (1999) Sucrose synthase in legume nodules is essential for nitrogen fixation. *Plant Physiol.* 120: 867–877.

Graham L, Graham J, Wilcox L. (2013) Plant biology: Pearson new international edition. 2nd ed. Harlow: Pearson.

Graham PH, Vance CP. (2003) Legumes: importance and constraints to greater use. *Plant Physiol.* 131: 872–877.

Griffiths CA, Paul MJ, Foyer CH. (2016) Metabolite transport and associated sugar signalling systems underpinning source/sink interactions. *Biochim. Biophys. Acta - Bioenerg*. 1857: 1715–1725.

Grillakis MG. (2019) Increase in severe and extreme soil moisture droughts for Europe under climate change. *Sci. Total Environ.* 660: 1245–1255.

Guo R, Shi L, Jiao Y, Li M, Zhong X, Gu F, *et al.* (2018) Metabolic responses to drought stress in the tissues of drought-tolerant and drought-sensitive wheat genotype seedlings. *AoB Plants*. 10: ply016.

Hasanuzzaman M, Bhuyan MHMB, Anee TI, Parvin K, Nahar K, Mahmud JA, *et al.* (2019) Regulation of ascorbate-glutathione pathway in mitigating oxidative damage in plants under abiotic stress. *Antioxidants*. 8: 384.

Hasibeder R, Fuchslueger L, Richter A, Bahn M. (2015) Summer drought alters carbon allocation to roots and root respiration in mountain grassland. *New Phytol.* 205: 1117–1127.

Hatch MD, Mau SL. (1973) Activity, location, and role of asparate aminotransferase and alanine aminotransferase isoenzymes in leaves with C4-pathway photosynthesis. *Arch. Biochem. Biophys.* 156: 195–206.

Hauser F, Horie T. (2010) A conserved primary salt-tolerance mechanism mediated by HKT transporters: a mechanism for sodium exclusion and maintenance of high K^+/Na^+ ratio in leaves during salinity stress. *Plant, Cell Environ.* 33: 552–565.

He M, Dijkstra FA. (2014) Drought effect on plant nitrogen and phosphorus: a meta-analysis. *New Phytol.* 204: 924–931.

Hennion N, Durand M, Vriet C, Doidy J, Maurousset L, Lemoine R, Pourtau N. (2019) Sugars en route to the roots. Transport, metabolism and storage within plant roots and towards microorganisms of the rhizosphere. *Physiol. Plant*. 165: 44–57.

Henry C, Bledsoe SW, Griffiths CA, Kollman A, Paul MJ, Sakr S, *et al.* (2015) Differential role for trehalose metabolism in salt-stressed maize. *Plant Physiol.* 169: 1072–1089.

Herrero-Martínez J, Simó-Alfonso EF, Ramis-Ramos G, Deltoro, Vicente I, Calatayud A, Barreno E. (2000) Simultaneous determination of L-ascorbic acid, glutathione, and their oxidized forms in ozone-exposed vascular plants by capillary zone electrophoresis. *Environ. Sci. Technol.* 34: 1331–1336.

Hessini K, Martínez JP, Gandour M, Albouchi A, Soltani A, Abdelly C. (2009) Effect of water stress on growth, osmotic adjustment, cell wall elasticity and water-use efficiency in *Spartina alterniflora*. *Environ. Exp. Bot.* 67: 312–319.

Hichri I, Boscari A, Castella C, Rovere M, Puppo A, Brouquisse R. (2015) Nitric oxide: a multifaceted regulator of the nitrogen-fixing symbiosis. *J. Exp. Bot.* 66: 2877–2887.

Hildebrandt TM. (2018) Synthesis *versus* degradation: directions of amino acid metabolism during Arabidopsis abiotic stress response. *Plant Mol. Biol*. 98: 121–135.

Hill CB, Jha D, Bacic A, Tester M, Roessner U. (2013) Characterization of ion contents and metabolic responses to salt stress of different arabidopsis AtHKT1;1 genotypes and their parental strains. *Mol. Plant*. 6: 350–368.

Hodges M, Flesch V, Gálvez S, Bismuth E. (2003) Higher plant $NADP^+$-dependent isocitrate dehydrogenases, ammonium assimilation and NADPH production. *Plant Physiol. Biochem.* 41: 577–585.

Hoekstra FA, Golovina EA, Buitink J. (2001) Mechanism of plant desiccation tolerance. *Trends Plant Sci.* 6: 431–438.

Horrer D, Flütsch S, Pazmino D, Matthews JSA, Thalmann M, Nigro A, *et al.* (2016) Blue light induces a distinct starch degradation pathway in guard cells for stomatal opening. *Curr. Biol.* 26: 362–370.

Hsiao TC. (1973) Plant responses to water stress. *Annu. Rev. Plant Physiol.* 24: 519–570.

Hsiao TC, Xu LK. (2000) Sensitivity of growth of roots *versus* leaves to water stress: biophysical analysis and relation to water transport. *J. Exp. Bot.* 51: 1595–1616.

Hu Y, Schmidhalter U. (2005) Drought and salinity: a comparison of their effects on mineral nutrition of plants. *J. Plant Nutr. Soil Sci.* 168: 541–549.

Huang B, Gao H. (2000) Root physiological characteristics associated with drought resistance in tall fescue cultivars. *Crop Sci.* 40: 196–203.

Huang T, Jander G. (2017) Abscisic acid-regulated protein degradation causes osmotic stress-induced accumulation of branched-chain amino acids in *Arabidopsis thaliana*. *Planta*. 246: 737–747.

Hummel I, Pantin F, Sulpice R, Piques M, Rolland G, Dauzat M, *et al.* (2010) Arabidopsis plants acclimate to water deficit at low cost through changes of carbon usage: an integrated perspective using growth, metabolite, enzyme, and gene expression analysis. *Plant Physiol.* 154: 357–372.

Hütsch BW, Osthushenrich T, Faust F, Kumar A, Schubert S. (2016) Reduced sink activity in growing shoot tissues of maize under salt stress of the first phase may be compensated by increased PEP-carboxylase activity. *J. Agron. Crop Sci.* 202: 384–393.

Hyden S. (1956) A turbidimetric method for the determination of higher polyethylene glycols in biological materials. *K. Lantbrukshogskolans Ann.* 22: 139–145.

Jacoby RP, Taylor NL, Millar AH. (2011) The role of mitochondrial respiration in salinity tolerance. *Trends Plant Sci.* 16: 614–623.

Jacomini E, Bertani A, Mapelli S. (1988) Accumulation of polyethylene glycol-6000 and its effects on water content and carbohydrate level in water-stressed tomato plants. *Can. J. Bot.* 66: 970–973.

Janes BE. (1974) The effect of molecular size, concentration in nutrient solution, and exposure time on the amount and distribution of polyethylene glycol in pepper plants. *Plant Physiol.* 54: 226–230.

Jeschke W, Pate J. (1991) Cation and chloride partitioning through xylem and phloem within the whole plant of *Ricinus communis* L. under conditions of salt stress. *J. Exp. Bot.* 42: 1105–1116.

Jha UC, Bohra A, Jha R, Parida SK. (2019) Salinity stress response and 'omics' approaches for improving salinity stress tolerance in major grain legumes. *Plant Cell Rep.* 38: 255–277.

Julius BT, Leach KA, Tran TM, Mertz RA, Braun DM. (2017) Sugar transporters in plants: new insights and discoveries. *Plant Cell Physiol.* 58: 1442–1460.

Jung H, Kim JH, Shin KD, Kim J, Lee HN, Chung T. (2017) Autophagic flux analysis of arabidopsis seedlings exposed to salt stress. *J. Plant Biol.* 60: 199–206.

Kachroo A, Venugopal SC, Lapchyk L, Falcone D, Hildebrand D, Kachroo P. (2004) Oleic acid levels regulated by glycerolipid metabolism modulate defense gene expression in arabidopsis. *PNAS*. 101: 5152–5157.

Kafkafi U, Xu G, Imas P, Magen H, Tarchitzky J, Johnston A. (**eds.**)(2001) Potassium and chloride in crops and soils: the role of potassium chloride fertilizer in crop nutrition. 1st ed. Switzerland: International Potash Institute.

Kamphuis LG, Williams AH, D'Souza NK, Pfaff T, Ellwood SR, Groves EJ, *et al.* (2007) The *Medicago truncatula* reference accession A17 has an aberrant chromosomal configuration. *New Phytol.* 174: 299–303.

Kaur G, Asthir B. (2015) Proline: a key player in plant abiotic-stress tolerance. *Biol. Plant.* 59: 609–619.

Kautz B, Noga G, Hunsche M. (2015) PEG and drought cause distinct changes in biochemical, physiological and morphological parameters of apple seedlings. *Acta Physiol. Plant.* 37: 162.

Keunen E, Peshev D, Vangronsveld J, van den Ende W, Cuypers A. (2013) Plant sugars are crucial players in the oxidative challenge during abiotic stress: extending the traditional concept. *Plant. Cell Environ.* 36: 1242–1255.

Khan A, Sovero V, Gemenet D. (2016) Genome-assisted breeding for drought resistance. *Curr. Genomics*. 17: 330–342.

Khan MA, Gemenet DC, Villordon A. (2016) Root system architecture and abiotic-stress tolerance: current knowledge in root and tuber crops. *Front. Plant Sci.* 7: 1584.

Khanna-Chopra R, Semwal VK, Lakra N, Pareek A. (2019) Proline – A key regulator conferring plant tolerance to salinity and drought. In: Hasanuzzaman M, Fujita M, Oku H, Islam MT (eds). *Plant tolerance to environmental stress. role of phytoprotectants*, Vol 1. 1st ed. Boca Ratón, FL: CRC Press, pp. 59–80.

Khelil A, Menu T, Ricard B. (2007) Adaptive response to salt involving carbohydrate metabolism in leaves of a salt-sensitive tomato cultivar. *Plant Physiol. Biochem.* 45: 551–559.

Kim TH, Lee BR, Jung WJ, Kim KY, Avice JC, Ourry A. (2004) *De novo* protein synthesis in relation to ammonia and proline accumulation in water-stressed white clover. *Funct. Plant Biol.* 31: 847–855.

King RW, Zeevaart JA. (1974) Enhancement of phloem exudation from cut petioles by chelating agents. *Plant Physiol.* 53: 96–103.

Kishor PBK, Sangam S, Amrutha RN, Laxmi PS, Naidu KR, Rao KRSS, *et al.* (2005) Regulation of proline biosynthesis, degradation, uptake and transport in higher plants: its implications in plant growth and abiotic stress tolerance. *Curr. Sci.* 88: 424–438.

Kishor PBK, Sreenivasulu N. (2014) Is proline accumulation *per se* correlated with stress tolerance or is proline homeostasis a more critical issue? *Plant. Cell Environ.* 37: 300–311.

Koevoets IT, Venema JH, Elzenga JTM, Testerink C. (2016) Roots withstanding their environment: exploiting root system architecture responses to abiotic stress to improve crop tolerance. *Front. Plant Sci.* 7: 1335.

Krasensky J, Jonak C. (2012) Drought, salt, and temperature stress-induced metabolic rearrangements and regulatory networks. *J. Exp. Bot.* 63: 1593–608.

Lalonde S, Tegeder M, Throne-Holst M, Frommer WB, Patrick JW. (2003) Phloem loading and unloading of sugars and amino acids. *Plant, Cell Environ.* 26: 37–56.

Larrainzar E, Molenaar JA, Wienkoop S, Gil-Quintana E, Alibert B, Limami A, *et al.* (2014) Drought stress provokes the down-regulation of methionine and ethylene biosynthesis pathways in *Medicago truncatula* roots and nodules. *Plant. Cell Environ.* 37: 2051–2063.

Lawlor DW. (1970) Absorption of polyethylene glycols by plants and their effects on plant growth. *New Phytol.* 69: 501–513.

Lawlor DW, Tezara W. (2009) Causes of decreased photosynthetic rate and metabolic capacity in water-deficient leaf cells: a critical evaluation of mechanisms and integration of processes. *Ann. Bot.* 103: 561–579.

Lee BR, Jin YL, Avice JC, Cliquet JB, Ourry A, Kim TH. (2009) Increased proline loading to phloem and its effects on nitrogen uptake and assimilation in water-stressed white clover (*Trifolium repens*). *New Phytol.* 182: 654–663.

Lemoine R, Lacamera S, Atanassova R, Dédaldéchamp F, Allario T, Pourtau N, *et al.* (2013) Source-to-sink transport of sugar and regulation by environmental factors. *Front. Plant Sci.* 4: 272.

Lesins KA, Lesins I. (**eds.**)(1979) Genus *Medicago* (*Leguminosae*). A taxogenetic study. 1st ed. London: Springer.

Lesk C, Rowhani P, Ramankutty N. (2016) Influence of extreme weather disasters on global crop production. *Nature*. 529: 84–87.

Li B, Tester M, Gilliham M. (2017) Chloride on the move. *Trends Plant Sci.* 22: 236–248.

Limami A, Ricoult C, Planchet E, González E, Ladrera R, Larrainzar E, *et al.* (2007) Response of *Medicago truncatula* to abiotic stress. In: Mathesius U, Journet EP, Sumner LW (eds). *The* Medicago truncatula *handbook*. ISBN 0-9754303-1-9. http://www.noble.org/*Medicago*Handbook.

Liu Y, Shi Y, Song Y, Wang T, Li Y. (2010) Characterization of a stress-induced NADP-isocitrate dehydrogenase gene in maize confers salt tolerance in arabidopsis. *J. Plant Biol.* 53: 107–112.

Lohaus G, Hussmann M, Pennewiss K, Schneider H, Zhu JJ, Sattelmacher B. (2000) Solute balance of a maize (*Zea mays* L.) source leaf as affected by salt treatment with special emphasis on phloem retranslocation and ion leaching. *J. Exp. Bot.* 51: 1721–32.

Long R, Li M, Zhang T, Kang J, Sun Y, Cong L, *et al.* (2016) Comparative proteomic analysis reveals differential root proteins in *Medicago sativa* and *Medicago truncatula* in response to salt stress. *Front. Plant Sci.* 7: 424.

Lou Y, Gou JY, Xue HW. (2007) PIP5K9, an arabidopsis phosphatidylinositol monophosphate kinase, interacts with a cytosolic invertase to negatively regulate sugar-mediated root growth. *Plant Cell*. 19: 163–181.

Luo J, Tang S, Peng X, Yan X, Zeng X, Li J, *et al.* (2015) Elucidation of cross-talk and specificity of early response mechanisms to salt and PEG-simulated drought stresses in *Brassica napus* using comparative proteomic analysis. *PLoS One*. 10: e0138974.

Luo SS, Sun YN, Zhou X, Zhu T, Zhu LS, Arfan M, *et al.* (2016) *Medicago truncatula* genotypes Jemalong A17 and R108 show contrasting variations under drought stress. *Plant Physiol. Biochem.* 109: 190–198.

Luo L, Xia H, Lu BR. (2019) Editorial: Crop breeding for drought resistance. *Front. Plant Sci.* 10: 314.

Lynch JP, Chimungu JG, Brown KM. (2014) Root anatomical phenes associated with water acquisition from drying soil: targets for crop improvement. *J. Exp. Bot.* 65: 6155–6166.

Lyon D, Castillejo MA, Mehmeti-Tershani V, Staudinger C, Kleemaier C, Wienkoop S. (2016) Drought and recovery: independently regulated processes highlighting the importance of protein turnover dynamics and translational regulation in *Medicago truncatula*. *Mol. Cell. Proteomics*. 15: 1921–37.

MacNeill GJ, Mehrpouyan S, Minow MAA, Patterson JA, Tetlow IJ, Emes MJ. (2017) Starch as a source, starch as a sink: the bifunctional role of starch in carbon allocation. *J. Exp. Bot.* 68: 4433–4453.

Mahajan S, Tuteja N. (2005) Cold, salinity and drought stresses: an overview. *Arch. Biochem. Biophys.* 444: 139–158.

Mailloux RJ, Bériault R, Lemire J, Singh R, Chénier DR, Hamel RD, *et al.* (2007) The tricarboxylic acid cycle, an ancient metabolic network with a novel twist. *PLoS One*. 2: e690.

Marino D, González EM, Arrese-Igor C. (2006) Drought effects on carbon and nitrogen metabolism of pea nodules can be mimicked by paraquat: evidence for the occurrence of two regulation pathways under oxidative stresses. *J. Exp. Bot.* 57: 665–673.

Meister R, Rajani MS, Ruzicka D, Schachtman DP. (2014) Challenges of modifying root traits in crops for agriculture. *Trends Plant Sci.* 19: 779–788.

Meng LS, Wei ZQ, Cao XY, Tong C, Lv MJ, Yu F, *et al.* (2020) Cytosolic invertase-mediated root growth is feedback regulated by a glucose-dependent signaling loop. *Plant Physiol.* 184: 895–908.

Mewis I, Khan MAM, Glawischnig E, Schreiner M, Ulrichs C. (2012) Water stress and aphid feeding differentially influence metabolite composition in *Arabidopsis thaliana* (L.). *PLoS One*. 7: e48661.

Miao Z, Xu W, Li D, Hu X, Liu J, Zhang R, *et al.* (2015) *De novo* transcriptome analysis of *Medicago falcata* reveals novel insights about the mechanisms underlying abiotic stress-responsive pathway. *BMC Genomics*. 16: 1–18.

Michaud R, Lehman WF, Rumbaugh MD. (1988) World distribution and historical development. In: Hanson AA, Barnes DK, Hill RR (eds). *Alfalfa and alfalfa improvement,* Vol 29. 1st ed. Madison, WI: American Society of Agronomy, Inc., Crop Science Society of America, Inc., Soil Science Society of America, Inc., pp. 25–91.

Millar AH, Whelan J, Soole KL, Day DA. (2011) Organization and regulation of mitochondrial respiration in plants. *Annu. Rev. Plant Biol.* 62: 79–104.

Miller G, Stein H, Honig A, Kapulnik Y, Zilberstein A. (2005) Responsive modes of *Medicago sativa* proline dehydrogenase genes during salt stress and recovery dictate free proline accumulation. *Planta*. 222: 70–79.

Moreau, **D.** (2006) Morphology, development and plant architecture of M. *truncatula*. In: Mathesius U, Journet EP, Sumner LW (eds). *The* Medicago truncatula *handbook*. ISBN 0-9754303-1-9. http://www.noble.org/*Medicago*Handbook.

Muller B, Pantin F, Génard M, Turc O, Freixes S, Piques M, *et al.* (2011) Water deficits uncouple growth from photosynthesis, increase C-content, and modify the relationships between C and growth in sink organs. *J. Exp. Bot.* 62: 1715–1729.

Munns R. (2002) Comparative physiology of salt and water stress. *Plant. Cell Environ.* 25: 239–250.

Munns R. (2011) Plant adaptations to salt and water stress: differences and commonalities. *Adv. Bot. Res.* 57: 1–32.

Munns R, James RA, Sirault XRR, Furbank RT, Jones HG. (2010) New phenotyping methods for screening wheat and barley for beneficial responses to water deficit. *J. Exp. Bot.* 61: 3499–3507.

Munns R, Tester M. (2008) Mechanisms of salinity tolerance. *Annu. Rev. Plant Biol.* 59: 651–681.

Nadeem M, Li J, Yahya M, Sher A, Ma C, Wang X, *et al.* (2019a) Research progress and perspective on drought stress in legumes: a review. *Int. J. Mol. Sci.* 20: 2541.

Nadeem M, Li J, Yahya M, Wang M, Ali A, Cheng A, *et al.* (2019b) Grain legumes and fear of salt stress: focus on mechanisms and management strategies. *Int. J. Mol. Sci.* 20: 799.

Naliwajski MR, Skłodowska M. (2018) The relationship between carbon and nitrogen metabolism in cucumber leaves acclimated to salt stress. *PeerJ*. 6: e6043.

Nefronus. (2019) Xylem and phloem diagram [Image]. Florida: Wikimedia Commons [Accessed 25th Otober 2020]. Available at: https://commons.wikimedia.org/wiki/File:Xylem_and_phloem_diagram.svg.

Nemati I, Moradi F, Gholizadeh S, Esmaeili MA, Bihamta MR. (2011) The effect of salinity stress on ions and soluble sugars distribution in leaves, leaf sheaths and roots of rice (*Oryza sativa* L.) seedlings. *Plant, Soil Environ.* 57: 26–33.

Nieves-Cordones M, García-Sánchez F, Pérez-Pérez JG, Colmenero-Flores JM, Rubio F, Rosales MA. (2019) Coping with water shortage: an update on the role of K^+, Cl^-, and water membrane transport mechanisms on drought resistance. *Front. Plant Sci.* 10: 1619.

Nunes-Nesi A, Fernie AR, Stitt M. (2010) Metabolic and signaling aspects underpinning the regulation of plant carbon-nitrogen interactions. *Mol. Plant*. 3: 973–996.

Nunes CC, de Sousa-Araújo S, da Silva JM, Fevereiro MPS, da Silva AB. (2008) Physiological responses of the legume model *Medicago truncatula* cv. Jemalong to water deficit. *Environ. Exp. Bot.* 63: 289–296.

Oelkers K, Goffard N, Weiller GF, Gresshoff PM, Mathesius U, Frickey T. (2008) Bioinformatic analysis of the CLE signaling peptide family. *BMC Plant Biol.* 8: 1.

Ogden AJ, Bhatt JJ, Brewer HM, Kintigh J, Kariuki SM, Rudrabhatla S, *et al.* (2020) Phloem exudate protein profiles during drought and recovery reveal abiotic stress responses in tomato vasculature. *Int. J. Mol. Sci.* 21: 1–20.

Osmolovskaya N, Shumilina J, Kim A, Didio A, Grishina T, Bilova T, *et al.* (2018) Methodology of drought-stress research: experimental setup and physiological characterization. *Int. J. Mol. Sci.* 19: 4089.

Page MJ, Cera E Di. (2006) Role of Na^+ and K^+ in enzyme function. *Physiol. Rev.* 86: 1049–1092.

Pandey V, Shukla A. (2015) Acclimation and tolerance strategies of rice under drought stress. *Rice Sci.* 22: 147–161.

Päpke C, Ramirez-Aguilar S, Antonio C. (2013) Oxygen consumption under hypoxic conditions. In: van Dongen J, Licausi F (eds). *Low-oxygen stress in plants. Plant cell monographs,* Vol 21. 1st ed. Vienna: Springer, pp. 185–208.

Parihar P, Singh S, Singh R, Singh VP, Prasad SM. (2015) Effect of salinity stress on plants and its tolerance strategies: a review. *Environ. Sci. Pollut. Res.* 22: 4056–4075.

Pei ZF, Ming DF, Liu D, Wan GL, Geng XX, Gong HJ, *et al.* (2010) Silicon improves the tolerance to water-deficit stress induced by polyethylene glycol in wheat (*Triticum aestivum* L.) seedlings. *J. Plant Growth Regul.* 29: 106–115.

Peng L, Lang S, Wang Y, Pritchard HW, Wang X. (2017) Modulating role of ROS in re-establishing desiccation tolerance in germinating seeds of *Caragana korshinskii* Kom. *J. Exp. Bot.* 68: 3585–3601.

Per TS, Khan NA, Reddy PS, Masood A, Hasanuzzaman M, Khan MIR, *et al.* (2017) Approaches in modulating proline metabolism in plants for salt and drought-stress tolerance: phytohormones, mineral nutrients and transgenics. *Plant Physiol. Biochem.* 115: 126–140.

Pérez-Alfocea F, Balibrea ME, Alarcón JJ, Bolarín MC. (2000) Composition of xylem and phloem exudates in relation to the salt tolerance of domestic and wild tomato species. *J. Plant Physiol.* 156: 367–374.

Phan HTT, Ellwood SR, Hane JK, Ford R, Materne M, Oliver RP. (2007) Extensive macrosynteny between *Medicago truncatula* and *Lens culinaris* ssp. *Culinaris*. *Theor. Appl. Genet.* 114: 549–558.

Phutela A, Jain V, Dhawan K, Nainawatee HS. (2000) Proline metabolism under water stress in the leaves and roots of *Brassica juncea* cultivars differing in drought tolerance. *J. Plant Biochem. Biotechnol.* 9: 35–39.

Pires M, Pereira-Junior AA, Medeiros DB, Daloso DM, Pham PA, Barros KA, *et al.* (2016) The influence of alternative pathways of respiration that utilize branched-chain amino acids following water shortage in arabidopsis. *Plant Cell Environ.* 39: 1304–1319.

Pommerrenig B, Papini-Terzi FS, Sauer N. (2007) Differential regulation of sorbitol and sucrose loading into the phloem of *Plantago major* in response to salt stress. *Plant Physiol.* 144: 1029–1038.

Poustini K, Siosemardeh A, Ranjbar M. (2007) Proline accumulation as a response to salt stress in 30 wheat (*Triticum aestivum* L.) cultivars differing in salt tolerance. *Genet. Resour. Crop Evol.* 54: 925–934.

Prinsi B, Negri AS, Failla O, Scienza A, Espen L. (2018) Root proteomic and metabolic analyses reveal specific responses to drought stress in differently tolerant grapevine rootstocks. *BMC Plant Biol.* 18: 1–28.

Puniran-Hartley N, Hartley J, Shabala L, Shabala S. (2014) Salinity-induced accumulation of organic osmolytes in barley and wheat leaves correlates with increased oxidative stress tolerance: *in planta* evidence for cross-tolerance. *Plant Physiol. Biochem.* 83: 32–39.

Qing DJ, Lu HF, Li N, Dong HT, Dong DF, Li YZ. (2009) Comparative profiles of gene expression in leaves and roots of maize seedlings under conditions of salt stress and the removal of salt stress. *Plant Cell Physiol.* 50: 889–903.

Rahmat Z, Turnbull C. (2013) Optimization of EDTA-exudation technique for proteome study of the phloem. *J. Teknol.* 64: 7–9.

Rai VK. (2002) Role of amino acids in plant responses to stresses. *Biol. Plant.* 45: 481–487.

Ramos J, López MJ, Benlloch M. (2004) Effect of NaCl and KCl salts on the growth and solute accumulation of the halophyte *Atriplex nummularia*. *Plant Soil*. 259: 163–168.

Ramos M, Gordon A, Minchin FR, Sprent JI, Parsons R. (1999) Effect of water stress on nodule physiology and biochemistry of a drought-tolerant cultivar of common bean (*Phaseolus vulgaris* L.). *Ann. Bot.* 83: 57–63.

Rao DE, Chaitanya KV. (2016) Photosynthesis and antioxidative defense mechanisms in deciphering drought-stress tolerance of crop plants. *Biol. Plant.* 60: 201–218.

Ren J, Xie T, Wang Y, Li H, Liu T, Zhang S, *et al.* (2020) Coordinated regulation of carbon and nitrogen assimilation confers drought tolerance in maize (*Zea mays* L.). *Environ. Exp. Bot.* 176: 104086.

Richter JA, Behr JH, Erban A, Kopka J, Zörb C. (2019) Ion-dependent metabolic responses of *Vicia faba* L. to salt stress. *Plant Cell Environ.* 42: 295–309.

Rochaix JD. (2011) Regulation of photosynthetic electron transport. *Biochim. Biophys. Acta - Bioenerg.* 1807: 375–383.

Rogers ED, Benfey PN. (2015) Regulation of plant root system architecture: implications for crop advancement. *Curr. Opin. Biotechnol.* 32: 93–98.

Roosens NH, Thu TT, Iskandar HM, Jacobs M. (1998) Isolation of the ornithine-delta-aminotransferase cDNA and effect of salt stress on its expression in *Arabidopsis thaliana*. *Plant Physiol.* 117: 263–271.

Rosa M, Prado C, Podazza G, Interdonato R, González JA, Hilal M, *et al.* (2009) Soluble sugars-metabolism, sensing and abiotic stress: a complex network in the life of plants. *Plant Signal. Behav.* 4: 388–393.

Rouached A, Slama I, Zorrig W, Jdey A, Cukier C, Rabhi M, *et al.* (2013) Differential performance of two forage species, *Medicago truncatula* and *Sulla carnosa*, under water-deficit stress and recovery. *Crop Pasture Sci.* 64: 254–264.

Ruan YL, Jin Y, Yang YJ, Li GJ, Boyer JS. (2010) Sugar input, metabolism, and signaling mediated by invertase: roles in development, yield potential and response to drought and heat. *Mol. Plant*. 3: 942–955.

Ryšlavá H, Müller K, Semorádová Š, Synková H, Čeřovská N. (2003) Photosynthesis and activity of phosphoenolpyruvate carboxylase in *Nicotiana tabacum* L. leaves infected by Potato virus A and Potato virus Y. *Photosynthetica*. 41: 357–363.

Saha B, Borovskii G, Panda SK. (2016) Alternative oxidase and plant stress tolerance. *Plant Signal. Behav.* 11: e1256530.

Sami F, Yusuf M, Faizan M, Faraz A, Hayat S. (2016) Role of sugars under abiotic stress. *Plant Physiol. Biochem.* 109: 54–61.

Savage JA, Clearwater MJ, Haines DF, Klein T, Mencuccini M, Sevanto S, *et al.* (2016) Allocation, stress tolerance and carbon transport in plants: how does phloem physiology affect plant ecology? *Plant. Cell Environ.* 39: 709–725.

Schertl P, Braun HP. (2014) Respiratory electron transfer pathways in plant mitochondria. *Front. Plant Sci.* 5: 163.

Scholander PF, Bradstreet ED, Hemmingsen EA, Hammel HT. (1965) Sap pressure in vascular plants: negative hydrostatic pressure can be measured in plants. *Science.* 148: 339–346.

Schroeder JI, Ward JM, Gassmann W. (1994) Perspectives on the physiology and structure of inward-rectifying K^+ channels in higher plants: biophysical implications for K^+ uptake. *Annu. Rev. Biophys. Biomol. Struct.* 23: 441–471.

Seager R, Ting M, Held I, Kushnir Y, Lu J, Vecchi G, *et al.* (2007) Model projections of an imminent transition to a more arid climate in Southwestern North America. *Science.* 316: 1181–1184.

Sergeeva LI, Keurentjes JJB, Bentsink L, Vonk J, van der Plas LHW, Koornneef M, *et al.* (2006) Vacuolar invertase regulates elongation of *Arabidopsis thaliana* roots as revealed by QTL and mutant analysis. *Proc. Natl. Acad. Sci. USA.* 103: 2994–2999.

Sevanto S. (2014) Phloem transport and drought. *J. Exp. Bot.* 65: 1751–1759.

Sevanto S. (2018) Drought impacts on phloem transport. *Curr. Opin. Plant Biol.* 43: 76–81.

Shabala S. (2009) Salinity and programmed cell death: unravelling mechanisms for ion specific signalling. *J. Exp. Bot.* 60: 709–712.

Shabala S, Pottosin I. (2014) Regulation of potassium transport in plants under hostile conditions: implications for abiotic and biotic stress tolerance. *Physiol. Plant.* 151: 257–279.

Shao HB, Chu LY, Jaleel CA, Manivannan P, Panneerselvam R, Shao MA. (2009) Understanding water-deficit stress-induced changes in the basic metabolism of higher plants - Biotechnologically and sustainably improving agriculture and the ecoenvironment in arid regions of the globe. *Crit. Rev. Biotechnol.* 29: 131–151.

Sharma P, Dubey RS. (2019) Protein synthesis by plants under stressful conditions. In: Pessarakli, M, ed. *Handbook of Plant and Crop Stress,* Vol. 1. 4th ed. Boca Raton, FL: CRC Press, pp. 405–449.

Sharma S, Villamor JG, Verslues PE. (2011) Essential role of tissue-specific proline synthesis and catabolism in growth and redox balance at low water potential. *Plant Physiol.* 157: 292–304.

Shen W, Wei Y, Dauk M, Tan Y, Taylor DC, Selvaraj G, *et al.* (2006) Involvement of a glycerol-3-phosphate dehydrogenase in modulating the $NADH/NAD^+$ ratio provides evidence of a mitochondrial glycerol-3-phosphate shuttle in arabidopsis. *Plant Cell*. 18: 422–441.

Shetty K. (2004) Role of proline-linked pentose phosphate pathway in biosynthesis of plant phenolics for functional food and environmental applications: a review. *Process Biochem.* 39: 789–804.

Shugaeva NA, Vyskrebentseva EI, Orekhova SO, Shugaev AG. (2007) Effect of water deficit on respiration of conducting bundles in leaf petioles of sugar beet. *Russ. J. Plant Physiol.* 54: 329–335.

Signorelli S, Imparatta C, Rodríguez-Ruiz M, Borsani O, Corpas FJ, Monza J. (2016) *In vivo* and *in vitro* approaches demonstrate proline is not directly involved in the protection against superoxide, nitric oxide, nitrogen dioxide and peroxynitrite. *Funct. Plant Biol.* 43: 870–879.

Signorelli S, Coitiño EL, Borsani O, Monza J. (2014) Molecular mechanisms for the reaction between $^{\bullet}OH$ radicals and proline: insights on the role as reactive oxygen species scavenger in plant stress. *J. Phys. Chem. B*. 118: 37–47.

Sima NAKK, Ahmad ST, Pessarakli M. (2013) Comparative study of different salts (sodium chloride, sodium sulfate, potassium chloride, and potassium sulfate) on growth of forage species. *J. Plant Nutr.* 36: 214–230.

Singh M, Kumar J, Singh S, Singh VP, Prasad SM. (2015) Roles of osmoprotectants in improving salinity and drought tolerance in plants: a review. *Rev. Environ. Sci. Bio/Technology*. 14: 407–426.

Slabu C, Zörb C, Steffens D, Schubert S. (2009) Is salt stress of faba bean (*Vicia faba*) caused by Na^+ or Cl^- toxicity? *J. Plant Nutr. Soil Sci.* 172: 644–650.

Sobhanian H, Razavizadeh R, Nanjo Y, Ehsanpour AA, Jazii FR, Motamed N, *et al.* (2010) Proteome analysis of soybean leaves, hypocotyls and roots under salt stress. *Proteome Sci.* 8: 19.

Sofo A, Cicco N, Paraggio M, Scopa A. (2010) Regulation of the ascorbate–glutathione cycle in plants under drought stress. In: Anjum N, Chan M, Umar S (eds). *Ascorbate-glutathione pathway and stress tolerance in plants*, Vol 1. 1st ed. Netherlands: Springer, pp. 137–189.

Somerville C, Briscoe J. (2001) Genetic engineering and water. *Science.* 292: 2217.

Sperry J, Stiller V, Hacke U. (2002) Soil water uptake and water transport through root systems. In: Waisel Y, Eshel A, Beeckman T, Kafkafi U (eds). *Plant roots: the hidden half*, Vol 1. 4th ed. Boca Ratón, FL: CRC Press, pp. 663–681.

Stagnari F, Maggio A, Galieni A, Pisante M. (2017) Multiple benefits of legumes for agriculture sustainability: an overview. *Chem. Biol. Technol. Agric.* 4: 2.

Staswick PE. (1994) Storage proteins of vegetative plant tissues. *Annu. Rev. Plant Physiol. Plant Mol. Biol.* 45: 303–322.

Staudinger C, Mehmeti V, Turetschek R, Lyon D, Egelhofer V, Wienkoop S. (2012) Possible role of nutritional priming for early salt and drought stress responses in *Medicago truncatula*. *Front. Plant Sci.* 3: 285.

Stein O, Granot D. (2019) An overview of sucrose synthases in plants. *Front. Plant Sci.* 10: 95.

Stitt M. (1998) Pyrophosphate as an energy donor in the cytosol of plant cells: an enigmatic alternative to ATP. *Bot. Acta*. 111: 167–175.

Stitt M. (2013) Progress in understanding and engineering primary plant metabolism. *Curr. Opin. Biotechnol.* 24: 229–238.

Stitt M, Zeeman SC. (2012) Starch turnover: pathways, regulation and role in growth. *Curr. Opin. Plant Biol.* 15: 282–292.

Stolte J, Tesfai M, Keizer J, Øygarden L, Kværnø S, Verheijen F, *et al.* (eds) (2016) Soil threats in Europe. Status, methods, drivers and effects on ecosystem services. Luxembourg: JRC Scientific and Technical Reports.

Sturm A, Tang GQ. (1999) The sucrose-cleaving enzymes of plants are crucial for development, growth and carbon partitioning. *Trends Plant Sci.* 4: 401–407.

Sui N, Tian S, Wang W, Wang M, Fan H. (2017) Overexpression of glycerol-3-phosphate acyltransferase from *Suaeda salsa* improves salt tolerance in arabidopsis. *Front. Plant Sci.* 8: 1337.

Sun J, Yang G, Zhang W, Zhang Y. (2016) Effects of heterogeneous salinity on growth, water uptake and tissue ion concentrations of alfalfa. *Plant Soil*. 408: 211–226.

Sun Y, Kong X, Li C, Liu Y, Ding Z. (2015) Potassium retention under salt stress is associated with natural variation in salinity tolerance among arabidopsis accessions. *PLoS One*. 10: e0124032.

Sutka MR, Manzur ME, Vitali VA, Micheletto S, Amodeo G. (2016) Evidence for the involvement of hydraulic root or shoot adjustments as mechanisms underlying water-deficit tolerance in two *Sorghum bicolor* genotypes. *J. Plant Physiol.* 192: 13–20.

Szabados L, Savouré A. (2010) Proline: a multifunctional amino acid. *Trends Plant Sci.* 15: 89–97.

Taiz L, Zeiger E. (eds.) (2010) Plant Physiology. 5th ed. Massachusetts: Sinauer Associates.

Takizawa K, Nakamura H. (1998) Separation and determination of fluorescein isothiocyanate-labeled amino acids by capillary electrophoresis with laser-induced fluorescence detection. *Anal. Sci.* 14: 925–928.

Tavakkoli E, Rengasamy P, McDonald GK. (2010) High concentrations of Na^+ and Cl^-ions in soil solution have simultaneous detrimental effects on growth of faba bean under salinity stress. *J. Exp. Bot.* 61: 4449–4459.

Thalmann M, Santelia D. (2017) Starch as a determinant of plant fitness under abiotic stress. *New Phytol.* 214: 943–951.

Thapa G, Dey M, Sahoo L, Panda SK. (2011) An insight into the drought stress-induced alterations in plants. *Biol. Plant.* 55: 603–613.

Tharanathan R, Mahadevamma S. (2003) Grain legumes - A boon to human nutrition. *Trends Food Sci. Technol.* 14: 507–518.

Theerawitaya C, Boriboonkaset T, Cha-Um S, Supaibulwatana K, Kirdmanee C. (2012) Transcriptional regulations of the genes of starch metabolism and physiological changes in response to salt stressed rice (*Oryza sativa* L.) seedlings. *Physiol. Mol. Biol. Plants*. 18: 197–208.

Tian H, De-Smet I, Ding Z. (2014) Shaping a root system: regulating lateral *versus* primary root growth. *Trends Plant Sci.* 19: 426–431.

Turnbull CGN, López-Cobollo RM. (2013) Heavy traffic in the fast lane: long-distance signalling by macromolecules. *New Phytol.* 198: 33–51.

Upadhyaya H, Sahoo L, Panda SK. (2013) Molecular physiology of osmotic stress in plants. In: Rout G, Das A (eds). *Molecular stress physiology of plants*, Vol 1. 1st ed. Bhubaneswar: Springer, pp. 179–192.

Vadez V. (2014) Root hydraulics: the forgotten side of roots in drought adaptation. *F. Crop. Res.* 165: 15–24.

van den Ende W, Valluru R. (2009) Sucrose, sucrosyl oligosaccharides and oxidative stress: scavenging and salvaging? *J. Exp. Bot.* 60: 9–18.

Vanlerberghe GC. (2013) Alternative oxidase: a mitochondrial respiratory pathway to maintain metabolic and signaling homeostasis during abiotic and biotic stress in plants. *Int. J. Mol. Sci.* 14: 6805–6847.

Vanlerberghe GC, Dahal K, Alber NA, Chadee A. (2020) Photosynthesis, respiration and growth: a carbon and energy balancing act for alternative oxidase. *Mitochondrion*. 52: 197–211.

Vanlerberghe GC, Martyn GD, Dahal K. (2016) Alternative oxidase: a respiratory electron transport chain pathway essential for maintaining photosynthetic performance during drought stress. *Physiol. Plant.* 157: 322–337.

Vargas WA, Salerno GL. (2010) The Cinderella story of sucrose hydrolysis: alkaline/neutral invertases, from cyanobacteria to unforeseen roles in plant cytosol and organelles. *Plant Sci.* 178: 1–8.

Vašák M, Schnabl J. (2016) Sodium and potassium ions in proteins and enzyme catalysis. In: Sigel A, Sigel H, Sigel R (eds). *The alkali metal ions: their role for life,* Vol 16. 1st ed. Switzerland: Springer, pp. 259–290.

Verbruggen N, Hermans C. (2008) Proline accumulation in plants: a review. *Amino Acids*. 35: 753–759.

Verdoy D, Coba-de la Pena T, Redondo FJ, Lucas MM, Pueyo JJ. (2006) Transgenic *Medicago truncatula* plants that accumulate proline display nitrogen-fixing activity with enhanced tolerance to osmotic stress. *Plant, Cell Environmen*. 29: 1913–1923.

Virlouvet L, Jacquemot MP, Gerentes D, Corti H, Bouton S, Gilard F, *et al.* (2011) The ZmASR1 protein influences branched-chain amino acid biosynthesis and maintains kernel yield in maize under water-limited conditions. *Plant Physiol.* 157: 917–936.

Waisel Y, Radunz A. (2006) Differences in lipid and in fatty acid composition of taproots and lateral roots of faba bean plants (*Vicia faba* L.) grown in saline media. *Plant Biosyst.* 140: 94–99.

Wang M, Zheng Q, Shen Q, Guo S. (2013) The critical role of potassium in plant stress response. *Int J Mol Sci*. 14: 7370–7390.

Wang Q, Wu C, Xie B, Liu Y, Cui J, Chen G, *et al.* (2012) Model analysing the antioxidant responses of leaves and roots of switchgrass to NaCl-salinity stress. *Plant Physiol. Biochem.* 58: 288–296.

Wang W, Vinocur B, Altman A. (2003) Plant responses to drought, salinity and extreme temperatures: towards genetic engineering for stress tolerance. *Planta*. 218: 1–14.

Wang XS, Han JG. (2007) Effects of NaCl and silicon on ion distribution in the roots, shoots and leaves of two alfalfa cultivars with different salt tolerance. *Soil Sci. Plant Nutr.* 53: 278–285.

Wood T. (1968) The inhibition of pyruvate kinase by ATP. *Biochem. Biophys. Res. Commun.* 31: 779–785.

Woodfield DR, Caradus JR, Cousins GR, Dunn T. (1996) Response to selection for increased taproot diameter. *Agron. Soc. New Zeal.* 11: 141–144.

Wu D, Cai S, Chen M, Ye L, Chen Z, Zhang H, *et al.* (2013) Tissue metabolic responses to salt stress in wild and cultivated barley. *PLoS One*. 8: e55431.

Wu H, Li Z. (2019) The importance of Cl^- exclusion and vacuolar Cl^- sequestration: revisiting the role of Cl^- transport in plant salt tolerance. *Front. Plant Sci.* 10: 1418.

Xiao W, Loscalzo J. (2020) Metabolic responses to reductive stress. *Antioxidants Redox Signal.* 32: 1330–1347.

Xu W, Cui K, Xu A, Nie L, Huang J, Peng S. (2015) Drought-stress condition increases root-to-shoot ratio via alteration of carbohydrate partitioning and enzymatic activity in rice seedlings. *Acta Physiol. Plant.* 37: 9.

Xue X, Liu A, Hua X. (2009) Proline accumulation and transcriptional regulation of proline biosynthesis and degradation in *Brassica napus*. *BMB Rep.* 42: 28–34.

Yang G, Wei Q, Huang H, Xia J. (2020) Amino acid transporters in plant cells: a brief review. *Plants*. 9: 1–17.

Yang H, Zhao L, Zhao S, Wang J, Shi H. (2017) Biochemical and transcriptomic analyses of drought-stress responses of LY1306 tobacco strain. *Sci. Rep.* 7: 17442.

Yaniv Z, Werker E. (1983) Absorption and secretion of polyethylene glycol by *Solanaceous* plants. *J. Exp. Bot.* 34: 1577–1584.

Yao S, Chen S, Xu D, Lan H. (2010) Plant growth and responses of antioxidants of *Chenopodium album* to long-term NaCl and KCl stress. *Plant Growth Regul.* 60: 115–125.

Young ND, Cannon SB, Sato S, Kim D, Cook DR, Town CD, *et al.* (2005) Sequencing the genespaces of *Medicago truncatula* and *Lotus japonicus*. *Plant Physiol.* 137: 1174–81.

Zagorchev L, Seal C, Kranner I, Odjakova M. (2013) A central role for thiols in plant tolerance to abiotic stress. *Int. J. Mol. Sci.* 14: 7405–7432.

Zahran HH. (1999) *Rhizobium*-legume symbiosis and nitrogen fixation under severe conditions and in an arid climate. *Microbiol. Mol. Biol. Rev.* 63: 968–989.

Zarattini M, Forlani G. (2017) Toward unveiling the mechanisms for transcriptional regulation of proline biosynthesis in the plant cell response to biotic and abiotic-stress conditions. *Front. Plant Sci.* 8: 927.

Zhan A, Schneider H, Lynch JP. (2015) Reduced lateral-root branching density improves drought tolerance in maize. *Plant Physiol.* 168: 1603–1615.

Zhang C, Shi S. (2018) Physiological and proteomic responses of contrasting alfalfa (*Medicago sativa* L.) varieties to PEG-induced osmotic stress. *Front. Plant Sci.* 9: 242.

Zhang JYY, Cruz DE, Carvalho MH, Torres-Jerez I, Kang Y, Allen SN, Huhman D V, *et al.* (2014) Global reprogramming of transcription and metabolism in *Medicago truncatula* during progressive drought and after rewatering. *Plant Cell Environ.* 37: 2553–2576.

Zhao Y, Li X, Wang F, Zhao X, Gao Y, Zhao C, *et al.* (2018) Glycerol-3-phosphate dehydrogenase (GPDH) gene family in *Zea mays* L.: identification, subcellular localization, and transcriptional responses to abiotic stresses. *PLoS One*. 13: e0200357.

Zhu JK, Hasegawa PM, Bressan RA, Bohnert HJ. (1997) Molecular aspects of osmotic stress in plants. *Crit. Rev. Plant Sci.* 16: 253–277.

Zobel RW. (2011) A developmental genetic basis for defining root classes. *Crop Sci.* 51: 1410.

Zobel RW, Waisel Y. (2010) A plant root system architectural taxonomy: a framework for root nomenclature. *Plant Biosyst*. 144: 507–512.

› SUPPLEMENTARY MATERIAL

upna

Universidad Pública de Navarra
Nafarroako Unibertsitate Publikoa

Table S1.1. Respiration analysis of the roots of *M. truncatula* under water-deficit stress. Respiration rates (as mmol O_2 s^{-1} g DW^{-1}) of the taproot and fibrous root regarding total respiration, residual respiration, alternative pathway and cytochrome pathway capacities under control (C), moderate (MD) and severe (SD) water-deficit stress. Each value represents the mean ± SE (n = 10). Different letters indicate statistically significant different averages [two-way ANOVA followed by the Bonferroni *post hoc* test ($p < 0.05$). See **Table S1.2** for the two-way ANOVA results].

		Total respiration	Residual respiration	Alternative pathway capacity	Cytochrome pathway capacity
Taproot	**C**	0.63 ± 0.01 [b]	0.17 ± 0.01 [ab]	0.16 ± 0.02 [b]	0.35 ± 0.02 [b]
	MD	0.50 ± 0.03 [b]	0.21 ± 0.01 [a]	0.11 ± 0.02 [bc]	0.20 ± 0.03 [c]
	SD	0.31 ± 0.02 [c]	0.15 ± 0.01 [b]	0.08 ± 0.01 [c]	0.08 ± 0.02 [cd]
Fibrous root	**C**	0.89 ± 0.07 [a]	0.20 ± 0.01 [a]	0.36 ± 0.04 [a]	0.60 ± 0.06 [a]
	MD	0.32 ± 0.01 [c]	0.09 ± 0.01 [c]	0.13 ± 0.01 [bc]	0.08 ± 0.01 [cd]
	SD	0.22 ± 0.03 [c]	0.09 ± 0.01 [c]	0.07 ± 0.02 [c]	0.04 ± 0.01 [d]

Table S1.2. Results of the two-way ANOVAs. Asterisks indicate the significance level: ns, $p > 0.05$; $^{*}p < 0.05$; $^{**}p < 0.01$; $^{***}p < 0.001$. *act*, activity; *ADH*, alcohol dehydrogenase; *AGPase*, ADP-glucose pyrophosphorylase; *FBPase*, fructose 1,6-bisphosphatase; *GAPDH*, glyceraldehyde-3-phosphate dehydrogenase; *GDH*, glutamate dehydrogenase; *HK*, hexokinase; *IDH*, isocitrate dehydrogenase; *MDH*, malate dehydrogenase; *ME*, malic enzyme; *PDC*, pyruvate decarboxylase; *PK*, pyruvate kinase; *UGPase*, UDP-glucose pyrophosphorylase.

	Two-way ANOVA results		
Parameter	**Organ**	**Treatment**	**Organ × Treatment**
Water content	***	***	***
Total respiration	ns	***	***
Residual respiration	***	***	***
% residual respiration (of total respiration)	**	***	ns
Alternative pathway capacity	**	***	***
Cytochrome pathway capacity	ns	***	***
Alternative/cytochrome pathway capacity ratio	ns	*	ns
Ala	*	*	*
Val	***	***	*
Leu	***	***	***
Ile	***	***	*
Pro	***	***	*
Phe	***	***	*
Trp	***	***	**
Met	***	***	**
Gly	ns	ns	**
Ser	***	ns	**
Thr	***	***	**
Tyr	*	**	ns
Asn	ns	***	ns
Gln	ns	*	***
GABA	***	*	***
Glu	***	*	*
Asp	*	ns	**
Lys	***	***	***
Arg	***	***	***
His	ns	***	ns
UGPase act	***	ns	ns
AGPase act	***	ns	ns
ME act	***	ns	ns
MDH act	ns	ns	ns
FBPase act	ns	ns	ns
HK act	***	ns	ns
GAPDH act	ns	ns	ns

Table S1.2. Results of the two-way ANOVAs (continued).

	Two-way ANOVA results		
Parameter	**Organ**	**Treatment**	**Organ × Treatment**
GHD act	***	ns	ns
IDH act	***	ns	ns
PK act	**	**	*
ADH act	***	*	ns
PDC act	*	ns	ns

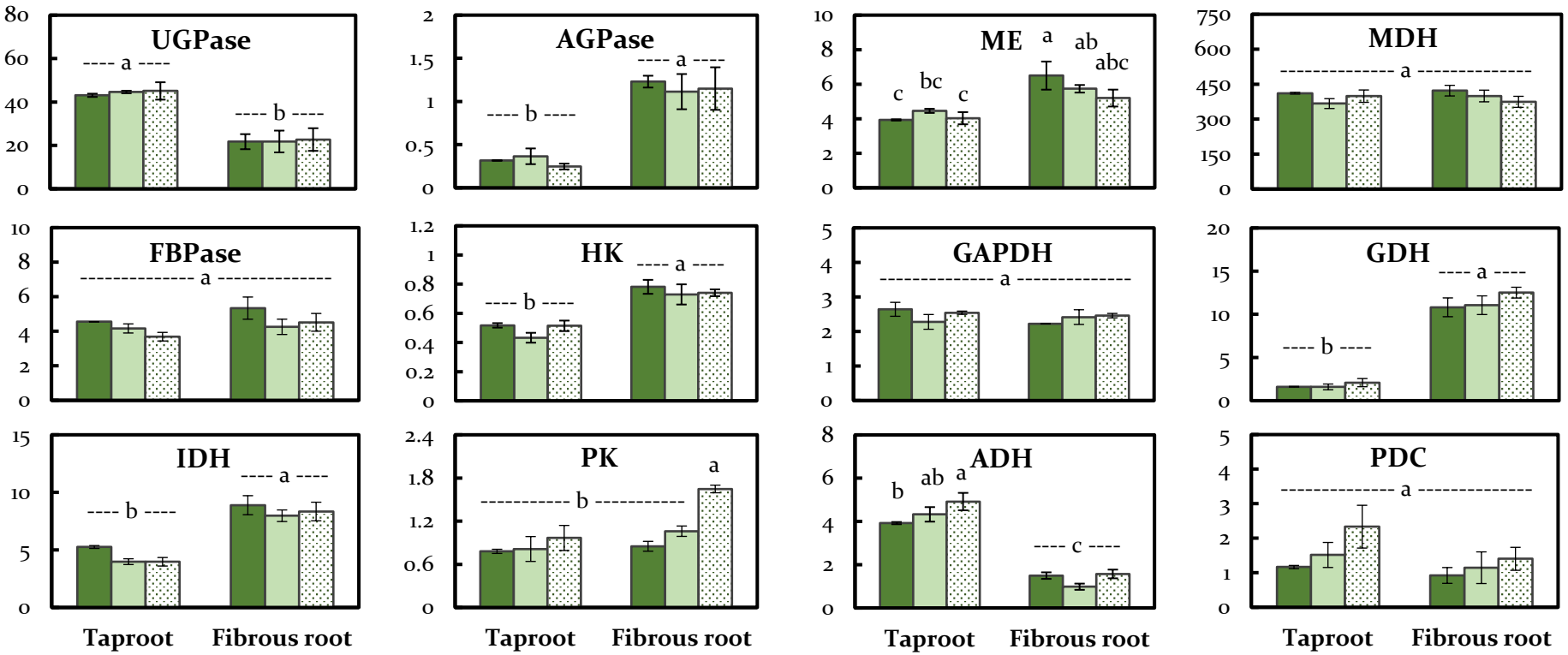

Figure S1.1. Various enzymatic activities in roots of *M. truncatula* under water-deficit stress. Enzymatic activities (as nmol NADH min^{-1} µg prot^{-1}) in the taproot and fibrous roots of *M. truncatula* under control (dark green), moderate (light green) and severe (dots) water-deficit stress conditions. Bars represent the mean ± SE (n = 4-10). Different letters indicate statistically significant different averages [two-way ANOVA followed by the Bonferroni *post hoc* test ($p < 0.05$). See **Table S1.2** for the two-way ANOVA results]. *ADH*, alcohol dehydrogenase; *AGPase*, ADP-glucose pyrophosphorylase; *FBPase*, fructose-1,6-bisphosphatase; *GAPDH*, glyceraldehyde-3-phosphate dehydrogenase; *GDH*, glutamate dehydrogenase; *HK*, hexokinase; *IDH*, isocitrate dehydrogenase; *MDH*, malate dehydrogenase; *ME*, malic enzyme; *PDC*, pyruvate decarboxylase; *PK*, pyruvate kinase; *UGPase*, UDP-glucose pyrophosphorylase.

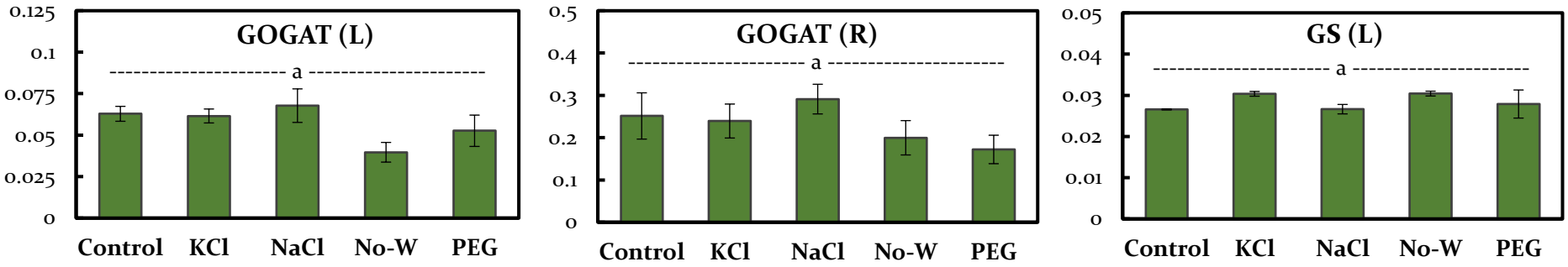

Figure S2.1. GS/GOGAT cycle enzymatic activities in response to different water-deficit treatments. Glutamine synthase (GS) and glutamate synthase (GOGAT) activities (as nmol NADH min^{-1} µg $prot^{-1}$) in leaves (L) and roots (R) of *M. truncatula* plants under NaCl, KCl, no-irrigation (No-W) and PEG-6000 conditions. Bars represent the means ± SE (n = 3). Letters represent statistical differences (Tukey`s test, $p < 0.05$) between treatments.

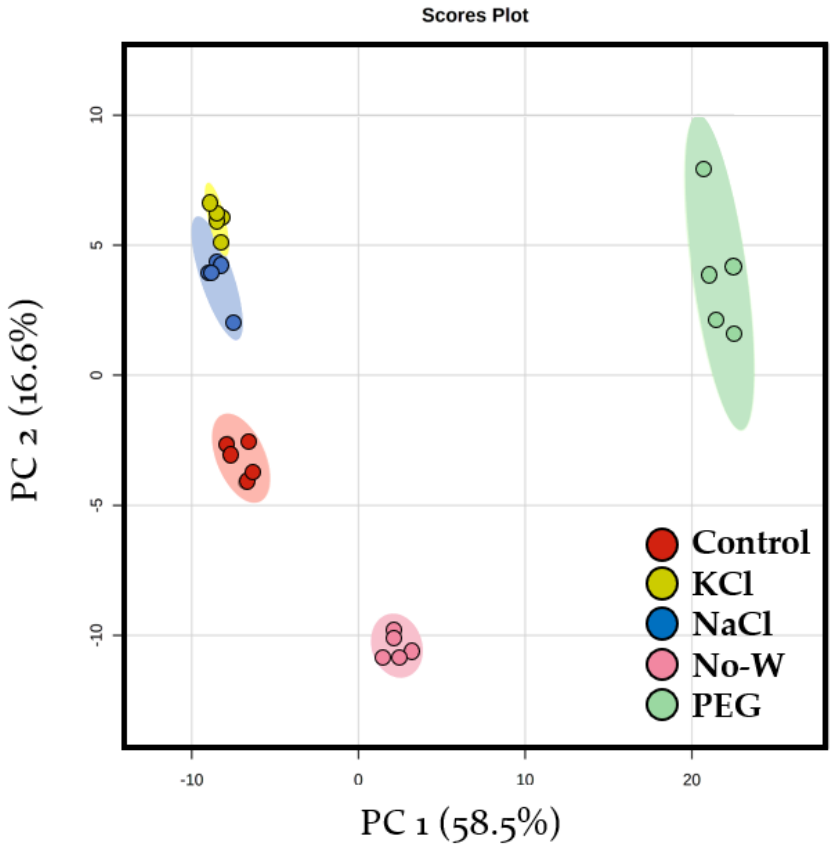

Figure S2.2. Principal Component Analysis conducted with all measured parameters in all treatments. PCA scores' plot showing the control, KCl, NaCl, non-irrigated (No-W) and PEG-6000 treated cases.

Table S2.1. Loading values resulting from the Principal Component Analyses (PCA) performed between treatments. Loading values in the first PC for all parameters after performing a PCA between non-irrigated (No-W) and PEG-6000-treated plants, NaCl and No-W plants as well as NaCl and KCl plants. *aa*, amino acids; *AAT*, aspartate aminotransferase; *act*, activity; *AlkINV*, alkaline invertase; *ASC*, reduced ascorbate; *Asc*, ascorbate; *DHA*, oxidized ascorbate; *ET*, evapotranspiration; *GDH*, glutamate dehydrogenase; *Glut*; glutathione; *GOGAT*, glutamate synthase; *G6PDH*, glucose-6-phosphate dehydrogenase; g_s, leaf conductivity; *GS*, glutamine synthase; *GSH*, reduced glutathione; *GSSG*, oxidized glutathione; *hGlut*; homoglutathione; *hGSH*, reduced homoglutathione; *hGSSG*, oxidized homoglutathione; *IDH*, isocitrate dehydrogenase; *α-KG*, α-ketoglutarate; *L*, leaves; *OAT*, ornithine aminotransferase; *P*, phloem sap; *P5CS*, Δ^1-1-pyrroline-5-carboxylate synthase; *ProDH*, proline dehydrogenase; *prot*, protein; *R*, roots; *SuSy*, sucrose synthase; *WC*, water content; Ψ_{leaf}, leaf water potential.

No-W *vs* PEG-6000		NaCl *vs* No-W		NaCl *vs* KCl	
Parameter	**Loading value**	**Parameter**	**Loading value**	**Parameter**	**Loading value**
Starch (L)	-0.887779	g_s	-0.577512	Na^+ (R)	0.511580
Fructose (R)	-0.143695	Fructose (R)	0.224002	Na^+ (L)	0.360261
Glucose (R)	-0.125668	Na^+ (L)	-0.212197	K^+ (R)	-0.239007
Succinate (R)	0.125463	Glucose (R)	0.203601	Met (P)	-0.216962
SO_4^{2-} (R)	-0.122215	Na^+ (R)	-0.197694	Asp (P)	-0.176480
Ca^{2+} (R)	-0.091684	Cl^- (R)	-0.171581	SuSy act (R)	0.175143
Na^+ (R)	-0.085489	Cl^- (L)	-0.164078	Val (P)	-0.161563
hGSSG (R)	-0.085019	Starch (L)	-0.138109	Trp (P)	-0.146466
Mg^{2+} (R)	-0.077836	SO_4^{2-} (R)	0.134215	Pro (P)	-0.144799
Total hGlut (R)	-0.077291	Ca^{2+} (R)	0.128653	Asn (R)	0.126747
NO_3^- (R)	-0.075811	hGSSG (R)	0.122023	Asn (P)	-0.124957
Total ions (R)	-0.075445	Total hGlut (R)	0.111009	Glu (P)	-0.121562
hGSH (R)	-0.074670	Ile (R)	0.105989	Ile (P)	-0.119927
GSH (R)	-0.072780	Citrate (L)	-0.102625	Total aa (P)	-0.119693
Pro (L)	0.072216	NO_3^- (R)	0.101899	Phe (P)	-0.117727
Sucrose (L)	0.066574	Mg^{2+} (R)	0.100902	Ala (P)	-0.115417
AlkINV act (R)	-0.062092	Glucose (L)	0.100769	GABA (P)	-0.111952
Ala (R)	0.061091	Val (R)	0.099913	Sucrose (R)	0.106338
OAT act (L)	-0.060567	Ser (P)	-0.099685	Malate (R)	0.100693
Total Glut (R)	-0.059920	Asn (R)	0.097426	Thr (P)	-0.094839
Thr (L)	-0.059640	Gln (P)	-0.097122	Sucrose (P)	-0.094679
Cl^- (R)	-0.059296	Ser (L)	-0.096311	Ca^{2+} (R)	-0.094422
GSSG (R)	-0.056464	Malate (R)	0.095884	Lys (P)	-0.094283
GABA (R)	0.054243	hGSH (R)	0.091603	Tyr (P)	-0.093545
K^+ (R)	-0.046714	Trp (R)	0.087039	Leu (P)	-0.091736
Glucose (L)	-0.046609	Pro (P)	-0.086297	Arg (P)	-0.090529
Asn (P)	0.044474	Fructose (L)	0.085594	DHA (R)	0.090164

Table S2.1. Loading values resulting from the Principal Component Analyses (PCA) performed between treatments (continued).

No-W *vs* PEG-6000		NaCl *vs* No-W		NaCl *vs* KCl	
Parameter	**Loading value**	**Parameter**	**Loading value**	**Parameter**	**Loading value**
Gln (P)	0.043759	Arg (L)	0.082706	Gly (P)	-0.089821
Asn (R)	-0.038990	GSSG (R)	0.078964	Citrate (R)	0.089066
Citrate (L)	-0.038613	GSH (R)	0.078715	Arg (R)	0.086941
GABA (P)	0.037361	Gln (L)	0.078585	K^+ (L)	-0.086598
Asp (L)	-0.037122	Total Glut (R)	0.078383	Gln (P)	-0.084790
hGSSG (L)	-0.036035	α-KG (L)	-0.078033	His (P)	-0.081439
Starch (R)	0.035203	His (R)	0.077902	Total asc (R)	0.071917
Fructose (L)	-0.035090	α-KG (R)	0.077863	Fructose (R)	0.068130
His (L)	0.033362	Phe (R)	0.077445	Sucrose (L)	-0.067586
Gln (R)	-0.033201	Leu (R)	0.076606	His (L)	-0.063896
Leu (L)	-0.032562	Total aa (R)	0.075955	Cl^- (R)	-0.062982
NO_3^- (L)	-0.032016	Lys (R)	0.074631	Met (L)	-0.061044
Glu (L)	-0.031761	Tyr (R)	0.072270	Citrate (L)	0.060578
Malate (R)	-0.030974	GABA (P)	-0.069238	IDH act (R)	0.059528
G6PDH act (L)	-0.030539	Arg (P)	-0.068861	Gln (R)	-0.059447
Ile (L)	-0.029826	Met (R)	0.068810	NH_4^+ (L)	0.055816
Trp (R)	-0.029805	Leu (L)	0.067736	hGSSG (L)	-0.055300
Tyr (P)	0.029725	Thr (R)	0.067192	Asn (L)	-0.054885
Ser (L)	0.029703	Asn (L)	0.066639	Mg^{2+} (R)	-0.054298
Total aa (P)	0.028089	Val (L)	0.064631	NO_4^- (R)	0.051398
Malate (L)	-0.027880	G6PDH act (R)	-0.062602	Gly (L)	-0.051107
Na^+ (L)	-0.027462	Starch (R)	-0.061863	Asp (L)	0.050690
Ser (P)	0.027186	Asp (R)	0.061176	Tyr (R)	-0.050234
PO_4^{3-} (L)	-0.026994	Ile (L)	0.059829	hGSH (L)	0.049796
Asp (R)	-0.026760	Met (L)	0.059461	ASC (R)	0.048254
Pro (P)	0.026523	Phe (L)	0.057426	Total aa (R)	0.048056
Ca^{2+} (L)	-0.026338	Ser (R)	0.056987	g_s	0.047118
GSH/total Glut (L)	-0.026035	Gly (R)	0.056335	hGSH/total hGlut (L)	0.045876
Lys (R)	-0.025717	Arg (R)	0.055484	Trp (R)	0.045662
Phe (R)	-0.025644	Lys (L)	0.054769	Leu (L)	-0.045516
GSSG (L)	0.024238	Sucrose (L)	-0.054705	Glucose (L)	-0.045313
Met (L)	-0.023060	AlkINV act (R)	0.054668	NO_4^- (L)	-0.044107
Citrate (R)	-0.022363	Pro (R)	0.054460	SO_4^{2-} (L)	-0.043968
Arg (P)	0.021731	PO_4^{3-} (R)	0.053823	GDH act (R)	0.042336
Gly (P)	0.021154	Ala (R)	0.053569	G6PDH act (R)	0.041603
Gly (R)	0.020710	Tyr (L)	0.052830	Val (L)	-0.041261
Ile (P)	-0.020588	Thr (L)	0.049816	Soluble prot (R)	0.040654
Mg^{2+} (L)	-0.020284	Leu (P)	-0.046047	Pro (L)	-0.037969
Gln (L)	-0.020221	Total ions (R)	-0.043093	Arg (L)	-0.037132

Table S2.1. Loading values resulting from the Principal Component Analyses (PCA) performed between treatments (continued).

No-W *vs* PEG-6000		NaCl *vs* No-W		NaCl *vs* KCl	
Parameter	**Loading value**	**Parameter**	**Loading value**	**Parameter**	**Loading value**
Phe (L)	0.019486	Tyr (P)	-0.042839	Starch (L)	-0.036376
Total hGlut (L)	-0.019236	Trp (L)	0.041763	Malate (L)	0.034432
Lys (L)	-0.018447	Total aa (P)	-0.040173	Cl^- (L)	-0.033318
ASC (L)	-0.018425	Ala (P)	-0.038869	Ile (L)	-0.033155
Asn (L)	-0.018409	Total ions (L)	-0.038176	G6PDH act (L)	-0.033021
K^+ (L)	-0.017985	GOGAT act (L)	-0.038015	GOGAT act (R)	0.033017
His (R)	0.017665	SO_4^{2-} (L)	0.037038	Val (R)	0.032653
GSH (L)	-0.017494	NH_4^+ (R)	-0.036758	Thr (R)	0.032584
Total aa (R)	-0.017401	GABA (L)	0.036626	Ser (P)	-0.031567
Total ions (L)	-0.017400	His (L)	0.036395	Ile (R)	0.030301
Succinate (L)	-0.016787	Thr (P)	-0.035364	Trp (L)	-0.030202
Thr (P)	0.016494	Total Asc (R)	-0.034794	α-KG (R)	-0.030013
GOGAT act (L)	0.016336	Met (P)	-0.034654	Gln (L)	-0.029999
Glu (R)	-0.016315	Sucrose (R)	0.034324	Ψ_{leaf}	-0.028984
Ala (L)	-0.014603	Gly (P)	-0.033069	Total ions (R)	-0.028795
Root WC	0.014193	hGSH (L)	-0.032445	NH_4^+ (R)	-0.027817
Total Asc (L)	-0.013530	ProDH act (R)	0.032260	Mg^{2+} (L)	0.027145
Trp (L)	0.013313	Gly (L)	0.032239	P5CS act (R)	-0.027006
Arg (L)	0.013229	Pro (L)	-0.031578	GABA (L)	0.026603
Lys (P)	-0.013057	Val (P)	0.031204	OAT act (L)	-0.026450
SO_4^{2-} (L)	-0.012882	DHA (L)	0.030200	PO_4^{3-} (R)	-0.025007
Ala (P)	0.012851	Asn (P)	-0.030076	Lys (L)	0.024778
His (P)	0.012762	G6PDH act (L)	0.029823	ProDH act (L)	-0.024687
Root biomass	-0.012132	Asp (P)	0.029571	Gly (R)	-0.024265
AAT act (R)	0.012023	K^+ (R)	0.028586	Fructose (L)	-0.023943
Val (R)	-0.011869	GOGAT act (R)	-0.027520	ASC/total Asc (R)	-0.023908
Tyr (L)	-0.011651	PO_4^{3-} (L)	0.026944	ET	0.023875
α-KG (R)	-0.011060	Glu (R)	0.026895	GSSG (R)	-0.022097
hGSH/total hGlut (L)	0.010843	GDH act (R)	-0.025793	AAT act (L)	-0.021987
NH_4^+ (R)	0.010602	Trp (P)	0.025738	P5CS act (L)	-0.021938
Gly (L)	0.010367	SuSy act (R)	-0.025636	Phe (L)	-0.021595
NH_4^+ (L)	-0.010340	ET	-0.025549	Total ions (L)	-0.021357
Asp (P)	0.010295	GABA (R)	0.025538	GDH act (L)	-0.021249
ProDH act (L)	0.010152	P5CS act (R)	0.021054	Tyr (L)	0.021087
Thr (R)	-0.010049	GSH (L)	0.020571	PO_4^{3-} (L)	-0.021067
Root/Shoot ratio	-0.009907	OAT act (L)	-0.020360	Starch (R)	0.020989
AAT act (L)	0.009412	hGSH/total hGlut (L)	-0.020025	Total aa (L)	-0.020165
SuSy act (R)	0.009234	hGSH/total hGlut (R)	-0.019610	hGSSG (R)	-0.020009
GOGAT act (R)	-0.009058	AAT act (R)	-0.019594	GS act (L)	-0.019509

Table S2.1. Loading values resulting from the Principal Component Analyses (PCA) performed between treatments (continued).

No-W *vs* PEG-6000		NaCl *vs* No-W		NaCl *vs* KCl	
Parameter	**Loading value**	**Parameter**	**Loading value**	**Parameter**	**Loading value**
Ser (R)	-0.009005	P5CS act (L)	-0.019475	GSH (R)	0.018937
IDH act (R)	0.008784	Total aa (L)	0.018975	Glucose (R)	-0.018499
Total aa (L)	0.008241	Sucrose (P)	0.018901	Phe (R)	0.018125
G6PDH act (R)	-0.008187	hGSSG (L)	0.018639	GABA (R)	0.017748
Total Glut (L)	0.008164	Ala (L)	0.017493	His (R)	0.016817
Leaf WC	-0.007071	NO_3^- (L)	0.017338	GOGAT act (L)	0.015024
PO_4^{3-} (R)	0.007045	Root/Shoot ratio	0.016284	ProDH act (R)	-0.014497
Met (R)	-0.006974	Root WC	-0.016247	Glu (R)	0.013344
Total biomass	-0.006959	Total Asc (L)	0.016215	AlkINV act (R)	-0.012570
hGSH (L)	-0.006953	Total Glut (L)	0.015836	Total hGlut (R)	-0.012547
GDH act (R)	0.006824	Glu (L)	0.015807	hGSH/total hGlut (R)	-0.011573
Leu (P)	0.006764	Gln (R)	0.014420	IDH act (L)	-0.010802
Phe (P)	0.006644	Root biomass	0.013827	Lys (R)	0.010742
P5CS act (R)	0.006628	IDH act (L)	-0.013615	Ala (R)	-0.010615
OAT act (R)	0.006511	Phe (P)	-0.013380	SO_4^{2-} (R)	-0.010603
GSH/total Glut (R)	0.006336	ProDH act (L)	0.013081	Ala (L)	0.010331
GS act (L)	-0.005933	GSSG (L)	0.012188	OAT act (R)	0.009911
Tyr (R)	-0.005840	Ile (P)	0.012096	hGSH (R)	-0.009092
Leu (R)	-0.005560	OAT act (R)	-0.011989	GSSG (L)	-0.008854
Arg (R)	-0.005476	IDH act (R)	-0.011690	Ca^{2+} (L)	0.008753
Val (P)	-0.005289	Total hGlut (L)	-0.011562	Soluble prot (L)	0.008487
Met (P)	0.005192	ASC (L)	0.010792	Thr (L)	0.007852
Soluble prot (L)	0.005083	Asp (L)	0.010413	Pro (R)	-0.007850
Cl^- (L)	-0.004980	Mg^{2+} (L)	-0.010178	ASC (L)	0.007365
ASC/total Asc (L)	-0.004843	GS act (L)	0.009865	DHA (L)	0.007273
Total Asc (R)	0.004650	Succinate (L)	-0.009559	Succinate (L)	0.007100
DHA (L)	-0.004028	GSH/total Glut (R)	-0.009391	Chlorophyll	0.006798
Soluble prot (R)	-0.003968	AAT act (L)	0.007680	Total Glut (L)	-0.006725
α-KG (L)	0.003748	Malate (L)	-0.007494	AAT act (R)	-0.006679
hGSH/total hGlut (R)	0.003517	Citrate (R)	0.007439	Total hGlut (L)	0.005825
Chlorophyll	-0.003504	Soluble prot (R)	-0.007274	GSH/total Glut (L)	0.005813
Pro (R)	-0.003405	Succinate (R)	-0.007172	Glu (L)	0.005641
IDH act (L)	-0.003128	Total biomass	0.005485	Leu (R)	0.005512
Ile (R)	-0.002879	ASC/total Asc (L)	-0.005452	Ser (L)	-0.005378
GDH act (L)	0.002554	GSH/total Glut (L)	0.004672	Total Glut (R)	-0.005251
Shoot biomass	-0.002225	K^+ (L)	-0.003952	Asp (R)	0.004862

Table S2.1. Loading values resulting from the Principal Component Analyses (PCA) performed between treatments (continued).

No-W *vs* PEG-6000		NaCl *vs* No-W		NaCl *vs* KCl	
Parameter	**Loading value**	**Parameter**	**Loading value**	**Parameter**	**Loading value**
Sucrose (P)	-0.002154	Glu (P)	-0.003815	Root WC	0.004589
P5CS act (L)	-0.001714	Shoot biomass	-0.003731	Shoot biomass	0.004177
Trp (P)	0.001465	NH_4^+ (L)	-0.002879	GSH/total Glut (R)	-0.004163
Glu (P)	-0.001139	Leaf WC	-0.002258	ASC/total Asc (L)	0.003677
Sucrose (R)	0.001085	Chlorophyll	-0.001447	Total Asc (L)	0.003400
Val (L)	0.001058	Ca^{2+} (L)	-0.001426	Ser (R)	0.003258
GABA (L)	0.000708	Soluble prot (L)	0.001303	Root biomass	0.002986
ET	0.000257	Lys (P)	0.001208	Met (R)	0.002802
ProDH act (R)	-0.000171	Ψ_{leaf}	0.000263	Leaf WC	0.002691
Ψ_{leaf}	-0.000078	His (P)	-0.000120	Root/Shoot ratio	0.002090
g_s	0.000000	GDH act (L)	-0.000031	Total biomass	0.001942
				α-KG (L)	-0.001884
				GSH (L)	-0.000864
				Succinate (R)	0.000020